Downregulation of glial fibrillary acidic protein by TNF-α – implications for the neurogenic ability of Müller glia

Erika Aquino

This thesis is submitted to University College London
for the degree of Doctor of Philosophy

UCL Institute of Ophthalmology
University College London
August 2018

Declaration

I, Erika Aquino, confirm that the work presented in this thesis is my own. Where information has been derived from other sources, I confirm that this has been indicated in the thesis.

London, August 2018

Acknowledgements

Firstly, I must thank Prof. Astrid Limb for having faith in me and giving me the opportunity to do this PhD. I am very fortunate to have had her supervision over the last three years, her guidance and support have been invaluable. Not only has she encouraged me to progress academically but has also allowed me to follow avenues for personal development. I would like to thank Prof. Sir Peng Khaw for all the wise words over the years, your enthusiasm and excitement for research is inspiring. Thank you, Joanne and Sudershana for the administrative help and the friendly chats. This work was funded by Moorfield's Eye Charity and I am very grateful for their support.

Thank you to everyone in the group and the Institute, past and present, for making my experience so great and the environment one I have enjoyed working in. Karen, the fountain of all laboratory knowledge, thank you for never making my stupid questions seem stupid and for having endless patience in teaching me everything I know. When I was still new, Phey Feng and Richard helped me find my feet, thank you both for all the fun memories. Thank you Angshu, Silke, Maureen, Damir, Justin, I-Ting, Rachel, Will, Mark, Josh and Celia for the constant help and advice in all those hours of lab meetings. Aida and Naheed have made my lab life run smoothly, for which I am grateful. And to the lunch crew: Rita, Carla, Isabel and Ashkon, thank you for providing that much needed time out from western blots, and filling it with laughter and knitting.

I would like to thank my friends, especially my housemates, who have kept me going through this process, for being there when I needed an ear and cheering me up after hard days. To Matthew, thank you for believing in me and building my confidence when I had doubts, your support has been vital during the course of this PhD.

And most importantly, thank you to my family Julia, Rafael, Marcio and Zelia. I couldn't have completed this without the unconditional support, reassuring phone calls and infinite encouragement. My parents' passion for research inspired me to pursue this dream of studying a PhD. This is dedicated to them.

Abstract

Müller glial cells can regenerate the retina in zebrafish throughout life. However, in the damaged adult human retina, upregulation of inflammatory cytokines, including TNF-α, leads to Müller cell gliosis, a hallmark of which is an increase in intermediate filament glial fibrillary acid protein (GFAP) production. However, a subset of these human cells has stem cell characteristics *in vitro*. This study investigated the role that inflammatory cytokines may play in regulating Müller cell gliosis-associated proteins and the implications this could have on the neurogenic ability of Müller glia *in vitro*.

As determined by gene and protein analysis, culture of the human Müller glial cell line MIO-M1 in the presence of TNF-α, causes downregulation of GFAP expression. Through upregulation of TNF-receptor2 and downstream activation of the NFκB signalling pathway, a cell survival signal is initiated. MIO-M1 cells co-cultured with TNF-α and factors known to induce rod photoreceptor precursor differentiation, showed increased expression of the photoreceptor marker NR2E3. These observations suggest that TNF-α may not inhibit the neurogenic ability of these cells.

A retroviral transfection method was developed to overexpress GFAP in MIO-M1 cells using molecular cloning techniques. Overexpression of GFAP resulted in no phenotypic changes as Müller cells maintained their stem cell characteristics. Culturing these transfected cells with TNF-α revealed differential transcriptional regulation of endogenous and exogenous GFAP. This indicates the importance of the GFAP promoter and transcriptional response elements in responding to TNF-α during gliosis.

In conclusion, the present study has identified the downregulation of GFAP expression by TNF-α in Müller glial cells as a target that could be further explored to control scarring of the human retina. These observations pave the way for further investigations to promote endogenous regeneration of the adult human retina by Müller glia.

Impact Statement

A major cause of visual impairment and blindness is the damage or degeneration of retinal tissue that occurs as a result of diseases such as age-related macular degeneration (AMD) and glaucoma. Current treatments for retinal degeneration are directed at limiting damage to the retina, preserving vision and managing disease. Treatments usually require life-long follow up and are not restorative so many patients still develop visual impairment. Therefore, novel approaches are needed to treat retinal degenerative diseases and research exploring endogenous regeneration and the use of Müller glial cells as a source of endogenous stem cells to restore vision is fast expanding. This concept comes from the knowledge that in damaged zebrafish retina, Müller glial cells can regenerate and replace retinal neurons to repair damage. In contrast, when human adult retina is damaged, Müller glial cells become reactive, releasing inflammatory cytokines and other factors responsible for gliosis which ultimately cause scarring of the retina. This thesis aimed to examine whether overexpression of a gliosis-associated protein, known as glial fibrillary acid protein (GFAP), plays a role in the proliferation and neural differentiation of the MIO-M1 cell line. To investigate the problem, inflammatory cytokines were examined for their ability to modify the expression of GFAP. It was found that TNF-α downregulated GFAP in MIO-M1 cells through activation of downstream signalling involving NFκB. It was also shown that TNF-α did not prevent these cells differentiating into rod photoreceptor precursors *in vitro*, indicating that this cytokine may not be detrimental during gliosis but may support the neurogenic potential of Müller glial cells. This knowledge is beneficial in furthering the understanding of how scarring in the human retina can be potentially controlled or reversed. In addition, molecular methods to control expression of GFAP were investigated and Müller cells overexpressing this protein were examined for their capacity to proliferate and differentiate into rod photoreceptor precursors. This methodology allowed the establishment of a stable cell line in the host laboratory which can be used by others in future to further investigate the role of this protein within Müller glia. Identifying molecular mechanisms that are capable of controlling gliosis whilst also encouraging self-repair by Müller glial cells, may eventually benefit patients affected by retinal degenerative diseases.

Contents

Table of figures

Abbreviations

AMD	Age-related macular degeneration
ASCL1A	Achaete-scute homolog 1 A
BCA	Bicinchoninic acid
BDNF	Brain derived neurotrophic factor
bFGF	Basic fibroblast growth factor
bHLH	basic Helix-Loop-Helix
BrdU	Bromodeoxyuridine
CAPE	Caffeic acid phenethyl ester
cGMP	Cyclic guanosine monophosphate
CDK	Cyclin-dependent kinase
CMV	Cytomegalovirus
CNS	Central nervous system
CNTF	Ciliary neurotrophic factor
CRALBP	Cellular retinaldehyde binding protein
DAPI	4',6-diamidino-2-phenylindole
DMEM	Dulbecco's Modified Eagle Medium
DNA	Deoxyribonucleic acid
ECM	Extracellular matrix
EGF-R	Epidermal growth factor receptor
ELISA	Enzyme-Linked Immunosorbent Assay
ERG	Electroretinogram
ERK	Extracellular signal-regulated kinases
FACS	Fluorescence-activated cell sorting
FCS	Fetal calf serum
FGF	Fibroblast growth factor
FTRI	FGF, Taurine, Retinoic acid, IGF
Fz	Frizzled family transmembrane receptors

GCL	Ganglion cell layer
GDNF	Glial cell-derived neurotrophic factor
GFAP	Glial fibrillary acidic protein
GFP	Green fluorescent protein
GLAST	Glutamate-aspartate transporter
HB-EGF	Heparin binding - epidermal growth factor
IκBα	Nuclear factor of kappa light polypeptide gene enhancer in B-cells inhibitor, alpha
IF	Intermediate filament
IFN	Interferon
IGF	Insulin like growth factor
IL	Interleukin
ILM	Inner limiting membrane
INL	Inner nuclear layer
IOP	Intraocular pressure
IPL	Inner plexiform layer
JAK	Janus kinase
LDH	Lactate dehydrogenase
MAPK	Mitogen-activated protein kinases
MCP	Monocyte chemotactic protein
MIO-M1	Moorfields/Institute of Ophthalmology-Müller 1
mRNA	Messenger Ribonucleic acid
NFkB	Nuclear factor kappa-light-chain-enhancer of activated B cells
NFL	Nerve fibre layer
NMDA	N-Methyl-D-aspartic acid
NOS	Nitric oxide synthase
NR2E3	Nuclear receptor subfamily 2, group E, member 3
OLM	Outer limiting membrane
ONL	Outer nuclear layer

OPL	Outer plexiform layer
PBS	Phosphate buffered saline
PCR	Polymerase chain reaction
PFA	Paraformaldehyde
PVDF	Polyvinylidene difluoride
PVR	Proliferative vitreoretinopathy
qPCR	Quantitative polymerase chain reaction
RGC	Retinal ganglion cell
RIPA	Radioimmunoprecipitation assay buffer
RNA	Ribonucleic acid
RPE	Retinal pigment epithelium
RT-PCR	Reverse transcriptase polymerase chain reaction
Shh	Sonic hedgehog
STAT	Signal transducer and activator of transcription
TBS	Tris buffered saline
TetO2	Tetracycline operator 2
TetR	Tetracycline regulatory molecule
TGF	Transforming growth factor
TNF	Tumour necrosis factor
TNFR	Tumour necrosis factor receptor
Trk	Tyrosine receptor kinases
VEGF	Vascular endothelial growth factor
Wnt	Wingless-type MMTV integration site family

Chapter 1 General introduction

1.1 The retina: structure and function

The visual system is responsible for translating light energy into an image of the world we see. When light penetrates the eye, it is refracted by the cornea through the pupil and is then focused by the lens onto the retina, which lies at the back of the eye (Barker, 1999). The retina is a thin sensory tissue, which relays the incoming information to the visual cortex in the brain. There are believed to be about 70 different cells in the vertebrate neural retina but the six main types of cells are photoreceptors, bipolar, horizontal, amacrine, glial and retinal ganglion cells (Kolb et al., 2001). The neural retina consists of three laminar layers, namely the outer nuclear layer (ONL), the inner nuclear layer (INL) and the ganglion cell layer (GCL) (Figure 1-1).

Light must travel through the full thickness of the retina to the photoreceptor cells, which have their light sensitive region facing away from incoming light. Photoreceptor cells have their cell bodies in the ONL arranged below the outer limiting membrane (OLM) and transduce the light energy into electrical signals. The most posterior part of the retina has a monolayer of pigmented cells known as the retinal pigment epithelium (RPE) which absorb light to prevent it reflecting back onto the photoreceptors causing a blurred image (Vander et al., 2003).There are two types of photoreceptor cells containing molecules called photopigments which absorb light: rod and cone cells. Rod cells are more numerous and also more sensitive. They respond to low light levels and are responsible for our vision in the dark. Cone cells are fewer but contain pigments that are sensitive to colour and are responsible for bright light colour vision (Wassle, 2004). Light causes the photopigments to absorb energy from photons, which activates biochemical processes involving cGMP, leading to changes in membrane potential. In the dark, photoreceptors are in fact depolarised and in response to light they hyperpolarise and subsequently inhibit neurotransmitter release (Vander et al., 2003).

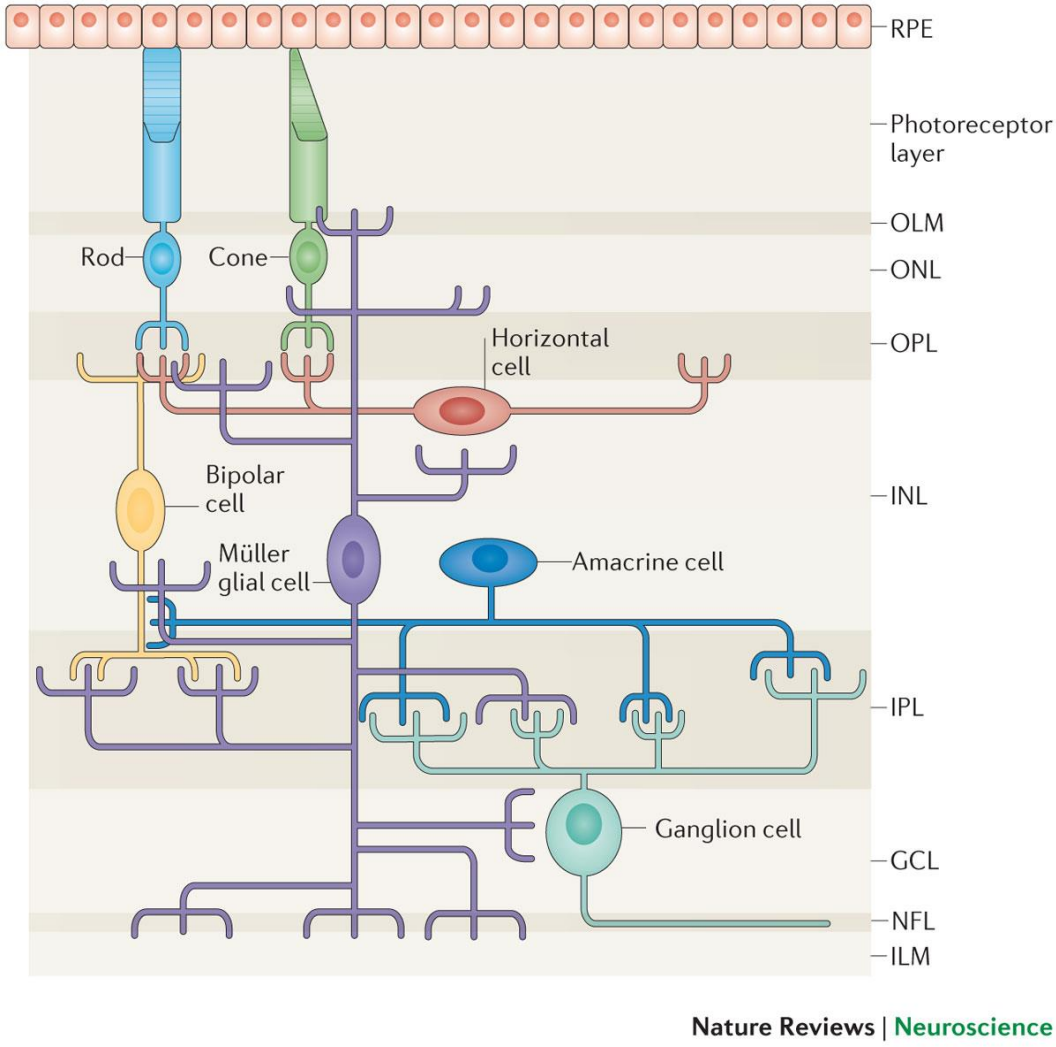

Figure 1-1: Illustration of the neural retina.
Adapted from (Goldman, 2014). The vertebrate retina contains six main cells types: rod and cone photoreceptors, horizontal, bipolar, amacrine, ganglion and Müller glial cells. There are three laminar layers: the outer nuclear layer (ONL), the inner nuclear layer (INL) and the ganglion cell layer (GCL). Cells synapse with each other in the outer plexiform layer (OPL) and the inner plexiform layer (IPL). Ganglion cell axons form the nerve fibre layer (NFL), whilst the Müller glia processes form the outer limiting membrane (OLM) and the inner limiting membrane (ILM).

Photoreceptors do not fire action potentials themselves but pass signals to bipolar cells via synapses at the outer plexiform layer (OPL). The INL contains the cell bodies of bipolar cells as well as other interneurons called horizontal and amacrine cells. The horizontal cells help modulate the connections between photoreceptors and bipolar cells to modify the response. Amacrine cells are mostly inhibitory interneurons and function to control the excitatory pathway between photoreceptors and bipolar cells (Kolb et al., 2001). The bipolar cells then synapse with ganglion cells in the inner plexiform layer (IPL), which are the first cells to produce action potentials. Via these synapses, ganglion cells respond differently to the visual image in terms of colour, intensity, movement and form. Ganglion cell bodies are found in the GCL and their axons extend along the nerve fibre layer (NFL) which converges into the optic nerve, allowing signals to pass to the visual cortex of the brain.

The macroglial cells of the retina include Müller glia and astrocytes. Astrocytes are restricted to the NFL, function as ganglion cell axonal sheaths and have a role in ionic homeostasis. Müller cells are the main glial cell of the retina and although their cell bodies lie in the INL they span the whole width of the retina and form the limits of the retina at the OLM and the inner limiting membrane (ILM). As well as providing structural support to retinal neurons, Müller cells also have a wide range of functions necessary for retinal health (Goldman, 2014).

1.2 Retinal development

Using a lineage-marking system, it was found that all retinal neural cell types, as well as Müller glia, share a common multipotent progenitor (Turner and Cepko, 1987, Turner et al., 1990). Furthermore, birth-dating studies showed that each cell type undergoes neurogenesis in a specific temporal order but that there is significant overlap between cell types. This provides evidence for the existence of retinal multipotent progenitor cells (Reese, 2011). In the rat retina, cell genesis begins around embryonic day (E) 10 and is complete by postnatal day (P) 12 with retinal ganglion cells being the first cell to be produced followed by horizontal cells, cone cells, amacrine cells, rod cells, bipolar cells, and Müller glia (Rapaport et al., 2004). The same pattern of development is seen in human retina with retinogenesis beginning at 6.5 weeks of gestation and retinal ganglion cells being the first to develop, followed by photoreceptors and finally Müller glia, with retinogenesis complete by 18 weeks (Spira and Hollenberg,

1973). Astrocytes are not derived from this single progenitor and instead migrate from the optic nerve head into the neural retina during retinogenesis (Watanabe and Raff, 1988).

The regulation of proliferation and cell fate specification are important in retinogenesis in order to generate a fully functional retina. There are intrinsic factors and extrinsic cues that influence cell fate in a complex manner and importantly, the progenitor cell itself has to be able to respond to these cues (Cepko et al., 1996). If progenitor cells exit the cell cycle too early then the ratio of early born cells (retinal ganglion cells) to later born cells (Müller glia) will be incorrect and there could be alterations in the size, shape and organisation of the retina (Dyer and Cepko, 2001). Therefore, it is important to maintain enough progenitor cells throughout retinogenesis to ensure that the correct number of different cells is generated (Hatakeyama and Kageyama, 2004).

The main regulation during retinal development is through the Notch receptor pathway. Upon activation of the Notch receptor via cell-to-cell signalling, the expression of target genes such as *Hes1* are upregulated. These genes are known as basic helix-loop-helix (bHLH) transcription factors, which control cell fate specification and can either be repressors or activators. *Hes1* is a bHLH repressor and acts by supressing bHLH activator genes, such as *Mash1*, and causing differentiation to be inhibited and a progenitor pool to be maintained. When Notch is not activated, *Hes1* is not expressed and bHLH activators induce neuronal specific gene expression.

To generate the specific neuronal subtypes found in the retina, it is necessary for bHLH genes to function together with homeodomain genes. The time and precise expression of these regulatory genes determines neuronal cell fate. For example, the homeodomain transcription factor Prox1 expression is known to change during retinogenesis. When *Prox1* is downregulated progenitor cells exit the cell cycle, reducing progenitor cell proliferation. Expression of this gene is turned on again specifically during horizontal cell differentiation (Dyer, 2003).

Another pathway which is important during retinal development is the wingless-type MMTV integration site family (Wnt) signalling pathway. Wnt proteins are a large family of glycoproteins which bind to Frizzled (Fz) family transmembrane receptors and activate the intracellular protein Disheveled (Dsh), initiating one

of three different pathways. Wnt and Fz expression patterns during development reflect different roles. For example, Wnt5a is restricted to the peripheral neural retina suggesting a role in maintaining multipotent progenitors (van Raay and Vetter, 2004). Additionally, familial cases of the degenerative disease vitreoretinopathy have been associated with mutations in the Fz gene *fz-4,* indicating that Wnt signalling may be required in the mature retina (Robitaille et al., 2002).

1.3 Photoreceptor cells

1.3.1 Genesis

The human retina has only one type of rod cell, expressing rhodopsin as its photopigment, but three types of cones cells. Each type of cone cell expresses a different opsin photopigment which is sensitive to different regions of the visual spectrum. S opsin is sensitive to short wavelengths such as blue light, M opsin is sensitive to medium wavelengths such as green light, and L opsin is sensitive to long wavelengths such as red light (Swaroop et al., 2010). Photoreceptors are generated after the multipotent progenitor cell commits to a photoreceptor precursor cell fate. Next, the immature photoreceptors are directed towards rod or cone cell fate and begin to express photoreceptor specific genes. Finally, during terminal differentiation towards functional photoreceptors, there is axonal growth, synapse formation and photopigment expression (Swaroop et al., 2010). Rod cell differentiation begins at foetal week 10 when specific markers are first identified but rhodopsin expression is not seen until week 15 (Hendrickson et al., 2008). Cone cells are born around foetal week 8 but S opsin appears at around week 11 and M and L opsin appear later at week 14 (Xiao and Hendrickson, 2000). According to the visual needs of different species, the amount and distribution of each photoreceptor subtype varies.

1.3.2 Signalling pathways

The genesis of photoreceptors is tightly regulated by many complex signalling pathways (Figure 1-2). It is known that the inhibition of Notch signalling promotes photoreceptor precursor differentiation. *In vivo* mammalian studies revealed that inactivation of the Notch receptor in retinal precursor cells considerably reduces proliferating cells and increases the proportion of

photoreceptor cells and expression of photoreceptor markers (Yaron et al., 2006) (Jadhav et al., 2006).

Another key regulator in early photoreceptor differentiation is the homeodomain transcription factor OTX2. *Otx2* is required for photoreceptor cell fate determination from precursors because in *Otx2* conditional knockout mice there is an absence of photoreceptors (Nishida et al., 2003). After becoming a photoreceptor precursor, cells must differentiate into rod or cone cells. *Otx2* is also involved in upregulating cone–rod homeobox protein CRX expression. *Crx* is a transcription factor acting downstream of *Otx2* and is found expressed in photoreceptor precursors (Koike et al., 2007). Retinal sections from *Crx* null mice contained photoreceptors that lacked outer segments and had reduced rod and cone specific genes. Furthermore, electroretinogram (ERG) assays showed huge loss of rod and cone activity (Furukawa et al., 1999) indicating that *Crx* is important in photoreceptor terminal differentiation but is not specific for rod or cone cell fate.

Rod cell fate is largely determined by the basic motif–leucine zipper transcription factor NRL. *Nrl* and *Crx* interaction is required for rod specific gene expression (Pittler et al., 2004). *In vivo* analysis of *Nrl* null mice showed complete ablation of rod cell function by ERG readings under dark adapted conditions (Mears et al., 2001). There was no expression of rod specific genes such as rhodopsin (*Rho*) but significantly increased expression of cone specific gene S-opsin (*Opn1sw*) signifying a functional change in photoreceptors. When *Nrl* is overexpressed in photoreceptor precursors differentiation is directed towards rod cells at the expense of cone cells (Oh et al., 2007). A direct downstream target of NRL is the orphan nuclear receptor NR2E3 which is required for suppression of cone specific genes, whilst directing rod cell fate (Oh et al., 2008). *Nr2e3* is exclusively expressed in rod photoreceptors in human foetal retina (O'Brien et al., 2004) as well as the developing mouse and zebrafish retina (Chen et al., 2005).

Activation of S-opsin cone cell development is controlled by retinoid-related orphan receptor β (RORβ) acting synergistically with CRX. *Rorβ*-deficient mice lack S-opsin in postnatal cone cells suggesting a key role in opsin organisation in the mature retina (Srinivas et al., 2006). Alternatively, the thyroid hormone receptor β2 (TRβ2) protein specifically identifies cone cells from initial

generation to mature M-opsin cones (Ng et al., 2009). Mice lacking TRβ2 show a selective loss of M-opsin cone cells with all cone cells expressing S-opsin, indicating that TRβ2 controls M-opsin cone genesis and without its expression cone cells “default” to S-opsin cone cells (Ng et al., 2001).

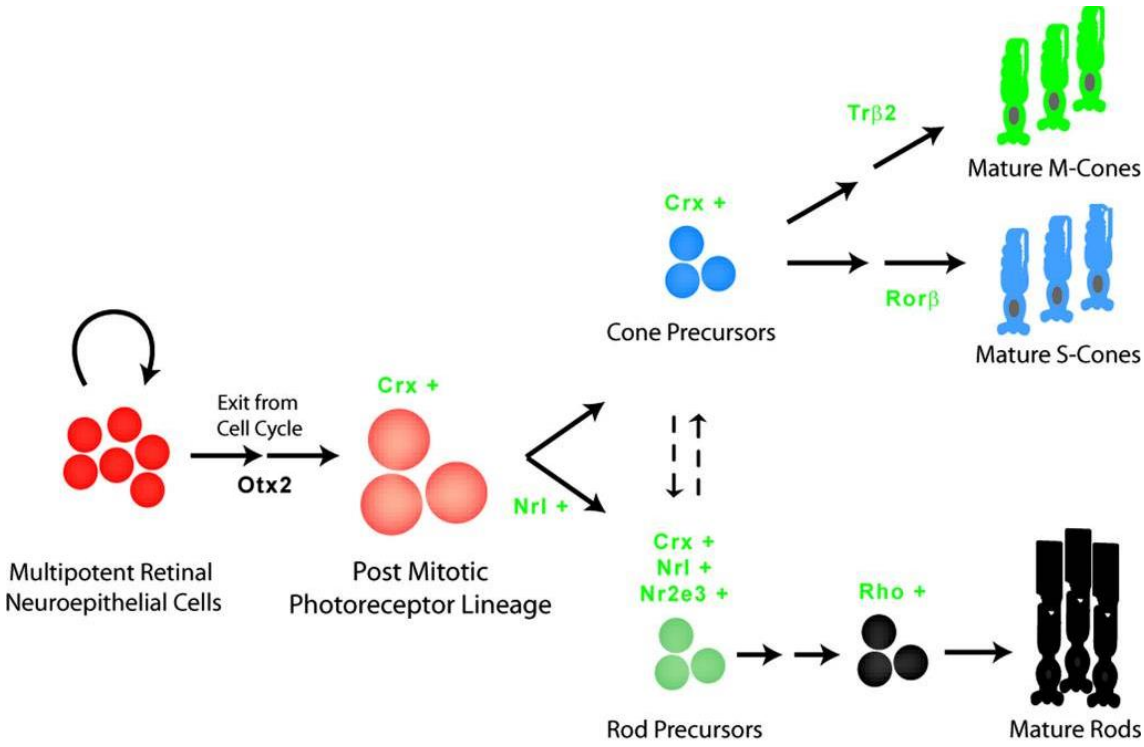

Figure 1-2: Rod and cone photoreceptor genesis from multipotent retinal progenitor cells.
Otx2 is required for cell cycle exit into photoreceptor lineage and *Crx+* cells are photoreceptor precursors. *Nrl* expression causes rod differentiation, *Nr2e3+* cells are rod lineage and *Rho* expression is a sign of a mature rod photoreceptor cell. *Trβ2* expression is found in M-opsin cone cells, whereas *Rorβ* expression is found in S-opsin cone cells. Adapted from (Oh et al., 2007).

1.4 Müller glial cells

1.4.1 Development

The development of Müller glial cells is not fully understood and there are various hypotheses about Müller cell fate determination (Jadhav et al., 2009). The concept that a single 'master gene' acts to regulate Müller glia differentiation arises from Notch signalling regulating the bHLH repressor gene *Hes1*. When *Notch1* is constitutively activated in rat retinal explants, 90-95% of cells express Müller cell markers. When there is forced expression of *Hes1* only Müller cell markers are seen, whilst markers for other retinal cell types are undetectable (Furukawa et al., 2000). However, as *Notch1* is expressed throughout development and Müller glia are only produced during later stages of retinogenesis this model appears to be too simple.

It has also been suggested that those cells that do not acquire neuronal cell fate during development default to a glial cell fate. The homeobox gene *Chx10* is essential for bipolar cell differentiation and misexpression of this gene in retinal explants increases Müller glial cell production (Hatakeyama et al., 2001, Burmeister et al., 1996). However, as *Chx10* null mice retain Müller glial cells, it is not simply a case of glial or neuronal cell fate specification; many signals and factors may be at play.

Cyclin-dependent kinases (CDKs) are important proteins controlling the cell cycle and CDK inhibitors act to negatively control cell cycle progression. CDK inhibitor gene expression patterns correlate with retinogenesis, gradually increasing during development. The CDK inhibitor $p27^{Kip1}$ is found expressed in the mammalian retina and $p27^{Kip1}$ null mice have shown disrupted retinal layers (Nakayama et al., 1996). In *Xenopus*, overexpression of $p27^{Kip1}$ causes a dramatic increase in Müller glia formation, indicating this as an intrinsic factor which influences retinal precursor cells into a glial rather than neuronal cell fate (Ohnuma et al., 1999).

Another factor regulating Müller glia differentiation is the expression of epidermal growth factor receptor (EGF-R) and its ability to respond to extracellular signals. By increasing EGF-R in progenitor cells *in vitro* there were more Müller glia produced (Lillien, 1995). This demonstrates that levels of receptor expression influences cell fate by modulating responsiveness to extracellular signals during retinogenesis. An extracellular signal shown to

influence Müller glia development is the cytokine ciliary neurotrophic factor (CNTF). Müller glial cells are the main cells in the retina that respond to CNTF as CNTF-receptor-α (CNTFRα) expression is mainly localised to Müller glia (Wen et al., 2012, Rhee and Yang, 2010, Kirsch et al., 1997). CNTF can promote Müller glia cell differentiation from progenitor cells *in vitro* in postnatal mouse retinal explants by i) inducing 'signal transducers and activators of transcription' (Stat) protein phosphorylation and by ii) regulating extracellular signal-mediated kinase (ERK) phosphorylation (Goureau et al., 2004). Bhattacharya et al postulated that CNTF-mediated signalling regulates a developmental switch from neuronal to glial generation in the retina (Bhattacharya et al., 2008). Using a rat neurosphere assay, retinal progenitor cells were stimulated to express markers of bipolar cells under low concentrations of CNTF. At high concentrations of CNTF, Müller specific markers such as GFAP and vimentin were increased. As well as responding to CNTF, Müller glia also produce CNTF, creating a feed forward influence during gliogenesis.

The high-mobility group box transcription factors *Sox9* and *Sox2* are also implicated in Müller glial cell fate determination. The *Sox* family genes are well established in their importance during development. The expression of *Sox9* gradually increases during retinogenesis, beginning in retinal progenitor cells and at postnatal stages restricting their expression to the INL, specifically by Müller glial cells but not in retinal neurons (Poche et al., 2008). In the *Sox9* mutant mouse postnatal retina, only Müller cell development is affected, by specific loss of Müller glia markers and not of neurons (Poche et al., 2008). Furthermore, *in vitro* downregulation of *Sox9* in retinal explants significantly reduced Müller glial cell population, indicating that *Sox9* is important in Müller cell differentiation (Muto et al., 2009). *Sox2* is also known to be expressed in postnatal and adult mice retina, implicating it in Müller glial cell development (Surzenko et al., 2013). *Sox2* mutant mice retinas have reduced density and aberrant morphology of Müller glia (Surzenko et al., 2013) and forced expression of *Sox2* in mouse retinal explants increases Müller glial cell number (Lin et al., 2009). In addition, adult human Müller glial cell lines express *Sox2* and silencing of the transcription factor decreases proliferation and increases apoptosis *in vitro,* implying that *Sox2* is important for adult Müller glia survival (Bhatia et al., 2011).

1.4.2 Structure and function

Heinrich Müller first described Müller glial cells in 1851 as “radial fibres” and in fact they are the most abundant type of radial glial cells that reside in the sensory retina. The Müller cell soma is located in the INL and its two main processes extend in opposite directions (Figure 1-3). The outer Müller cell process projects into the subretinal space, reaching in between the photoreceptor inner segments using microvilli. The inner process runs towards the vitreous, expanding at the end forming the endfoot and touching the basal lamina between the vitreous body and neuroretina, forming the ILM. Both the processes and the soma have lateral branches that expand into all the layers of the retina and contact all neuronal cells of this tissue. The soma and processes of Müller glia are similar in all vertebrate species but the overall morphology varies due to the needs of each retina, for example, the mammalian retina has a thick ONL and so the outer processes of the Müller glia are rather long (Reichenbach and Bringmann, 2010).

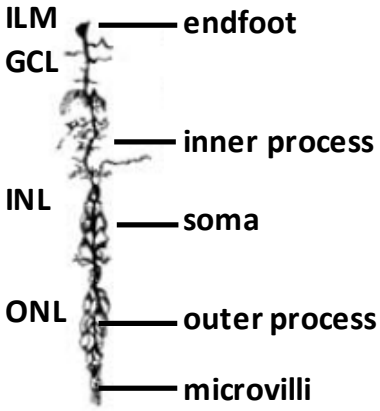

Figure 1-3: Human Müller glial cell. The soma is in the inner nuclear layer (INL) and the cell expands through all the layers of the retina including the outer nuclear layer (ONL) and the ganglion cell layer (GCL). The inner process runs towards the vitreous with the endfoot reaching the inner limiting membrane (ILM), whilst the outer process runs towards the subretinal space. Adapted from (Reichenbach and Bringmann, 2010).

The outer process has a large surface-to-volume ratio due to the numerous, long microvilli that are needed for nutrient and molecule exchange with the subretinal space. The outer process contains the Golgi complexes, multivesicular bodies for secretory functions, microtubules for intracellular transport and densely packed mitochondria. The inner process is where the majority of the cytoplasmic volume of the cell is contained with bundles of intermediate filaments (IFs) and densely packed smooth endoplasmic reticulum. The endfoot membrane is involved in exchange of molecules and biological signals between Müller cells and the vitreous via specific membrane proteins. The side branches are important for interacting with neurons of the retina but have barely any organelles suggesting that neuronal activity may stimulate local protein synthesis. There are many proteins that are selectively expressed in

Müller cells and are used as specific markers. These are vimentin, glial fibrillary acid protein (GFAP), cellular retinaldehyde-binding protein (CRALBP), glutamate-aspartate transporter (GLAST) and glutamine synthetase amongst others (Reichenbach and Bringmann, 2010).

Müller glial cells have many important roles, acting in a symbiotic way with the retinal neurons by providing homeostatic and metabolic support to the retina (Reichenbach and Bringmann, 2013). Müller cells regulate synaptic activity through neurotransmitter uptake, such as glutamate via GLAST, which is responsible for 50% of glutamate transport in the retina (Sarthy et al., 2005). Glutamate uptake by Müller cells is important to prevent the neurotoxic effects of glutamate as shown by experimentally blocking glutamate transporters in the retina causing neuronal degeneration, even when low concentrations of glutamate were administered (Izumi et al., 2002). Glutamate uptake by Müller glia is also used to make glutamine via the glia specific enzyme glutamine synthetase. This glutamine is then transported from the Müller cells into retinal neurons to be used as precursors for neurotransmitter production (Pow and Crook, 1996). Furthermore, glutamate can be converted into the antioxidant glutathione and released from Müller cells to provide protection for the photoreceptors, which experience high levels of oxidative stress due to light exposure (Schütte and Werner, 1998).

Müller glia can adapt their morphology either when neurons are activated and change their cell body and synapse size or when the vitreous shrinks with age and increases tractional forces onto the Müller cells. This adaptability is due to the viscoelastic properties of Müller cells, which makes them twice as flexible as neurons. This can be seen by electron microscopy images of Müller cell somata indented by smoothly rounded bipolar cell somata (Lu et al., 2006). By surrounding neurons in this way Müller cells facilitate neuronal plasticity during development and in the mature retina, as well as offering protection from mechanical trauma.

Müller glial cells are also important in supporting photoreceptor function and viability. Müller cells can act as optical fibres. The endfeet cover the entire inner retinal surface and have a low refractive index, which allows for efficient light entry which is then guided through the retina, helped by the Müller cell’s funnel shape and parallel arrangement, to the photoreceptor cells, which improves the

image seen (Franze et al., 2007). Moreover, Müller glial cells produce chromophores, the most common in vertebrate retina being 11-*cis* retinal, needed by cone cells for the visual cycle, during which bleached pigment is recycled into new photopigment (Wang and Kefalov, 2011). Conditional ablation of Müller cells causes photoreceptor damage and apoptosis, as well as disruption of the retinal histology and function (Shen et al., 2012). Retinal neurons depend on Müller glia, therefore selectively killing Müller cells leads to secondary photoreceptor death (Dubois-Dauphin et al., 1999).

In addition, Müller glia are known to be active in the formation and maintenance of the blood-retina barrier (Tout et al., 1993). For example, Müller glia can release the glial cell line-derived neurotrophic factor (GDNF) to enhance the barrier function of endothelial cells in retinal blood vessels (Igarashi et al., 2000). The blood-retina barrier can also be broken down with the loss of Müller cells, as shown by increased retinal vascular permeability when Müller cells are ablated (Shen et al., 2010). Many of these features are found in retinal degeneration indicating a role of Müller glia dysfunction in retinal disease.

1.5 Müller glia in disease

1.5.1 Protecting the retina

During disease states Müller cells provide protection to retinal neurons by, among others, taking up excess neurotoxic glutamate and releasing protective antioxidants (Bringmann et al., 2009). Hypertrophied Müller cells can support neuronal outgrowths and synaptic remodelling to aid regeneration (Sethi et al., 2005). Additionally, activated Müller glia release neurotrophic factors, growth factors and cytokines, which encourage survival of retinal neurons (Bringmann et al., 2006). Basic fibroblast growth factor (bFGF), brain-derived neurotrophic factor (BDNF), ciliary neurotrophic factor (CNTF), interleukin 1 (IL-1), neurotrophin-3 (NT-3), insulin-like growth factor-1 (IGF-1) and glial cell line-derived neurotrophic factor (GDNF) are amongst some of the factors known to rescue photoreceptors in retinal degeneration models (LaVail et al., 1992) (Frasson et al., 1999). These factors can have direct effects on the neurons by acting on specific receptors, such as bFGF increasing photoreceptor survival *in vitro* by activation of FGF receptors found on photoreceptor cells (Fontaine et al., 1998). However, *in vivo* studies have shown that intravitreal injection of

neurotrophins cause activation of intracellular signalling pathways in Müller cells but not in photoreceptors (Wahlin et al., 2000).

Neurotrophins act on two different receptors to control neuronal survival, Trk receptor tyrosine kinases (TrkA, TrkB, TrkC) and p75 neurotrophin receptor ($p75^{NTR}$), which are both upregulated in Müller glia during photoreceptor degeneration (Harada et al., 2000). Binding of neurotrophins to Trk receptor initiates cell survival and differentiation signals whereas $p75^{NTR}$ binding activates cell death signals (Casaccia-Bonnefil et al., 1999). Specifically, inhibiting Trk receptor *in vivo* decreased production of bFGF and subsequently increased cell death in the retina, while inhibiting $p75^{NTR}$ increased retinal bFGF and decreased cell apoptosis (Harada et al., 2000). Likewise, *in vitro* production and secretion of bFGF by Müller cells was increased by $p75^{NTR}$ inhibition and decreased by Trk inhibition (Harada et al., 2000). This suggests that neurotrophins that are released from Müller glia themselves can act in an autocrine manner to further increase neurotrophin release from Müller glia. Müller glia activation by neurotrophic factors also causes release of pro-survival factors that enhance neuronal survival during retinal degeneration.

1.5.2 Gliosis and retinal degeneration

Activation of glial cells in the central nervous system (CNS) is known as reactive gliosis. Gliosis is not a simple response but is seen as a spectrum of characteristic changes which range from reversible alterations in gene expression, cell morphology and biochemical and physiological properties, to permanent tissue reorganisation (Reichenbach and Bringmann, 2010, Sofroniew, 2015b). Müller glial cells become activated during all pathological stimuli (Bringmann and Reichenbach, 2001) and gliosis is characterised by three unspecific responses, which are independent of the type of stimuli: cellular hypertrophy, proliferation (Fisher et al., 1991) and increase in the intermediate filaments (IFs) nestin, vimentin and GFAP (Reichenbach and Bringmann, 2010). As a first response, acute gliosis is a beneficial reaction in disease. Gliosis initially acts to limit further damage, restrict inflammation and provide neuroprotection. However, chronic gliosis is detrimental, causing direct or indirect harm to retinal neurons and inhibiting repair. Reactive gliosis is prominent in degenerative diseases such glaucoma, AMD and diabetic retinopathy (Wu et al., 2003, Rungger-Brandle et al., 2000, Graf et al., 1993).

This destructive gliosis often occurs due to expression of the acute-phase proteins at high concentrations for prolonged periods (Coorey et al., 2012). Müller cells attempt to limit damage to the retina but in doing so can actually hinder repair (Bringmann et al., 2009). After *in vivo* retinal detachment followed by reattachment, which mimics human conditions where surgical reattachment is used, attempts at photoreceptor regeneration varies widely between adjacent areas of the same retina and recovery is always poor in areas beneath gliotic regions (Anderson et al., 1986). Therefore, gliosis is associated with both protective and degenerative properties and it is important to define which components are detrimental to neuronal survival.

Müller cell gliosis leads to cellular alterations which can contribute to neurodegeneration and the more severe the damage to the retina the higher the degree of these alterations. During early stages of gliosis, any normal supportive functions of Müller cells are impaired and neurons are more vulnerable to pathological stimuli. For example, after photoreceptor degeneration Müller cells reduce glutamine synthetase and subsequently there is a decrease in glutamate uptake and thus neurons are exposed to glutamate toxicity (Lieth et al., 1998). In addition, reactive Müller cells can have direct or indirect cytotoxic effects. In stressed conditions Müller glia produce pro-inflammatory cytokines such as tumour necrosis factor-α (TNF-α) and excessive nitric oxide synthase (NOS), which can directly cause apoptosis of retinal neurons (Tezel and Wax, 2000). *In vivo* damage to Müller glia causes upregulation of GFAP and cell proliferation leading to disorganisation of retinal layers and increase in invading inflammatory cells (Byrne et al., 2013). The increased release of chemokines such as monocyte chemoattractant protein 1 (MCP-1) by Müller glia indirectly causes photoreceptor apoptosis by attracting and increasing the number of macrophages and microglia in the retina (Nakazawa et al., 2007a, Nakazawa et al., 2006a). However, Müller glia are one but not the only source of elevated expression of inflammatory and immune related cytokines in the retina during injury, as local immune responsive cells can also contribute to Müller cell activation (Hollborn et al., 2008). It has also been suggested that Müller cells with a high degree of gliosis can induce gliotic changes in neighbouring cells and therefore gliosis spreads. Consequently, degeneration of initially unharmed retinal tissue occurs (Francke et al., 2005).

1.5.3 The glial scar

Reactive Müller cells form a glial scar, which is new fibrotic-like tissue generated in place of degenerated photoreceptors, neurons, RPE cells and blood vessels (Reichenbach and Bringmann, 2010). The glial scar is formed as reactive Müller glial cells proliferate and migrate through the ONL to the subretinal space (Burke and Smith, 1981, Fan et al., 1996, Lewis and Fisher, 2000). Hypertrophied Müller cell cytoplasmic processes accumulate around the cell bodies and inner segments of degenerated photoreceptors, which completely inhibits the ability of photoreceptor cells to regenerate their outer segments (Lewis and Fisher, 2000). Moreover, these processes also fill the gaps between the photoreceptors' retracted and degenerated synapses and other interneurons, preventing any reconnections from being established (Erickson et al., 1983). The proliferating Müller cells, which have highly increased IF content, form a fibrotic sheet of multiple layers of cell bodies and processes in the subretinal space (Erickson et al., 1983). In addition, gliotic Müller cells exhibit increased stiffness which correlates with increased density of IFs (Lu et al., 2011). The stiff Müller glial cells create a physical barrier, aided by the production of extracellular matrix proteins, which obstruct neuron regeneration. This has been suggested because neurite branching is directly affected by the biomechanical properties of their surrounding environment as they can grow more branches on softer substrates (Flanagan et al., 2002).

This all leads to the assumption that controlling Müller cell gliosis and glial scarring may be therapeutically beneficial (Fisher and Lewis, 2003). However, in the CNS astrogliosis and scar formation serves as a functional barrier to neurotoxic inflammation (Sofroniew, 2015b). In this way, astrocytes can regulate CNS inflammation which can affect outcome after neurodegenerative disease (Sofroniew, 2015a). *In vivo* knockout of scar forming astrocytes in spinal cord injury models lead to increased infiltration of leukocytes, increased neuronal loss and impaired recovery in the CNS (Faulkner et al., 2004). Although inflammatory responses are beneficial during injury to restore tissue homeostasis, uncontrolled inflammation in the retina is detrimental and can worsen disease (Xu et al., 2009). Therefore, the glial scar can actually protect the retina from invading inflammatory cells. Consequently, understanding the basic and fundamental physiology of the Müller glial cell under normal and disease conditions is essential.

1.6 Inflammatory cytokines involved in gliosis

The retina is considered to be an immune privileged site and is therefore very sensitive to inflammation. The inflammatory immune response causes non-specific tissue destruction, leading to gliosis and consequently to retinal neurodegeneration. Inflammatory cytokines, such as IL-6 and TNF-α have been found elevated in the vitreous from patients with diabetic retinopathy (Franks et al., 1992, Limb et al., 1996) as well as in cells invading the retina during proliferative vitreoretinopathy (PVR) (Limb et al., 1994b, Limb et al., 1994a). PVR is considered an undesired wound healing response to retinal detachment caused by upregulation of inflammatory factors such as TNF-α, IL-6, VEGF and TGF-β amongst others (Eastlake et al., 2016). TGF-β has been thought to play a key role in PVR because treatment with a TGF-β inhibitor can prevent epiretinal membrane formation in an *in vivo* rabbit model of PVR (Nassar et al., 2014). There is also evidence of altered cytokine production and inflammation in AMD (Muether et al., 2013) whilst in glaucoma there is upregulation of proteins involved in the innate immune response which lead to cytokine production and inflammation (Luo et al., 2010) (Yang et al., 2011). Additionally, increased levels of TNF-α and IL-6 in the aqueous humor of patients with glaucoma, correlate to the severity of visual field loss (Ghanem AA, 2010). In a mouse model of glaucoma causing raised intraocular pressure (IOP) and ageing, significantly increased IL-6 production is observed in the whole retina, although IL-6 receptor expression is only increased in retinal ganglion cells (RGC) (Sims et al., 2012). Elevated levels of all three TGF-β isoforms have also been observed in the aqueous humor of patients with glaucoma (Prendes et al., 2013) and TGF-β2 is increased in human optic nerve heads with glaucoma and in samples of gliotic retina (Pena et al., 1999b, Eastlake et al., 2016). When the TGF-β1 gene is overexpressed in the anterior segment of the rat eye, IOP is raised as a result of altered trabecular meshwork morphology, leading to glaucoma (Robertson et al., 2010). This suggests that TGF-β contributes to the clinical damage seen in the optic nerve in glaucoma.

Studies have shown that many cell types in the retina are involved in mediating the inflammatory response, both producing and reacting to inflammatory cytokines including the retinal pigment epithelium (RPE), microglia and Müller glia (Holtkamp et al., 2001, Langmann, 2007, Bringmann et al., 2006). The

response of Müller glial cells to inflammatory cytokines plays a major role in reactive gliosis in the human retina during disease. Human Müller glial cells have been shown to produce IL-6 (Yoshida et al., 2001) and in retinal degeneration and injury models, CNTF, a member of the IL-6 family of cytokines, is markedly upregulated in the retina, localised to the Müller glia (Wen et al., 1995, Walsh et al., 2001). This increase in CNTF also correlated to increase in the glial marker GFAP, suggesting a role of CNTF in reactive gliosis. When CNTF is injected into mouse eyes, Müller glial cells show increased expression of genes associated with immune and inflammatory responses (Xue et al., 2011). Müller cells exposed to CNTF also increased production of cytokines such as TNF-α and TGF-β, suggesting a role of Müller glia in creating a destructive inflammatory environment in the retina.

Human Müller glial cells express all Toll-like receptors (TLRs), which are pattern recognition receptors able to recognise microbial-associated molecular patterns (MAMPs) from pathogens. Müller glia are activated by TLR ligands and bacterium challenge and downstream signalling results in production of pro-inflammatory cytokines IL-8, IL-6 and TNF-α (Kumar and Shamsuddin, 2012). Pro-inflammatory cytokines have chemotactic activities, specialising in recruiting leukocytes to the damaged area; TNF-α upregulates endothelial adhesion molecules facilitating leukocyte migration into the tissue, initiating the inflammatory cascade and causing tissue damage (Dinarello, 2000). This is further evidence of Müller glia as a source of cytokines and involvement in the immune response, contributing to the aetiology of retinal pathologies (Kumar et al., 2013).

As well as causing damage, these inflammatory cytokines may create an environment which could potentially prevent regeneration of the retina. In the zebrafish retina, which spontaneously regenerates after damage by harnessing the stem cell properties of Müller glial cells, TGF-β signalling needs to be regulated. When the TGF-β corepressors Tgif1 and Six3b are knocked down in zebrafish, Müller glia proliferate less and cone photoreceptor regeneration is decreased (Lenkowski et al., 2013). TGF-β can significantly reduce the proliferation rate of isolated human Müller glial cells *in vitro*, implying that this cytokine could be preventing regeneration (Romo et al., 2011).

Interestingly, cytokines have also been implicated in tissue regeneration. It has been demonstrated that IL-6 plays an important role in regenerative proliferation of liver hepatocytes and intestinal epithelial cells in mice (Scheller et al., 2011). CNTF is also known to influence retinal regeneration. Injection of CNTF into the zebrafish retina induces Müller glia proliferation and is sufficient to generate neuronal progenitors from Müller glial cells (Kassen et al., 2009). As well as inducing regeneration, CNTF is a neuroprotective factor in the retina. In light-damaged zebrafish retina, injection of CNTF can prevent photoreceptor cell death by activation of the MAPK signalling pathway (Kassen et al., 2009). In a mouse photoreceptor degeneration model, lentiviral-mediated expression of CNTF prevented photoreceptor cell death, inhibiting degeneration and improving morphology (Rhee et al., 2013). This suggests a complex role for inflammatory cytokines in retinal gliosis and regeneration.

1.7 Role of intermediate filaments in Müller cell gliosis

Glial cells have abundant amounts of two class III intermediate filament (IF) proteins, GFAP and vimentin, which are both structural constituents of the cellular cytoskeleton. These proteins can form homopolymer filaments or can occur as heteropolymers with each other. Because these proteins are associated with each other it has proven difficult to distinguish and clarify the exact biological function of each in the mammalian retina (Sarthy, 2007). Under normal conditions Müller glia mainly contain vimentin but very low levels of GFAP or none at all, however in the degenerating retina there is an increase in both GFAP and vimentin expression (Okada et al., 1990).

The upregulation of GFAP has become the universal marker of retinal stress and Müller cell gliosis because it is an early and highly sensitive indicator in a variety of retinal injury models and diseases (Figure 1-4) (Dahl, 1979, Bringmann and Reichenbach, 2001, Smith et al., 1997). GFAP increase is due to transcriptional activation of the gene specifically within Müller cells (Sarthy and Fu, 1989) and begins as early as 2 hours after retinal stress such as elevated intraocular pressure in experimental glaucoma (Xue et al., 2006). GFAP is normally seen in Müller cell bodies but after photoreceptor degeneration is found across the entire retina as Müller cells expand and proliferate and in particular, GFAP accumulates in distal processes and the endfoot region (Sarthy and Egal, 1995).

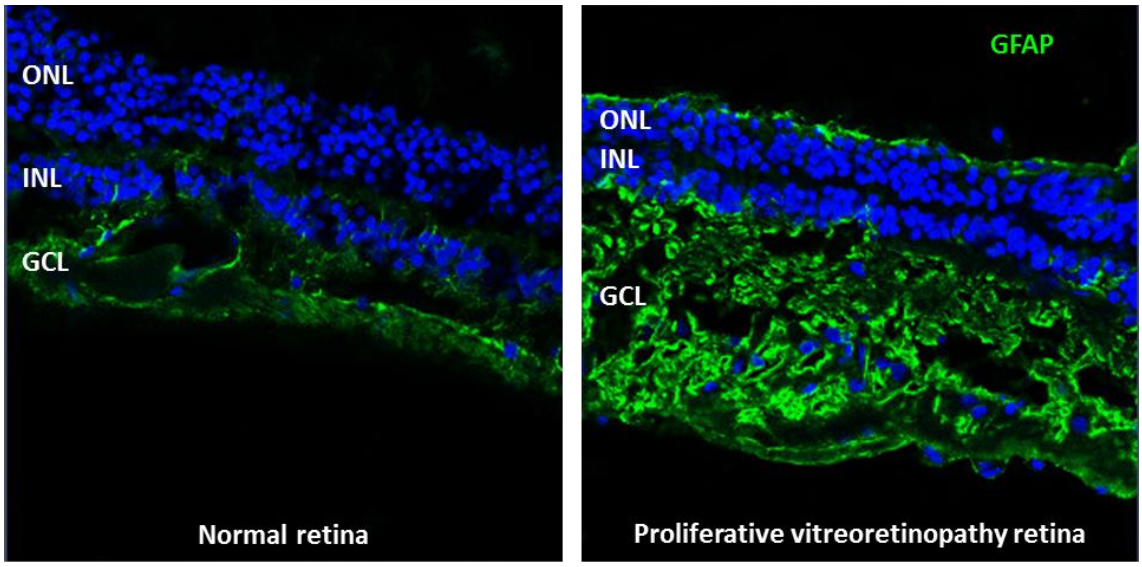

Figure 1-4: Immunocytochemical staining for GFAP (green) of normal human retina from a healthy eye and diseased retina from a patient with proliferative vitreoretinopathy. After injury GFAP is upregulated whilst the INL and ONL layers become thinner.

1.7.1 Upregulation of intermediate filament is crucial for the gliotic response

Without IFs glial cells do not form normal scars after CNS injury, as observed in *GFAP* or/and *vimentin* null mice. Interestingly, *GFAP-/-* or *vimentin-/-* mice have completely normal scar formation after spinal cord or brain injury but *GFAP-/-vimentin-/-* mice have defective glial scars (Pekny et al., 1999). The scar in these animals is less dense, contains more cellular debris and has fissures throughout, which leads to impaired wound healing and disrupted astrocytic function. After CNS injury astrocytes lacking GFAP and vimentin have altered morphology and the characteristic hypertrophy is abolished. Reduced astrocyte hypertrophy in *GFAP-/-vimentin-/-* mice resulted in a greater loss of neuronal synapses, indicating an important function of IFs in acute phases after injury. However, a few days after injury, neuronal synapses were restored in the *GFAP-/-vimentin-/-* mice and there was better regeneration compared to wild-type mice, implicating reactive astrocytes as inhibitors of neuroregeneration (Wilhelmsson et al., 2004). This suggests that there may be a fine balance between IFs role in scarring and regeneration.

In the retinas of *GFAP-/-vimentin-/-* mice Müller glia have impaired homeostatic function (Wunderlich et al., 2015). After retinal detachment, Müller glia of *GFAP-/-vimentin-/-* mice have altered morphology with irregular lateral protrusions and their endfeet become broken away from the rest of the retina (Verardo et al., 2008). These Müller glial cells are less able to withstand mechanical stress of the retina, suggesting an important role for IFs during gliosis. Reactive gliosis is supressed in these Müller glial cells as indicated by reduced signalling pathway activation and chemokine MCP-1 expression (Nakazawa et al., 2007b). These mutant mice have less monocyte recruitment after retinal detachment and reduced photoreceptor cell apoptosis. This strongly suggests that GFAP and vimentin are critical for the reactive Müller glia response to injury and scar formation.

1.8 Endogenous regeneration of the neural retina

Endogenous regeneration refers to the ability to renew tissue and restore function by growing new and healthy cells to replace those lost after degeneration caused by injury or disease. Regeneration is possible in the CNS and the retina of lower vertebrate species and is well characterised in teleost

fish such as the zebrafish. On the other hand, endogenous regeneration in the human retina is non-existent and a scar is formed with loss of tissue function instead of regenerating. However, recent studies, which will be discussed below, have shown that although limited, there is potential for retinal regeneration through Müller glia and this could be exploited to treat human eye diseases. Regeneration of the retina by Müller glia derived progenitors would require neural dedifferentiation and proliferation of these cells, followed by migration into all the retinal layers. In addition, these new neurons should display functional properties (Gallina et al., 2014). Therefore, understanding the regenerative abilities of different species and the inability of humans to regenerate is necessary for the future of retinal regenerative medicine.

1.9 Endogenous regeneration in zebrafish

1.9.1.1 Müller glia as the source of retinal progenitors

It is known that following surgical excision, chemical induced damage or light induced damage in the adult zebrafish retina there is retinal regeneration as cells proliferate and produce a variety of retinal neurons (Brown and Regillo, 2007). Lineage tracing studies have identified Müller glia as the source of progenitor cells needed for retinal regeneration in this species. The first study used transgenic zebrafish that labelled Müller glia with green fluorescent protein (GFP) and found that after stab injury these cells divide and proliferate as seen by bromodeoxyuridine (BrdU) incorporation (Fausett and Goldman, 2006). These Müller glial cells became injury-induced retinal progenitors and expressed the multipotent progenitor marker Pax6 (paired box gene 6). The recently dividing cells derived from Müller glia could migrate to all nuclear cell layers and begin expressing markers for retinal neurons starting with ganglion cells, then photoreceptors, amacrine, bipolar and Müller cells. However, as there were still 6% of BrdU labelled cells that were not Müller glia there is the possibility that there are other stem cells contributing to regeneration.

Similarly, a second study used transgenic zebrafish with a glial-specific promoter for GFAP to drive GFP expression in differentiated Müller glia. After specific retinal injury inducing photoreceptor cell death, Müller glial cells were activated as GFAP expression increased. Müller cells then proliferated and initially expressed Pax6. After downregulating Pax6, the photoreceptor marker Crx was expressed, suggesting that these injury-induced progenitors take on a

photoreceptor lineage to replace the damaged cells (Bernardos et al., 2007). Also, because photoreceptors do not normally express GFAP but these cells did, this indicates that the cells inherited the proteins from the Müller glia. Even though the injury-induced Müller glia are dedifferentiating they still express specific Müller markers indicating that they can still maintain glia characteristics (Lenkowski and Raymond, 2014). However, the third experiment damaged the retinal ganglion cells, which caused transgenic GFP labelled Müller glia to downregulate GFAP and not exhibit reactive gliosis. This suggested that increased GFAP expression in Müller glia before their proliferation is not essential to re-enter the cell cycle (Fimbel et al., 2007).

1.9.2 Müller glia sense injury in the zebrafish

Müller glia undergo reprogramming in response to a variety of insults in order to regenerate the retinal neurons and there are a number of ways that injured cells communicate with Müller glia to relay this information (Goldman, 2014). This includes secretion of signalling molecules from the damaged cells, Müller glia or infiltrating microglia. The expression of TNF-α is increased in the damaged retina, which is caused by initial increased secretion from dying photoreceptors and then by Müller glia when proliferation begins. This TNF-α secretion by dying cells is required to induce Müller glia to re-enter the cell cycle and is necessary for maximal proliferation of Müller glia, whereas TNF-α secretion by Müller glia themselves is needed to amplify the number of proliferating Müller glia (Nelson et al., 2013). However, TNF-α knockdown does not completely stop regeneration as *tnf-α* mutants still regenerated photoreceptors, albeit at a much slower rate. This could be due to other cells releasing TNF-α or an alternative delayed signal. Another secreted factor which affects Müller glia during injury is heparin-binding epidermal-like growth factor (HB-EGF). HB-EGF works in an autocrine manner as it is released by Müller glia and induces Müller glia to dedifferentiate into multipotent progenitors and stimulates proliferation (Wan et al., 2012).

Likewise, the IL-6 family of cytokines can potentially act in an autocrine and paracrine way because cytokine expression is usually increased in response to injury and numerous IL-6 family member genes are upregulated in injury-induced Müller glia-derived progenitors. Knocking down the IL-6 receptor signal transduction component Gp130, prevented expression of injury-induced *ascl1a*

(achaete-scute complex-like 1a) and reduced proliferation of Müller glia (Zhao et al., 2014). Ascl1a is a transcription factor vital for inducing Müller glia to actively divide into retinal progenitors during regeneration (Fausett et al., 2008). This suggests that Müller glia respond to the IL-6 family of cytokines, which can mediate reprogramming and proliferation.

An additional mechanism that may activate Müller glia following injury is phagocytosis of apoptotic photoreceptor cell debris. Indeed, inhibition of phagocytosis reduced the number of proliferating Müller glia and although there was regeneration, the number of cone photoreceptor cells was significantly reduced (Bailey et al., 2010). It is also thought that altered contact between Müller glia and damaged neighbouring cells may alter signalling by Notch, which works via cell-to-cell contact (Goldman, 2014). However, this has not been yet tested

1.9.2.1 Activation of signalling pathways in Müller glia from the zebrafish

There are many signalling cascades and pathways involved in retinal regeneration in the zebrafish. These signalling pathways alter gene expression needed for Müller glia cell reprogramming. Reprogramming is when the Müller glia genome acquires retinal stem cell properties in order to produce a proliferating population of progenitor cells.

HB-EGF mediates Müller glia dedifferentiation through activation of the MAPK-ERK signalling pathway by acting on the EGF-R (Wan et al., 2012). Knockdown of HB-EGF prevents gene expression of Pax6 and Ascl1a, indicating that HB-EGF acts upstream of Ascl1a and Pax6. Similarly, increased TNF-α signalling is also required for the injury-induced expression of Ascl1a and Stat3 (Nelson et al., 2013). Stat3 expression is activated by Ascl1 and is only required for proliferation by a subset of Müller glia (Nelson et al., 2012).

Another signalling cascade crucial for Müller glia reprograming is the canonical Wnt pathway. There is induction and suppression of a number of Wnt pathway genes in injury-induce Müller glia-derived progenitor cells (Ramachandran et al., 2011). The expression of *dkk1b*, which is a Wnt signalling antagonist, declines after injury, whereas *ascl1a* expression increases in a mutually exclusive fashion. Therefore, *ascl1a* can suppress *dkk* expression, which allows activation of Wnt signalling. Further evidence that there is activation of Wnt signalling in

the injured retina comes from increased expression of nuclear β-catenin, which is only translocated to the nucleus when the Wnt signalling pathway is activated. β-catenin is a protein that, once in the nucleus, acts as a coactivator of transcription factors of the T cell factor (Tcf) and lymphoid enhancer-binding factor (Lef) family members. Therefore, injury-induced stabilisation of β-catenin is necessary for progenitor proliferation and retinal regeneration (Ramachandran et al., 2011). Moreover, inhibiting Wnt signalling prevents Müller glia re-entering the cell cycle following photoreceptor loss (Meyers et al., 2012).

An alternative pathway that can be activated to induce Müller cell reprogramming is the Jak/Stat (Janus kinase-Signal transducer and activator of transcription) signalling. Injecting CNTF, a member of the IL-6 family of cytokines, into undamaged zebrafish retina can promote Müller glia proliferation and generation of progenitor cells (Kassen et al., 2009) but requires Stat3 expression. Indeed, Stat3 expression is increased in all Müller glia after injury and knockdown of Stat3 produces fewer proliferating Müller glia (Kassen et al., 2007). Moreover, Zhao et al were able to locate activated Stat3 in the Müller glia-derived progenitors at the site of injury and inhibition of Jak/Stat signalling suppressed progenitor formation (Zhao et al., 2014). Furthermore, Jak/Stat inhibition prevented injury-induced expression of *ascl1a* as two Stat3 binding sites were identified in the *ascl1a* promoter. Therefore, Jak/Stat3 signalling is required for Müller glia gene expression reprogramming and re-entry into the cell cycle.

1.9.2.2 Factors antagonising Müller glia proliferative response in the zebrafish

As well as factors that stimulate Müller glia reprogramming there are factors that promote cell differentiation and quiescence during retinal regeneration. TGF-β and its signalling pathway are one of these factors because expression of the TGF-β corepressors Tgif1 and Six3b is upregulated in Müller glia-derived progenitors following retina injury (Lenkowski et al., 2013). The *tgif1-/-* zebrafish have a normal number of Müller glial cells but higher expression of GFAP in these cells suggesting that they are in a state of gliosis. After photoreceptor destruction there is significantly decreased proliferating Müller glia-derived progenitors and photoreceptor regeneration in *tgif1-/-;six3b-/-* fish. This

suggests that regulation of TGF-β through the inhibitors Tgif1 and Six3b is needed for retinal regeneration. Moreover, during regeneration in *tgif1-/-* fish, there are significantly higher levels of Smad2/3 target genes, such as *ascl1a*, indicating that in normal zebrafish retina Tgif1 acts by downregulating Smad2/3-mediated TGF-β signalling in response to injury in order for Müller glia to proliferate and form progenitors.

Unlike the TGF-β inhibitory pathway, which is downregulated after injury, the inhibitory Notch pathway is activated as Notch signalling components and target genes are upregulated after injury (Raymond et al., 2006). This Notch activity has been demonstrated to be targeted to Müller glia-derived progenitor cells at the site of injury (Wan et al., 2012). Inhibition of Notch signalling significantly increased the number of dedifferentiating and proliferating progenitors and expanded the area that these cells covered in the injured retina, whereas overexpression of Notch signalling reduced the number of proliferating cells. Additionally, injury-induced expression of *ascl1a* was stimulated by Notch inhibition whilst overexpression of Notch signalling supressed *ascl1a* expression. Interestingly, Notch inhibition in the uninjured retina does not cause proliferation or dedifferentiation of Müller glia which indicates that Notch is activated by an injury-induced signalling pathway to ensure the number of Müller glia recruited is appropriate to the severity of the injury.

1.10 Partial retinal regeneration in the postnatal chick

The postnatal chick retina is capable of regeneration after retinal injury by proliferation of Müller glia, however adult birds do not respond to injury. Following chemical induced damage by N-methyl-D-aspartate (NMDA), which selectively kills amacrine and bipolar cells in the retina, Müller glia re-enter the cell cycle and proliferate into retinal progenitor cells expressing Pax6 and Chx10 (Fischer and Reh, 2001). *In vivo* a small number of these cells differentiate into retinal neurons expressing markers for amacrine and bipolar cells but not photoreceptor cells or ganglion cells. Similarly, when retinas are treated with kainite or colchicine, which destroys ganglion cells, new cells proliferated and differentiated specifically into ganglion cells (Fischer and Reh, 2002). This suggests that, like the fish, Müller glia are the source of retinal progenitor cells required for regeneration in the chicken and the regeneration of the certain cell type depends on which cells have been injured. However, even

though some retinal progenitor cells differentiate into neurons or Müller glia that express glutamine synthetase, the majority remain as undifferentiated progenitors. This implies that potentially the progenitor cells lack intrinsic factors required for differentiation or/and that the mature retinal environment lacks the appropriate signals needed for differentiation of the progenitors (Fischer, 2005).

To investigate the signals needed for Müller glia reprogramming Fischer et al (2002) injected growth factors into postnatal chick eyes. They found that a combination of insulin and FGF-2 at a sustained dose induced a wave of proliferating Müller glia starting from the peripheral of the retina towards the central regions, in a time dependent manner (Fischer et al., 2002). These proliferating Müller cells gave rise to progenitor cells expressing Pax6 and Chx10, but only a few cells (~4%) went on to express neuronal markers and some (~24%) formed new Müller glia, whilst most of the cells remained in the progenitor-like state. There were no molecular differences in the Müller glia to account for the differences in their ability to proliferate but it has been noted that those Müller glia with increased expression of GFAP after injury do not re-enter the cell cycle, whilst those that do not increase GFAP take up BrdU (Fischer and Reh, 2003).

The Mitogen-activated protein kinase (MAPK) signalling pathway is involved in chick retina regeneration because insulin and FGF bind to receptor tyrosine kinases which activate the MAPK-pathway. After NMDA induced retinal damage, phosphorylated ERK1/2 (pERK1/2) and phospho-CyclicAMP Response Element Binding-protein (pCREB), which are phosphorylated due to signalling activation, significantly increase in proliferating Müller glia. In addition, gene expression of Egr1 is enhanced, which is downstream of MAPK signalling (Fischer et al., 2009). Inhibition of MAPK-signalling and blocking FGF receptor causes suppression of Müller glia proliferation after injury and reduces expression of pERK, pCREB and Erg1. This indicates that MAPK-signalling is required for Müller glia-derived progenitor proliferation, which acts through activation of both FGF receptor and ERK1/2-pathway.

Similar to regeneration in the fish, some components of the Notch signalling pathway (Notch1 and Hes 5) are upregulated in proliferating Müller glia following retinal injury in the postnatal chick. The inhibition of Notch signalling at day 2 after NMDA treatment by DAPT, which is an inhibitor of γ-secretase,

supressed the upregulation of Notch1 and Hes5 and decreased the number of proliferating cells (Hayes et al., 2007). This suggests that Notch signalling is necessary for Müller glia to re-enter the cell cycle and early inhibition of Notch prevents Müller glia dedifferentiation and progenitor formation. However, treatment with DAPT at day 4 post injury caused an increase in newly generated neurons. This indicates that blocking Notch signalling after Müller glia have generated progenitors causes neuronal differentiation. However, these neurons do not persist in the retina. These observations propose two phases of Notch signalling; an initial increased expression leading to dedifferentiation of Müller glia into progenitor cells and sustained Notch activity inhibiting differentiation of these progenitors into neurons which impedes regeneration of the retina (Hayes et al., 2007).

1.11 Limited regeneration of the mammalian retina

1.11.1 Rodent retinal regeneration

It was believed that the mammalian retina did not contain retinal stem cells and thus did not have the ability to regenerate following injury. However, pigmented cells from the ciliary margin of the adult rodent retina were shown to proliferate into a neurosphere colony, indicating that these cells have the capacity to self-renew (Tropepe et al., 2000). Although the frequency of neurosphere forming cells was very rare (~0.2%) in this study, the cells did express Chx10 and nestin, which are markers of retinal progenitor cells. Additionally, *in vitro* culturing of these sphere colonies with certain exogenous growth factors induced them to express retinal neuronal markers, indicating that these cells are multipotent (Ballios et al., 2012). However, furthering of these studies towards translational medicine have not been yet repeated despite these cells having been identified about 18 years ago.

Similar to the zebrafish and chick, reactive Müller glia increase expression of GFAP after injury in the rodent retina, indicating a gliotic response (Xue et al., 2006). Additionally, there is increased expression of nestin, which is an intermediate filament initially found to be expressed in dividing cells during development in the CNS and so has been used as a marker of neural stem cells (Lendahl et al., 1990). There is also significantly increased expression of nestin by Müller glia during retinal injury, induced by both chemicals and high intraocular pressure (Xue et al., 2006, Chang et al., 2007). Therefore, the

expression of nestin by reactive Müller cells in the mature rodent retina suggests a dedifferentiation potential of the cells towards becoming neurogenic progenitor cells and an attempt at regeneration (Chang et al., 2007).

Indeed, *in vivo* the Müller glial cells in the rodent retina are endogenous progenitors, much like in the zebrafish and chick. Following NMDA injection Müller glia proliferate and can differentiate into neurons because a small proportion of cells incorporating BrdU expressed specific markers for bipolar cells and rod photoreceptors (Ooto et al., 2004). Injection of exogenous growth factors, such as retinoic acid, EGF and FGF plus insulin, at the same time as injury induces differentiation into retinal neurons more effectively, indicating that the mammalian retina has the potential for regeneration but unknown extrinsic cues partially control this (Ooto et al., 2004, Karl et al., 2008).

In vitro culturing of rodent Müller glial cells with exogenous growth factors, such as FGF-2, induces proliferation of neurospheres and expression of neural stem cell markers Notch1, Sox2 and nestin (Das et al., 2006). These primary neurospheres are self-renewing as they could produce secondary neurospheres with multipotent ability as they expressed neuronal and glial markers. Moreover, when these proliferating Müller glial cells were co-cultured with embryonic chick retinal cells, which have retinal ganglion cell inducing activity, or rat retinal cells, which can induce later born retinal neurons, they were able to differentiate into retinal ganglion cells and bipolar and rod photoreceptor cells, respectively.

One of the factors that Müller glial cells use to proliferate in the rodent retina is the Notch signalling pathway. After NMDA injury and EGF injection to induce proliferation of Müller glia, gene expression of *Notch1*, and one of its ligands, *Delta1*, are significantly upregulated in the mouse retina (Karl et al., 2008). There is also increased expression of Notch and Wnt pathway genes in neurotoxin-injured rodent retinas (Das et al., 2006). In mouse retinal explants, Notch activation increased the number of proliferating Müller glial cells expressing neural progenitor markers (Del Debbio et al., 2010). When Wnt2b, which induces Wnt signalling, was injected with neurotoxins there were more proliferating Müller glia, and when Notch signalling was inhibited by DAPT there was a decrease in Pax6 and Sox2 expression (Das et al., 2006). Similarly, when injured retinal explants were cultured with Wnt3a there was increased proliferation of Müller glia as well as the number of retinal progenitors derived

from Müller glia (Osakada et al., 2007). This suggests that Wnt and Notch signalling are involved in injury-induced activation of the stem cell properties of Müller glia *ex vivo* and *in vivo*.

Another signalling pathway that mammalian Müller glia may utilise that the bird and fish do not is the Sonic hedgehog (Shh) pathway. Shh is a signalling molecule that regulates progenitor cell proliferation in the adult CNS (Machold et al., 2003) and *in vitro* can induce the proliferation of retinal progenitor cells (Levine et al., 1997). Treating Müller glia *in vitro* with Shh significantly increases proliferation, and inhibition of Shh by cyclopamine reduces Müller glia proliferation (Wan et al., 2007). Additionally, culture with exogenous Shh induced expression of Pax6, Sox2 and nestin, indicating that Müller glia differentiate into progenitor cells. After further days in culture without Shh, these cells expressed Nrl, Crx and rhodopsin, which are found in rod photoreceptors, suggesting Müller glia-derived progenitors have neurogenic potential. *In vivo*, after chemical induced injury, Shh injection can stimulate Müller glia to proliferate and form retinal progenitor cells but only a few Müller glia-derived cells expressed markers for rhodopsin but no other neuronal markers. Therefore, Müller glial cells have the possible ability to act as stem cells in the mammalian retina, which is enhanced by Shh.

It has also been proposed that regeneration in mammals is age dependent because in mouse retinal explants post damage and mitogen stimulation, Müller glial cell cycle re-entry and proliferation significantly declined with increasing mouse age (Löffler et al., 2015). It could be that regeneration is more likely when Müller glia are young in the developmental progenitor stage and that reactive gliosis in adult mammals may be a mis-regulated or incomplete regenerative program.

1.11.2 Human retinal regeneration

In the human foetal retina, neural progenitor cells express nestin along with CRALBP, suggesting that Müller glia and progenitor cells are the same class during development (Walcott and Provis, 2003). In the adult human eye, expression of nestin is co-localised with the Müller glia markers vimentin, CRALBP and GFAP mainly in the anterior neural retina and not the ciliary margin like the neural stem cells found in other species (Bhatia et al., 2009). A small subpopulation of these Müller glial cells expressing nestin also expressed

Chx10 and Sox2, indicating that there are Müller glial cells that express neural progenitor markers *in situ*. These cells can be isolated from human neural retina and become spontaneously immortalised. A cell line derived from the adult human retina and named Moorfields/Institute of Ophthalmology–Müller 1 (MIO-M1) has been thoroughly characterised (Limb et al., 2002). In the presence of foetal calf serum (FCS) these cells can grow to a confluent monolayer *in vitro* and exhibit a characteristic Müller cell morphology. This cell line is morphologically identical to a primary Müller cell culture, as characterised by scanning and transmission electron microscopy and expression of Müller glial cell markers vimentin, CRALBP and glutamine synthetase (Limb et al., 2002). Because these cells became spontaneously immortalised, which is a main property of stem cells, it was further investigated if these cells had stem cell potential. Indeed, *in vitro* these cells express retinal stem cell markers Sox2, Pax6, Chx10, and Notch 1 (Lawrence et al., 2007). When cultured on extracellular matrix proteins with neurogenic factors FGF or retinoic acid, between 10 to 20% of individual Müller cells formed neurospheres, expressed nestin and acquired neural morphology. Further culturing with FGF or retinoic acid differentiated the cells into mature retinal neurons as there was increased expression of the ganglion cell marker HuD, the bipolar cell marker PKC and the photoreceptor marker peripherin whilst showing a significant decrease in the Müller glia marker CRALBP. Cells cultured without growth factors maintained expression of Sox2 but only a very small proportion expressed makers of retinal neurons (Lawrence et al., 2007). This indicates that *in vitro* human Müller glial cells are sources of retinal progenitors but certain extracellular matrix proteins and growth factors are required to promote their neural differentiation. However, there is no evidence of neural differentiation in the human retina *in vivo* where instead, Müller glial cells cause gliosis. When these differentiated cells are transplanted into rodent retinal degeneration models, integration does not occur, indicating that these cells may need developmental cues to survive.

When these same cells were differentiated *in vitro* into retinal ganglion cell precursors and then transplanted into rats depleted of retinal ganglion cells they migrated into the GCL and formed synapses with host cells but did not extend axons into the optic nerve (Singhal et al., 2012). In addition, the transplanted cells partially restored retinal ganglion cell function. Nonetheless, migration of

the grafted cells had to be promoted by anti-inflammatory immunosuppressant drugs and local extracellular matrix degradation therapy (Singhal et al., 2008).

Although there has been a lot of research into stem cell based therapies in animal models of retinal degeneration there are no therapies available for patients yet. This is mainly due to the barriers encountered with transplantation; major issues that prevent successful transplantation include the host immune response, abnormal extracellular matrix accumulation in retinal degeneration, glial scarring, and possibly the developmental age of the transplanted cells (Jayaram et al., 2011, MacLaren et al., 2006). If we can find a method to promote the host's Müller glia to self-repair and control reactive gliosis with chemical compounds rather than transplant, it would be a much-preferred option. Therefore, promoting endogenous regeneration of the retina may be a better treatment to restore vision.

1.12 Objectives of this thesis

Current knowledge indicates that Müller glial cells can regenerate the zebrafish retina throughout life and that the human retina harbours Müller glia that exhibit stem cell characteristics *in vitro*. However, human retina does not have the ability to regenerate *in vivo*, but upon injury or disease, the main feature that characterises retinal degeneration is Müller cell gliosis. It has been hypothesised that gliosis may prevent regeneration, therefore the present research aimed to investigate some aspects of the proliferative and neurogenic ability of Müller glia upon induction of gliotic features *in vitro*. The objectives of this thesis were:

1. To investigate the role that inflammatory cytokines may play in regulating Müller cell gliosis-associated proteins and the implications that this could have on the neurogenic ability of Müller glia *in vitro*.
2. To investigate how TNF-α signalling and downstream activation of the transcription factor NFκB regulates GFAP expression in Müller cells *in vitro*.
3. To investigate *in vitro* methods to overexpress GFAP in Müller glial cells and to study the effects that this intermediate filament has on Müller cell proliferation, viability and rod photoreceptor precursor differentiation *in vitro*.

4. To examine how overexpression of GFAP in Müller glia may be regulated by TNF-α and the implications for the neurogenic ability of these cells *in vitro.*

Chapter 2 Effect of inflammatory cytokines on expression of gliosis-associated proteins and on the differentiation of the Müller glial cell line MIO-M1 into rod photoreceptor precursors

2.1 Introduction

Proteomic studies using animal models of retinal diseases have identified various upregulated proteins associated with gliosis. An *in vivo* ischemic retinopathy model revealed that several protein markers of Müller cell gliosis were upregulated, including GFAP, vimentin, galectin and tenascin (Kim et al., 2012). A comparative investigation of the proteomic profiles of gliotic and normal human retina and the contribution of Müller glia to these profiles were undertaken in our lab previously. A number of proteins in the retina which were upregulated during gliosis in patients with PVR as compared to healthy normal retina were identified. Of these proteins, five were selected for investigation in this study. They were GFAP, vimentin, galectin, tenascin and procollagen galactosyltransferase. Study of proteins associated with gliosis may provide insight into mechanisms that may be targeted to induce endogenous regeneration of the retina following disease or injury.

2.1.1 Intermediate filament proteins in the gliotic retina

Even though Müller glia provide homeostatic support within the retina, they rapidly react to environment changes caused by injury or cell death. Reactive gliosis is characterised by Müller glia over-production of proteins such as intermediate filaments (IFs) and cell proliferation and hypertrophy, that leads to degeneration of the retina. The most prominent IFs in Müller glia are GFAP and vimentin and increase in expression of these proteins in the retina is a universal hallmark for reactive gliosis (Sarthy, 2007). IFs are components of the cell cytoskeleton, along with actin and microtubules and the term intermediate simply refers to their size (Pekny, 2001). In the normal retina, these IFs are localised to the Müller glia endfeet and they can be independent or co-localise with each other. However, they are present in low amounts (Lewis and Fisher, 2003). In virtually all models studied there is dramatic increase in Müller glia GFAP and vimentin expression when the retina is under stress, such as retinal detachment, PVR, photoreceptor damage and inherited retinal dystrophies

(Dahl, 1979, Erickson et al., 1987, Eisenfeld et al., 1984, Okada et al., 1990, Lewis et al., 1995, Kuo et al., 2012). After trauma and injury, accumulation is rapid, whereas in degenerative disease and ageing it can be gradual (Lewis and Fisher, 2003). However, vimentin also has a role in regeneration because vimentin deficient mice have reduced wound healing *in vivo* and fibroblasts from these animals have impaired migration (Eckes et al., 2000, Eckes et al., 1998, Chernoivanenko et al., 2013). After optic nerve damage in goldfish, vimentin positive glial cells migrate to the injury site to regenerate the nerve axons (Cohen et al., 1994).

2.1.2 Extracellular matrix in the gliotic retina

Within the extracellular matrix, collagen is the most abundant protein in gliotic retina. It normally undergoes significant posttranslational modification by enzymes such as procollagen galactosyltransferase to form collagen fibril bundles. This collagen fibre network is required in normal homeostasis of the extracellular matrix, maintaining structural and functional integrity. Inflammation can modify this network and induce stiff scar formation (Frantz et al., 2010).

Tenascin, another extracellular matrix protein, is expressed in the developing retina and in the adult retina tenascin is produced by retinal neurons such as horizontal and amacrine cells, as well as Müller glia (Siddiqui et al., 2009, Reinhard et al., 2017, Klausmeyer et al., 2007). In the CNS, astrocytes upregulate tenascin production in response to TGF-β1 released from activated macrophages, suggesting a role of tenascin in inflammation (Smith and Hale, 1997). In injury models, tenascin is found highly expressed within the glial scar along with GFAP and this correlates to the reduced ability of axon regeneration *in vivo* and inhibited neurite outgrowth *in vitro* (McKeon et al., 1991). After cerebral stab wound injury in tenascin deficient mice, astrogliosis is delayed and inflammatory cytokines TNF-α and IL-6 expression is increased in astrocytes (Ikeshima-Kataoka et al., 2008). Tenascin, is also highly upregulated in retinal degenerative diseases such as PVR, diabetic retinopathy and glaucoma, where it is associated with reactive gliosis (To et al., 2013, Pena et al., 1999a, Ioachim et al., 2005). Tenascin is implicated in glaucoma disease pathology because *in vivo* models of raised IOP found increased tenascin in damaged optic nerve heads (Johnson et al., 2007). Therefore, tenascin may not only promote gliosis but also modulate cytokine production to inhibit inflammation in the injured brain

(Jakovcevski et al., 2013). Moreover, tenascin is associated with a regulatory role in stem cell environments and glial progenitor cell proliferation in the CNS (Faissner et al., 2017). When Müller glia from tenascin knockout mice were induced to de-differentiate by addition of FGF-2 to the culture medium, there was reduced cell proliferation and impaired production of progenitor cells and newly generated neurons (Besser et al., 2012). This suggests tenascin is an important protein in regulating endogenous regeneration by modulating the responsiveness of retinal progenitor cells and supporting de-differentiation of Müller glia (Reinhard et al., 2015).

2.1.3 Galectins in the gliotic retina

Galectins belong to the family of carbohydrate binding molecules of lectins with affinity for β-galactosides and have both intracellular and extracellular functions, including regulation of cell cycle, apoptosis and proliferation (Camby et al., 2006, Liu et al., 2002). Galectins are involved in pathological fibrosis and scar formation in various tissues, including galectin-1 in the liver and galectin-3 in the lungs, where it induces production of pro-inflammatory cytokines TNF-α and IL-8 by invading macrophages (Nishi et al., 2007, Smetana et al., 2015, Bacigalupo et al., 2013). Galectin-1 is also extensively studied in cancer progression and is known to inhibit the immune response by causing T cell apoptosis, as well as promote tumour angiogenesis and encourage metastasis, contributing to a tumour pro-growth microenvironment (Ito et al., 2012). *In vitro*, galectin-1 can induce astrocyte differentiation and inhibit proliferation whilst promoting production of brain-derived neurotrophic factor (BDNF) (Sasaki et al., 2004). This suggests that galectin-1 has a protective neurotrophic role, which could be harnessed to prevent neuron loss after CNS injury. In the mammalian retina, galectin-1 has a role in mediating retinal adhesion because injection of anti-galectin-1-antibody causes retinal detachment (Uehara et al., 2001). Galectins are also implicated in gliosis as they are found in human PVR samples and the trabecular meshwork of patients with glaucoma (Alge et al., 2006, Fautsch et al., 2003).

2.1.4 Gliosis versus endogenous regeneration

In light-damaged zebrafish retina, Müller glia re-enter the cell cycle to produce neural progenitor cells, which proliferate and migrate to the INL to differentiate into photoreceptors. Interestingly the pro-inflammatory cytokines implicated in

human disease can play a part in endogenous regeneration in zebrafish. When CNTF is injected into this model, Müller glia proliferation and production of neural progenitor cells is inhibited, likely a consequence of reduced photoreceptor degeneration, suggesting that Müller glia respond to this cell death signal in the zebrafish retina (Kassen et al., 2009). Indeed, it has been shown that the release of TNF-α from dying photoreceptors is necessary to promote Müller glia proliferation in this experimental model (Nelson et al., 2013). Additionally, inhibiting Notch signalling after photoreceptor damage, increases the number of proliferating Müller glia that express the dedifferentiation marker Ascl1a (Conner et al., 2014). This expression was enhanced when zebrafish were exposed to TNF-α as well as Notch inhibitor and acted synergistically to stimulate proliferation of neural progenitor cells and commitment of these cells into neural lineage. These observations suggest that it is necessary to have both activation of TNF-α and elimination of the Notch inhibitory signal for maximal regeneration by Müller glial cells in zebrafish. Proteins associated with gliosis in mammalian retina have been shown to be involved in zebrafish regeneration. The zebrafish galectin-like protein Drgal1-L2, is expressed by proliferating Müller glia after light-induced photoreceptor damage and knock-down of this protein decreases rod photoreceptor regeneration (Craig et al., 2010). Supporting these observations, Eastlake et al found that mRNA and protein expression of galectin increased in the Ouabain damaged zebrafish retina preceding regeneration (Eastlake et al., 2017). This indicates that galectin has a regulatory role during Müller glia regeneration in zebrafish.

The retina of the postnatal chick has potential to regenerate because induced damage causes Müller glia to re-enter the cell cycle but only a small number of these cells differentiate into neurons. Most cells remain as progenitor-like cells that could be harnessed to stimulate endogenous regeneration (Fischer and Bongini, 2010). The regenerative capacity of Müller glia in the chick retina changes with age as Müller glial cells of younger animals can proliferate in the central retina, whilst older animals only have residual activity in the peripheral retina (Fischer and Reh, 2003). It may be that in the chick, Müller glia can only undergo dedifferentiation for a limited period. Additionally, it was observed that Müller glia that upregulate GFAP in response to retinal damage do not re-enter the cell cycle, which may explain the heterogeneity of these cells in the avian

retina. Injection of insulin and FGF-2 into undamaged chick retinas depleted of microglia have fewer Müller glia progenitor cells, suggesting reactive microglia may be necessary for regeneration in the avian retina (Fischer et al., 2014). This evidence indicates that a pro-inflammatory environment may provide signals for endogenous regeneration.

It is possible that the local retinal environment in the mammalian retina plays a significant role in preventing Müller glia from regenerating neurons. Reactive mouse microglia co-cultured *in vitro* with mouse Müller glia induced production of inflammatory cytokines such as IL-6 by Müller cells, which resulted in activation of other microglia (Wang et al., 2011). It is possible that this early response to injury serves to spread the inflammatory response across all layers of the retina and create an environment that prevents regeneration. Mammalian retinae have been shown to have regenerative potential *in vitro*. Extracted rodent Müller glia grown in the presence of FGF-2 form neurospheres and express neural progenitor markers (Das et al., 2006). However, when enriched Müller cells were transplanted into rodent eyes, the cells did not acquire photoreceptor morphology and rarely expressed photoreceptor-specific markers. This indicates that a permissive environment is needed for mammalian Müller glia to regenerate retinal neurons, which is achievable *in vitro* but lacking *in vivo*. It suggests that mammalian Müller glia have an inherent but dormant ability to regenerate.

In humans, Müller glial cells do not regenerate retinal neurons as that seen in lower vertebrates. Instead, Müller glial cells establish a glial scar, which acts as a physical barrier to halt inflammation but also prevents endogenous regeneration (Vecino et al., 2016). *In vivo* photoreceptor degeneration reveals that reactive Müller cells form a glial scar which contributes to negative retinal remodelling (Jones et al., 2003). Remodelling is when neurons reposition within the neural retina causing disrupted rewiring and cell loss meaning the retina cannot process visual information correctly and the function is lost. Glial scarring may also inhibit regeneration by blocking progenitor cell migration and new synapse formation (Belecky-Adams et al., 2013). However, in the CNS, reactive astrogliosis and scarring can prevent infiltration of pro-inflammatory cytokines and cells, maintain the blood-brain barrier after injury and preserve tissue function (Sofroniew, 2015a, Faulkner et al., 2004, Bush et al., 1999).

Therefore, complete scarring prevention may not be the right approach to promote endogenous regeneration of the mammalian retina.

The human MIO-M1 Müller glial stem cell line can be induced to differentiate into neuronal photoreceptor precursor cells *in vitro* through a combination of growth and differentiation factors as previously described (Jayaram et al., 2014). These factors include human basic fibroblast growth factor 2 (FGF-2), taurine, retinoic acid and insulin-like growth factor 1 (IGF-1). Upon culture with these factors MIO-M1 cells acquire characteristic photoreceptor morphology *in vitro* and express gene and protein markers of rod photoreceptor precursors. Therefore, this cell line was used to better understand the potential role of inflammatory cytokines and gliosis-associated proteins on the regenerative ability of human Müller glia. In designing methods to modulate the expression of these molecules, pharmacological interventions could promote endogenous regeneration within the retina.

2.2 Objectives

After injury in zebrafish Müller glial cells spontaneously repair the retina by producing new neurons. However, this endogenous regeneration is not seen in humans. Instead, inflammation in the human retina causes activation of Müller glial cells, causing their uncontrolled proliferation, with consequent retinal degeneration and glial scarring. Yet there is a subset of Müller glial cells with stem cell characteristics in the human retina, which have the ability to differentiate into neurons *in vitro*, suggesting that these cells have the potential for regeneration *in vivo*. However, we need to identify the factors in the human diseased retina that prevent Müller glia from proliferating and differentiating into retinal neurons. The aims of this chapter were therefore to examine the influence that inflammatory cytokines have on reactive gliosis in MIO-M1 cells and to investigate gliosis-associated proteins for their ability to inhibit neuronal differentiation of MIO-M1 cells *in vitro*.

The objectives of this chapter were:

1. To investigate the effect of the inflammatory cytokines TGF-β1, TNF-α, IL-6 and CNTF (found upregulated in human gliotic retina) on the expression of gliosis-associated proteins in MIO-M1 cells *in vitro*.

2. To examine the effect of these inflammatory cytokines on the ability of MIO-M1 cells to differentiate into rod photoreceptor precursors *in vitro*.
3. To assess the expression of GFAP in MIO-M1 cells treated with these inflammatory cytokines in the absence or presence of factors that induce rod photoreceptor precursor differentiation of these cells *in vitro.*

Experimental design:

I. RNA extracted from MIO-M1 cells cultured with the inflammatory cytokines TGF-β1, TNF-α, IL-6 and CNTF at concentrations previously determined in the host laboratory, was used to examine expression of mRNA coding for the gliosis-associated proteins GFAP, vimentin, galectin-1, tenascin and procollagen galactosyltransferase.

II. MIO-M1 cells were cultured for 6 days in the absence or presence of the inflammatory cytokines TGF-β1, TNF-α, IL-6 and CNTF in a dose-response experiment. Expression of mRNA GFAP and protein coding for GFAP was analysed using RT-PCR and western blot protocols established in our laboratory.

III. To assess the viability and proliferation of MIO-M1 cells cultured with the inflammatory cytokine TNF-α, LIVE/DEAD and hexosaminidase assays were undertaken.

IV. MIO-M1 cells were cultured with FGF-2, taurine, retinoic acid and IGF-1 (FTRI) to induce rod photoreceptor precursor differentiation in the absence or presence of the inflammatory cytokines. Isolated RNA was used in RT-PCR and qPCR using corresponding primers to examine expression of the rod photoreceptor markers NR2E3 and recoverin, whilst protein was analysed by western blot using antibodies against NR2E3 and GFAP. Protocols were previously established in our laboratory.

V. Semi-quantitative statistical analysis was done using ImageJ and GraphPad Prism.

2.3 Results

2.3.1 Effect of TGF-β1, TNF-α, IL-6 and CNTF on mRNA expression of gliosis-associated proteins by MIO-M1 cells

Preliminary work, carried out with RNA from other lab members, revealed that recombinant TGF-β1 at a final concentration of 50ng/ml did not modify mRNA expression of vimentin, galectin or procollagen galactosyltransferase in Müller glial cell line MIO-M1 when compared to control untreated cells (Figure 2-1). However, there was a significant downregulation of tenascin and GFAP mRNA expression in cells cultured with TGF-β1 as compared to controls ($p<0.01$) (Figure 2-2).

mRNA obtained from MIO-M1 cells cultured with 50ng/ml of recombinant TNF-α showed that expression of vimentin, galectin, procollagen galactosyltransferase or tenascin was not modified by this cytokine (Figure 2-3). However, the mRNA expression of GFAP was significantly downregulated by culturing MIO-M1 cells with TNF-α when compared to control untreated cells ($p<0.05$) (Figure 2-4).

mRNA obtained from MIO-M1 cells cultured with 10ng/ml of recombinant IL-6 showed that there was no difference in mRNA expression of vimentin, galectin, procollagen galactosyltransferase or tenascin between control untreated cells and cells cultured with this cytokine (Figure 2-5). Conversely, there was a significant increase in mRNA expression of GFAP in MIO-M1 cells cultured with IL-6 compared to control untreated cells ($p<0.01$) (Figure 2-6).

When MIO-M1 cells were cultured with 10ng/ml of recombinant CNTF the mRNA expression of vimentin, galectin, procollagen galactosyltransferase, tenascin or GFAP were not modified when compared to control untreated cells (Figure 2-7).

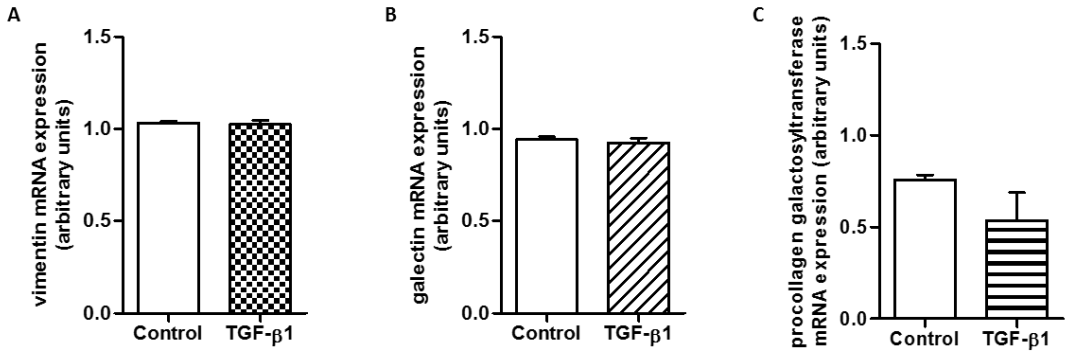

Figure 2-1: Expression of mRNA coding for proteins associated with gliosis by MIO-M1 cells cultured in the absence or presence of TGF-β1.
Bar chart shows relative expression of mRNA normalised to β-actin (mean +/- SEM) of **(A)** vimentin, **(B)** galectin and **(C)** procollagen galactosyltransferase. There was no significant difference in mRNA expression between control untreated cells and cells cultured with TGF-β1. Paired student's T-test (p>0.05 vs. control). Vimentin and galectin N=4, procollagen galactosyltransferase N=3.

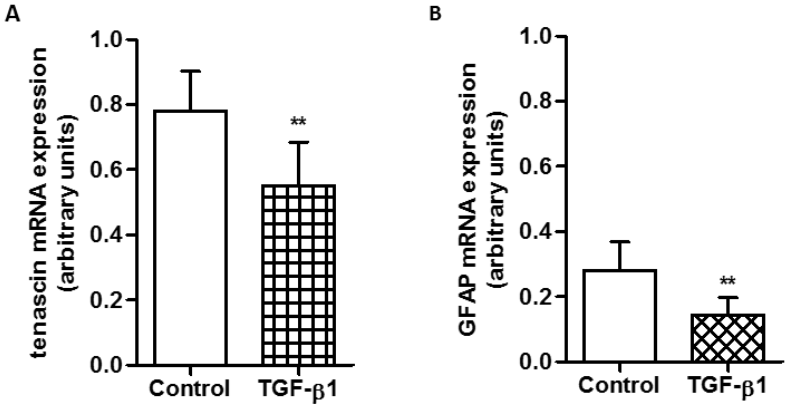

Figure 2-2: Expression of mRNA coding for (A) tenascin and (B) GFAP by MIO-M1 cells cultured in the absence or presence of TGF-β1.
Bar chart shows relative expression of mRNA normalised to β-actin (mean +/- SEM). Both genes were significantly downregulated by TGF-β1 in Müller glial cells. Paired student's T-test (p< 0.05 vs. control). GFAP N=12, Tenascin N=7.

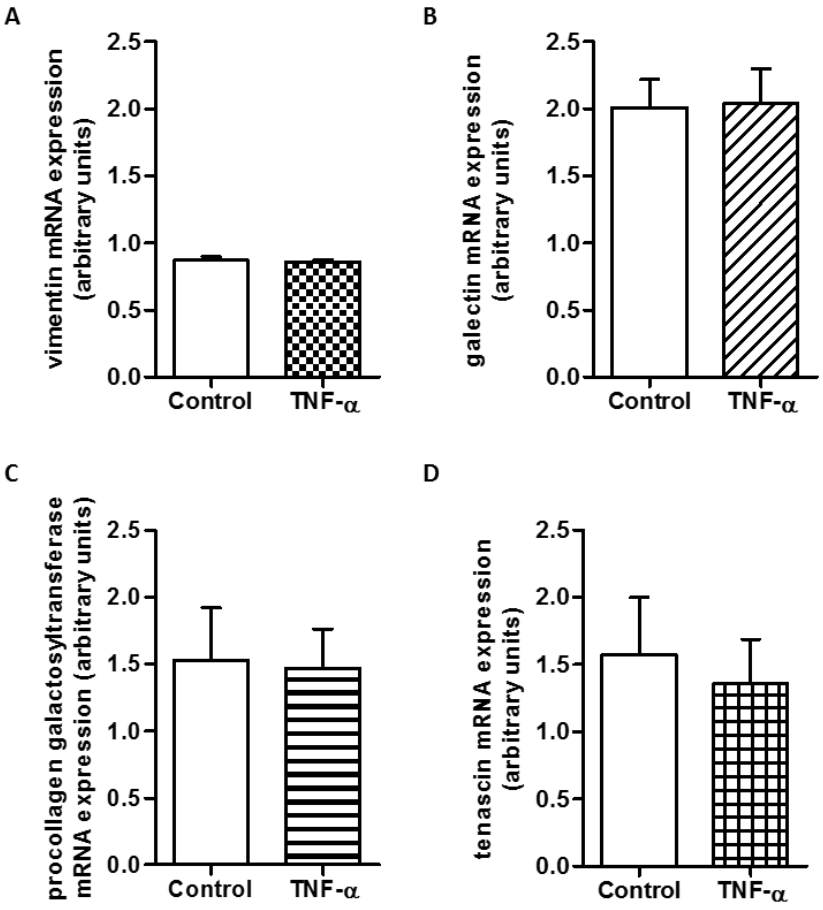

Figure 2-3: Expression of mRNA coding for proteins associated with gliosis by MIO-M1 cells cultured in the absence or presence TNF-α.
Bar chart shows relative expression of mRNA normalised to β-actin (mean +/- SEM) of **(A)** vimentin, **(B)** galectin, **(C)** procollagen galactosyltransferase and **(D)** tenascin. Culturing MIO-M1 cells with TNF-α did not modify the mRNA expression of these proteins when compared to untreated control cells. Paired student's T-test ($p>0.05$ vs. control). N= 5.

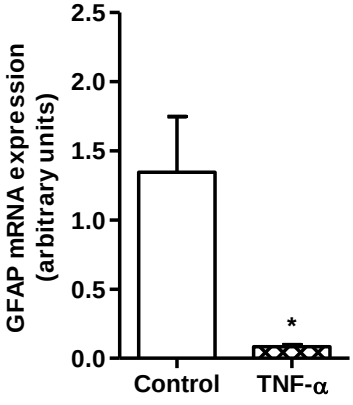

Figure 2-4: mRNA expression of GFAP by MIO-M1 cells cultured in the presence of TNF-α.
Bar chart shows relative expression of mRNA normalised to β-actin (mean +/- SEM). GFAP expression was significantly decreased when cells were cultured with TNF-α when compared to control untreated cells. Paired student's T-test ($p<0.05$ vs. control). N= 5.

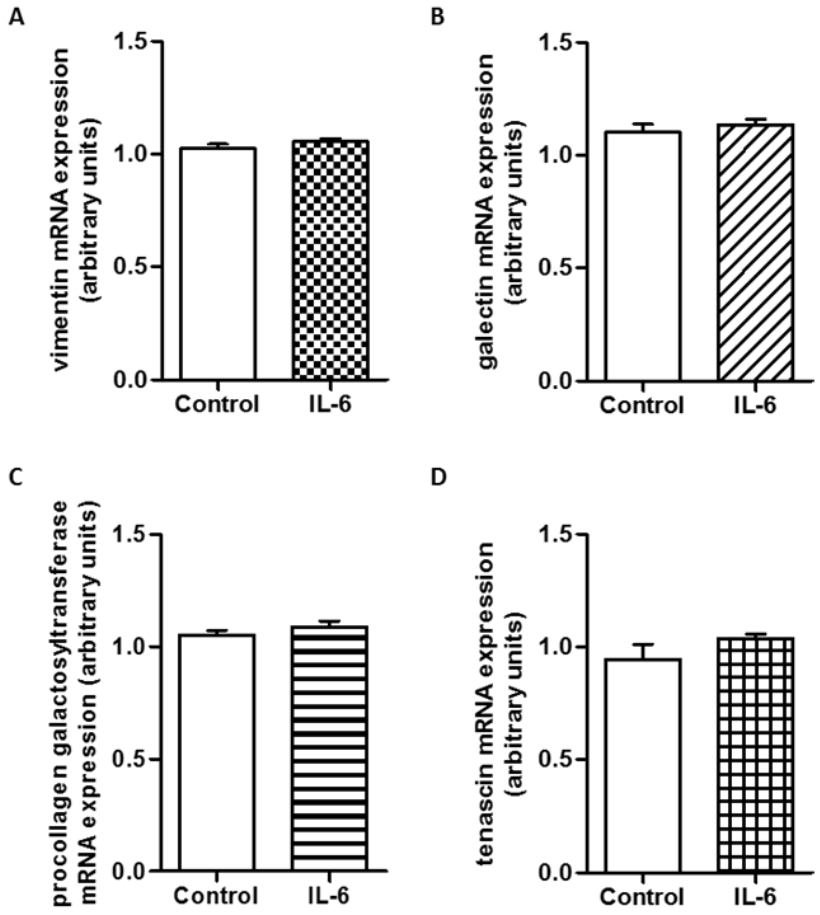

Figure 2-5: Expression of mRNA coding for proteins associated with gliosis by MIO-M1 cells cultured in the absence or presence of IL-6. Bar chart shows relative expression of mRNA normalised to β-actin (mean +/- SEM) of **(A)** vimentin, **(B)** galectin, **(C)** procollagen galactosyltransferase and **(D)** tenascin. Culturing MIO-M1 cells with IL-6 did not modify expression of these genes when compared to untreated control cells. Paired student's T-test ($p>0.05$ vs. control). N=5.

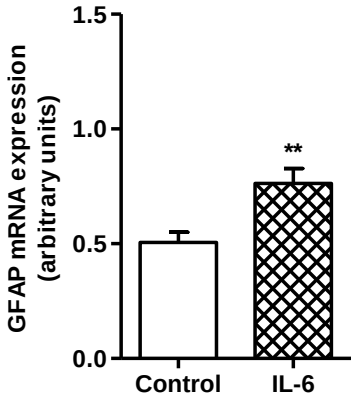

Figure 2-6: mRNA expression of GFAP by MIO-M1 cells cultured in the presence of IL-6.
Bar chart shows relative expression of mRNA normalised to β-actin (mean +/- SEM). GFAP expression was significantly increased when cells were cultured with IL-6 when compared to control untreated cells. Paired student's T-test ($p<0.01$ vs. control). N= 5.

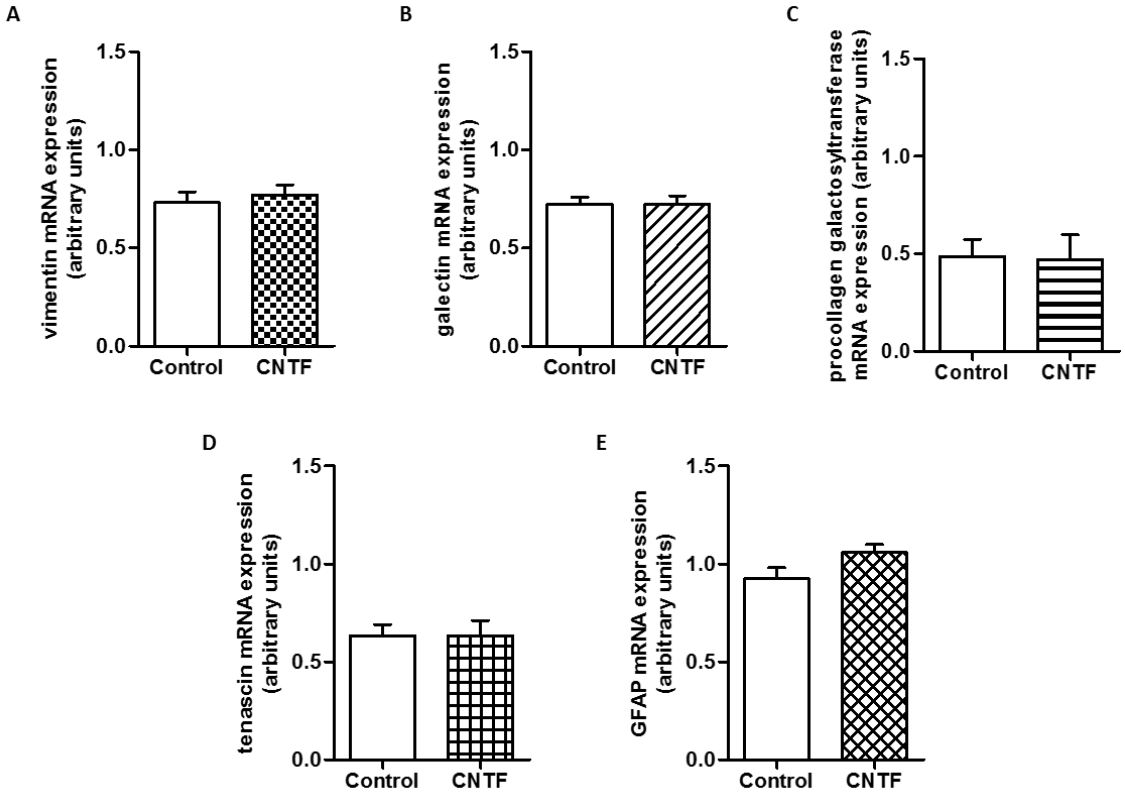

Figure 2-7: Expression of mRNA coding for proteins associated with gliosis by MIO-M1 cells cultured in the absence or presence of CNTF.
Bar chart shows relative expression of mRNA normalised to β-actin (mean +/- SEM). There was no change in mRNA expression of **(A)** vimentin, **(B)** galectin, **(C)** procollagen galactosyltransferase, **(D)** tenascin and **(E)** GFAP when MIO-M1 cells were cultured with CNTF as compared to untreated control cells. Paired student's T-test ($p>0.05$ vs. control). N=3.

2.3.2 Regulation of GFAP expression by inflammatory cytokines in MIO-M1 cells

Based on the above data that mRNA expression of GFAP was significantly downregulated in MIO-M1 cells cultured in the presence of TGF-β1 and TNF-α, whilst being significanly upregulated by the presence of IL-6, further work was focused on the investigation of GFAP regulation by these cytokines. Culture of MIO-M1 cells with these cytokines was repeated to confirm what was observed using RNA supplied by other lab members.

2.3.2.1 TGF-β1 downregulated GFAP expression

MIO-M1 cells were cultured with increasing concentrations of recombinant TGF-β1 in a dose-response manner. The results showed that there was a significant downregulation of GFAP mRNA expression when MIO-M1 cells were cultured with 1ng/ml and 100ng/ml of TGF-β1 when compared to control untreated cells ($p<0.05$) (Figure 2-8). There was no change in GFAP mRNA expression between control untreated cells and cells cultured with TGF-β1 concentrations of 0.1ng/ml and 10ng/ml. Furthermore, GFAP expression was significantly different between cells cultured with 0.1ng/ml of TGF-β1 and cells cultured with 10ng/ml and 100ng/ml ($p<0.05$).

The protein expression of GFAP confirmed the downregulation of GFAP expression by TGF-β1 (Figure 2-9). GFAP protein was significantly downregulated by 1ng/ml and 100ng/ml of TGF-β1 ($p<0.05$).

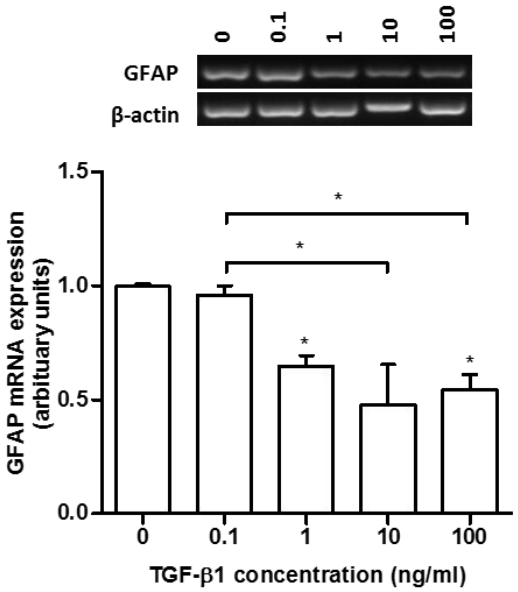

Figure 2-8: mRNA expression of GFAP by MIO-M1 cells cultured with increasing concentrations of TGF-β1.
Representative image of PCR bands for GFAP and β-actin are shown above the bar chart. Bar chart shows the relative expression of mRNA normalised to β-actin (mean +/- SEM). There was a significant downregulation of GFAP mRNA expression in cells cultured with 1ng/ml and 100ng/ml TGF-β1 as compared to control untreated cells. There was also a significant difference between cells cultured with 0.1ng/ml and cells cultured with the two highest concentrations of TGF-β1 used. One-way repeated-measures ANOVA and Tukey's post-test $p<0.05$, N=3.

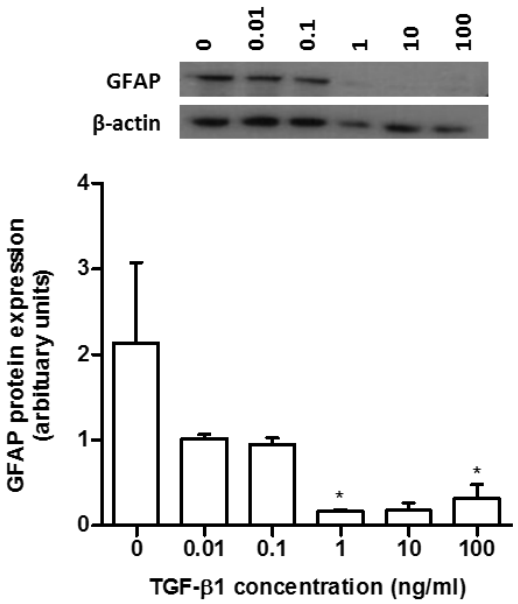

Figure 2-9: Protein expression of GFAP by MIO-M1 cells cultured with increasing concentrations of TGF-β1.
Representative western blot bands of GFAP and β-actin are shown above the bar chart. Bar chart shows the relative GFAP protein expression normalised to β-actin (mean +/- SEM). Cells cultured with 1ng/ml and 100ng/ml of TGF-β1 had GFAP protein expression significantly downregulated when compared to control untreated cells. One-way repeated-measures ANOVA and Tukey's post-test, $p<0.05$, N=3.

2.3.2.2 TNF-α downregulated GFAP expression

MIO-M1 cells cultured with increasing concentrations of recombinant TNF-α showed a decrease in mRNA expression of GFAP in a dose-response manner (Figure 2-10). There was a significant downregulation of GFAP mRNA in MIO-M1 cells treated with 5ng/ml, 50ng/ml and 500ng/ml of TNF-α when compared to control untreated cells ($p<0.01$). There was no difference in GFAP mRNA expression between control cells and cells treated with 0.1% BSA, which was the vehicle used to dilute the TNF-α, or cells treated with 0.5ng/ml of TNF-α. Furthermore, there was a significant difference in GFAP mRNA expression between cells treated with the BSA vehicle control and 5 ng/ml, 50 ng/ml and 500ng/ml of TNF-α ($p<0.05$).

Western blot analysis of cell lysate protein from MIO-M1 cells cultured with TNF-α showed that the expression of GFAP protein also decreased significantly when cells were treated with 5ng/ml, 50 ng/ml and 500ng/ml of TNF-α as compared to control cells and cells treated with BSA vehicle control ($p<0.01$) (Figure 2-11). However, GFAP protein expression in cells cultured with 0.5ng/ml TNF-α was not significantly changed when compared to untreated control cells.

2.3.2.3 IL-6 and CNTF did not modify GFAP expression

MIO-M1 cells were cultured with increasing concentrations of recombinant IL-6 and CNTF and analysed for mRNA and protein expression of GFAP. The results showed that mRNA expression of GFAP was not modified in MIO-M1 cells cultured with increasing concentrations of IL-6 (Figure 2-12). Similarly, culturing cells with CNTF did not modify the expression of mRNA coding for GFAP by these cells (Figure 2-14). However, there was a significant increase in GFAP mRNA expression in cells cultured with 100ng/ml of IL-6 or CNTF when compared to cells cultured with BSA vehicle ($p<0.05$), suggesting that physiologically higher concentrations of these cytokines may cause significant upregulation of GFAP mRNA.

Western blot analysis of protein from MIO-M1 cells cultured with IL-6 confirmed that protein expression of GFAP was not modified in cells cultured with increasing concentrations of IL-6 (Figure 2-13). Protein expression of GFAP was not examined in cells treated with CNTF.

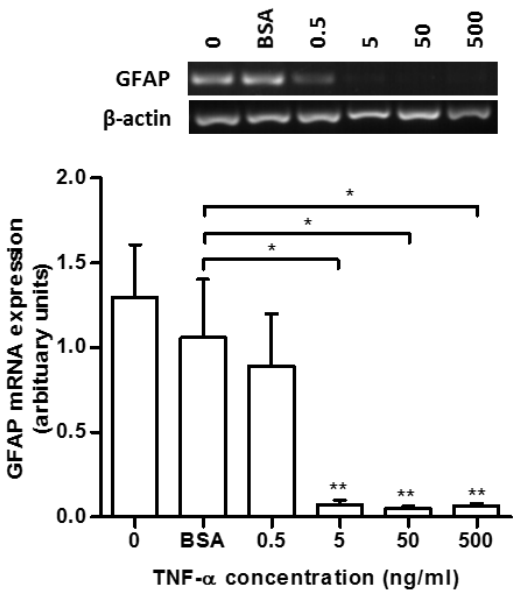

Figure 2-10: mRNA expression of GFAP by MIO-M1 cells cultured with increasing concentrations of TNF-α.
Representative PCR bands of GFAP and β-actin are shown above bar chart. Bar chart shows relative expression of GFAP mRNA normalised to β-actin (mean +/- SEM). There was a significant decrease in GFAP mRNA expression in cells cultured with 5ng/ml, 50ng/ml and 500ng/ml of TNF-α when compared to control untreated cells. There was also a significant difference in GFAP mRNA expression between cells cultured with the vehicle BSA and cells cultured with 5ng/ml, 50ng/ml and 500ng/ml of TNF-α. One-way repeated measures ANOVA and Tukey's post-test, $p<0.05$, N=3.

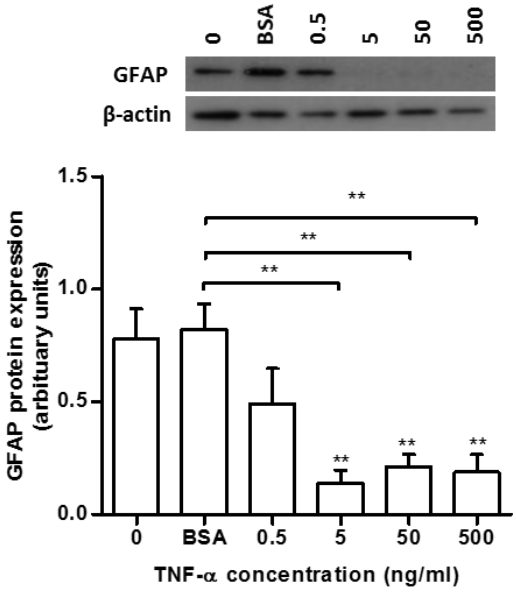

Figure 2-11: Protein expression of GFAP by MIO-M1 cells cultured with increasing concentrations of TNF-α.
Representative western blot bands of GFAP and β-actin are shown above bar chart. Bar chart shows relative GFAP protein expression normalised to β-actin (mean +/- SEM). There was a significant decrease in GFAP protein expression between cells cultured with 5ng/ml, 50ng/ml and 500ng/ml TNF-α and control untreated cells. One-way repeated measures ANOVA and Tukey's post-test, $p<0.05$, N=3.

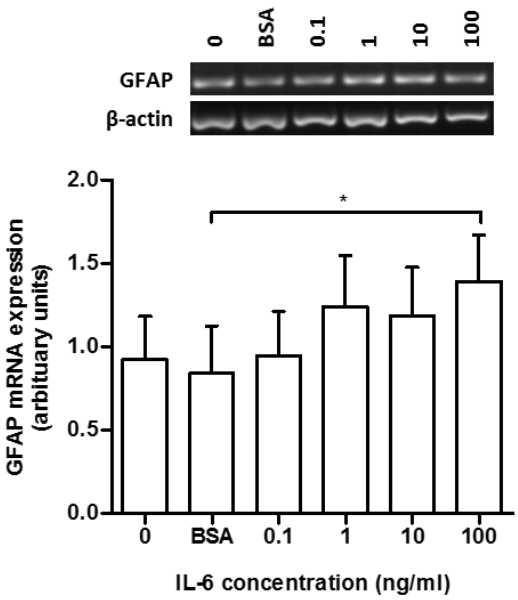

Figure 2-12: mRNA expression of GFAP by MIO-M1 cells cultured with increasing concentrations of IL-6.
Representative PCR bands of GFAP and β-actin are shown above bar chart. Bar chart shows relative expression of GFAP mRNA normalised to β-actin (mean +/- SEM). There was no difference in GFAP mRNA expression between untreated control cells and cells cultured with IL-6. One-way repeated measures ANOVA and Tukey's post-test, $p>0.05$, N=7.

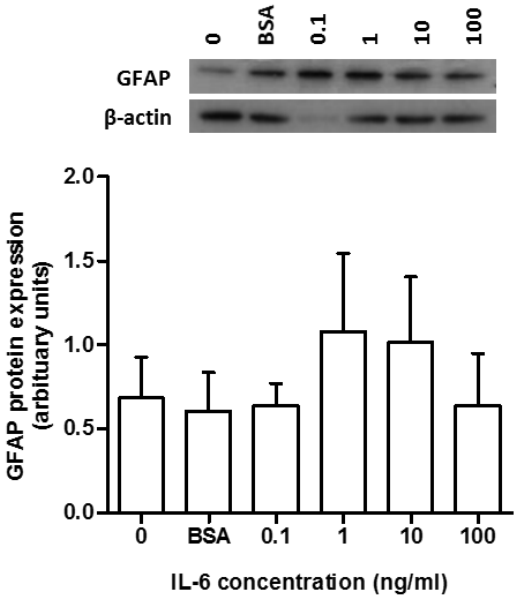

Figure 2-13: Protein expression of GFAP by MIO-M1 cells cultured with increasing concentrations of IL-6.
Representative image of western blot bands for GFAP and β-actin are shown above the bar chart. Bar chart shows relative expression of GFAP protein normalised to β-actin (mean +/- SEM). There was no significant difference in GFAP protein expression between control untreated cells and cells cultured with IL-6 at any concentration. One-way repeated measures ANOVA and Tukey's post-test, $p>0.05$, N=3.

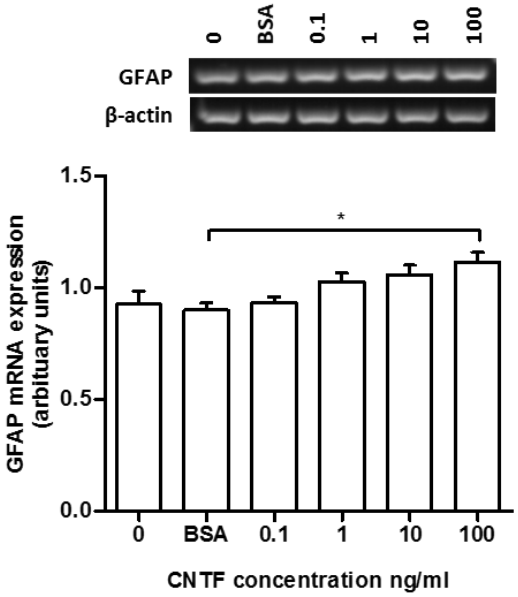

Figure 2-14: mRNA expression of GFAP by MIO-M1 cells cultured with increasing concentrations of CNTF.
Representative image of PCR bands for GFAP and β-actin are shown above bar chart. Bar chart shows relative expression of GFAP mRNA normalised to β-actin (mean +/- SEM). There was no significant difference between control cells and cells cultured with increasing concentrations of CNTF. There was a significant difference between cells cultured with BSA vehicle and cells cultured with 100ng/ml of CNTF. One-way repeated measures ANOVA and Tukey's post-test, $p<0.05$, N=3.

2.3.3 Effect of TNF-α on the cell viability and proliferation of MIO-M1 cells

Based on previous observations that TNF-α induced downregulation of GFAP mRNA and protein in MIO-M1 cells cultured with this cytokine, it was important to rule out the possibility that this effect was due to TNF-α causing cell death or altering cell proliferation.

2.3.3.1 TNF-α did not affect viability of MIO-M1 cells

To determine whether cell viability was affected by the concentrations of TNF-α used in the dose-response experiment, a cytotoxicity test was carried out. After culturing cells with increasing concentrations of TNF-α, a LIVE/ DEAD assay was used. This test simultaneously stains live and dead cells with two different fluorescent dyes. Live cells are stained green by calcein and dead cells are stained red by ethidium homodimer-1 (Figure 2-15). The proportion of red and green fluorescent cells was analysed under confocal fluorescence microscopy. Quantification of the number of positive cells for each marker revealed that an average of less than 3% cell death was observed across all samples. There was no significant difference in cell death when MIO-M1 cells were cultured with increasing concentrations of TNF-α ranging from 0.5 to 500 ng/ml (Figure 2-16)

2.3.3.2 TNF-α did not alter the proliferation rate of MIO-M1 cells

To investigate whether different concentrations of TNF-α influenced cell proliferation when MIO-M1 cells were cultured with this cytokine, a proliferation assay using hexosaminidase was performed. Hexosaminidase is a lysosomal enzyme, the total activity of which is directly proportional to the number of living cells in a homogenous population. This assay is a robust method of measuring cell proliferation over time because relative absorbance readings are directly proportional to cell numbers. Over 6 days the untreated MIO-M1 cells increased 1.3-fold, equating to a 17% increase in the number of cells per day (Figure 2-17). Addition of TNF-α at varying concentrations from 0.5ng/ml to 500ng/ml did not have a significant effect on MIO-M1 cell proliferation (Figure 2-18).

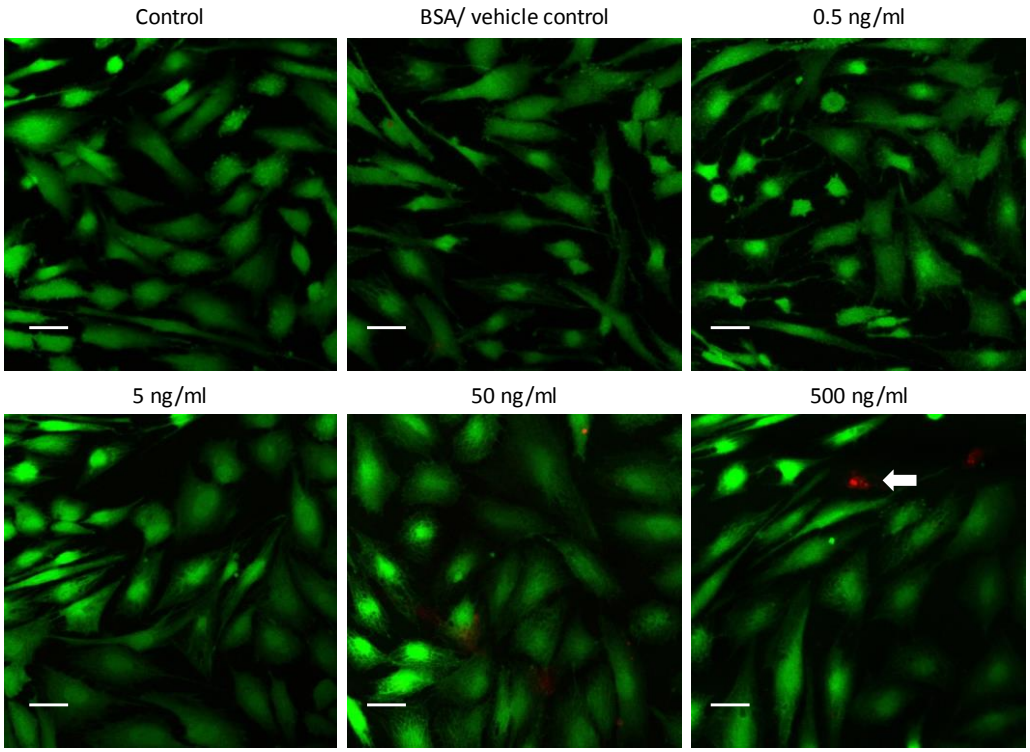

Figure 2-15: LIVE/DEAD cell cytotoxicity assay in MIO-M1 cells cultured with increasing concentrations of TNF-α.
Live cells fluoresce green and dead cells fluoresce red. The majority of cells cultured with BSA, 0.5ng/ml, 5ng/ml, 50ng/ml an 500ng/ml of TNF-α showed to be viable (green) whilst only occasional cells were shown to be dead (red, white arrow). Scale bar represents 35µm.

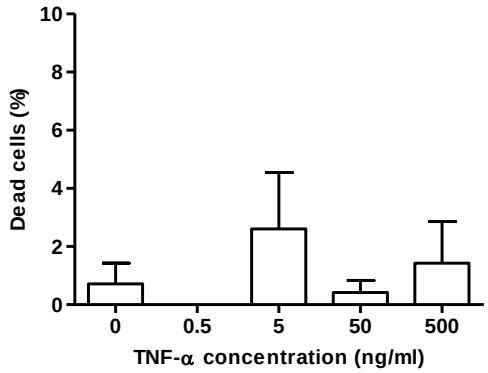

Figure 2-16: Müller glial cell viability following culture with increasing concentrations of TNF-α.
Bar chart represents the percentage of dead red cells (mean +/- SEM). There was no significant difference in cell death in cells cultured with various concentrations of TNF-α when compared to untreated control cells. One-way ANOVA and Tukey's post-test, p> 0.05, N=3.

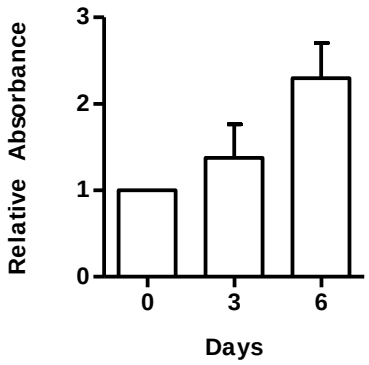

Figure 2-17: Proliferation of MIO-M1 cells as measured by hexosaminidase assay.
Bar chart shows relative absorbance (mean +/- SEM), which represents the number of MIO-M1 cells at day 0, 3 and 6 of culturing under standard conditions. Rate of proliferation was 17% per day (N=4).

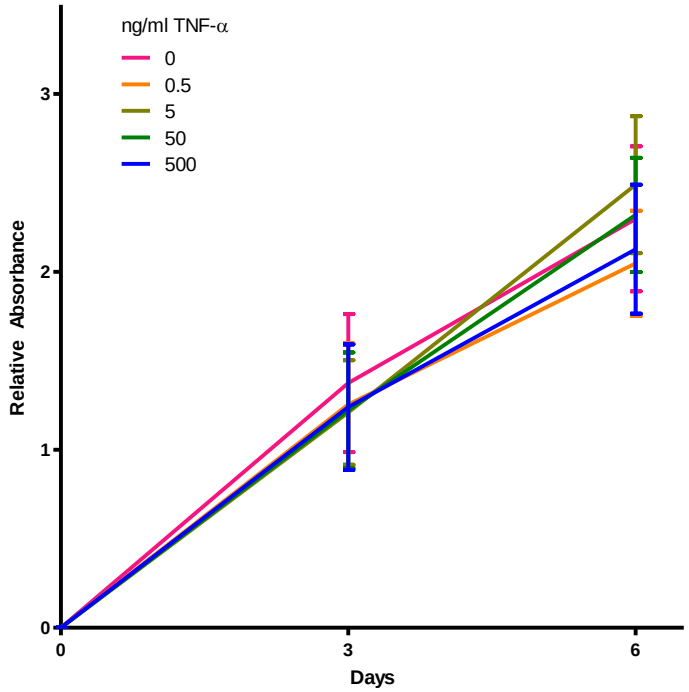

Figure 2-18: Proliferation rate of MIO-M1 cells cultured with increasing concentrations of TNF-α as determined by hexosaminidase assay.
Coloured lines represent the different concentrations of TNF-α. There was no significant effect on cell proliferation at 3 and 6 days in culture. Two-way ANOVA and Bonferroni post-test, $p>0.05$, N=4.

2.3.4 Effect of inflammatory cytokines on the rod photoreceptor precursor differentiation of MIO-M1 cells

To better understand the potential role of inflammatory cytokines on the neurogenic ability of Müller glia, MIO-M1 cells were induced to differentiate into rod photoreceptor precursors by culture on matrigel in the presence of FGF-2, taurine, retinoic acid and IGF-1 (hereafter referred to as FTRI) for 6 days in the presence or absence of TGF-β1, TNF-α, IL-6 or CNTF.

2.3.4.1 Validation of the method used to induce rod photoreceptor precursor differentiation of MIO-M1 cells

Morphological changes of MIO-M1 cells in response to culture with FTRI

Culturing MIO-M1 cells on matrigel and FTRI for 6 days, caused a distinct change in cell morphology that resemble photoreceptors *in vitro* (Figure 2-19). Whereas untreated control cells had a glial morphology, the majority of cells cultured with FTRI acquired condensed, rounder cell bodies with more prominent nuclei and short neurite-like processes, confirming the morphology previously observed using this protocol (Jayaram et al., 2014).

MIO-M1 cell proliferation in response to culture with FTRI

Culturing MIO-M1 Müller glial cells on matrigel in the presence of FTRI slightly increased their proliferation rate but this was not significant compared to control untreated cells, as analysed by hexosaminidase assay (Figure 2-20).

Expression of rod photoreceptor precursor genes NR2E3 and recoverin and NR2E3 protein by MIO-M1 cells in response to culture with FTRI

To further examine MIO-M1 cell response to FTRI, gene expression of NR2E3 and recoverin were examined in MIO-M1 cells after 6 days of culture with these factors. These genes are associated with rod photoreceptor development. Using RT-PCR, cDNA of cells cultured in the absence or presence of FTRI were analysed. When compared to control, cells cultured with FTRI showed a small upregulation of both NR2E3 and recoverin mRNA (Figure 2-21). However, this was not statistically significant. When cDNA was analysed by qPCR to validate these results, cells cultured with FTRI had a 1.09-fold increase in NR2E3 gene expression compared to untreated cells (Figure 2-22), which confirmed that there were no significant changes in gene expression of NR2E3 by these cells.

Western blot analysis was performed on cell lysates to examine the protein expression of NR2E3. The results showed that MIO-M1 cells cultured with FTRI had a significant increase in NR2E3 protein expression compared to untreated control cells ($p<0.01$) (Figure 2-23).

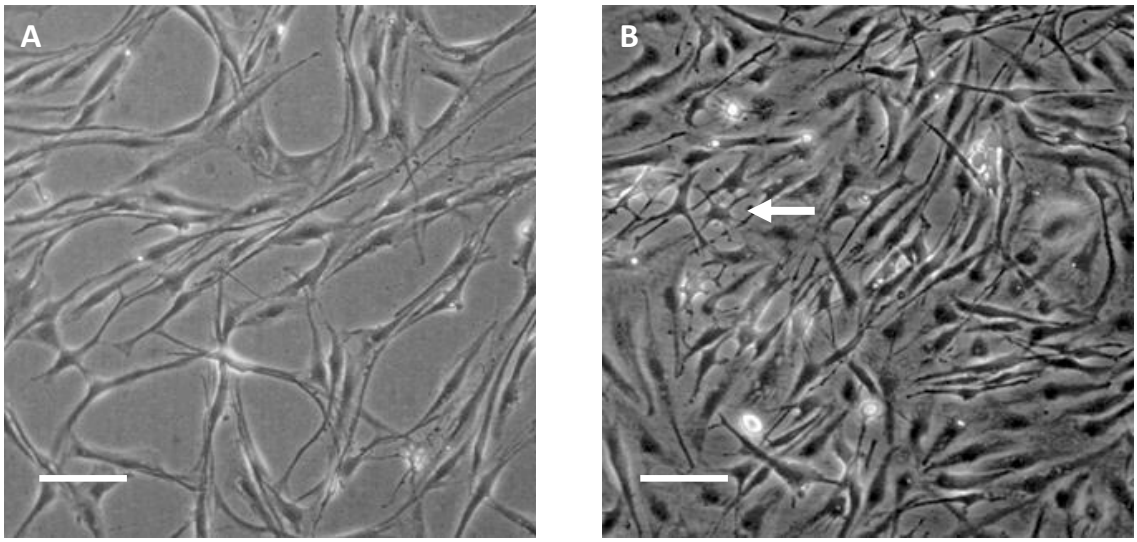

Figure 2-19: Phase contrast microscope images of (A) control untreated MIO-M1 cells and (B) cells cultured with differentiation factors FGF-2, taurine, retinoic acid and IGF-1 (FTRI).
Cells cultured without differentiation factors have elongated glia morphology, whilst cells cultured with FTRI acquired a characteristic photoreceptor morphology *in vitro* with condensed cell bodies, round bulging nuclei and short projections (indicated by white arrow). Scale bar represents 100µm.

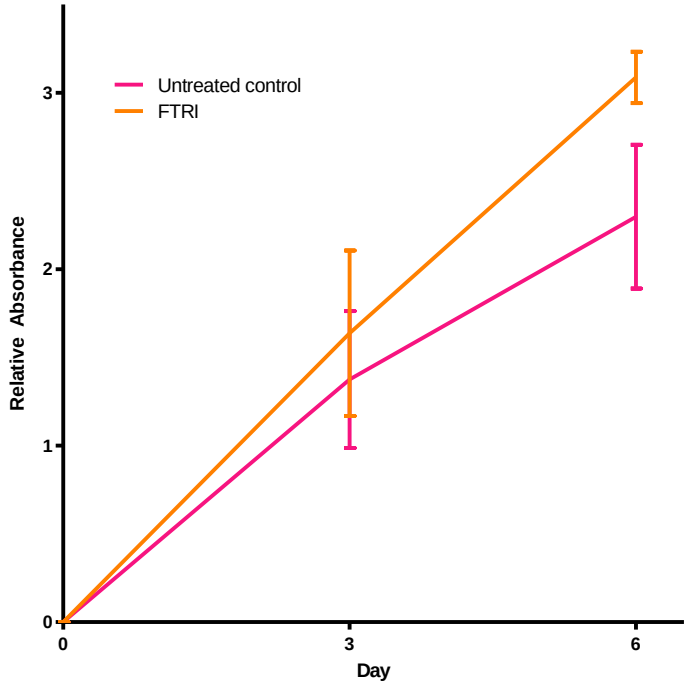

Figure 2-20: Proliferation rate of MIO-M1 cells cultured in the absence or presence of FTRI as determined by hexosaminidase assay.
Pink coloured line represents untreated control cells and orange line represents FTRI treated cells after 6 days in culture (mean +/- SEM). Rod photoreceptor precursor differentiation caused a slight increase in cell proliferation, which was not significant at 3 and 6 days in culture. Two-way ANOVA and Bonferroni post-test, $p>0.05$, N=4.

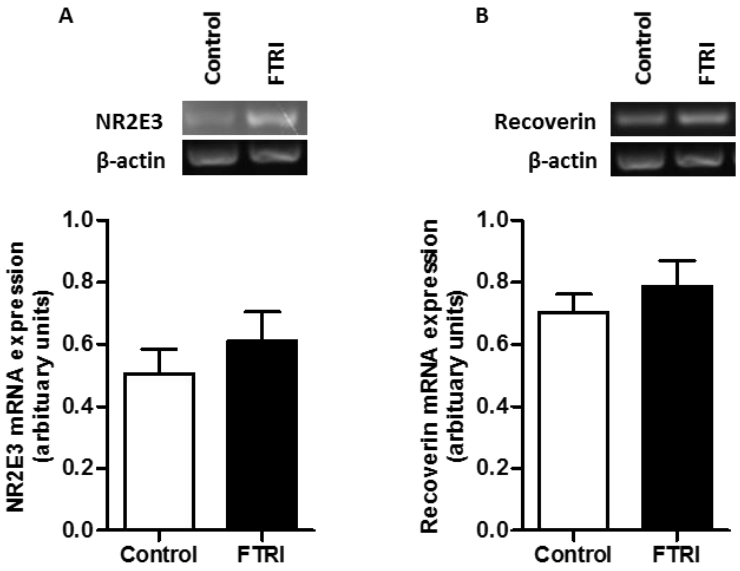

Figure 2-21: mRNA expression of rod photoreceptor markers by MIO-M1 cells cultured with FTRI as determined by RT-PCR.
Representative images of PCR bands for gene of interest and β-actin shown above bar charts. Bar charts represent mRNA expression of rod photoreceptor genes normalised to β-actin (mean +/- SEM). **(A)** NR2E3 mRNA is slightly increased in cells induced to differentiate into photoreceptor precursors (N=11). **(B)** Recoverin mRNA expression also showed a small increase in the presence of FTRI (N= 12). Although both genes slightly increased expression in cells cultured with differentiation factors compared to untreated control cells, this was not statistically significant. Paired student's T-test, p>0.05.

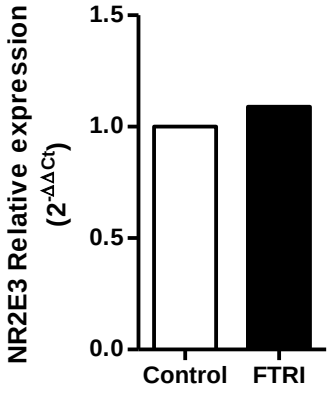

Figure 2-22: qPCR analysis of NR2E3 gene expression by MIO-M1 cells cultured in the absence or presence of FTRI.
Bar chart represents relative expression of NR2E3 (mean +/- SEM). Results confirmed a non-significant increase of NR2E3 gene expression in cells cultured in the presence of FTRI when compared to untreated control cells. Paired student's T-test p>0.05, N=3.

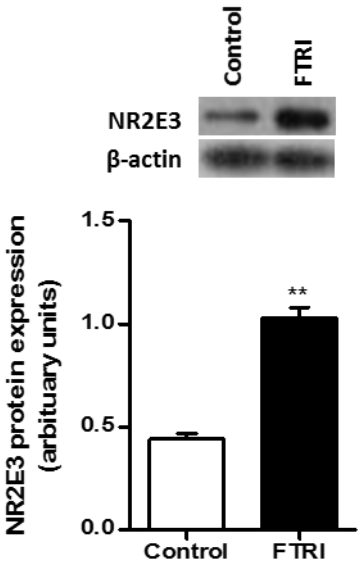

Figure 2-23: Protein expression of NR2E3 by MIO-M1 cells cultured with FTRI. Representative western blot bands for NR2E3 and β-actin shown above the bar chart. Bar chart represents NR2E3 protein expression normalised to β-actin (mean +/- SEM). There was a significant increase in NR2E3 protein expression in cells cultured with FTRI compared to untreated control cells. Paired student's T-test $p < 0.01$, N=3.

2.3.5 Expression of NR2E3 mRNA in MIO-M1 cells cultured with FTRI in the presence of inflammatory cytokines

High variability in the FTRI protocol was observed throughout the experiments. Although a slight increase in the expression of NR2E3 mRNA was previously observed in cells cultured with FTRI alone, there was no significant difference in expression of this marker in MIO-M1 cells cultured with FTRI in further experiments investigating the effect of cytokines on the rod photoreceptor precursor differentiation of these cells (Figure 2-24).

Culture of these cells with either TGF-β1 (Figure 2-24A) or CNTF (Figure 2-24B) alone did not modify the expression of NR2E3 mRNA when compared to untreated control cells. In addition, the expression of this marker was not modified when Müller glia were cultured with FTRI in the presence of TGF-β1 or CNTF when compared to untreated control cells. Similarly, culture of these cells with TNF-α alone or with FTRI in the presence of this cytokine did not alter the expression of NR2E3 mRNA when compared to controls (Figure 2-24C). Whilst culture of cells with IL-6 alone showed a slight decrease in NR2E3 mRNA expression as compared to control cells, this was not statistically significant. Addition of IL-6 to cells cultured with FTRI did not modify the mRNA expression of NR2E3 when compared to control cells (Figure 2-24D).

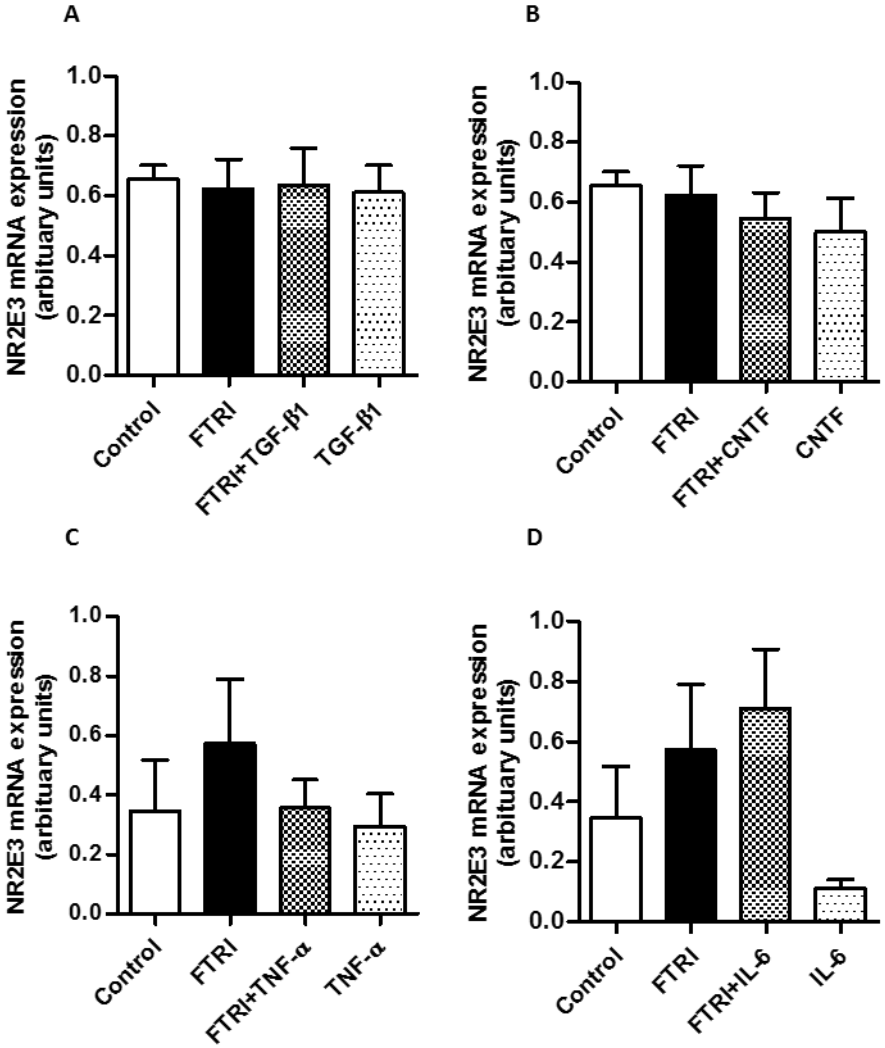

Figure 2-24: NR2E3 mRNA expression by MIO-M1 cells cultured with FTRI alone, FTRI combined with inflammatory cytokines or cytokines alone.

Bar charts represent NR2E3 mRNA expression normalised to β-actin (mean +/- SEM) **(A)** Culture of Müller glia with FTRI in the presence of TGF-β1 or **(B)** CNTF did not modify the expression of NR2E3 mRNA when compared to untreated control cells. Addition of **(C)** TNF-α or **(D)** IL-6 to cells cultured with FTRI did not change expression of NR2E3 mRNA when compared to controls. Two-way ANOVA and Tukey post-test, $p>0.05$, N= 4.

2.3.6 Expression of recoverin mRNA in MIO-M1 cells cultured with FTRI in the presence of inflammatory cytokines

As previously observed, there was not a significant difference in mRNA expression of recoverin in cells cultured with FTRI when compared to untreated control cells (Figure 2-25). Like NR2E3 expression, MIO-M1 cells cultured with FTRI in combination with TGF-β1 (Figure 2-25A) or CNTF (Figure 2-25B) did not show change in the mRNA expression of recoverin when compared to controls. Culture of cells with TGF-β1 or CNTF alone also did not alter the mRNA expression of this gene. Likewise, culture of MIO-M1cells with IL-6 alone or with the addition of this cytokine to cells cultured with FTRI did not modify recoverin mRNA expression when compared to untreated control cells (Figure 2-25D).

However, there was a significant increase in recoverin mRNA expression in MIO-M1 cells cultured with FTRI in the presence of TNF-α when compared to control untreated cells ($p<0.001$) (Figure 2-25C). The mRNA expression of recoverin in cells cultured with FTRI in the presence of TNF-α was significantly higher than cells cultured with FTRI ($p<0.05$) or TNF-α alone ($p<0.001$). Furthermore, the mRNA expression of recoverin was unchanged in MIO-M1 cells cultured with TNF-α alone compared to untreated control cells and was significantly lower than in cells cultured with FTRI alone ($p<0.05$). This suggests that TNF-α is not causing the increase in recoverin expression but may be indirectly potentiating the differentiation of MIO-M1 cells by FTRI. It would therefore be interesting to investigate the downstream signalling of TNF-α in MIO-M1 cells.

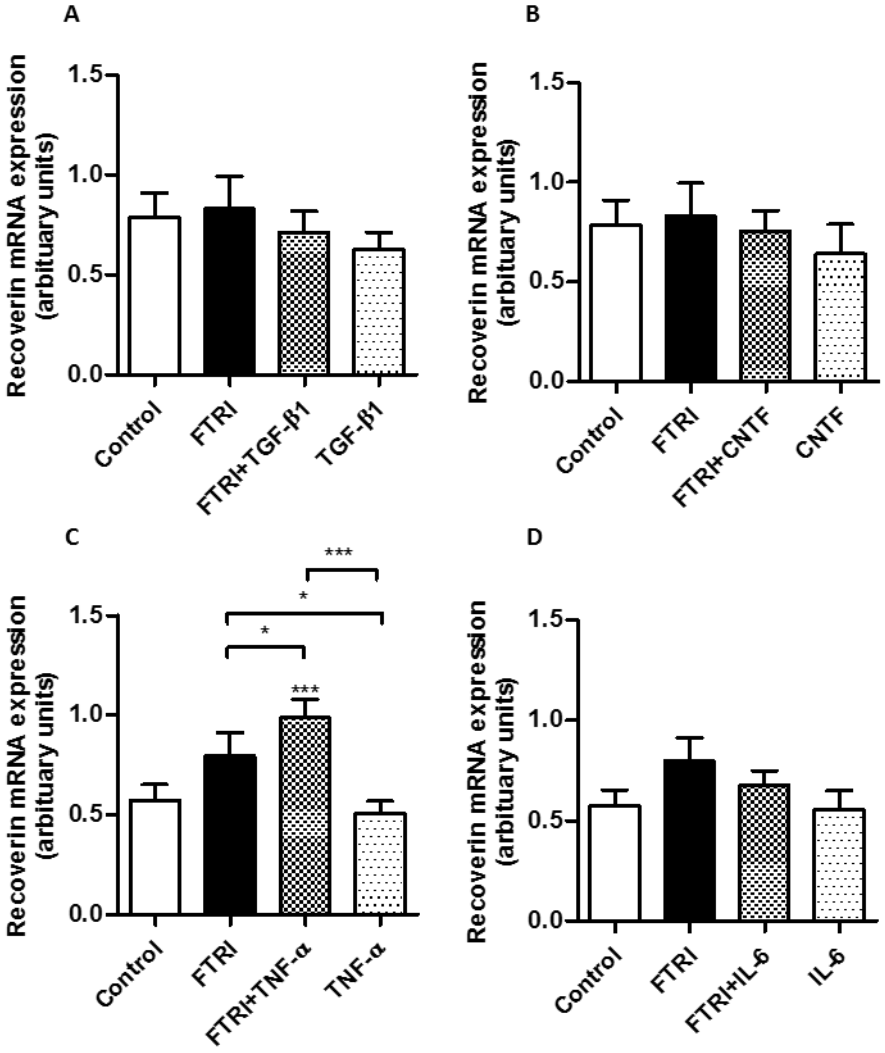

Figure 2-25: Recoverin mRNA expression by MIO-M1 cells cultured with FTRI alone, FTRI combined with inflammatory cytokines and cytokines alone.

Bar charts represent recoverin mRNA expression normalised to β-actin (mean +/- SEM). Culture of cells with FTRI alone or in combination with **(A)** TGF-β1, **(B)** CNTF or **(D)** IL-6 did not modify mRNA expression of recoverin when compared to untreated control cells. **(C)** Although there was not a significant increase in recoverin mRNA expression in cells cultured with FTRI alone, there was a significant increase in the expression of this gene when cells were cultured with FTRI in conjunction with TNF-α as compared to control cells. Two-way ANOVA and Tukey post-test, $p<0.05$, N= 5.

2.3.7 Expression of NR2E3 protein in MIO-M1 cells cultured with FTRI in the presence of inflammatory cytokines

Because mRNA expression was variable, protein from extracted lysates of cells cultured with FTRI was also examined. Western blot analysis was performed to examine protein expression of NR2E3 in cells cultured with FTRI in the absence or presence of TGF-β1, CNTF, TNF-α and IL-6. In all sets of experiments, there was a significant increase in NR2E3 protein expression when MIO-M1 cells were cultured with FTRI when compared to untreated control cells ($p<0.01$) (Figure 2-26).

The protein expression of NR2E3 was not modified in cells cultured with TGF-β1 alone or in combination with FTRI when compared to control (Figure 2-26A). However, when compared to cells cultured with FTRI alone, cells cultured with FTRI in the presence of TGF-β1 showed downregulation of NR2E3 protein expression ($p<0.01$). This suggests that the addition of TGF-β1 to cells cultured with FTRI prevents MIO-M1 cells from differentiating into rod photoreceptor precursors.

When MIO-M1 cells were cultured with CNTF alone ($p<0.05$) or FTRI in the presence of CNTF ($p<0.01$) the protein expression of NR2E3 increased compared to untreated control (Figure 2-26B). There was no difference in expression of this protein between cells cultured with CNTF alone or cells cultured with FTRI combined with CNTF. This suggests that CNTF can increase expression of NR2E3 by itself but does not potentiate the effect of FTRI.

The expression of NR2E3 protein in cells cultured with FTRI in the presence of TNF-α was increased when compared to untreated control cells ($p<0.05$) (Figure 2-26C). However, there was no difference in NR2E3 protein expression between cells cultured with FTRI in the absence or presence of TNF-α and the expression of this protein was not modified by culturing cells with TNF-α alone. This suggests that TNF-α does not inhibit the rod photoreceptor precursor differentiation of MIO-M1 cells induced by FTRI.

Likewise, cells cultured with FTRI in the presence of IL-6 showed a similar increased expression of NR2E3 protein when compared to untreated control cells ($p<0.01$) (Figure 2-26D). NR2E3 protein expression was not altered in cells cultured with IL-6 alone as compared to untreated control cells. This suggests

that IL-6 does not affect the induced differentiation of MIO-M1 cells into rod photoreceptor precursors by FTRI.

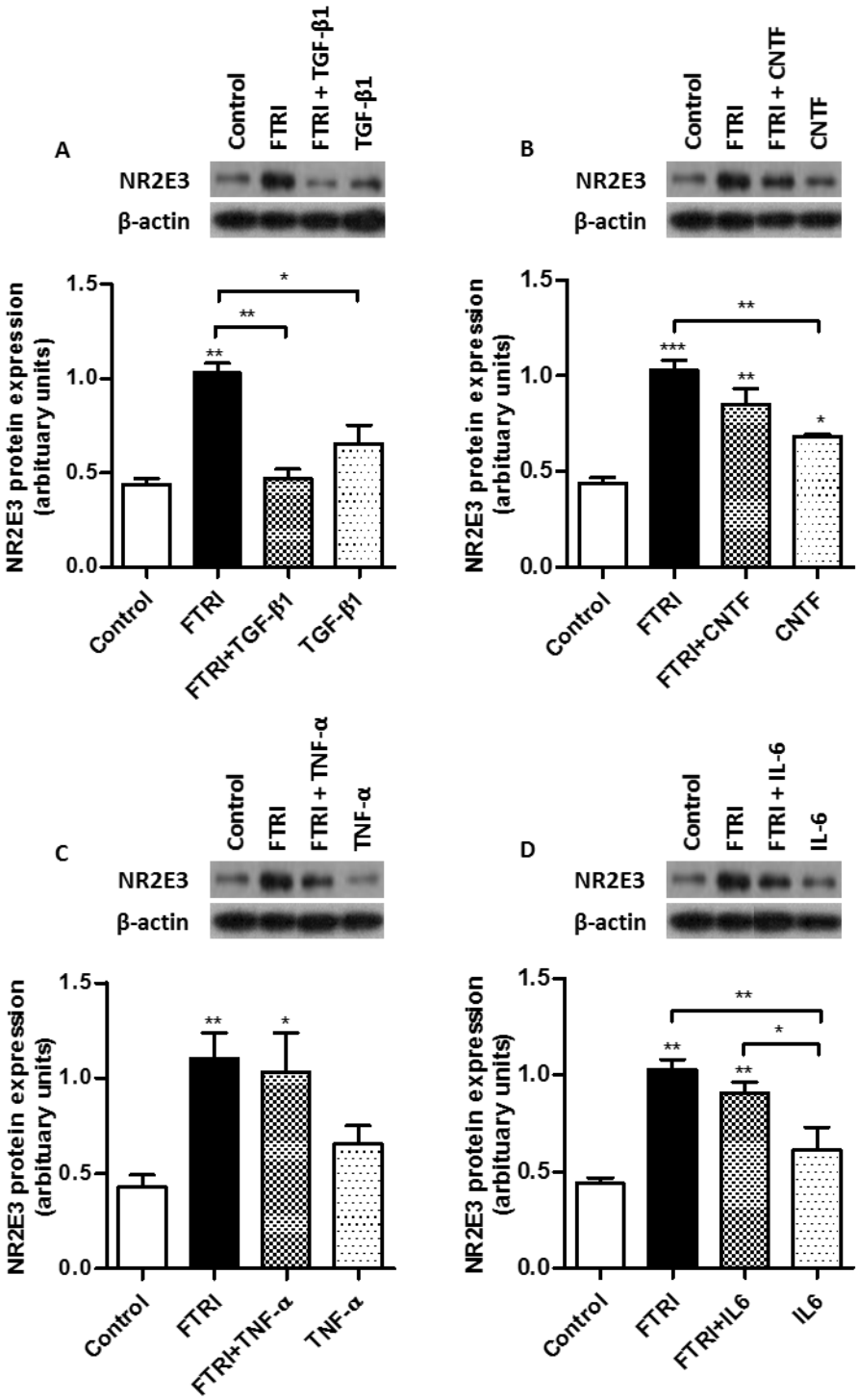

Figure 2-26: Protein expression of NR2E3 by MIO-M1 cells cultured with FTRI in the presence or absence of inflammatory cytokines.
Representative western blot bands showing NR2E3 and β-actin expression shown above bar charts. Bar charts represent NR2E3 protein normalised to β-actin (mean +/- SEM). **(A)** Cells cultured with FTRI in the presence of TGF-β1 showed decreased NR2E3 protein expression when compared to cells cultured with FTRI alone. **(B)** Cells cultured with CNTF alone or FTRI combined with CNTF showed increased NR2E3 protein expression as compared with untreated control cells. **(C)** Addition of TNF-α to cells cultured with FTRI did not modify protein expression of NR2E3 induced by FTRI alone. **(D)** Müller glia cultured with FTRI in the presence of IL-6 showed a similar increased NR2E3 protein expression as in cells cultured with FTRI alone. One-way ANOVA and Tukey post-test, $p<0.05$, N= 3.

2.3.8 GFAP expression in MIO-M1 cells cultured with FTRI

mRNA and protein expression of GFAP was investigated in MIO-M1 cells after 6 days culture with FTRI, used to induce differentiation of these cells into rod photoreceptor precursors. There was a statistically significant decrease in GFAP mRNA expression in cells cultured with FTRI when compared to untreated control cells ($p<0.001$) (Figure 2-27). Protein expression of GFAP was also decreased in cells cultured with FTRI compared to untreated control cells but this was not statistically significant (Figure 2-28)

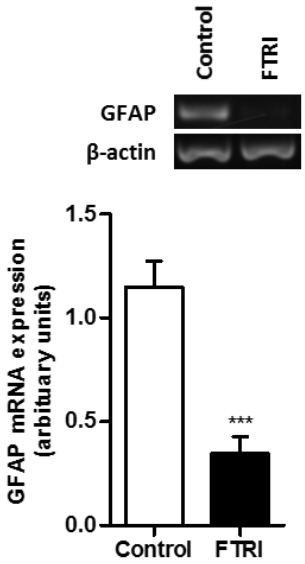

Figure 2-27: mRNA expression of GFAP by untreated control cells and cells cultured with FTRI. Representative PCR bands showing GFAP and β-actin expression above bar chart. Bar chart represents GFAP mRNA expression normalised to β-actin (mean +/- SEM). There was a significant downregulation of GFAP mRNA in cells induced to differentiate by FTRI as compared to control cells. Student's T-Test, $p< 0.001$, N= 17.

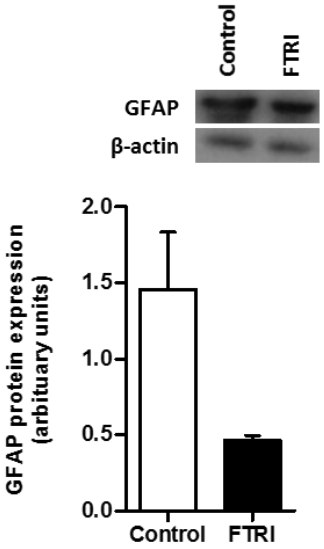

Figure 2-28: Protein expression of GFAP by MIO-M1 cells induced to differentiate into photoreceptor precursors by FTRI. Representative western blot bands showing GFAP and β-actin expression above bar chart. Bar chart represents GFAP protein expression normalised to β-actin (mean +/- SEM). Expression of GFAP protein was decreased in cells cultured with FTRI although this was not significant. Student's T-test, $p>0.05$, N=3**.**

2.3.9 Effect of inflammatory cytokines on GFAP expression by MIO-M1 cells cultured with FTRI

Because there was evidence of GFAP regulation in MIO-M1 cells cultured with FTRI, it was investigated whether the mechanisms of GFAP downregulation could be potentiated or inhibited by the inflammatory cytokines. For this purpose, Müller glia were cultured in the presence of FTRI alone, FTRI in combination with TGF-β1, IL-6, TNF-α or IL-6 and each cytokine alone.

2.3.9.1 Expression of GFAP mRNA in MIO-M1 cells cultured with FTRI in the presence of inflammatory cytokines

As previously observed, there was a significant downregulation of GFAP mRNA expression when MIO-M1 cells were cultured with FTRI alone when compared to untreated control cells ($p<0.05$) (Figure 2-29).

When MIO-M1 cells were cultured with TGF-β1 alone there was no change in GFAP mRNA expression as compared to untreated control cells (Figure 2-29A). However, when these cells were induced to differentiate in the presence of TGF-β1 there was a significant decrease in GFAP mRNA expression compared to untreated control cells ($p<0.05$). In this experiment, cells cultured with FTRI alone showed downregulation of GFAP mRNA expression although this was not statistically significant when compared to untreated control cells. Yet, there was no difference in GFAP mRNA expression between cells cultured with FTRI in the absence or presence of TGF-β1, which suggests the that induced differentiation into photoreceptor precursors is responsible for the GFAP downregulation regardless of TGF-β1 presence.

Experiments in which MIO-M1 cells were cultured with CNTF (Figure 2-29B) or IL-6 (Figure 2-29D) alone, showed that GFAP mRNA expression was not modified when compared to untreated controls. This correlated with previous results. When cells were cultured with FTRI in the presence of CNTF or IL-6 there was a significant decrease in GFAP mRNA expression similar to that seen in cells cultured with FTRI alone when compared to untreated controls ($p<0.05$). This suggests that induction of MIO-M1 cell differentiation into photoreceptor precursors modifies GFAP mRNA expression irrespective of the presence of these cytokines.

MIO-M1 cells cultured with TNF-α alone showed a significant downregulation of GFAP mRNA expression when compared to untreated control cells ($p<0.01$) (Figure 2-29C). Also, when cells were cultured with FTRI in combination with TNF-α there was a significant decrease in GFAP mRNA expression compared to untreated control cells ($p<0.01$). However, there was no difference in mRNA expression of GFAP between cells cultured with FTRI alone or cells cultured with FTRI in the presence of TNF-α, suggesting that the two mechanisms of GFAP downregulation by these factors may be driven by separate pathways.

2.3.9.2 Expression of GFAP protein in MIO-M1 cells cultured with FTRI in the presence of inflammatory cytokines

GFAP protein expression was also investigated in MIO-M1 cells cultured with FTRI in the absence and presence of TGF-β1, IL-6, TNF-α or CNTF. Results showed that although GFAP protein expression was downregulated in MIO-M1 cells cultured with FTRI alone, this was not statistically significant in all experiments (Figure 2-30).

When MIO-M1 cells were cultured with FTRI combined with TGF-β1 there was a significant decrease in GFAP protein expression when compared to untreated control cells ($p<0.05$) (Figure 2-30A). The downregulation of GFAP protein was also observed in cells cultured with TGF-β1 alone when compared to controls, which does not correlate with that seen in mRNA expression.

MIO-M1 cells cultured with CNTF alone significantly upregulated GFAP protein expression when compared to cells cultured with FTRI alone ($p<0.05$) but not when compared to control untreated cells (Figure 2-30B). Culturing these cells with FTRI in the presence of CNTF caused a decrease in protein expression of GFAP when compared to controls, similar to that seen in mRNA expression, but this was not statistically significant.

Similar to that observed with mRNA expression, GFAP protein expression was significantly downregulated by FTRI in the presence of TNF-α when compared to untreated control cells ($p<0.05$) and did not differ from that seen in cells cultured with TNF-α alone (Figure 2-30C). There was no difference in GFAP protein expression when cells were cultured with FTRI in the absence or the presence of TNF-α.

When MIO-M1 cells were cultured with FTRI in the presence of IL-6, GFAP protein expression was slightly decreased when compared to untreated control cells (Figure 2-30D). Although not significant, this observation matched what was seen with GFAP mRNA expression. Cells cultured with IL-6 alone did not show any changes in GFAP protein expression compared to control cells, similar to previous observations.

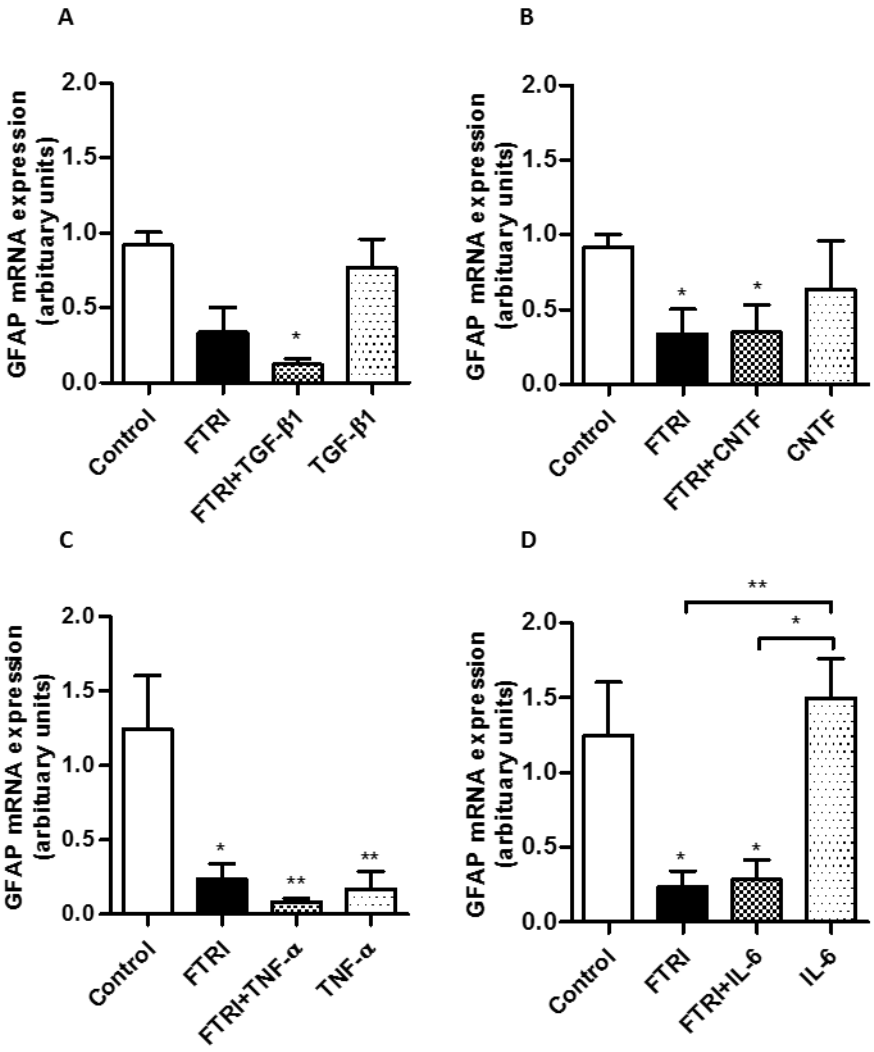

Figure 2-29: GFAP mRNA expression by MIO-M1 cells cultured with FTRI in the absence or presence of inflammatory cytokines.
Bar charts represent GFAP mRNA expression normalised to β-actin (mean +/- SEM). **(A)** Cells cultured with FTRI in the presence of TGF-β1 showed decreased GFAP mRNA expression when compared to control untreated cells. Culture with TGF-β1 alone did not modify expression of GFAP mRNA (N=4). **(B)** Cells cultured with FTRI in the presence of CNTF showed decreased GFAP mRNA expression when compared to untreated control cells, similar to that seen in cells cultured with FTRI alone. Cells cultured with CNTF alone showed no change in GFAP mRNA expression as compared to control cells (N=4). **(C)** MIO-M1 cells cultured with FTRI in the presence of TNF-α showed significant downregulation of GFAP mRNA expression when compared to untreated control cells. Additionally, cells cultured with TNF-α alone showed significant decrease in mRNA expression of GFAP when compared to control cells (N= 5). **(D)** Cells cultured with FTRI in the presence of IL-6 also showed a significant decrease in mRNA expression of GFAP when compared to untreated control cells. However, GFAP mRNA expression was not modified in cells cultured with IL-6 alone (N=5). One-way ANOVA and Tukey post-test, $p<0.05$.

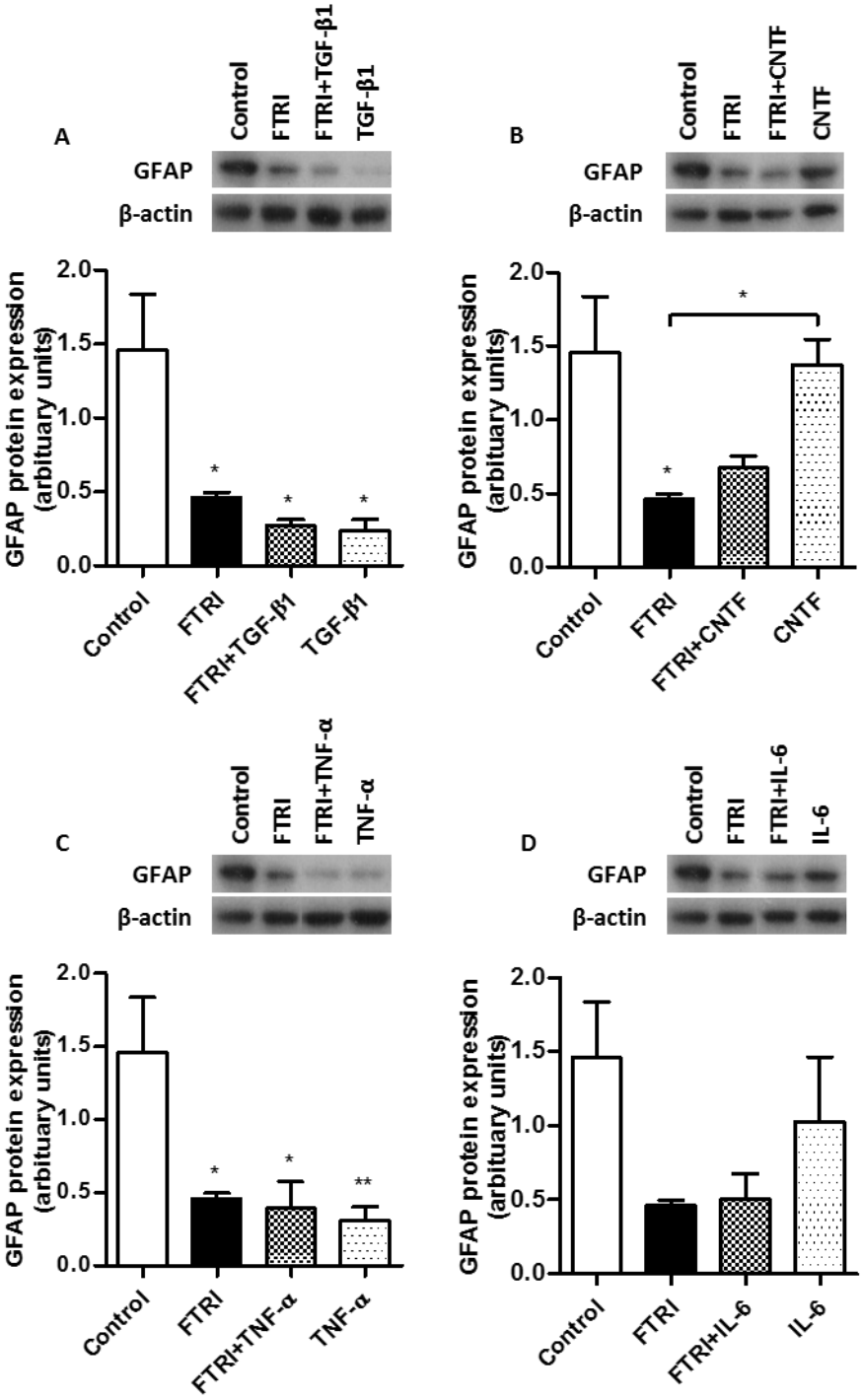

Figure 2-30: Protein expression of GFAP by MIO-M1 cells cultured with FTRI in the absence or presence of inflammatory cytokines.
Representative western blot bands show GFAP and β-actin expression shown above bar charts. Bar charts represent GFAP protein normalised to β-actin (mean +/- SEM). **(A)** Cells cultured with FTRI in the presence of TGF-β1 showed decreased GFAP protein expression when compared to control untreated cells. Culture with TGF-β1 alone also significantly decreased GFAP protein expression. **(B)** Cells cultured with FTRI in the presence of CNTF showed slightly decreased GFAP protein expression when compared to untreated control cells. Cells cultured with CNTF alone showed no change in GFAP protein expression as compared to control cells. **(C)** MIO-M1 cells cultured with FTRI in the presence of TNF-α showed significant downregulation of GFAP protein expression when compared to untreated control cells. Additionally, cells cultured with TNF-α alone showed significant decrease in protein expression of GFAP when compared to control cells. **(D)** Cells cultured with FTRI in the presence of IL-6 showed a decrease in protein expression of GFAP when compared to untreated control cells, although this was not significant. GFAP protein expression was not modified in cells cultured with IL-6 alone. One-way ANOVA and Tukey post-test, $p<0.05$, N=3.

2.4 Discussion

2.4.1 Pro-inflammatory cytokines modulate expression of gliosis-associated proteins in MIO-M1 cells

Of the gliosis-associated proteins investigated for modulation by pro-inflammatory cytokines in the MIO-M1 cell line, only GFAP was downregulated by TNF-α. Culture of MIO-M1 cells with increasing concentrations of TNF-α significantly downregulated gene and protein expression of GFAP in a dose-dependent manner. This was surprising because TNF-α is implicated in gliosis in mammals and is increased in retinal diseases such as glaucoma (Tezel et al., 2001) and diabetic retinopathy (Demircan et al., 2006). Other studies have shown that when rat cerebral astrocytes are cultured with TNF-α there is a powerful upregulation of GFAP, caused by activation of mitogen activated protein kinase Erk2 (Zhang et al., 2000). Additionally, porcine retinal explants treated with TNF-α have shown an increased GFAP expression in the cell bodies and processes of Müller cells which extended across the entire retina (Fernandez-Bueno et al., 2013). However, the present results suggest that in MIO-M1 cells, TNF-α may not be promoting gliosis. This is in accordance to that observed in rat brain astrocytes, in which TNF-α reduces protein expression of GFAP *in vitro* and may not be responsible for reactive changes in astrocytes during neurodegenerative diseases (Edwards and Robinson, 2006). This downregulation of GFAP induced by TNF-α in MIO-M1 cells may also resemble the anti-gliotic properties of this cytokine observed in zebrafish, in which TNF-α induces Müller glia to re-enter the cell cycle (Nelson et al., 2013). In this present study, it was found that TNF-α is not cytotoxic for MIO-M1 cells. This is in agreement with observations by others that TNF-α does not affect viability of astrocytes (Edwards and Robinson, 2006). Proteomic analysis of human glaucomatous retina detected not only apoptotic and cell death signals, but activation of NFκB, which promotes cell survival and can protect cells from TNF-α cytotoxicity (Beg and Baltimore, 1996, Yang et al., 2011). On this basis, it would be important to investigate the downstream targets of TNF-α in MIO-M1 cells and this was explored later in this thesis.

The present results show that MIO-M1 cells cultured with TGF-β1 caused downregulation of both mRNA and protein expression of GFAP, which conflicts with existing literature. Stimulation of bovine Müller glia *in vitro* with exogenous

TGF-β1 has been shown to increase GFAP expression in a dose-dependent manner (Hisatomi et al., 2002). This cytokine has also been shown to have an important role in scar formation in rodent CNS as brain lesions are associated with an increase in TGF-β1 and GFAP expression *in vivo*. In addition, infusion of TGF-β1 into the uninjured rat lateral ventricle, induced GFAP mRNA expression in a dose-dependent manner (Laping et al., 1994). This suggests that TGF-β1 plays a role in promoting gliosis and inducing GFAP expression, which was not seen in MIO-M1 cells cultured with TGF-β1 *in vitro*.

TGF-β1 is also known to regulate expression of the IF protein vimentin within the retina. Induction of PVR in rabbits results in increased TGF-β1 in the aqueous humor and vitreous, with a correlated increase in vimentin protein expression in the retina (Hoerster et al., 2014). Additionally, neurotoxin damage to rodent retinae has shown to increase vimentin protein expression in Müller glia (Das et al., 2006). However, Wu et al found that the human vimentin gene does not contain a canonical TGF-β1 response element (Wu et al., 2007), which could explain why vimentin is not modified by TGF-β1 in MIO-M1 cells. Extensive research has been carried out on GFAP/vimentin knockout mice to better understand the roles of these two IFs. Double knockout astrocytes can encourage neuronal proliferation *in vitro* and *in vivo* in mouse retinas lacking GFAP and vimentin, significantly improves migration and integration of transplanted retinal cells (Menet et al., 2001, Kinouchi et al., 2003). This suggests that regulation of vimentin, as well as GFAP, would be beneficial for regeneration but this was not observed in MIO-M1 cells cultured with any of the inflammatory cytokines investigated.

Of the pro-inflammatory cytokines tested, TNF-α and TGF-β1 downregulated the expression of the gliosis-associated protein tenascin in MIO-M1cells. Genetically modified mice lacking tenascin had significantly reduced Müller glia and inducing Müller glia from these animals to de-differentiate by FGF-2 showed reduced proliferation *in vitro* (Besser et al., 2012). This suggests that tenascin influences Müller glia behaviour of retinal progenitor cells. It was surprising that TGF-β1, which is significantly elevated in gliosis (Prendes et al., 2013), downregulated tenascin expression in MIO-M1 cells because in astrocytes this cytokine robustly increases tenascin expression (Smith and Hale, 1997). Additionally, astrocytes cultured with IL-6, CNTF or TNF-α did not

show changes in tenascin expression. This correlates with the current results in which IL-6 and CNTF did not modify tenascin expression in MIO-M1 cells, whilst it also does not correlate with the results in which TNF-α downregulates tenascin expression. However, in a rat glaucoma model, tenascin upregulation occurs before Müller cell gliosis, suggesting that pro-inflammatory cytokines associated with gliosis may not regulate this protein in the retina (Reinehr et al., 2016). Alternatively, it may be that other mechanisms control the production of tenascin in Müller glial cells.

Expression of IL-6 increases in patients with glaucoma and in animal models of retinal neurodegeneration (Chen et al., 1999, Sims et al., 2012) and it is possible that Müller glia are a source of local IL-6 production in the retina (Yoshida et al., 2001). It has been previously shown that culture of human astrocytes with IL-6 significantly increased expression of GFAP and vimentin (Pogue et al., 2010). In this investigation, culturing MIO-M1 cells with exogenous IL-6 did not modify the expression of gliosis-associated proteins tenascin, vimentin, procollagen galactosyltransferase or galectin. Studies by others showed that in the chick retina, intraocular injection of IL-6 did not activate Müller glia and did not modify GFAP expression (Fischer et al., 2014). Furthermore, IL-6 injection into mouse eyes caused a weak upregulation of GFAP in Müller glia (Wang et al., 2002) and immunohistochemical staining of mouse retina revealed a spatial variation in IL-6 signalling. Sims et al found that there was a mosaic staining of IL-6 and its receptor within the different cell layers of the retina, which is of interests as in animal models with raised IOP, RGCs are the main target of IL-6 signalling (Sims et al., 2012). From the present results and observations by others, it may be possible to suggest that MIO-M1 cells do not respond to IL-6 during reactive gliosis. However, the current study only used one reference gene (β-actin) in the semi-quantitative analysis, which may not maintain a constant level of expression in MIO-M1 cells in the different culture conditions, in particular TNF-α, which has been previously reported to affect its expression in other conditions (Kohno et al., 1993). As such, the data presented here would be strengthened by validating the expression of both the genes of interest and β-actin against a second reference gene.

As CNTF is a member of the IL-6 family of pro-inflammatory cytokines, the effect of CNTF on gliosis-associated proteins was also examined. In the mouse retina *in vivo* injection of CNTF can increase GFAP expression throughout the retina and specifically induces GFAP gene expression in Müller glia through Stat3-phosphorylation (Wang et al., 2002). However, culture of MIO-M1 cells with CNTF did not upregulate GFAP mRNA expression. This contrasts with other reports that found that retinal progenitor cells show specific concentration-dependent increase in GFAP expression by CNTF (Bhattacharya et al., 2008). In these studies, only concentrations of CNTF above 100ng/ml caused increased expression of GFAP and vimentin. In the present study the highest concentration of CNTF used was 100ng/ml, so it may be that higher doses are required to induce changes in the expression of gliosis-associated proteins in MIO-M1 cells. Another explanation could be that CNTF does not affect gliosis but instead promotes neuroprotection in the retina. This is suggested by observations that human CNTF expressed in mouse retina acts directly on Müller glia to induce production of neurotrophic factors that promote photoreceptor survival (Rhee et al., 2013).

None of the inflammatory cytokines examined showed any effect on the expression of the gliosis-associated protein galectin-1. In the zebrafish retina, galectin-1-like protein Drgal1-L2 becomes increased in proliferating Müller glia and neural progenitors after photoreceptor damage (Craig et al., 2010). In rats, photoreceptor degeneration caused by constant light exposure has also been reported to increase the expression of galectin-1 in Müller glia (Uehara et al., 2001). Exogenous TGF-β1 can also induce galectin expression in HKC cells, an immortalized human renal epithelial cell line (Okano et al., 2010). In addition, human lung fibroblasts treated *in vitro* with TGF-β1 showed increased expression of galectin-1, accelerating fibrosis (Jin Lim et al., 2014). It is of interest however, that neither TGF-β1 or any of the inflammatory cytokines investigated in this study had any effect on galectin-1 expression in MIO-M1 cells.

2.4.2 Rod photoreceptor precursor differentiation of MIO-M1 cells

When MIO-M1 cells were induced to differentiate into rod photoreceptor precursors by culturing with FGF-2, taurine, retinoic acid and IGF-1 (FTRI) there was an obvious morphological difference in the treated cells as compared to

controls. However, it was not possible to show that mRNA expression of *NR2E3* and recoverin, which are genes associated with photoreceptor development, significantly increased after FTRI treatment. Even though the PCR primers were designed based on their specificity to each gene and rigorously tested to optimise the PCR method, PCR tests performed on different occasions showed inconsistent results. On this basis, real-time qPCR was performed as it is a more robust method. However, significant changes in expression of these genes were not observed. It may be that these genes of interest are very sensitive to the PCR methods used or they may be constitutively expressed at high levels and therefore it is difficult to assess changes using PCR methods. Nonetheless, protein expression of NR2E3 significantly increased in MIO-M1 cells cultured with FTRI, which is in agreement with previous studies (Jayaram et al., 2014). Recoverin protein expression was not tested.

In this study it was also observed that GFAP mRNA and protein expression significantly decreased in MIO-M1 cells cultured with FTRI. Fischer and Reh noted that after retinal damage in postnatal chick, those Müller glial cells which do not increase GFAP expression are the ones which re-enter the cell cycle (Fischer and Reh, 2003). It could be possible that when Müller glial cells are induced to differentiate they downregulate GFAP expression to allow entry into the cell cycle. Furthermore, as GFAP is not expressed in photoreceptor cells in the retina and the MIO-M1 cells showed reduction in GFAP expression following FTRI treatment, this may indicate that these cells were differentiating. Additionally, cells induced to differentiate in the presence of TGF-β1 or TNF-α also showed downregulation of GFAP mRNA and protein expression compared to untreated control cells. This decreased GFAP expression was similar in cells treated with FTRI alone or with TNF-α or TGF-β1 alone. This suggests that these inflammatory cytokines and FTRI treatment do not act synergistically to regulate GFAP. Even though differentiation in the presence of IL-6 or CNTF decreased protein expression of GFAP in MIO-M1 cells, this was not statistically significant, indicating cytokine specific functions in gliosis.

Examination of cells cultured with FTRI in conjunction with the inflammatory cytokines TGF-β1, TNF-α, IL-6 or CNTF did not significantly modify NR2E3 mRNA expression. Recoverin mRNA expression was also not modified in cells cultured with FTRI in the presence of TGF-β1, IL-6 or CNTF. However, when

Müller glial cells were cultured with FTRI in the presence of TNF-α there was a significant increase in recoverin mRNA expression compared to controls. This suggests that TNF-α may be potentiating the differentiation of Müller glial stem cells by FTRI. In zebrafish, *in vivo* co-injection of TNF-α and a Notch inhibitor into undamaged retina, significantly increased the number of proliferating Müller glia which re-entered the cell cycle (Conner et al., 2014). This combination produced neuronal progenitors that differentiated into some but not all retinal neurons, mimicking the regenerating retina. As TNF-α also caused down regulation of GFAP, it may allow the MIO-M1 cells to adopt a neural lineage in the presence of FTRI, in a similar way to that seen in the zebrafish.

When examining protein expression of MIO-M1 cells cultured with FTRI in the presence of inflammatory cytokines, there was a significant increase in NR2E3 expression. Cells induced to differentiate into rod photoreceptor precursors in the presence of TNF-α, CNTF and IL-6 also significantly increased protein expression of NR2E3, suggesting that these cytokines are not inhibiting Müller glia differentiation induced by FTRI. In contrast, protein expression of NR2E3 was significantly downregulated in cells cultured with FTRI in the presence of TGF-β1 when compared to cells cultured with FTRI alone. This suggests that TGF-β1 inhibits rod photoreceptor precursor differentiation of Müller glia induced by FTRI, and this confirms previous published studies (Angbohang et al., 2015).

Interestingly, compared to controls, cells cultured with CNTF alone showed increased NR2E3 protein expression, suggesting that CNTF alone has the ability to induce a degree of rod photoreceptor precursor differentiation in MIO-M1 cells. However, this is not as marked as differentiation induced by FTRI alone. In early postnatal mouse retina, CNTF has been shown to regulate rod photoreceptor differentiation (Rhee et al., 2004) supporting the suggestion that CNTF may cause rod photoreceptor precursor differentiation of MIO-M1 cells *in vitro*.

In conclusion, this chapter has shown that GFAP is significantly downregulated by TNF-α and TGF-β1 but only TNF-α does not prevent induced rod photoreceptor precursor differentiation of MIO-M1 cells. These results suggest a role of TNF-α in MIO-M1 cell GFAP regulation and further investigation of this

mechanism is required. Downstream signalling of TNF-α was studied further in the next chapter of this thesis.

Chapter 3 TNF-α signalling in Müller glial MIO-M1 cells

3.1 Introduction

3.1.1 Role of TNF-α in gliosis and neurodegenerative disease

The inflammatory cytokine TNF-α may have degenerative properties in the retina. TNF-α is found upregulated in the retina from patients with many retinal degenerative diseases including PVR, diabetic retinopathy, retinitis pigmentosa and glaucoma (Eastlake et al., 2016, Limb et al., 1996, Ghanem AA, 2010, Martínez-Fernández de la Cámara et al., 2014). Chronic high IOP in mouse models has shown to cause rapid upregulation of TNF-α leading to loss of RGCs, whilst injection of TNF-α into normal eyes induces significant RGC loss, implicating TNF-α and inflammation in the pathogenesis of glaucoma (Nakazawa et al., 2006b). After *in vivo* optic nerve crush injury leading to RGC cell death, astrocytes increase expression of TNF-α along with GFAP, further suggesting a role for this cytokine in retinal degenerative gliotic responses (Tezel et al., 2004). TNF-α can act directly on Müller glial cells, as demonstrated by studies in which porcine retinal explants cultured with exogenous TNF-α showed marked upregulation of GFAP in Müller glial cells. This coincided with extensive photoreceptor disorganisation, indicating that TNF-α plays an integral part in reactive retinal gliosis (Fernandez-Bueno et al., 2013).

Explant studies in which retinitis pigmentosa, characterised by retinal degeneration and reactive Müller cell gliosis, is induced, blocking TNF-α with Infliximab significantly reduced Müller glia expression of GFAP and prevented photoreceptor cell death (Martínez-Fernández de la Cámara et al., 2014). Moreover, *in vitro* stimulation of mouse Müller glia with TNF-α resulted in increased expression of genes coding for pro-inflammatory cytokines, neurotoxic chemokines and enzymes producing reactive oxygen and nitrogen species, which all contribute to cell death (Dvoriantchikova and Ivanov, 2014). During gliosis, Müller glial cells can also be a source of elevated TNF-α (Xue et al., 2011, Kumar and Shamsuddin, 2012, Eastlake et al., 2016). Indeed, glaucoma-related induced stress of rat Müller glia *in vitro* does not affect cell death but amplifies secretion of TNF-α (Tezel and Wax, 2000). This production of TNF-α by Müller glia can target other retinal cell types.

Another TNF-α regulated signalling cascade involved in neurodegeneration is through production of reactive nitrogen species; TNF-α activation of Müller glia induces nitric oxide expression which is cytotoxic to retinal neurons (Agarwal and Agarwal, 2012). An enzyme that produces reactive nitrogen species is nitric oxide synthase-2 (NOS2) and Müller glia from TNF-α knockout mice produce less NOS2 after stimulation. This suggests that endogenous TNF-α production by Müller glia causes a detrimental inflammatory response in the retina (Goureau et al., 1997).

TNF-α and TNF-α regulated signalling is capable not only of mediating neurotoxicity and degeneration, but also neuroprotection. In mammalian CNS astrocytes, TNF-α reduces GFAP expression and does not affect viability *in vitro* (Edwards and Robinson, 2006). In addition, *in vivo* injury-induced gliosis does not require elevated expression of TNF-α in rodents (Little et al., 2002). This suggests that TNF-α may not cause reactive astrogliosis in neurodegenerative diseases. In human glaucomatous retinal samples, the survival-promoting pathways of TNF-α signalling are also activated indicating a protective role of TNF-α (Yang et al., 2011). Additionally, TNF-α deficient Müller glia in zebrafish have reduced proliferation suggesting that TNF-α produced by Müller glial cells themselves may encourage cell-cycle re-entry (Nelson et al., 2013). This identifies TNF-α signalling as essential in endogenous regeneration in the zebrafish and potentially protective in the mammalian retina.

3.1.2 TNF-α signalling pathway

It is apparent that TNF-α can have both neuroprotective and neurodegenerative effects depending on signalling through its two receptor (TNFR1 or TNFR2) (Agarwal and Agarwal, 2012). TNFR1 is proapoptotic in neurodegenerative diseases, where activation of TNFR1 recruits Fas-Associated Death Domain (FADD) and TNF Receptor-Associated Death Domain (TRADD) and downstream caspase 8 and subsequently caspase 3 are activated, which have a crucial role in initiating the proteolysis cascade, resulting in apoptosis (Figure 3-1). Using an *in vivo* retinal ischemia model, upregulation of TNF-α and both receptors TNFR1 and TNFR2 has been shown to precede neuronal cell death (Fontaine et al., 2002). In human glaucomatous eyes TNF-α immunostaining is localised to Müller glial cell bodies and processes, whereas TNF-α receptor-1 (TNFR1) is mainly localised to the RGC layer (Tezel et al., 2001). When

conditioned medium of cultured Müller glia was used to culture RGCs there was increased RGC apoptosis (Tezel and Wax, 2000). Furthermore, mice deficient in TNFR1 when subjected to optic nerve crush injury show well-preserved retinal structure, minimal axonal degeneration and reduced RGC loss compared to wild type mice (Tezel et al., 2004). This implicates TNFR1 signalling in neurodegeneration.

Cell death after injury in TNF-α deficient mice surprisingly was not altered compared to wild type controls, but TNFR1 deficiency reduced cell death whilst TNFR2 knockout enhanced cell death (Fontaine et al., 2002). This indicates that TNF-α itself does not cause retinal neurodegeneration but the receptor it signals through can regulate injury-induced damage. TNFR2 promotes neuroprotection, as shown by evidence that TNFR2 causes release of the inhibitory protein Silencer of Death Domain (SODD) and allows it to be bound by TRADD, recruiting TNF Receptor Associated Factor 2 (TRAF2) and Receptor Interacting Protein (RIP). This leads to downstream activation of the transcription factor Nuclear Factor Kappa-light-chain-enhancer of activated B cells (NFκB) (Figure 3-1). NFκB activation by TNF-α induces genes involved in cell survival and cell proliferation (Agarwal and Agarwal, 2012, Beg and Baltimore, 1996).

The mammalian NFκB family consists of five subunits: NFκB1/p105, NF-κB2/p100, NFκB p65 (also known as RelA), RelB and c-Rel and these can form homodimers or heterodimers. The NFκB1/p105 and NF-κB2/p100 proteins are cytoplasmic inhibitory precursors and their degradation leads to formation of the active NFκB p50 and p52 proteins respectively (Albert S. Baldwin, 1996). Normally these active subunits are sequestered in the cytoplasm by complexing with the inhibitory protein Nuclear factor of kappa light polypeptide gene enhancer in B-cells inhibitor, alpha (IκBα). However, following TNF-α stimulation the IκBα protein dissociates, followed by rapid phosphorylation and degradation by the proteasome (Brown et al., 1995, Chen et al., 1995). The active NFκB complex can translocate to the nucleus where the different dimers recognise different DNA binding sites to regulate transcription of a variety of genes (Albert S. Baldwin, 1996). As well as being activated by TNF-α, NFκB can also stimulate production of TNF-α, consequently creating an autoregulation feedback loop (Sankar Ghosh et al., 1998).

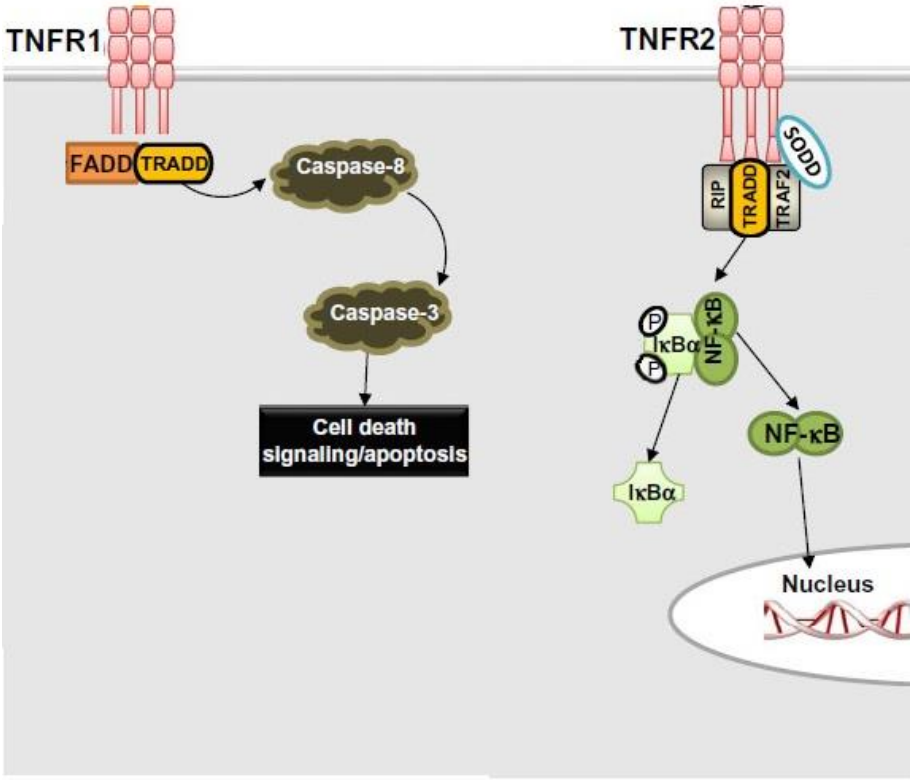

Figure 3-1:Illustration of the TNF-α signalling pathway through TNFR1 and TNFR2.
Adapted from (Urschel and Cicha, 2015). TNF-α can signal through two receptors, which are different from each other. The TNFR1 recruits FADD and TRADD, which activate caspase 8 followed by caspase 3, terminating in cell apoptosis. Meanwhile, TNFR2 signalling causes recruitment of TRADD, RIP, TRAF2 and SODD and downstream activation of NFκB. IκBα is phosphorylated and degrades, resulting in NFκB subunit being free to translocate to the nucleus where they behave as transcription factors for genes associated with cell survival.

Another regulatory process of TNF-α signalling results from the cell shedding of soluble TNF-receptors (sTNFR), which can act as inhibitors by binding free TNF-α and competing against cell surface TNFR1 and TNFR2. However, at lower concentrations sTNFRs can augment TNF-α activity by stabilising its structure and preserving its activity. This is illustrated by studies in human leukocytes incubated with TNF-α in the presence of exogenous sTNFR, in which cell death by TNF-α is initially prevented, but after 7 days of incubation stable cell death occurs (Aderka et al., 1992). Additionally, although TNF-α protein decays, sTNFR attenuates decay and augments TNF-α activity. It is of interest that soluble receptors are found increased in patients with diabetic retinopathy and inflammatory eye diseases (Limb et al., 1999, Bessa et al., 2012), indicating a possible regulatory role within the retinal environment during neurodegeneration.

Within the CNS and the retina TNF-α can have both toxic, including gliosis, and protective affects. This reaction could be tipped either way in a cell by a variety of factors including the extent of TNF-α activation in a cell, the concentration of and duration of exposure to TNF-α, the presence of other cytokines that act on a cell at the same time, the temporal exposure of other cytokines acting on the cell and the context of injury (Shohami et al., 1999, Tezel, 2008). For example, early rapid exposure to excessive TNF-α may recruit reactive nitrogen species causing a toxic response, while in later stages when TNF-α levels have declined, it may regulate NFκB to promote cell survival.

3.2 Objectives

The signalling pathway of TNF-α in Müller glial cells is not fully understood and exploration of this signalling may create insight into the regulatory role that TNF-α plays within the retinal environment during disease. TNF-α is found upregulated in retinal neurodegenerative diseases and can stimulate and be released by Müller glial cells. Depending on which receptor TNF-α activates determines the effect it can have on a cell, whether it be pro cell survival or detrimental apoptosis. Therefore, the aims of this chapter were to investigate the expression of TNF receptors by MIO-M1 cells and the activation of downstream targets including NFκB signalling. It is hypothesised that by identifying the downstream targets of TNF-α and investigating methods to

regulate these within the retinal environment may potentially have therapeutic potential for treating gliosis-associated retinal diseases.

The objectives of this chapter were:

1. To investigate the expression of TNFR1 and TNFR2 in MIO-M1 cells and how these receptors are affected by TNF-α *in vitro*.
2. To examine whether MIO-M1 cells release soluble TNF receptors when cultured with TNF-α.
3. To investigate the expression of NFκB signalling, including that of NFκB p105/50, NFκB p100/52, NFκB p65 and IκBα, in MIO-M1 cells stimulated by TNF-α *in vitro.*
4. To investigate the effect of inhibiting NFκB signalling on TNF-α mediated regulation of GFAP in MIO-M1 cells *in vitro*.
5. To examine whether factors that induce MIO-M1 cells to differentiate into rod photoreceptor precursors *in vitro* modified expression of NFκB signalling.

Experimental design:

I. RNA extracted from MIO-M1 cells that had been cultured with TNF-α for 6 days was used to examine the expression of mRNA coding for TNFR1, TNFR2, NFκB1 and NFκB2 using RT-PCR methods established in the laboratory.

II. Protein lysates from MIO-M1 cells cultured with increasing concentrations of TNF-α in the absence or presence of factors (FGF-2, taurine, retinoic acid and IGF-1) known to induce rod photoreceptor precursor differentiation were used to assess the expression of NFκB p105/50, NFκB p100/52 and IκBα. Western blot analysis was carried out using primary antibodies against proteins of interest and protocols established in our laboratory.

III. MIO-M1 cells cultured with TNF-α were immunostained with antibodies to NFκB p105/50 and NFκB p100/52 and examined under confocal fluorescence microscopy.

IV. Protein lysates from MIO-M1 cells cultured with 5ng/ml TNF-α over a 24 hour time lapse experiment were used to measure phosphorylation of NFκB p65 and IκBα using an ELISA kit. ELISA methods were also used

to measure concentrations of human soluble TNFR2 in supernatants collected from MIO-M1 cells cultured with increasing concentrations of TNF-α.

V. NFκB signalling was inhibited in MIO-M1 cells *in vitro* and protein expression of NFκB p105/50, IκBα and GFAP was assessed by western blot analysis. For this purpose, MIO-M1 cells were cultured with increasing concentrations of caffeic acid phenethyl ester (CAPE) for 24 hours and subsequently cultured with 5ng/ml of TNF-α for 5 days. Alternatively, cells were cultured with increasing concentrations of RO1069920 in the absence or presence of 5ng/ml of TNF-α for 6 days.

VI. Semi-quantitative statistical analysis of gene and protein expression was performed using Excel and GraphPad Prism programmes.

3.3 Results

3.3.1 Modulation of TNF-α receptors expression by TNF-α in MIO-M1 cells

In the previous chapter it was shown that TNF-α induced downregulation of GFAP in MIO-M1 cells. This led us to examine whether TNF-α receptors are also regulated by TNF-α. The actions of TNF-α are produced subsequent to binding to its cell surface receptors TNFR1 and/or TNFR2, which are functionally different. On this basis expression of these receptors was explored in MIO-M1 cells cultured with TNF-α for 6 days.

MIO-M1 cells were cultured with increasing concentrations of TNF-α in a dose-response manner and mRNA expression of the TNFR1 and TNFR2 genes were analysed (Figure 3-2). The results showed that there was no change in TNFR1 mRNA expression when MIO-M1 cells were cultured with TNF-α when compared to controls. However, there was a trend of increasing TNFR2 mRNA expression with increasing TNF-α concentration but this was only significant between cells cultured with the BSA vehicle control and cells cultured with TNF-α at a concentration of 50ng/ml ($p<0.05$) (Figure 3-2B).

Analysis by western blot was highly variable but untreated MIO-M1 cells expressed TNFR1 and TNFR2 proteins. Culturing MIO-M1 cells with increasing concentrations of TNF-α did not modify protein expression of TNFR1 (Figure 3-3A). However, expression of TNFR2 protein was altered in MIO-M1 cells cultured with increasing concentration of TNF-α (Figure 3-3B). The lower concentrations of TNF-α used, 0.5 and 5ng/ml, caused a significant increase in TNFR2 protein expression when compared to untreated control cells ($p<0.05$). The higher concentrations of TNF-α did not modify protein expression of TNFR2 when compared to untreated control cells.

An ELISA was used to measure the release of soluble TNFR2 (sTNFR2) into the cell culture medium of MIO-M1 cells cultured with TNF-α. Soluble TNFR2 derives from shedding of the extracellular domain of TNFR2 and the ELISA measurements included the amount of free receptor plus the amount of receptor bound to TNF-α. MIO-M1 cells cultured with 5, 50 and 500ng/ml TNF-α released significantly increased concentrations of sTNFR2 protein into cell supernatants when compared to untreated control cells and cells cultured with 0.5ng/ml TNF-α ($p<0.001$) (Figure 3-4). At a concentration of 0.5ng/ml, TNF-α

did not modify the release of sTNFR2. Additionally, there was a significant difference in concentration of sTNFR2 in supernatants of cells treated with both 5 and 50 ng/ml TNF-α and 5 and 500ng/ml ($p<0.001$).

3.3.2 Modulation of TNF-α receptors in MIO-M1 cells cultured with FTRI

MIO-M1 cells were induced to differentiate by addition of FTRI and the protein expression of TNFR1 and TNFR2 was measured. Culture with FTRI in the absence or presence of TNF-α did not modify the protein expression of TNFR1 or TNFR2 when compared to untreated control cells (Figure 3-5). Release of sTNFR2 was also not modified by culturing MIO-M1 cells with FTRI alone when compared to controls (Figure 3-6). However, the concentration of sTNFR2 in supernatants from cells cultured with FTRI in the presence of TNF-α was significantly upregulated when compared to supernatants from untreated control cells and cells cultured with FTRI alone ($p<0.05$).

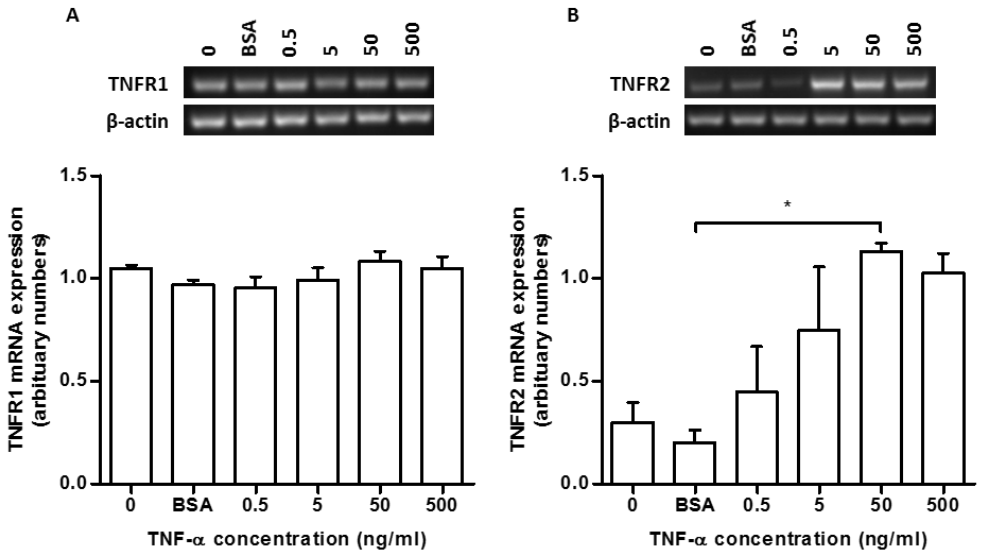

Figure 3-2: mRNA expression of TNF receptors by MIO-M1 cells cultured with increasing concentrations of TNF-α.
Representative images of PCR bands for TNF receptors and β-actin shown above bar charts. Bar charts show relative expression of receptor mRNA normalised to β-actin (mean +/- SEM). **(A)** There was no difference in TNFR1 mRNA expression in cells cultured with increasing concentrations of TNF-α when compared to untreated control cells. **(B)** TNFR2 mRNA expression was significantly upregulated in cells cultured with 50ng/ml TNF-α when compared to cells cultured with BSA control. One-way ANOVA and Tukey's post-test, $p<0.05$, N=3.

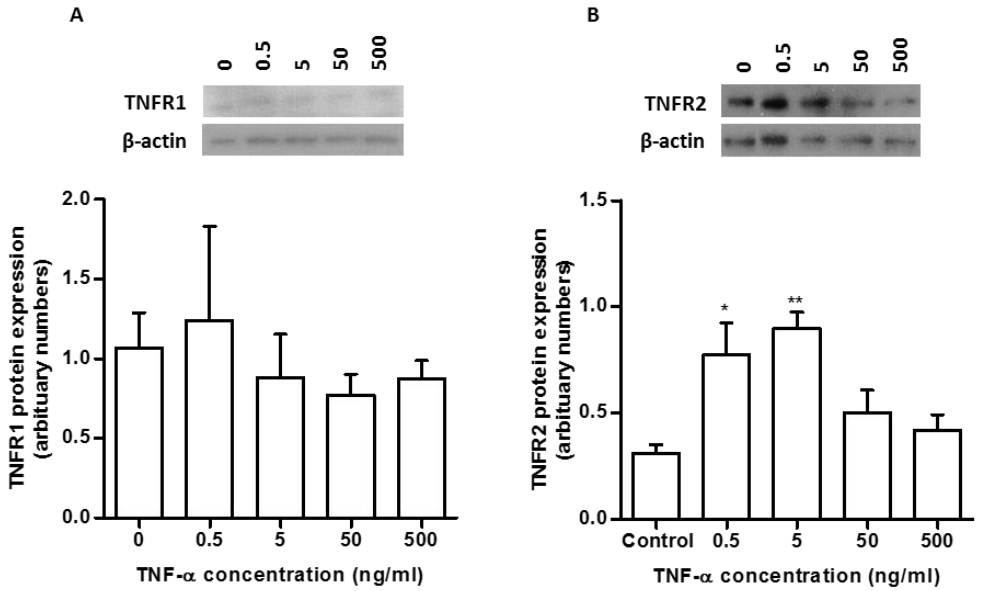

Figure 3-3: Protein expression of TNF receptors by MIO-M1 cells cultured with increasing concentrations of TNF-α.
Representative images of western blot bands for receptors and β-actin shown above bar charts. Bar charts show relative expression of protein normalised to β-actin (mean +/- SEM). **(A)** There was no significant difference in protein expression of TNFR1 in cells cultured with increasing concentrations of TNF-α when compared to untreated control cells. **(B)** TNFR2 protein expression was significantly increased in MIO-M1 cells cultured with 0.5 and 5ng/ml TNF-α when compared to control cells. One-way ANOVA and Tukey's post-test, $p<0.05$, N=3.

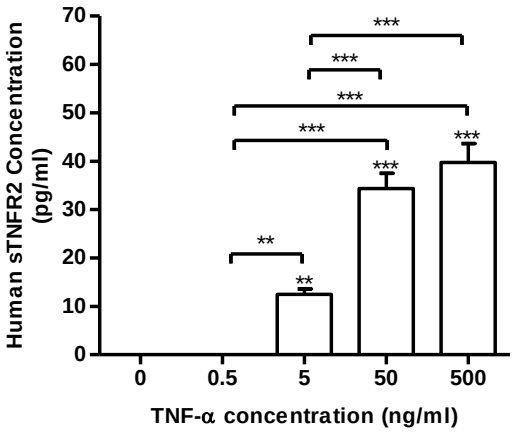

Figure 3-4: ELISA results for concentration of human sTNFR2 released by MIO-M1 cells cultured with increasing concentrations of TNF-α.
Bar chart represents sTNFR2 concentration (mean +/- SEM). There was a significant upregulation of sTNFR2 concentration in cell supernatant of MIO-M1 cells cultured with 5, 50 and 500ng/ml TNF-α as compared to untreated control cells and cells cultured with 0.5ng/ml TNF-α. One-way ANOVA and Tukey post-test, $p<0.005$, N=3.

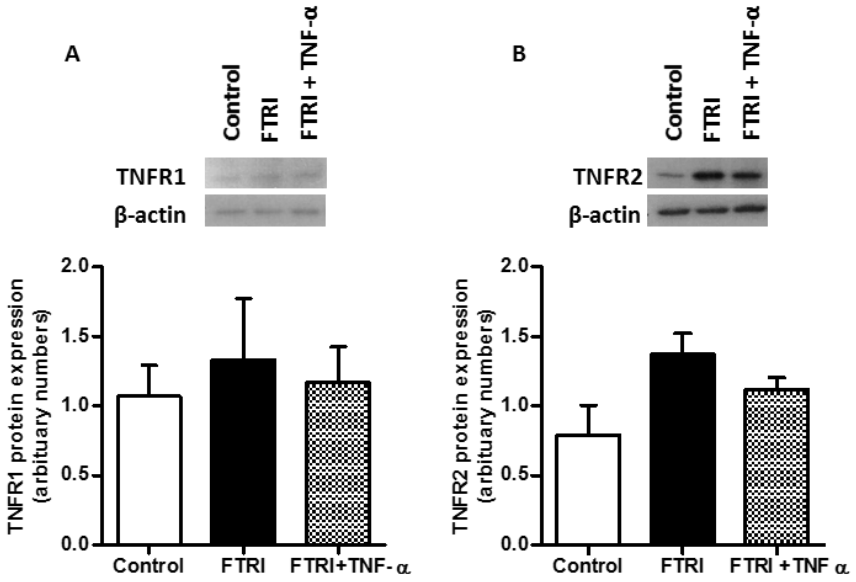

Figure 3-5: Protein expression of TNF receptors by MIO-M1 cells cultured with FTRI in the absence or presence of TNF-α.
Representative western blot bands showing receptors and β-actin expression shown above bar charts. Bar charts represent receptor protein expression normalised to β-actin (mean +/- SEM). **(A)** There was no significant difference in TNFR1 protein expression by cells cultured with FTRI in the absence or presence of TNF-α when compared to untreated control cells. **(B)** TNFR2 protein expression was not modified by culturing cells with FTRI in the absence or presence of TNF-α when compared to control cells. One-way ANOVA and Tukey post-test, $p>0.05$, N= 3.

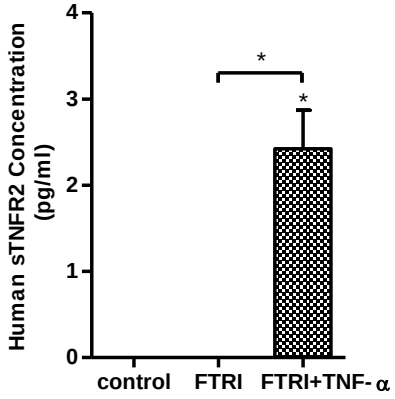

Figure 3-6: Concentration of released sTNFR2 protein by MIO-M1 cells cultured with FTRI in the absence or presence of TNF-α.
Bar chart represents sTNFR2 concentration (mean +/- SEM) as measured by ELISA. Cells cultured with FTRI in combination with TNF-α released significantly higher levels of sTNFR2 when compared to untreated control cells and cells cultured with FTRI alone. One-way ANOVA and Tukey post-test, $p<0.05$, N= 3.

3.3.3 Modulation by TNF-α of NFκB subunits expression in MIO-M1 cells

TNF-α binding to cell surface receptors induces downstream signalling and activation of NFκB. MIO-M1 cells were cultured with increasing concentrations of TNF-α and expression of NFκB mRNA and protein were examined.

MIO-M1 cells cultured for 6 days with increasing concentrations of TNF-α showed upregulation of NFκB1 and NFκB2 gene expression in a dose-response manner. mRNA expression of both NFκB1 and NFκB2 were significantly increased by cells cultured with 5, 50 and 500ng/ml TNF-α when compared to untreated control cells and when compared to cells cultured with 0.5ng/ml TNF-α ($p<0.05$) (Figure 3-7). There was also a significant upregulation in mRNA expression of NFκB1 between MIO-M1 cells cultured with 5 and 50ng/ml of TNF-α ($p<0.01$).

The protein expression regulated by the NFκB1 gene is NFκB p105/50. The NFκB p105 protein subunit is processed by proteolysis into NFκB p50, which forms a dimeric complex with Rel proteins and translocates to the nucleus to regulate gene transcription. Both NFκB p105 and NFκB p50 protein expression were increased by culturing MIO-M1 cells for 6 days with increasing concentrations of TNF-α (Figure 3-8). However, there was only a statistically significant upregulation of NFκB p50 protein expression in cells cultured with 5, 50 and 500ng/ml TNF-α when compared to untreated control cells ($p<0.05$) (Figure 3-8B).

The protein NFκB p100/52 is regulated by the NFκB2 gene. The NFκB p100 protein is proteolysed into NFκB p52, which forms a dimeric complex with Rel proteins and translocates to the nucleus to regulate gene transcription. NFκB p100 protein expression was significantly increased in MIO-M1 cells cultured for 6 days with increasing concentrations of TNF-α (Figure 3-9). However, this increase was not seen in NFκB p52 protein expression. The expression of NFκB p100 protein was significantly upregulated in MIO-M1 cells cultured with 500ng/ml TNF-α when compared to untreated control cells ($p<0.001$) and cells cultured with TNF-α at concentrations of 0.5 ($p<0.001$), 5 ($p<0.01$) and 50ng/ml ($p<0.05$) (Figure 3-9A).

MIO-M1 cells cultured with TNF-α were also analysed by immunofluorescence for expression of NFκB proteins. The proportion of stained cells was analysed

under confocal fluorescence microscopy. Immunofluorescent staining of untreated control MIO-M1 cells showed positive nuclei staining for both NFκB p105/50 and NFκB p100/52 proteins, at proportions of 12% and 42%, respectively. Quantification of the number of positive cells for NFκB p105/50 in MIO-M1 cells cultured in the presence of 50ng/ml of TNF-α revealed that an average of 31% of cells had stained their nuclei, which was a significant increase when compared to untreated control cells ($p<0.05$) (Figure 3-10). There was no significant difference in the number of NFκB p100/52 positive stained nuclei in MIO-M1 cells cultured with both 5 and 50ng/ml of TNF-α when compared to untreated control cells (Figure 3-11).

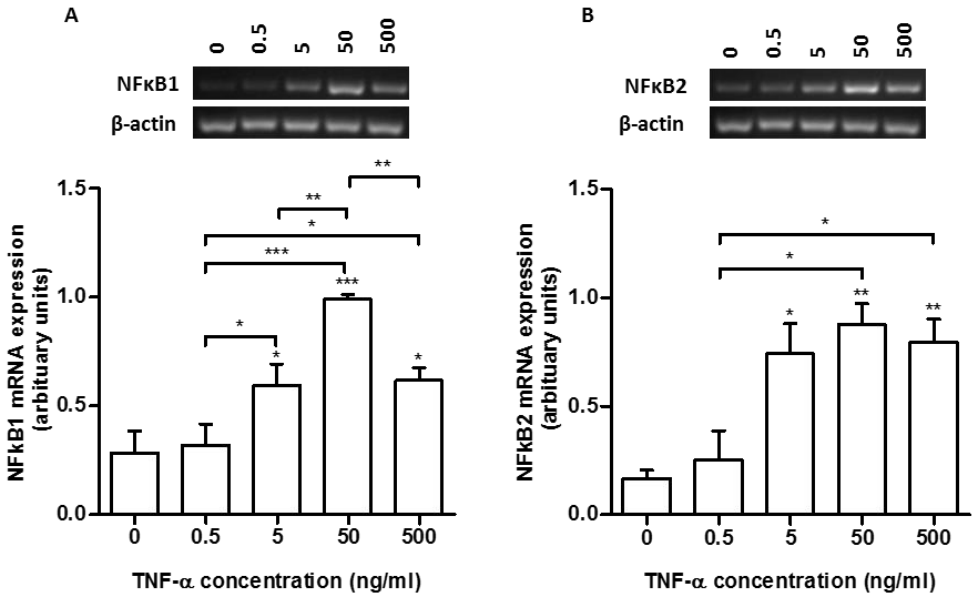

Figure 3-7: mRNA expression of NFκB genes by MIO-M1 cells cultured with increasing concentrations of TNF-α.
Representative images of PCR bands for NFκB genes and β-actin shown above bar charts. Bar charts show relative expression of NFκB mRNA normalised to β-actin (mean +/- SEM). **(A)** There was a significant upregulation of NFκB1 mRNA expression in cells cultured with 5, 50 and 500ng/ml of TNF-α when compared to untreated control cells. **(B)** mRNA expression of NFκB2 was also significantly upregulated in cells cultured with increasing concentrations of TNF-α when compared to control cells. One-way ANOVA and Tukey's post-test, $p<0.05$, N=3.

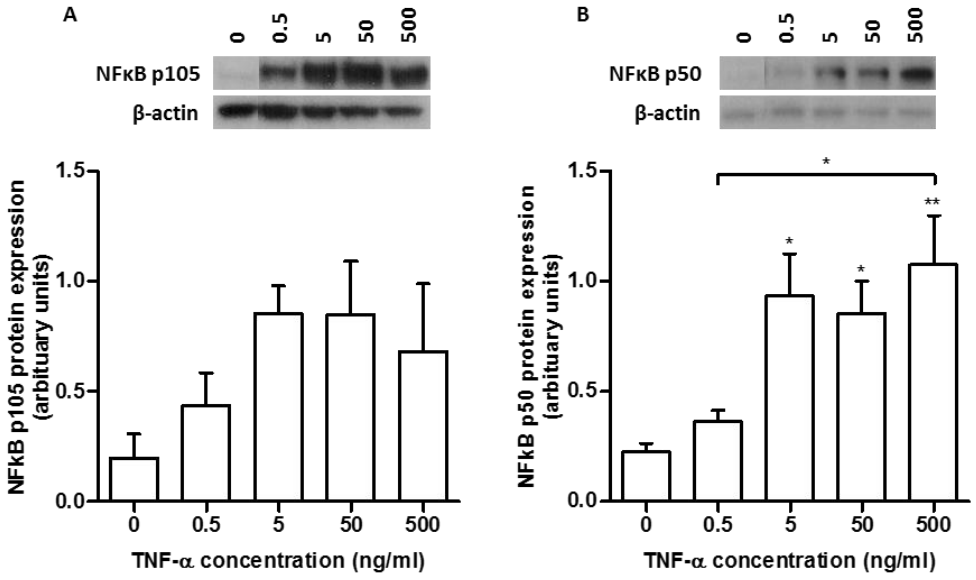

Figure 3-8: NFκB p105/50 protein expression by MIO-M1 cells cultured with increasing concentrations of TNF-α.
Representative images of western blot bands for NFκB p105, p50 and β-actin shown above bar charts. Bar charts show relative expression of NFκB proteins normalised to β-actin (mean +/- SEM). **(A)** NFκB p105 protein expression increased in cells cultured with TNF-α when compared to control, although this was not statistically significant (N=3). **(B)** NFκB p50 protein expression was significantly increased in MIO-M1 cells cultured with 5, 50 and 500ng/ml of TNF-α when compared to untreated control cells (N=5). One-way ANOVA and Tukey's post-test, $p<0.05$.

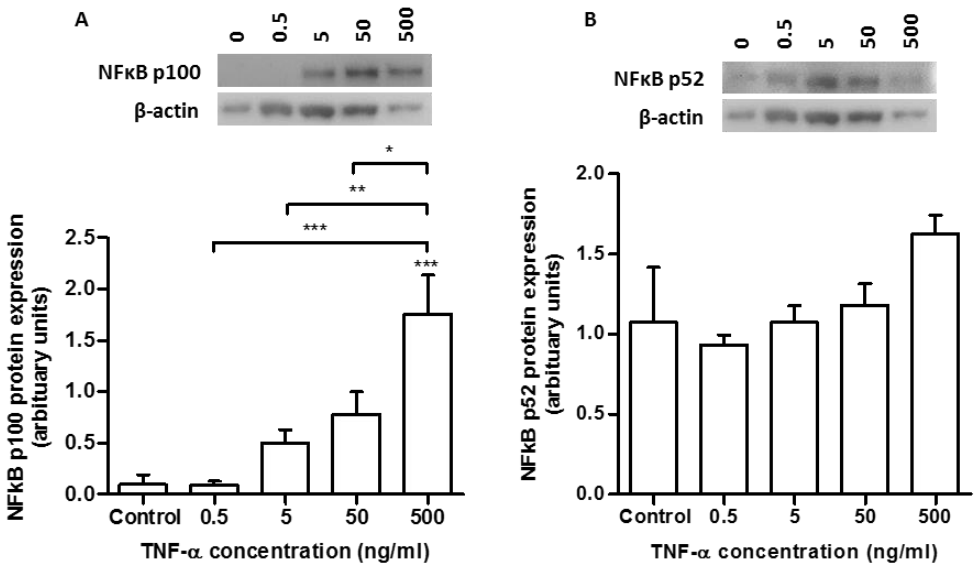

Figure 3-9: Protein expression of NFκB p100/52 by MIO-M1 cells cultured with increasing concentrations of TNF-α.
Representative images of western blot bands for NFκB p100, p52 and β-actin proteins shown above bar charts. Bar charts show relative expression of NFκB proteins normalised to β-actin (mean +/- SEM). **(A)** NFκB p100 protein expression was significantly increased in cells cultured with 500ng/ml TNF-α when compared to control cells and cells cultured with 0.5, 5 and 50ng/ml of TNF-α. **(B)** NFκB p52 protein expression was slightly not but significantly increased in Müller cells cultured with TNF-α when compared to untreated control cells. One-way ANOVA and Tukey's post-test, $p<0.05$, N=3.

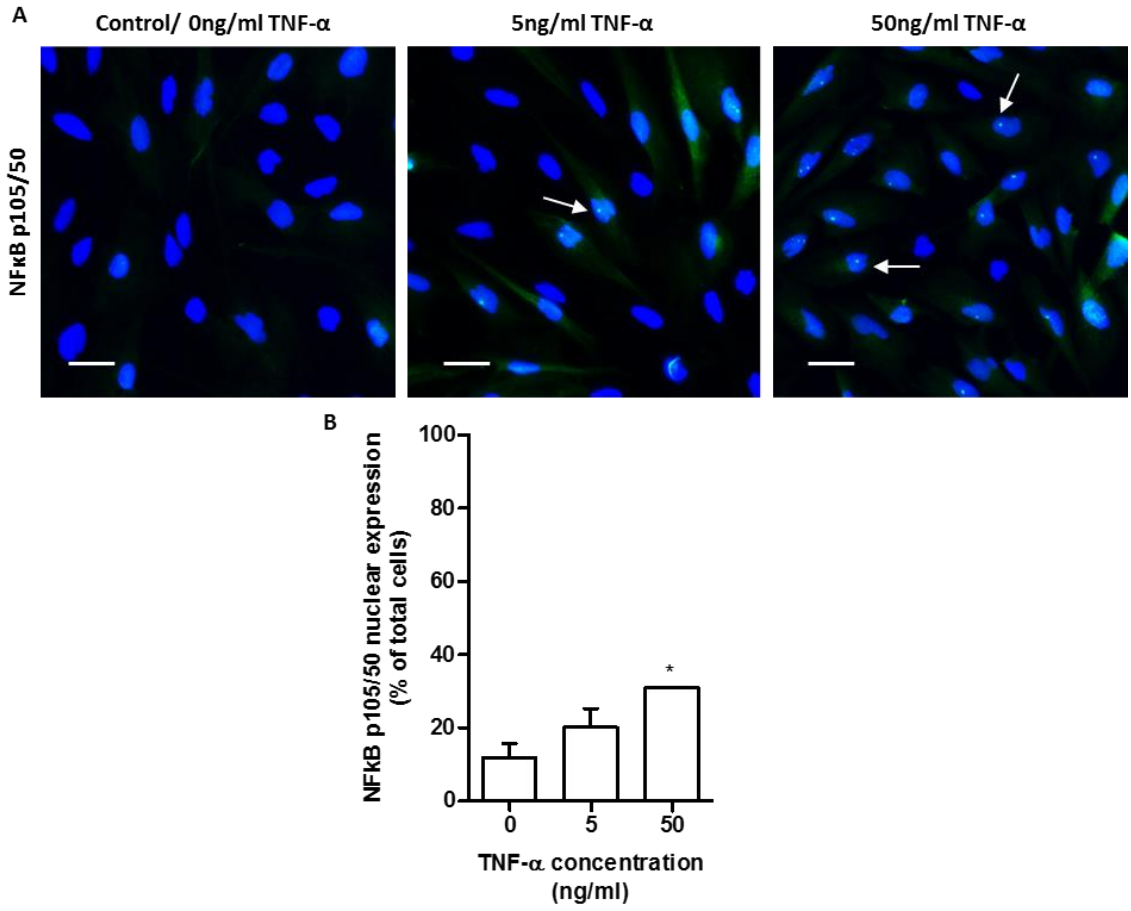

Figure 3-10: Immunofluorescence analysis of MIO-M1 cells cultured with increasing concentrations of TNF-α stained with anti-NFκB p105/50
(A) Representative fluorescent images of Müller cells cultured with 0, 5 or 50ng/ml of TNF-α and stained with anti-NFκB p105/50 (Alexa Flour 488, green). White arrows indicate nuclei immunostaining. **(B)** Quantification of the percentage of positive cells revealed an increase in number of MIO-M1 cells expressing NFκB p105/50 when cultured with TNF-α. This increase was only significant in cells cultured with 50ng/ml TNF-α when compared to untreated control cells. Bar chart represents the proportion of stained cells out of total cell number (mean +/- SEM). One-way ANOVA and Tukey's post-test, $p<0.05$, N=3. Scale bar represents 35μm.

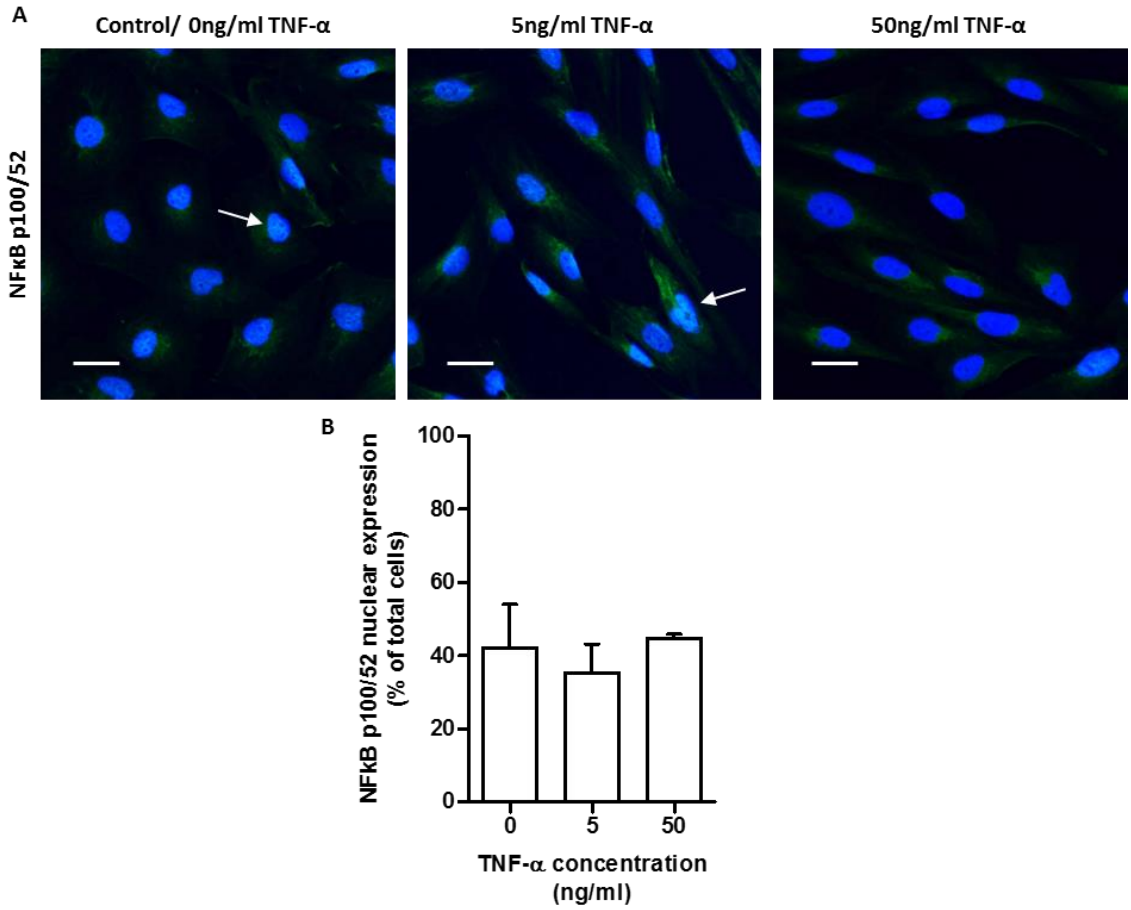

Figure 3-11: Immunofluorescence analysis of MIO-M1 cells cultured with increasing concentrations of TNF-α stained with anti-NFκB p100/52.
(A) Representative fluorescent images of Müller cells cultured with 0, 5 or 50ng/ml of TNF-α and stained with anti-NFκB p100/52 (AlexaFlour 488, green). White arrows indicate positive nuclei immunostaining. **(B)** Quantification of the percentage of positive nuclei revealed no significant difference in the percentage of cells staining for NFκB p100/52 upon culture with 5 or 50ng/ml of TNF-α when compared to untreated control cells. Bar chart represents proportion of stained cells out of total cell number (mean +/- SEM). One-way ANOVA and Tukey's post-test $p<0.05$, N=3. Scale bar represents 35μm.

3.3.4 Expression of NFκB protein by MIO-M1 cells cultured with FTRI

MIO-M1 cells were cultured with FTRI in the absence or presence of TNF-α. Protein expression of NFκB p105/50 and NFκB p100/52 by these cells was then measured (Figure 3-12). Treatment with FTRI did not modify NFκB p105/50 or NFκB p100/52 protein expression. However, protein expression of both NFκB p105/50 and NFκB p100 subunit increased significantly in MIO-M1 cells cultured with FTRI in the presence of TNF-α when compared to untreated control cells ($p<0.05$) (Figure 3-12A-C). This suggests that TNF-α regulates NFκB protein expression regardless of the presence of FTRI factors and that these factors used to induce differentiation of MIO-M1 cells do not modify NFκB protein expression. In addition, there was no significant change in NFκB p52 protein expression in MIO-M1 cultured with FTRI in the presence of TNF-α when compared to untreated control cells (Figure 3-12D).

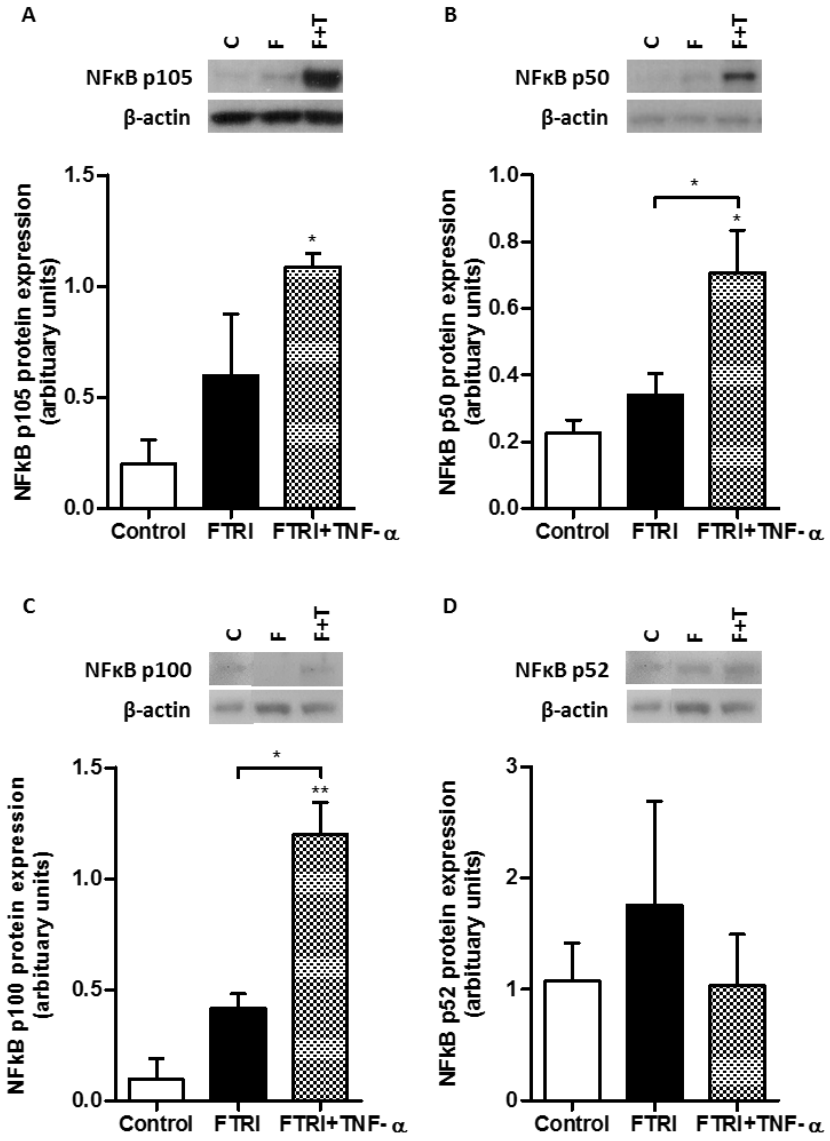

Figure 3-12: Protein expression of NFκB in MIO-M1 cells cultured with FTRI in the absence or presence of TNF-α.
Representative images of western blot bands for NFκB p105, p50, p100, p52 and β-actin proteins shown above bar charts. Bar charts show relative expression of NFκB proteins normalised to β-actin (mean +/- SEM). There was a significant upregulation of **(A)** NFκB p105 **(B)** NFκB p50 and **(C)** NFκB p100 protein expression in Müller cells cultured with FTRI in the presence of TNF-α when compared to untreated control cells. Protein expression of NFκB p50 and NFκB p100 were also significantly increased in MIO-M1 cells cultured with FTRI in the presence of TNF-α when compared to cells cultured with FTRI alone. **(D)** There was no significant different in NFκB p52 protein expression in MIO-M1 cells cultured with FTRI in the absence or presence of TNF-α when compared to control. One-way ANOVA and Tukey's post-test, $p<0.05$, N= 3.

3.3.5 Rapid NFκB p65 phosphorylation by MIO-M1 cells cultured with TNF-α was not accompanied by GFAP protein downregulation

MIO-M1 cells cultured with TNF-α over 6 days had shown to modulate NFκB protein expression. However, phosphorylation of NFκB and translocation to the nucleus occurs rapidly after stimulation with TNF-α. For this reason, MIO-M1 cells were cultured with 5ng/ml of TNF-α during a short time lapse experiment where protein from cell lysates were collected at 15 and 30 minutes, 3, 6 and 24 hours. An ELISA kit was used to measure phosphorylated NFκB p65 (also known as RelA), which forms dimeric complexes by binding to NFκB p50 or NFκB p52 for nuclear import. The results showed a significant increase in phosphorylated NFκB p65 protein in MIO-M1 cells cultured with TNF-α when compared to untreated control cells after 15 and 30 minutes ($p<0.05$) (Figure 3-13). Phosphorylated NFκB p65 protein expression in MIO-M1 cells cultured with TNF-α then returned to baseline after 3, 6 and 24 hours, when expression was unchanged when compared to untreated control cells.

Although TNF-α caused phosphorylation of NFκB p65 protein by MIO-M1 cells within 15 minutes of exposure, GFAP protein regulation in MIO-M1 cells did not occur rapidly. Culturing cells with 5ng/ml TNF-α did not modify GFAP protein expression at 15 or 30 minutes, 3, 6 or 24 hours when compared to untreated control cells (Figure 3-14). Furthermore, when MIO-M1 cells were cultured with increasing concentrations of TNF-α over 3 days, GFAP protein expression was not modified when compared to control untreated cells (Figure 3-15).

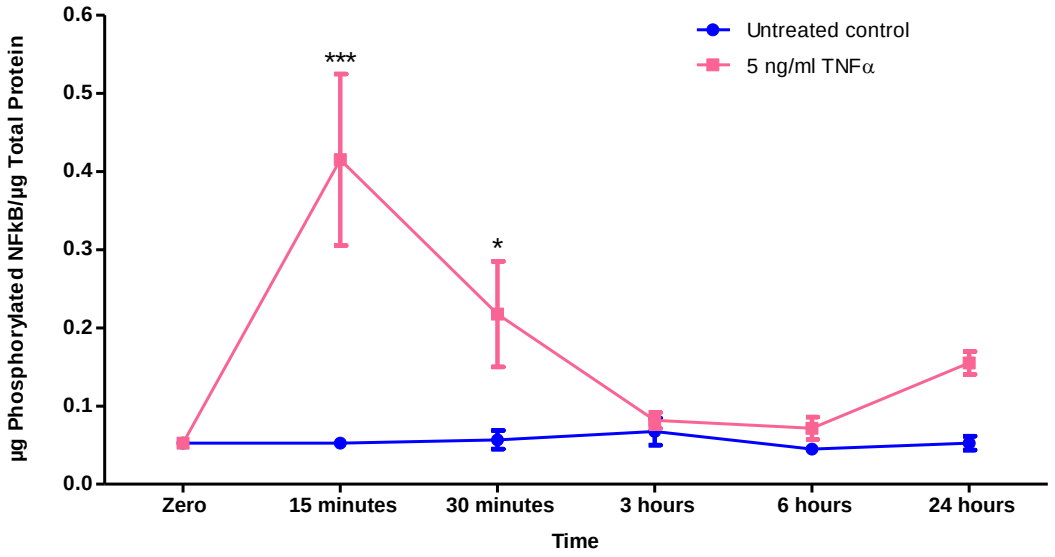

Figure 3-13: Protein expression of phosphorylated NFκB p65 by MIO-M1 cells cultured in the absence or presence of 5ng/ml TNF-α over a 24-hour period as examined by ELISA.
Blue coloured line represents untreated control cells and pink coloured line represents cells cultured with 5ng/ml of TNF-α. Time points are mean value +/- SEM. There was a significant increase in phosphorylated NFκB p65 protein at 15 and 30 minutes by Müller cells treated with 5ng/ml TNF-α when compared to untreated control cells. Two-way ANOVA and Bonferroni post-test, $p<0.05$, N=3.

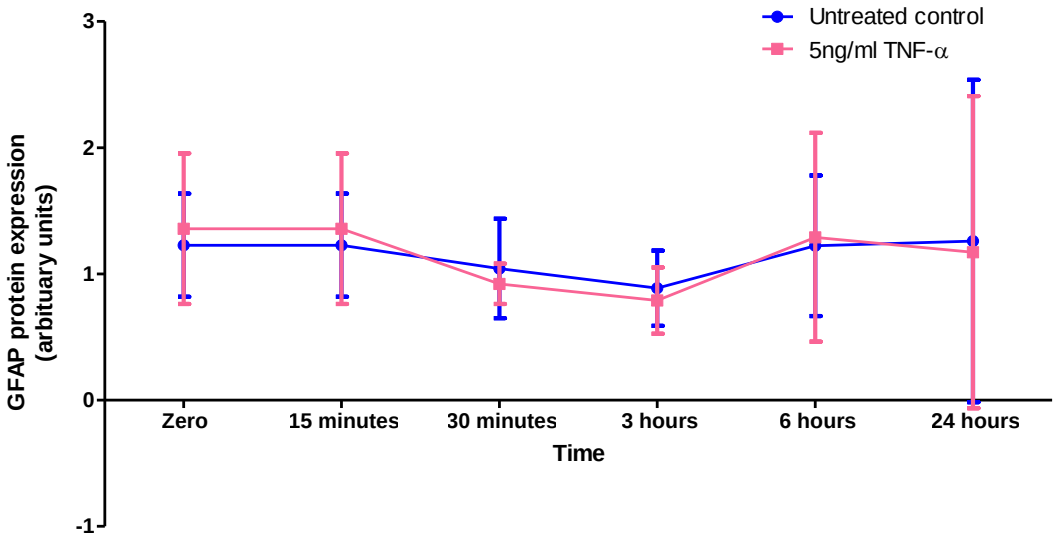

Figure 3-14: Protein expression of GFAP as examined by western blot analysis of lysates from MIO-M1 cells cultured with 5ng/ml TNF-α over a 24-hour period.
Blue coloured line represents untreated control cells and pink coloured line represents cells cultured with 5ng/ml of TNF-α. Time points are mean value +/- SEM. There was no difference in protein expression of GFAP in cells cultured with TNF-α when compared to untreated control cells at any time point. Two-way ANOVA and Bonferroni post-test, $p>0.05$, N=3.

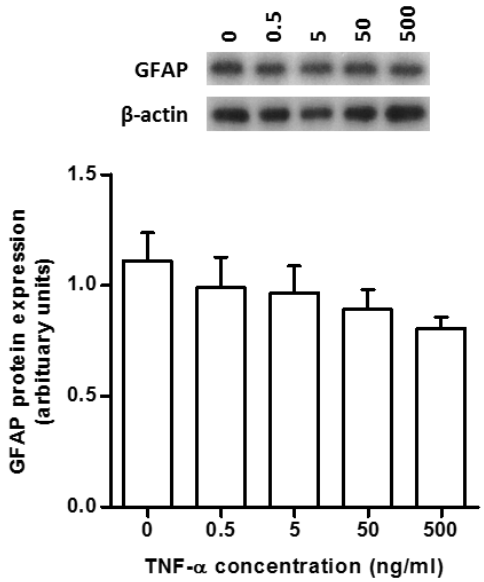

Figure 3-15: Protein expression of GFAP after three-day culture of MIO-M1 cells with increasing concentrations of TNF-α.
Representative western blot bands of GFAP and β-actin proteins are shown above bar chart. Bar chart represents protein expression of GFAP normalised to β-actin (mean +/- SEM). There was a trend of decreasing GFAP protein expression with increasing concentration of TNF-α but this was not statistically significant. One-way ANOVA and Tukey's post-test, $p>0.05$, N=4.

3.3.6 Expression of IκBα in MIO-M1 cells cultured with TNF-α and FTRI

The TNF-α signalling pathway stimulates IκBα, which is a regulatory protein that inhibits NFκB. IκBα exerts its effect by binding to NFκB and sequestering it in the cell cytoplasm to inhibit its translocation to the nucleus where it functions as a transcription factor. When TNF-α binds to its receptors IκBα is phosphorylated, promoting ubiquitination and degradation. This frees NFκB proteins to allow dimers to translocate to the nucleus and activate transcription. It was examined whether culturing MIO-M1 cells with TNF-α would modulate the protein expression of total and phosphorylated IκBα in these cells and whether FTRI factors modify the expression of this molecule.

Western blot analysis of cell lysates from MIO-M1 cells cultured with increasing concentrations of TNF-α over 6 days revealed no significant difference in protein expression of total IκBα (both non-phosphorylated and phosphorylated forms) (Figure 3-16). Phosphorylated IκBα was measured by ELISA analysis using lysates of MIO-M1 cells cultured with 5ng/ml TNF-α for 15 and 30 minutes and 3,6 and 24 hours (Figure 3-17). Protein expression of phosphorylated IκBα in MIO-M1 cells cultured with 5ng/ml of TNF-α was slightly elevated, peaking at 15 minutes. However, this increase was not significant over 24 hours culture when compared to untreated control cells.

MIO-M1 cells were cultured with FTRI in the absence or presence of TNF-α and protein expression of total IκBα was analysed. The results showed that protein expression of total IκBα was not modified in MIO-M1 cells induced to differentiate into rod photoreceptor precursors in the absence or presence of TNF-α when compared to untreated control cells (Figure 3-18).

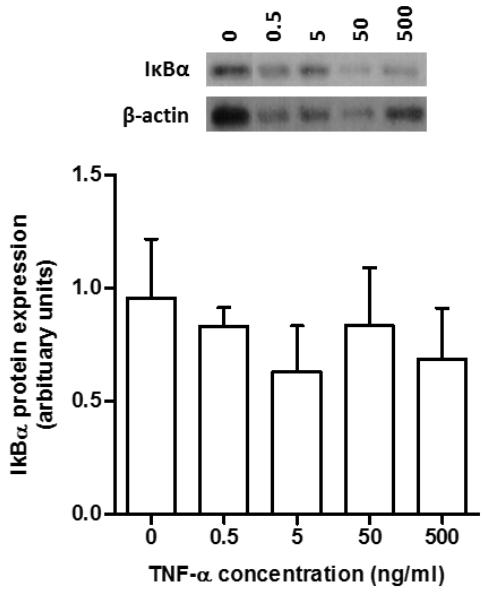

Figure 3-16: Protein expression of total IκBα by MIO-M1 cells cultured with increasing concentrations of TNF-α over six days.
Representative western blot bands of IκBα and β-actin proteins shown above bar chart. Bar chart represents protein expression of IκBα normalised to β-actin (mean +/- SEM). There was no significant difference in total IκBα protein expression by cells cultured with increasing concentrations of TNF-α when compared to untreated control cells. One-way ANOVA and Tukey's post-test, p>0.05, N=3.

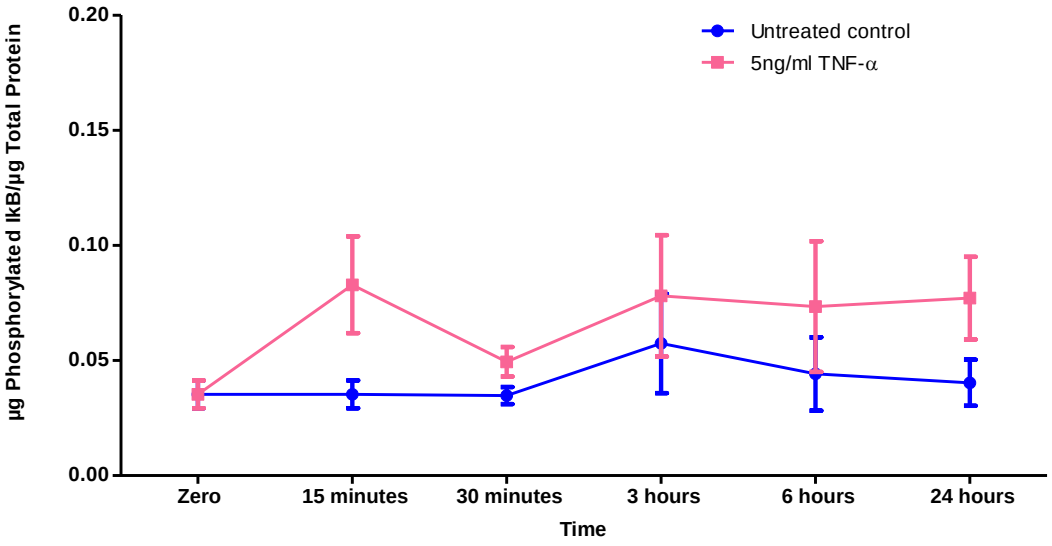

Figure 3-17: ELISA analysis of phosphorylated IκBα protein expression by MIO-M1 cells cultured in the absence or presence of 5ng/ml TNF-α over a 24-hour period.
Blue coloured line represents untreated control cells and pink coloured line represents cells cultured with 5ng/ml of TNF-α. Time points are mean value +/- SEM. There was a slight, but not significant, increase in phosphorylated IκBα protein expression by cells treated with TNF-α when compared to untreated control cells. Two-way ANOVA and Bonferroni post-test, p<0.05, N=3.

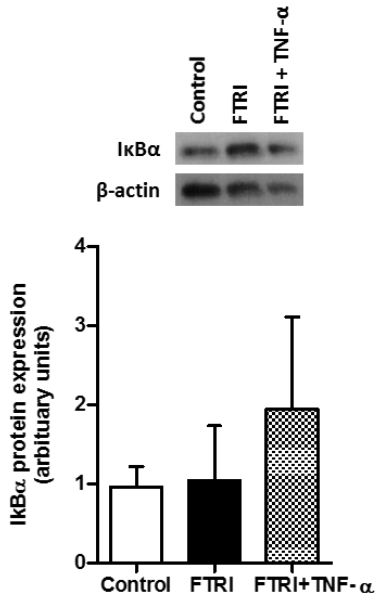

Figure 3-18: Protein expression of total IκBα by MIO-M1 cells cultured with FTRI in the absence or presence of TNF-α.
Representative western blot bands of IκBα and β-actin proteins shown above bar chart. Bar chart represents protein expression of IκBα normalised to β-actin (mean +/- SEM). There was no significant difference in IκBα protein expression by cells cultured with FTRI in the absence or presence of TNF-α when compared to untreated control cells. One-way ANOVA and Tukey's post-test, $p>0.05$, N=3

3.3.7 Effect of NFκB inhibition in MIO-M1 cell expression of GFAP

Based on the present observations that TNF-α caused downregulation of GFAP and activation of NFκB signalling in MIO-M1 cells, it was examined whether inhibiting NFκB would prevent the downregulation of GFAP by TNF-α in these cells. Cells were cultured with NFκB inhibitors caffeic acid phenethyl ester and RO1069920 for 6 days because GFAP protein downregulation by TNF-α occurs after this period of time in culture.

3.3.7.1 Caffeic acid phenethyl ester (CAPE) and RO1069920 did not have long term inhibitory activity in MIO-M1 cells

MIO-M1 cells were cultured for 6 days with increasing concentrations of caffeic acid phenethyl ester (CAPE), followed by examination of NFκB p105/50 and IκBα protein expression in cell lysates by western blot. Results showed that culture of MIO-M1 cells with CAPE alone did not modify protein expression of NFκB p105/50 when compared to untreated control cells (Figure 3-19A/B). However, addition of TNF-α to cells that had been cultured with 5 and 10μg/ml of CAPE inhibitor, caused a significant increase in NFκB p105/50 protein expression when compared to cells cultured with CAPE alone ($p<0.05$). Protein expression of IκBα was slightly decreased in cells cultured with 5 and 10μg/ml of CAPE alone but this was not statistically significant when compared to untreated control cells (Figure 3-19C). The presence of TNF-α significantly downregulated IκBα protein expression in MIO-M1 cells when compared to untreated controls ($p<0.05$) but the presence of CAPE did not modify expression of this protein.

Likewise, culturing MIO-M1 cells for 6 days with increasing concentrations of the RO1069920 inhibitor alone did not modify the protein expression of NFκB p105/50 or IκBα when compared to untreated control cells (Figure 3-20). However, addition of TNF-α to cell cultures did significantly upregulate protein expression of NFκB p105/50 by MIO-M1 cells when compared to untreated control cells irrespective of RO1069920 concentration. Expression of NFκB p105/50 proteins was significantly increased in cells cultured with 0, 0.1, 1 and 3μM RO1069920 in the presence of 5ng/ml TNF-α when compared to cells cultured with the increasing concentrations of RO1069920 alone ($p<0.05$) (Figure 3-20A/B). Furthermore, protein expression of IκBα was not modified in cells cultured with increasing concentrations of RO1069920 when compared to

untreated control cells (Figure 3-20C). MIO-M1 cells cultured with RO1069920 in the presence of TNF-α showed a slight decrease in IκBα protein expression. However, this was not significant when compared to untreated control cells.

The results suggest that these inhibitors did not downregulate NFκB signalling in MIO-M1 cells over a 6 day period.

3.3.7.2 CAPE and RO1069920 inhibitors did not modify TNF-α induced downregulation of GFAP in MIO-M1 cells

Culturing MIO-M1 cells with increasing concentrations of CAPE inhibitor caused a slight decrease in GFAP protein expression, although this was not statistically significant when compared to untreated control cells (Figure 3-21). Addition of TNF-α to the cell cultures caused a slight downregulation of GFAP protein expression in MIO-M1 cells when compared to cells cultured with CAPE alone, regardless of the initial CAPE concentration. However, GFAP downregulation was only significant in MIO-M1 cells cultured with TNF-α in the absence of CAPE when compared to untreated control cells ($p<0.01$). Inhibiting NFκB by CAPE in MIO-M1 cells followed by addition of TNF-α did not prevent the downregulation of GFAP protein caused by TNF-α.

Similarly, culturing MIO-M1 cells with increasing concentrations RO1069920 inhibitor slightly decreased GFAP protein expression, although this response was not statistically significant when compared to untreated control cells (Figure 3-22). MIO-M1 cells cultured with TNF-α in the presence of 0.1, 1 and 3 μM RO1069920 showed downregulation of GFAP protein expression when compared to untreated control cells and compared to cells treated with RO1069920 alone. However, this decrease in GFAP protein expression was only significant in MIO-M1 cells cultured with TNF-α in the absence of RO1069920 when compared to untreated control cells ($p<0.05$). NFκB inhibition by culturing MIO-M1 cells with RO1069920 did not prevent the downregulating effect that TNF-α has on GFAP protein expression in these cells.

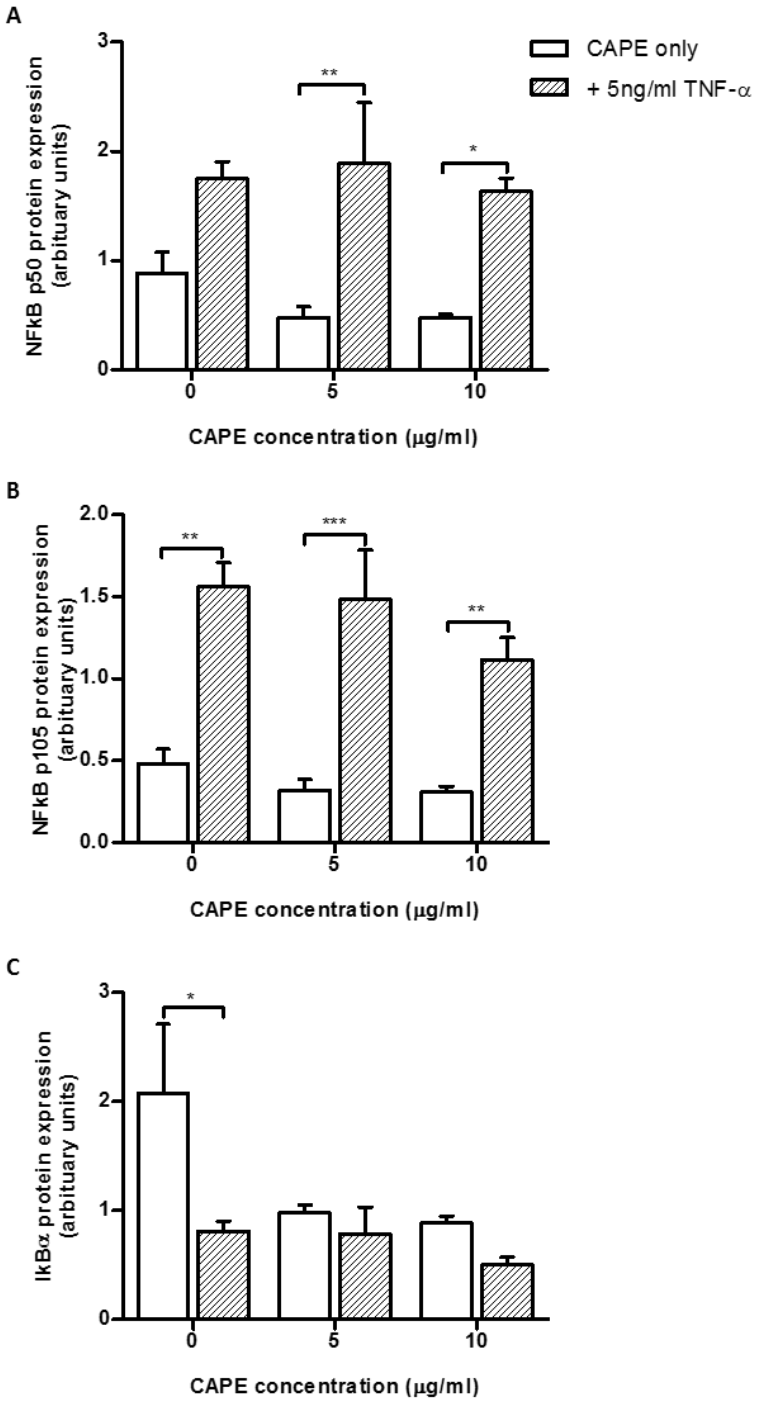

Figure 3-19: Protein expression of NFkBp105/50 and IκBα by MIO-M1 cells cultured with increasing concentrations of CAPE inhibitor in the absence or presence of TNF-α.
Bar charts represent protein expression normalised to β-actin (mean +/- SEM). Empty white bars represent protein expression by cells cultured with CAPE alone, whilst filled bars represent protein expression by cells cultured with the inhibitor in the presence of TNF-α. **(A)** Protein expression of NFkBp50 was not modified in cells cultured with increasing concentrations of CAPE when compared to untreated control cells. Müller cells cultured with TNF-α after inhibition showed increased NFkBp50 protein expression when compared to cells cultured with inhibitor alone. **(B)** Likewise, NFkBp105 protein expression was also not modified in cells cultured with increasing concentrations of CAPE when compared to untreated control cells. Cells cultured with TNF-α after inhibition showed increased NFkBp105 protein expression when compared to cells cultured with inhibitor alone. **(C)** IκBα protein expression was slightly but not significantly downregulated in MIO-M1 cells cultured with increasing concentrations of CAPE when compared to untreated control cells. Cells cultured with TNF-α alone showed decreased IκBα protein expression when compared to untreated control cells. Two-way ANOVA and Bonferroni post-test, $p<0.05$, N=4.

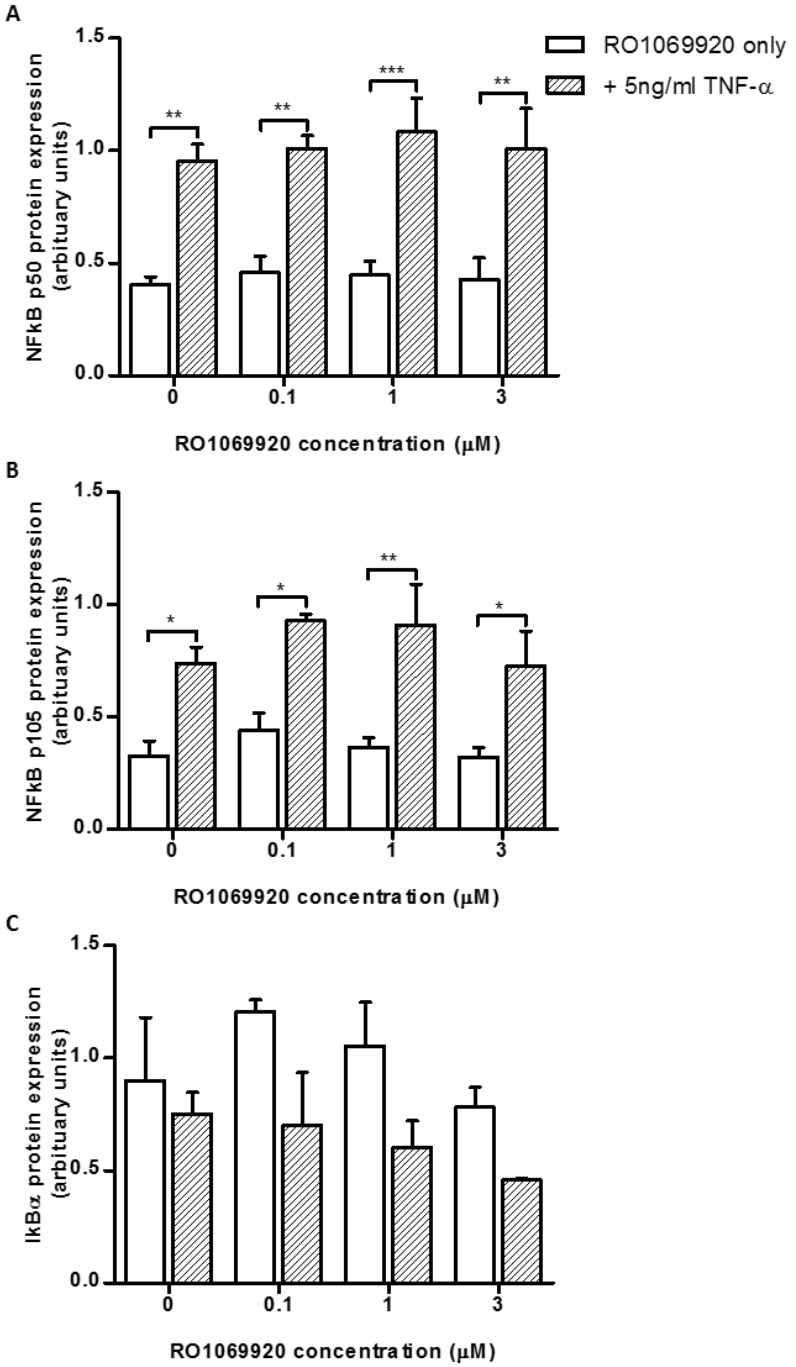

Figure 3-20: Protein expression of NFkBp105/50 and IκBα by MIO-M1 cells cultured with increasing concentrations of RO1069920 inhibitor in the absence or presence of TNF-α. Bar chart represents protein expression normalised to β-actin (mean +/- SEM). Empty white bars represent protein expression by cells cultured with RO1069920 alone, whilst filled bars represent protein expression by cells cultured with the inhibitor in the presence of TNF-α **(A)** Protein expression of NFkBp50 was not modified in cells cultured with increasing concentrations of RO1069920 when compared to untreated control cells. MIO-M1 cells cultured with RO1069920 in the presence of TNF-α showed increased NFkBp50 protein expression when compared to cells cultured with inhibitor alone. **(B)** Likewise, NFkBp105 protein expression was also not modified in cells cultured with increasing concentrations of RO1069920 when compared to untreated control cells. Cells cultured with RO1069920 in the presence of TNF-α showed increased NFkBp105 protein expression when compared to cells cultured with inhibitor alone. **(C)** IκBα protein expression was not modified in MIO-M1 cells cultured with increasing concentrations of RO1069920 when compared to untreated control cells. Cells cultured with RO1069920 in the presence of TNF-α showed slightly decreased, but not significant, IκBα protein expression when compared to untreated control cells. Two-way ANOVA and Bonferroni post-test, $p<0.05$, N=4.

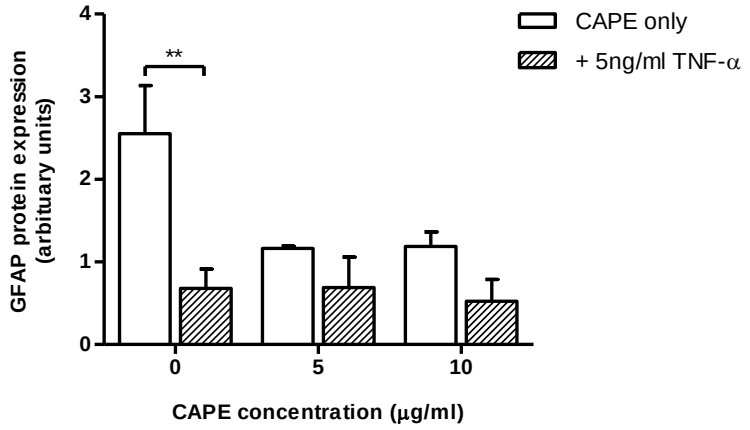

Figure 3-21: Protein expression of GFAP by MIO-M1 cells cultured with increasing concentrations of CAPE in the absence or presence of TNF-α.
Bar chart represents GFAP protein expression normalised to β-actin (mean +/- SEM). Empty white bars represent GFAP protein expression by cells cultured with CAPE alone, whilst filled bars represent protein expression by cells cultured with the inhibitor in the presence of TNF-α. Culturing MIO-M1 cells with TNF-α significantly downregulated GFAP protein expression when compared to untreated control cells. Cells cultured with CAPE at increasing concentrations showed a slight decrease in GFAP protein expression compared to untreated control cells but this was not significant. Addition of TNF-α to cultures of cells inhibited by CAPE slightly decreased GFAP protein expression when compared to cells cultured with CAPE alone. Two-way ANOVA and Bonferroni post-test, $p<0.05$, N=4.

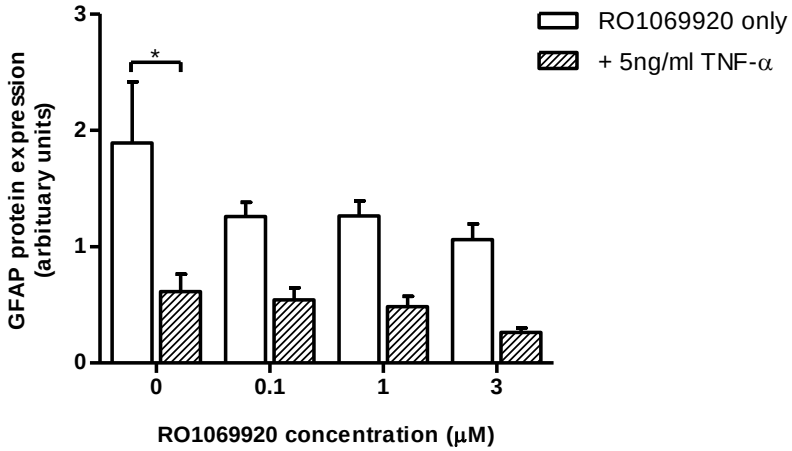

Figure 3-22: Protein expression of GFAP by MIO-M1 cells cultured with increasing concentrations of RO1069920 in the absence or presence of TNF-α.
Bar chart represents GFAP protein expression normalised to β-actin (mean +/- SEM). Empty white bars represent protein expression by cells cultured with RO1069920 alone, whilst filled bars represent protein expression by cells cultured with the inhibitor in the presence of TNF-α. Culturing cells with TNF-α significantly downregulated GFAP protein expression when compared to untreated control cells. Cells cultured with increasing concentrations of RO1069920 showed no change in GFAP protein expression when compared to untreated control cells. Addition of TNF-α to cultures of cells inhibited by RO1069920 slightly decreased GFAP protein expression when compared to cells cultured with RO1069920 alone. Two-way ANOVA and Bonferroni post-test, $p<0.05$, N=4.

3.4 Discussion

3.4.1 MIO-M1 cells express TNF-α receptors which are modified by TNF-α

The MIO-M1 cell line expressed mRNA and protein coding for both TNF-α receptors TNFR1 and TNFR2. Normally, these TNF-α receptors are found at low levels in the retina but after injury expression levels increase and can be found in the Müller glia cell processes (Fontaine et al., 2002). Indeed, when MIO-M1 cells were cultured with exogenous inflammatory cytokine TNF-α there was a robust upregulation of TNFR2 protein when low concentrations of TNF-α (0.5 and 5ng/ml) were added to the cultures. However, the expression of TNFR1 was not modified. It has been reported that TNF-α does not modulate the expression of TNFR1 in other cells such as lymphocytes either, although it has been shown that in the retina TNF-α does upregulate TNFR1 expression in RGC cells (Ware et al., 1991, Tezel et al., 2001). It is thought that RGC express TNFR1 in response to glaucomatous damage because they are targets of TNF-α, which results in cell death and neurodegeneration. In contrast, glial cells, which do not express high levels of TNFR1 survive this TNF-α insult (Tezel, 2008, Agarwal and Agarwal, 2012). The current results are therefore in accordance with these observations as MIO-M1 cells do not respond to TNF-α in a destructive way. They do not modulate their expression of the apoptosis-inducing receptor TNFR1 but increase the expression of TNFR2, which initiates neuroprotective signalling (Sedger and McDermott, 2014).

Whereas TNFR1 is found throughout the body, TNFR2 is found primarily on immune cells and some CNS cells, with the ratio of receptors determining the biological response to TNF-α. Although both TNFR1 and TNFR2 can bind soluble TNF-α, as observed in MIO-M1 cell cultures, it has been shown that TNFR2 has a lower affinity for soluble TNF-α but instead preferentially binds to transmembrane TNF-α (tmTNF) (Grell et al., 1998, Grell et al., 1995). Transmembrane TNF-α is a precursor to soluble TNF-α expressed on the cell surface of TNF-α producing cells and exerts its biological effect by acting as a ligand for TNFRs in a cell-to-cell contact manner (Horiuchi et al., 2010). Cells expressing tmTNF interacting with cells expressing TNFR2 can produce signalling in both directions hence, tmTNF mediates signalling forward to the TNFR2 bearing target cell but also signals in the reverse direction towards the tmTNF bearing cell (Qu et al., 2017). It may be possible that Müller glial cells,

as TNF-α producing cells, contain tmTNF and in cell culture conditions, where cell-to-cell contact is enhanced, there is this forward and reverse signalling in MIO-M1 cells. In cancer cells *in vitro*, this reverse signalling can promote constitutive NFκB activation and can enhance cell survival (Zhang et al., 2008). In the CNS, tmTNF can have important homeostatic functions. In an *in vivo* autoimmune inflammation model, mice exclusively expressing tmTNF showed supressed onset and disease progression, suggesting a beneficial effect of the tmTNF (McCoy and Tansey, 2008, Alexopoulou et al., 2006). This is supported by other studies, such as in a rat glaucoma model, in which soluble TNF-α is blocked without interfering with tmTNF. In these animals RGC survival is promoted, indicating a neuroprotective role for tmTNF in the retina (Cueva Vargas et al., 2015). From the present observations that MIO-M1 cells cultured with TNF-α increase TNFR2 expression, it can be suggested that this receptor may bind to and initiate signalling through tmTNF on neighbouring MIO-M1 cells to promote cell survival. However, expression of tmTNF was not examined in this project and could be a subject of future work.

Another regulator of TNF-α activity are the soluble TNFRs. When MIO-M1 cells were cultured with 0.5ng/ml TNF-α there was no change in the release of sTNFR2 into the culture medium. However, with higher concentrations of TNF-α there was a dose-response effect. MIO-M1 cells cultured with 5ng/ml TNF-α exhibited increased expression of sTNFR2 compared to untreated control cells. When cells were exposed to 50 and 500ng/ml TNF-α there was further increase in sTNFR2, significantly higher than cells cultured with 5ng/ml. This might explain why in cells cultured with 50 and 500ng/ml TNF-α the expression of TNFR2 protein decreased to the levels seen in untreated cells. It is possible that, at these higher concentrations of TNF-α, the TNFR2 is shed, resulting in the release of increasing amounts of sTNFR2 observed in the cell culture supernatants. Increasing the concentration of sTNFR2 in cell culture medium may potentially augment TNF-α activity by stabilising its structure and preserving its activity. Aderka et al suggested that tissue culture experiments are closed compartments where sTNFRs can act as slow release reservoirs of TNF-α in long term experiments (Aderka et al., 1992). As the current experiments were undertaken over 6 days this could apply to the present

results, which correlate with an increased NFκB activation in MIO-M1 cells cultured with TNF-α over this relatively long period.

3.4.2 TNF-α regulates NFκB signalling in MIO-M1 cells

TNFR1 signalling often leads to cell death because the receptor contains an intracellular death domain. However, TNFR2 does not have this domain and instead signalling through this receptor results in activation of NFκB, which was clearly seen in MIO-M1 cells. The protein expression of the active NFκB p50 subunit increased significantly in MIO-M1 cells cultured with 5, 50 and 500ng/ml TNF-α over 6 days. This could be attributed to sTNFR2 delaying TNF-α decay and prolonging signalling. Additionally, NFκB p50 activation in MIO-M1 cells cultured with TNF-α correlated with increased nuclear immunostaining of NFκB p105/50, suggesting that this factor translocates to the nucleus to initiate transcription. Protein expression of the active NFκB p52 subunit and immunostaining for NFκB p100/52 was not modified in MIO-M1 cells cultured with increasing concentrations of TNF-α. Interestingly, the protein expression of inhibitory NFκB subunits p105 and p100 was increased in MIO-M1 cells cultured with TNF-α, although this affect was more prominent at higher concentrations of TNF-α. Normally these subunits remain in the cytoplasm and initial NFκB activation would lead to protein degradation. However, the p105 and p100 genes themselves have κB binding sites and NFκB activation can cause de novo synthesis of the p105 and p100 subunits (Finco and Baldwin, 1995). This could explain the increase in protein expression of p105 and p100 subunits seen in MIO-M1 cells, since these proteins may have been resynthesised after 6 days by TNF-α mediated NFκB targeted gene transcription. Indeed, NFκB signalling targets many genes for transcription, including the TNF-α gene for TNF-α production by Müller glial cells (Lebrun-Julien et al., 2009), potentially creating a feedback loop in these cells, where exogenous TNF-α leads to endogenous TNF-α production, which might explain the long term activation of NFκB seen in MIO-M1 cells.

Phosphorylation of the NFκB p65 subunit, which is essential for binding to the p50 or p52 subunits to create a complex that translocates to the nucleus, occurs much quicker. Treating retinal astrocytes with TNF-α causes a peak of NFκB p65 phosphorylation within 15 minutes (Dvoriantchikova and Ivanov, 2014). This was also observed in the present study, in which there was rapid transient

NFκB p65 phosphorylation in MIO-M1 cells following 15 and 30 minutes treatment with TNF-α. These then retreated to basal levels after 3 hours. The most common NFκB complex occurs between the p50 and p65 subunits. Mice deficient in p65 subunit die during embryonic development due to cell death, suggesting that signalling through this NFκB subunit is important in protecting cells from apoptosis (Beg et al., 1995). Thus it can be suggested that the TNF-α induced NFκB p65 phosphorylation along with enhanced p50 subunit activation seen in MIO-M1 cells may help protect these cells from death.

In previous reports, in which human lymphocytes were stimulated by TNF-α, there was rapid NFκB activity within 10 minutes and this correlated with rapid loss of IκBα protein, which reappeared after 40 minutes. The IκBα protein degradation was followed by increase in IκBα mRNA expression and de novo protein synthesis (Brown et al., 1993). This has been attributed to the fact that the IκBα gene has a κB binding site in its promoter and therefore, IκBα protein synthesis is dependent on the presence of activated NFκB complex (Chiao et al., 1994). This then leads to increased IκBα protein expression which inhibits NFκB and stops NFκB signalling, maintaining a transient activation of NFκB responsive genes in an autoregulatory feedback loop (Thompson et al., 1995). In MIO-M1 cells IκBα phosphorylation, which precedes protein degradation, coincides with NFκB p65 phosphorylation peaking at 15 minutes after culture with TNF-α. Once IκBα phosphorylation in MIO-M1 cells cultured with TNF-α returned to basal levels after 30 minutes, NFκB p65 phosphorylation also began to decrease. These observations of transient activation correspond to previous reports in the literature. When measuring total IκBα protein after 6 days of culturing MIO-M1 cells with increasing concentrations of TNF-α there was no statistically significant change in expression of this protein. However, in cells cultured with 5ng/ml TNF-α there was a slight decrease in total IκBα protein when compared to control, which could be due to the prolonged NFκB activation in these cells causing IκBα protein degradation. Although, in MIO-M1 cells cultured with higher concentrations of TNF-α this effect was not obvious, possibly due to NFκB continuously inducing protein synthesis of IκBα and then this being degraded by NFκB activation in a repeated cycle. On the other hand, this discrepancy could be caused by experimental error in the western blot technique not being consistent between cell passage samples and therefore

creating high variation in the data and reducing statistical power. Another possible explanation of this high variability seen in expression could be attributed to the intrinsic variation within MIO-M1 cell passages. As different cell passages were used as biological repeats in these experiments, this could have contributed to differences in protein expression.

3.4.3 Culturing MIO-M1 cells with FTRI in the presence of TNF-α

MIO-M1 cells were cultured with FTRI in the absence or presence of TNF-α. Protein expression of TNFR2 was increased, although not significantly, in cells cultured with FTRI alone. Potentially, the factors may cause increased expression of TNFR2 by MIO-M1 cells. Signalling through TNFR2 has been shown to induce cardiac stem cell differentiation as that seen in TNFR2 knockout mouse heart organ cultures, which upon treatment with TNF-α exhibited negligible amounts of activated cardiac stem cells entering the cell cycle and differentiate into a cardiogenic lineage (Al-Lamki et al., 2013). Additionally, in the CNS after neurotoxin demyelination, these TNFR2 knockout mice had decreased oligodendrocyte progenitor cells and reduced remyelination, indicating TNF-α binding to TNFR2 may promote progenitor proliferation (Arnett et al., 2001). From the present results it can be suggested that MIO-M1 cells cultured with FTRI upregulate TNFR2 protein, which could potentially contribute to enhance signalling to promote neural differentiation.

In damaged new born chick retinae, where there is some regeneration, ablating reactive microglia with consequential massive decrease in retinal levels of TNF-α decreased proliferating Müller glial cells and progenitors (Fischer et al., 2014). This suggests a role for TNF-α in formation of Müller glial progenitor cells during regeneration. This could be triggered by TNFR2 downstream signalling, as suggested by studies in the CNS of TNFR2 knock out mice, in which reduced numbers of active astrocytes stimulate oligodendrocyte progenitor proliferation. As a result, activation of astrocytes by TNFR2 signalling facilitates myelin repair (Patel et al., 2012). Culturing MIO-M1 cells with FTRI in the presence of TNF-α increased protein expression of activated NFκB p50 significantly more than in cells cultured with FTRI alone. This may suggest that TNF-α signalling through TNFR2 and NFκB may facilitate MIO-M1 cell differentiation. However, further investigations are required.

3.4.4 GFAP downregulation by TNF-α occurs after NFκB activation

Although culture of MIO-M1 cells with exogenous TNF-α for 6 days caused downregulation of GFAP protein, this was not seen in cells cultured with TNF-α for 24 hours or 3 days. In astrocytes *in vitro* GFAP protein downregulation is slow, persisting for longer in these cells because even though there is a small pool of GFAP that decays rapidly, the majority of GFAP proteins have a half-life of 8 days (Chiu and Goldman, 1984). There is some similarity with MIO-M1 cells, in which decreased GFAP protein expression was only observed at significant levels after 6 days in culture with TNF-α. The concentration of TNF-α used in the 24 hour time lapse study was 5ng/ml because this produced a significant reduction in GFAP over 6 days. In bovine astrocytes cultured with 60U/ml TNF-α, equivalent to 6ng/ml, GFAP protein expression was decreased after 5 days (Selmaj et al., 1991), which is similar to the timeframe used in the present experiments. It may also be possible that GFAP mRNA is regulated faster than protein translation because rat astrocytes treated with 5ng/ml TNF-α show GFAP mRNA decreased in a time-dependent manner, beginning at 12 hours and reaching the lowest expression at 3 days (Oh et al., 1993). However, mRNA expression of the GFAP coding gene was not tested in MIO-M1 cells during this time scale and needs further investigations.

In this study, protein regulation of GFAP by TNF-α occurs after TNFR2 mediated NFκB activation in MIO-M1 cells, suggesting that NFκB activation can drive GFAP regulation in Müller glial cells. Indeed, there is a conserved NFκB binding site in the upstream promoter sequence of the human GFAP gene (Bae et al., 2006). Rat astrocytes increase GFAP mRNA after treatment with TGF-β1 but decrease GFAP mRNA when treated with IL-1β via this NFκB binding domain *in vitro* (Krohn et al., 1999). This indicates that the same binding element upstream of the GFAP promoter mediates opposite transcriptional responses of GFAP to inflammatory cytokines. This could also be regulated by the type of NFκB subunit complex which binds to the GFAP regulatory element. For example, the p50-p50 complex can repress transcription and the p50-p65 complex can promote expression of the IL-2 gene in lymphocytes (Kang et al., 1992). Therefore, this could explain the possibility of GFAP downregulation being mediated by NFκB in MIO-M1 cells cultured with TNF-α.

3.4.5 Inhibition of NFκB in MIO-M1 cells does not modify GFAP downregulation by TNF-α

NFκB was inhibited in MIO-M1 cells to examine if this would prevent TNF-α mediated downregulation of GFAP protein. Caffeic acid phenethyl ester (CAPE) is an active component of propolis from honey bees, with anti-inflammatory properties which acts as a specific inhibitor of NFκB by preventing p65 subunit translocation to the nucleus. Cells must be pre-treated with CAPE, for a few hours followed by TNF-α (or any other NFκB activating agent) to observe this NFκB inhibition as co-treatment does not work. This is suggested by studies in human histiocytic cells, in which culture with CAPE for 2 hours and then exposure to TNF-α for 15 minutes showed potent NFκB inhibition (Natarajan et al., 1996). In the present study, MIO-M1 cells were cultured for 24 hours with CAPE, which was then removed and TNF-α was added for 5 days so there was a total incubation time of 6 days. However, when protein expression of the NFκB subunits p105 and p50 or total IκBα were examined at 6 days, there was no significant changes in their expression, in cells cultured with 5 or 10μg/ml CAPE, indicating that it did not inhibit NFκB activation in MIO-M1 cells. It might be possible that after 5 days culture without CAPE present, NFκB is no longer inhibited in MIO-M1 cells. Moreover, in MIO-M1 cells pre-treated with CAPE and then cultured with TNF-α the downregulation of GFAP expression did not differ from that seen in cells treated with TNF-α alone, further confirming that this inhibitor does not prevent TNF-α mediated downregulation of GFAP.

A similar effect was observed with another NFκB inhibitor, RO1069920. This small molecule inhibitor selectively blocks TNF-α induced IκBα ubiquitination, meaning that there must be co-treatment to induce its affects (Swinney et al., 2002). However, in MIO-M1 cells cultured with increasing concentrations of RO1069920 in the presence of 5ng/ml TNF-α there was no change in IκBα total protein expression when compared to untreated control. There was instead a slight decrease in IκBα total protein, which is opposite to inhibiting IκBα ubiquitination, suggesting that this inhibitor does not function in MIO-M1 cells over a period of 6 days. Additionally, NFκB p105/50 protein expression was not modified in cells cultured with RO1069920 in the presence of TNF-α when compared to cells cultured with TNF-α alone. When MIO-M1 cells were cultured with RO1069920 in the presence of 5ng/ml TNF-α, GFAP protein expression

decreased when compared to untreated cells. In conclusion, this inhibitor does not prevent TNF-α mediated downregulation of GFAP because it is not consistently inhibiting NFκB signalling. Therefore, methods of inhibiting NFκB, which act within minutes or hours and then examining GFAP regulation by TNF-α after 6 days, are not compatible *in vitro*. To specifically inhibit NFκB in glia *in vivo,* transgenic animals with an IκBα supperrepressor under transcriptional control of the GFAP promoter have been developed (Zhang et al., 2005), but this was not possible in this project and could be a matter for further research.

Chapter 4 Development of methods to induce GFAP overexpression in the MIO-M1 cell line

4.1 Introduction

4.1.1 Regulation of GFAP in Müller glial cells

GFAP is a class III intermediate filament found in glial cells in the CNS and in Müller glia and astrocytes in the retina. Although low expression of GFAP is normally found in Müller cell bodies, in the degenerating retina there is an increase in GFAP expression as Müller cells expand and proliferate (Okada et al., 1990). GFAP overexpression is an early and highly sensitive indicator of degeneration in a variety of human retinal diseases and *in vivo* models of retinal degeneration (Dahl, 1979, Bringmann and Reichenbach, 2001, Smith et al., 1997, Lewis et al., 1995, Kuo et al., 2012, Kim et al., 2012). Upregulation of this intermediate filament has become the universal marker of retinal stress and is crucial for the Müller cell gliotic response (Sarthy, 2007). Experiments with GFAP knockout mice found altered and reduced Müller glial response to injury, strongly suggesting a critical role for GFAP within Müller glial cells (Nakazawa et al., 2007b, Verardo et al., 2008).

The human *GFAP* gene is composed of nine exons and eight introns distributed over 10kb of DNA and has eight mRNA splice variants (Middeldorp and Hol, 2011). Although gene expression of *GFAP* is regulated by the promoter which is essential for transcription, other elements on this promoter can also determine specificity. Experiments in transgenic mice have demonstrated that the *Gfap* promoter proximal sequences are able to drive high level, Müller cell specific expression, however 5' sequences longer than 2.5kb inhibit this expression (Kuzmanovic et al., 2003). In the CNS, *GFAP* gene promoter elements control astrocyte specific expression, but neurons do not express GFAP because of a sequence which silences gene transcription (Lee et al., 2008). The *GFAP* gene is tightly controlled not just by activation of transcription factors but also by negative regulatory elements. In addition, epigenetic mechanisms such as phosphorylation and DNA methylation can alter *GFAP* transcription (Middeldorp and Hol, 2011).

In the rat retina *Gfap* gene expression appears after the triggering of transcriptional activators as a result of neurodegeneration or a sustained

response due to inflammation (Vázquez-Chona et al., 2004). After induced degeneration, where 50% of the photoreceptors cells are lost after 2 weeks and 80% are lost after 4 weeks, GFAP mRNA increases significantly in Müller glial cells after 2 weeks. However, gene expression then declines whilst GFAP protein content increases after 2 weeks, remaining high 6 months later (Sarthy and Egal, 1995). This suggests that a quick and transient activation of GFAP gene transcription occurs soon after retinal damage in Müller cells with sustained GFAP protein levels as a result of low turnover rather than de novo synthesis.

4.1.2 GFAP overexpression in the mammalian CNS

GFAP overexpression has been widely studied in mammalian astrocytes in the CNS context. Transgenic mice that carry the human GFAP gene were created to study the effects of elevated GFAP on astrocytes without the need for injury or drug treatment (Messing et al., 1998). Most of the transgenic animals died prematurely but the cause of death was not known. However, they only showed CNS abnormalities. Reactive gliosis is seen in the astrocytes from transgenic mice as cells showed hypertrophy and contained intermediate filament aggregates called Rosenthal fibres, a pathological hallmark for Alexandre disease, a rare neurodegenerative disorder of astrocytes in the CNS mainly affecting children. Thus, these transgenic mice overexpressing wild-type GFAP, named TgGFAP-wt, have been used as an animal model for Alexandre disease (Brenner et al., 2001). The consequences of how cells cope with excess GFAP is not fully understood. Murine astrocytes with mutant GFAP have similar characteristics to TgGFAP-wt mice, indicating that it is not only increased GFAP protein but also the quality of this protein that causes disease pathology (Tanaka et al., 2007, Cho and Messing, 2009).

Furthermore, primary astrocytes from TgGFAP-wt mice in culture exhibit Rosenthal fibre-like GFAP inclusions, suggesting that GFAP accumulation is specific to astrocytes and does not require interaction with other cells (Eng et al., 1998). In these studies it was also observed that these GFAP inclusions occurred in a subset but not all astrocytes (Cho and Messing, 2009), indicating that cell to cell variation in GFAP expression may occur, or that some cells may have better ability to breakdown GFAP than others. In this astrocyte disease model, GFAP overexpression inhibits proteasomal activity and activates the

JNK pathway, which further inhibits proteasomal activity causing a positive feedback loop that allows GFAP accumulation to rise (Tang et al., 2006). Normal protein turnover mechanisms are insufficient to handle excess GFAP, instead it has been suggested that GFAP accumulation induces autophagy as a mechanism to reduce GFAP levels. This is supported by findings that autophagosomes are found near Rosenthal fibres in the CNS tissue of Alexandre disease patients (Tang et al., 2008). GFAP protein is found in the cerebrospinal fluid of mouse models of Alexander disease, possibly due to increased cell apoptosis and protein release (Jany et al., 2013). Whilst in intact astrocytes GFAP is insoluble, after injury and cell lysis elevated levels of soluble GFAP breakdown products can be found in interstitial fluid in patients with traumatic brain injury, and is indicative of severity of injury (McMahon et al., 2014). This suggests that GFAP accumulation and breakdown may play an important role in CNS disorders. However, there are limited studies on GFAP overexpression in the retina and this merits further investigations.

4.1.3 Molecular biology techniques used to induce gene overexpression

Overexpression of wild-type genes can cause mutant phenotypes and contribute to disease pathology, not just in Alexandre disease but other neurodegenerative diseases and cancers, indicating the importance of gene regulation in human health (Shastry, 1995). Studies of genetic overexpression began in yeast in the 1980s and has since been exploited by geneticists as a useful tool to examine biological pathways (Prelich, 2012). Overexpression of a given gene can result in inhibition of functions by either i) reducing transcription of another gene, ii) preventing translation of another gene to reduce protein expression, iii) increasing the rate of protein degradation, iv) inactivating another protein, or v) competing with another protein. On the other hand, induced gene overexpression, resulting in overexpression of the encoded protein can cause activation by i) increasing the total protein activity over a critical threshold, ii) initiating a step in a pathway, or iii) overcoming an inhibitor. This indicates that gene overexpression can have complex and widespread implications in a biological system.

4.1.3.1 Use of retroviral vectors to induce gene overexpression

A popular and extensively used method for genetic overexpression are retroviral vectors that permit the long-term stable expression of the transferred gene

(Maier et al., 2010). These vectors facilitate the introduction of additional copies of a given gene causing the encoded protein to be overexpressed. In gene therapy, this approach can produce a curative biological effect as well as replacing a defective gene or manipulating a disease related gene.

The retroviral genome has three important genes required for its lifecycle. The *gag* gene which encodes the core and structural viral proteins, the *pol* gene which encodes the reverse transcriptase, integrase and protease and the *env* gene which encodes the virus envelope coat protein (Makrides, 2003). The widely used γ-retroviral vectors require not only the viral vector but also a packaging cell line for production of viral particles which infect the target cell. The retroviral pCLNCx vector contains the inserted transgene (the gene of interest), a so-called packaging signal and long-term repeats (LTRs) at the 3' end of the viral RNA. The packaging cell line GP2-293 provides the viral proteins as the *gag* and *pol* genes are stably integrated in these cells. The *env* gene must be supplied by co-transfection. The envelope coat protein determines which species the retrovirus can infect (tropism) and the pMD.G plasmid contains the *env* gene coding for the VSV-G envelope protein which allows for transfection of mammalian cells. Only when all elements come together will the packaging cells create viral particles because this process requires the packaging signal and all viral proteins (Figure 4-1). In this process, the viral particles are released by the packaging cells into the culture medium, which is filtered and applied to the target cell line for transfection. The retrovirus then enters the target cell by interacting with cell surface receptors and fusing lipid membranes.

Once the viral RNA is transferred to the target cell, reverse transcription occurs, mediated by the viral reverse transcriptase. The newly transcribed dsDNA integrates with the host cell genome through the viral integrase, recognising the LTRs on the viral DNA. The host cell transcription machinery will then transcribe the viral genome and the transgene will be translated into protein. For safety reasons the GP2-293 packaging cell line only produces replication-incompetent retrovirus so it cannot propagate and transfects only one target cell. For integration of the retroviral DNA into the host DNA the target cells must be proliferating because this requires the absence of the nuclear membrane during the M phase of the cell cycle.

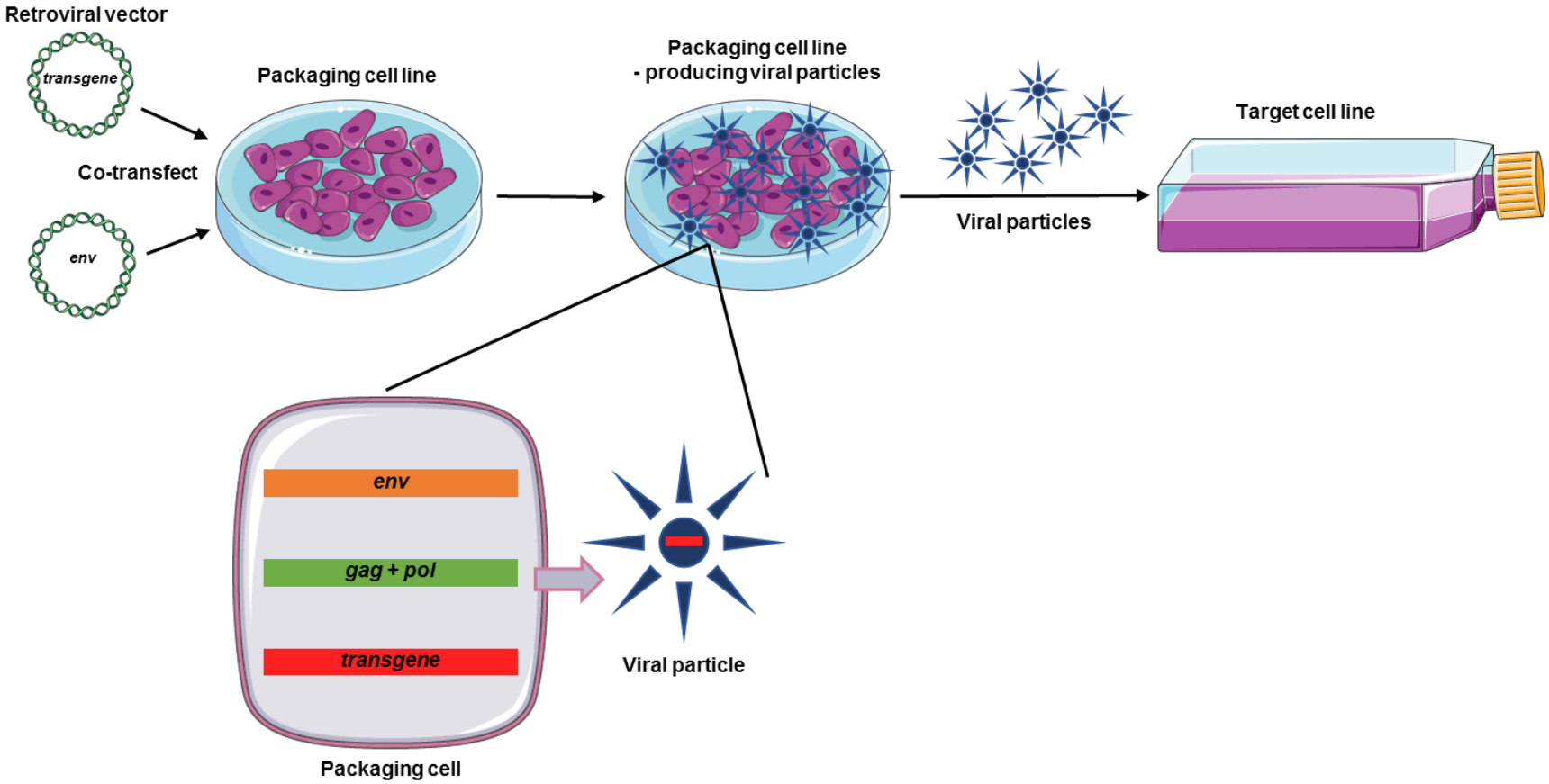

Figure 4-1: Schematic diagram of a retroviral vector system.
The retroviral vector system requires a packaging cell line, expressing the *gag* and *pol* genes, to be co-transfected with the viral vector containing the inserted transgene and a plasmid with the *env* gene. When all components come together the packaging cells create viral particles, which require the packaging functions and all viral proteins. The viral particles, containing the transgene, are released by the packaging cells into the culture medium, which is then applied to the target cell line for transfection.

4.1.3.2 Controlling gene overexpression

A method of controlling the expression of individual genes in mammalian cells was first devised as a means to mediate “on/off” activity of genes in a reversible way and at a defined level (Gossen and Bujard, 1992). This would need to be controlled exogenously by which gene expression is turned “on/off” pharmacologically. The tetracycline-resistance operon from the Tn10 in *E. coli* was exploited to develop a highly efficient regulatory system in mammalian cells. The tetracycline repressor (TetR) is very specific for its operator sequence and has very high affinity to tetracycline, which made it an ideal candidate. The binding of tetracycline to the TetR leads to derepression of the promoter controlling the gene of interest. There are two components required for this system (Yao et al., 1998). Firstly, the gene of interest is cloned into an expression vector controlled by the CMV promoter which has two tetracycline operator 2 (TetO2) sequences inserted. Secondly, a TetR-expressing plasmid is stably integrated into the mammalian host cell line so TetR is highly expressed. In the absence of tetracycline, the TetO2 sequences are binding sites for TetR and this represses transcription of the gene of interest. Upon addition, tetracycline binds the TetR and causes a conformational change in the protein that renders it unable to bind TetO2, thus dissociating from the TetO2 site and allowing induction of transcription of the gene of interest (Figure 4-2). This inducible expression system was also used in this study to control the expression of the GFAP encoding gene in Müller glial cells.

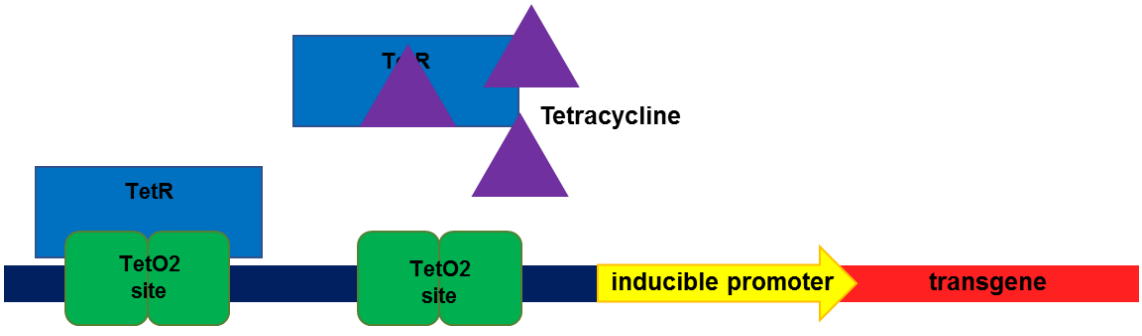

Figure 4-2: Schematic diagram of a tetracycline gene induction system.
The promoter is controlled by two tetracycline operator 2 (TetO2) sequences, which are repressed by the tetracycline repressor (TetR). The host cell line is stably expressing TetR. The addition of tetracycline to the culture causes derepression of the promoter because tetracycline binds to the TetR, removing it from the TetO2 site and allowing transcription of the transgene.

4.2 Objectives

As GFAP is a gliosis associated protein and a universally used marker of Müller glia activation and retinal gliosis, it was of special interest to investigate the effects of GFAP upregulation in Müller glial cells. Overexpression of GFAP in astrocytes has been extensively studied and used as an *in vivo* model for Alexander disease. However, the effect of GFAP overexpression in the retina, and specifically the Müller glia, of these animals has never been investigated. To begin to elucidate the role of GFAP in Müller glia during gliosis, it would be important to examine the effects of overexpression of GFAP in MIO-M1 cells *in vitro*. The methodology for investigating this intermediate filament at the cellular level are however limited. On this basis, various molecular biology techniques were used in this study for inducing genetic overexpression of GFAP. Controlling the expression of GFAP and being able to exogenously switch on gene transcription is an essential step when exploring the effects of this protein in Müller glial cell functions within the retina. Therefore, the object of this chapter was to develop a protocol to induce upregulation of GFAP in MIO-M1 cells and the following approaches were used.

The transfection methods used in this chapter were:

1. Examination of an *in vitro* protocol to transfect MIO-M1 cells with a plasmid containing the GFAP encoding gene using a lipid-based transfection reagent to overexpress this protein.
2. Examination of an *in vitro* protocol to regulate on/off GFAP overexpression in MIO-M1 cells using tetracycline to induce gene expression.
3. Optimisation of an *in vitro* methods to induce GFAP overexpression in MIO-M1 cells, combining the retroviral vector transfection method with the tetracycline inducible system.
4. Optimisation of an *in vitro* protocol using retroviral transfection of MIO-M1 cells to overexpress GFAP at increasing levels.

Experimental design:

I. MIO-M1 cells were transfected with a plasmid containing the GFAP encoding gene tagged to a fluorescent mCherry protein using EndoFectin™ Max, which is a lipid-based transfection reagent.

II. An MIO-M1 cell line was established which stably expressed the pcDNA4/TR plasmid and thus produced tetracycline regulatory protein. The mCherry-GFAP sequence including an upstream tetracycline operator promoter was cloned into the retroviral vector pCLNCx (pCLNC-mCherry-GFAP-TO). This cloning step involved removal of the vectors CMV promoter. The MIO-M1 pcDNA4/TR cell line was transduced with viral construct. GFAP expression was induced in these cells using the tetracycline “turn on” system.

III. Due to insufficient tetracycline regulatory protein expression achieved by using the pcDNA4/TR plasmid, a new vector was created. The gene encoding for the tetracycline regulatory protein was cloned into the retroviral vector pCLNCx (pCLNC-TetR). This plasmid was co-transfected with the pCLNC-mCherry-GFAP-TO vector into MIO-M1 cells to optimise tetracycline controlled induction of GFAP.

IV. MIO-M1 cells were transfected with a newly created retroviral vector pCLNCx cloned with the mCherry-GFAP sequence controlled by a CMV promoter (pCLNC-mCherry-GFAP). The virus was titrated onto the MIO-M1 cells in order to produce cells with low or high expression of the GFAP gene.

V. Fluorescence-activated cell sorting was used to analyse transfection efficiency and median mCherry fluorescence intensity in transfected MIO-M1 cells.

VI. To assess levels of transfection, RNA was extracted from co-transfected cells and used in qPCR to measure relative expression ratios of the genes encoding for the tetracycline regulatory protein and mCherry-GFAP.

4.3 Results

4.3.1 Transient transfection of MIO-M1 cells with the mCherry-GFAP-N-18 plasmid

A plasmid containing an mCherry-N-18 vector backbone which expresses the human GFAP protein tagged to the N-terminus of the mCherry fluorescent protein (see appendix 4), a gift from Michael Davidson (Addgene plasmid # 55051), was initially used to overexpress GFAP in the MIO-M1 cell line. MIO-M1 cells were transfected with the plasmid DNA using the EndoFectin Max transfection reagent. For this purpose, various combinations of plasmid DNA concentrations and volumes of EndoFectin Max transfection reagent were tested to optimise the protocol in MIO-M1 cells.

After 48 hours incubation with the transfection reagent cells were imaged under a fluorescence microscope and counted manually using ImageJ. Using 0.5µg of plasmid DNA yielded very low percentage of transfected cells; when 0.5µg of plasmid DNA was used with 0.5µl of transfection reagent 2% of cells expressed mCherry and when 0.5µg of plasmid DNA was used with 1µl of transfection reagent, 4% of cells were transfected (Figure 4-3). Very low cell death was observed after incubation with EndoFectin Max at low volumes. However, when higher volumes of this reagent were used, cell debris was often observed. The amount of plasmid DNA was increased to 1µg and combined with 2µl, 3µl or 4µl of transfection reagent (Figure 4-3). When 1µg of plasmid DNA was incubated with 2µl of EndoFectin Max, there was 30% transfection efficiency, which was the highest proportion of transfected cells observed. When 3µl of transfection reagent was used, 19% transfection was observed. Although using 1µg of plasmid DNA with 4µl of reagent generated 25% of transfected cells, higher cell mortality was observed causing fewer cells to count, which appeared to skew the results (Figure 4-4).

Based on the above results, attempts to expand the number of transfected cells for further studies were made. For this purpose, the optimised condition selected was 1µg of plasmid DNA per 2µl of EndoFectin Max reagent. After 48 hours incubation with the transfection reagent, positive cells were selected by incubation with G418 antibiotic for 48 hours and imaged under a fluorescence microscope (Figure 4-5A). A large proportion of cells were observed to be mCherry positive, therefore cell sorting through FACS was undertaken. After

FACS sorting and growth for 3 days, there were only a few mCherry positive cells within the population (Figure 4-5B). These cells that had become confluent were passaged and allowed to grow to confluence for 5 days before being imaged again. One passage after FACS sorting the cells were no longer positive for mCherry fluorescence and therefore did not contain the GFAP expressing plasmid (Figure 4-5C). The proportion of mCherry fluorescence positive cells declined upon expansion, suggesting that using the EndoFectin Max reagent resulted in a transient transfection of MIO-M1 cells with the mCherry-GFAP-N-18 plasmid. Therefore, different permanent transfection methods were explored that would also produce a higher transfection efficiency.

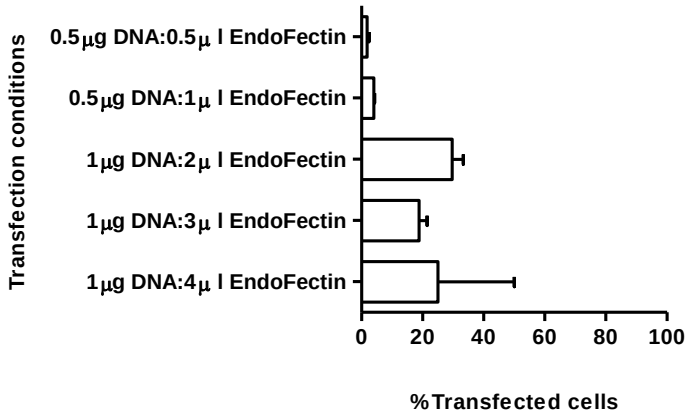

Figure 4-3: Percentage of MIO-M1 cells expressing mCherry fluorescence following transfection with the mCherry-GFAP-N-18 plasmid.
Graph shows the efficiency of transfection conditions, in which various levels of plasmid DNA and EndoFectin reagent were used. Bar chart represents transfection rate which was calculated as the average percentage of mCherry positive cells (mean +/- SEM), N=3 images.

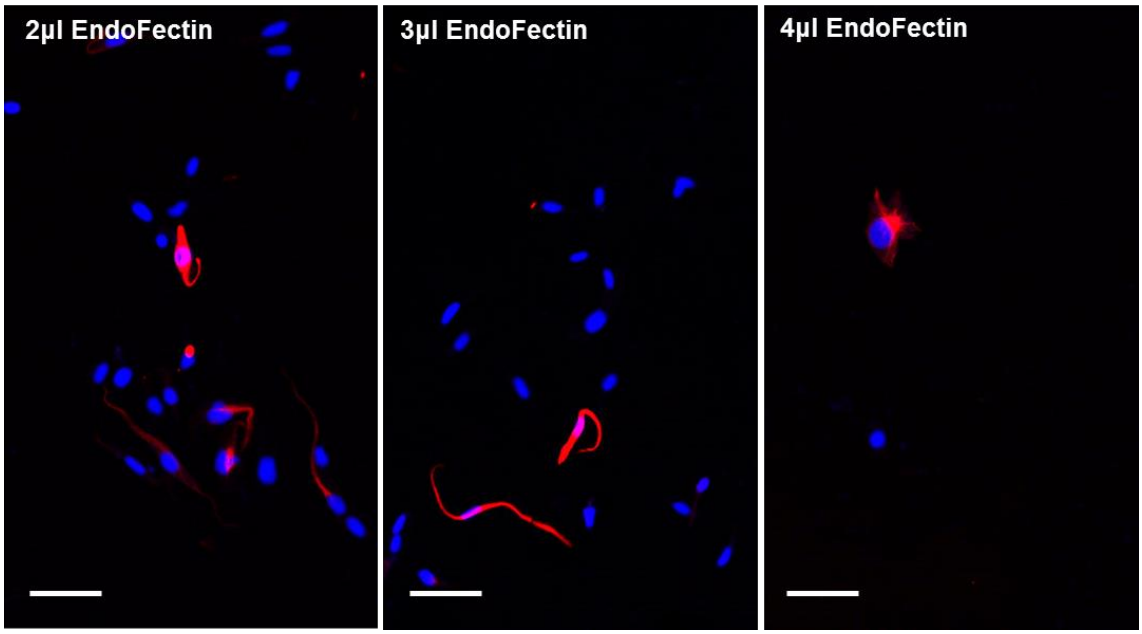

Figure 4-4: Confocal images of MIO-M1 cells after transfection with 1µg mCherry-GFAP-N-18 plasmid and 2µl, 3µl or 4µl of EndoFectin Max transfection reagent.
Representative images showing nuclei staining DAPI (blue) and mCherry fluorescence (red) merged. mCherry positive cells indicated transfection and GFAP overexpression. Use of 4µl of EndoFectin reagent caused cell death and reduced cell numbers. Scale bars represent 100µm.

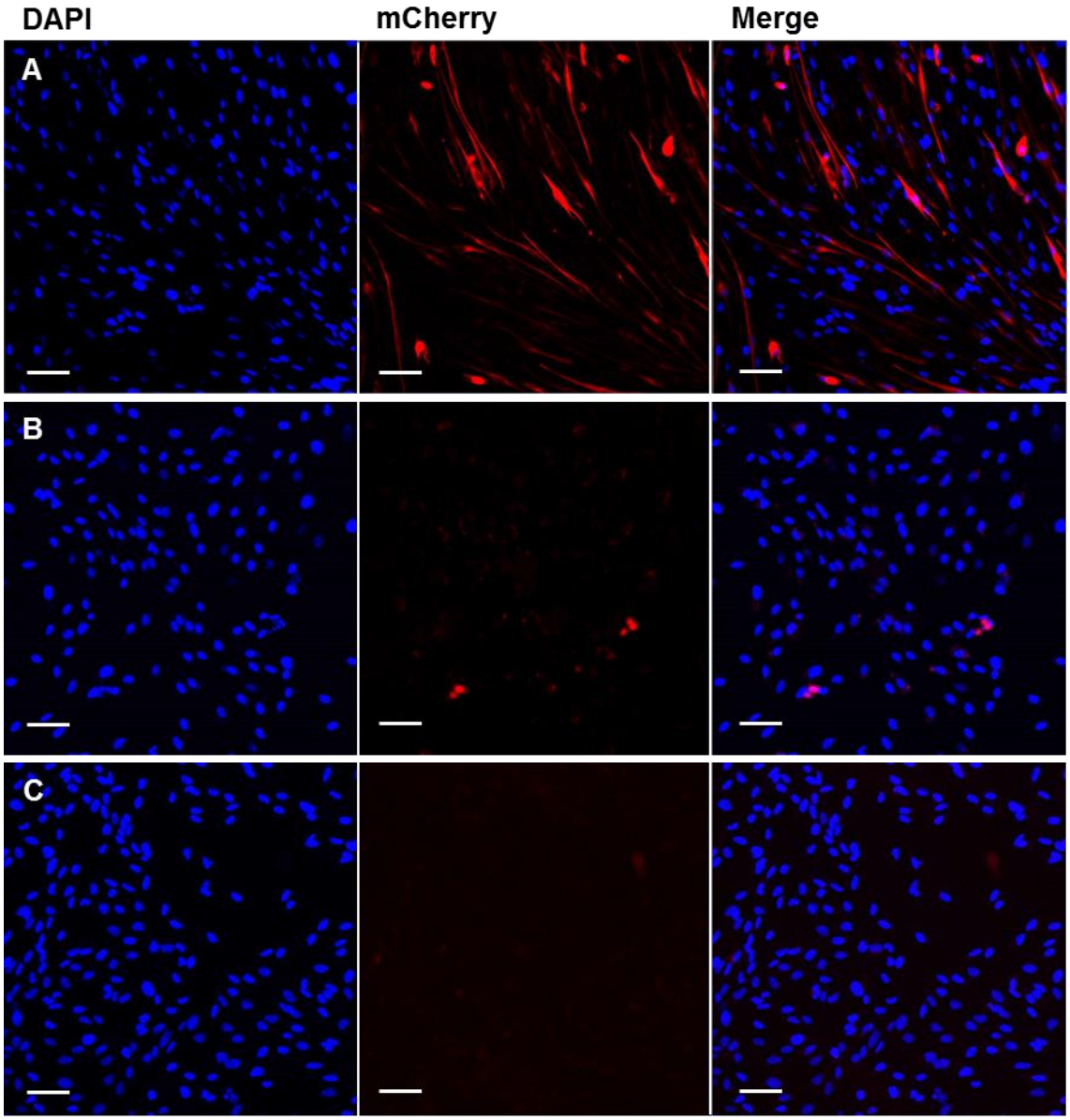

Figure 4-5: Confocal images of MIO-M1 cells transfected with mCherry-GFAP-N-18 plasmid.
Representative images showing nuclei staining DAPI (blue), mCherry fluorescence (red) and both merged. **(A)** After 48 hour of antibiotic selection by G418, the majority of Müller glial cells were positive for mCherry fluorescence. **(B)** After FACS selection for mCherry and 3 days in culture, few cells were positive for mCherry fluorescence. **(C)** Passaging cells after FACS and culturing for 5 days completely eliminated mCherry fluorescence in MIO-M1 cells. Scale bars represent 80µm.

4.3.2 Transfection of MIO-M1 cells with the retroviral pCLNCx vector expressing GFAP under the control of an inducible promoter

Using a retroviral vector would allow for permanent transfection of MIO-M1 cells with a GFAP-overexpressing plasmid. Schematic of the pCLNCx retroviral expression vector used in this study is shown in appendix 6 and was a gift from Dr. Amanda Carr. Firstly, the mCherry-GFAP sequence was cut from the Addgene plasmid and cloned into the pCLNCx retroviral vector to create a new pCLNC-mCherry-GFAP plasmid. Since the pCLNCx retroviral vector is under the control of the CMV promoter which is constitutively activated in mammalian cells it was decided that an inducible promoter would allow for better control of GFAP expression in MIO-M1 cells. The Invitrogen T-REx™ System, which is tetracycline regulated, was explored. Both plasmids pcDNA4™/TO/*myc*-His B and pcDNA4/TR were a gift from Prof. Karl Matter. The inducible expression plasmid pcDNA4™/TO/*myc*-His has the CMV promoter with two tetracycline operator 2 (TetO2) sites inserted to allow transcriptional control as indicated above. This inducible promoter was cloned into the pCLNC-mCherry-GFAP retroviral vector to allow retroviral transfection of MIO-M1 cells with GFAP under inducible promoter control (Figure 4-6). Methods used for this cloning and transfection are explained in detail in the Material and Methods section. The newly created plasmid was named pCLNC-mCherry-GFAP-TO (Figure 4-7). A control vector containing the mCherry sequence under the control of the TetO2 inducible promoter was also created (pCLNC-mCherry-TO) in order to confirm that any effects observed in the transfected MIO-M1 cells were not caused by the mCherry protein itself.

Before the retroviral transfection, a stable MIO-M1 cell line expressing the regulatory vector pcDNA4/TR containing the TetR gene and expressing high levels of tetracycline regulatory molecule, was established for use as hosts for the inducible promoter-based constructs. MIO-M1 cells were transfected with the regulatory plasmid pcDNA4/TR, which contained the blasticidin resistance gene allowing for selection of the plasmid using blasticidin antibiotic. A stable MIO-M1 cell line was established after 2 weeks in culture with selective medium, which killed negative untransfected control cells (Figure 4-8)

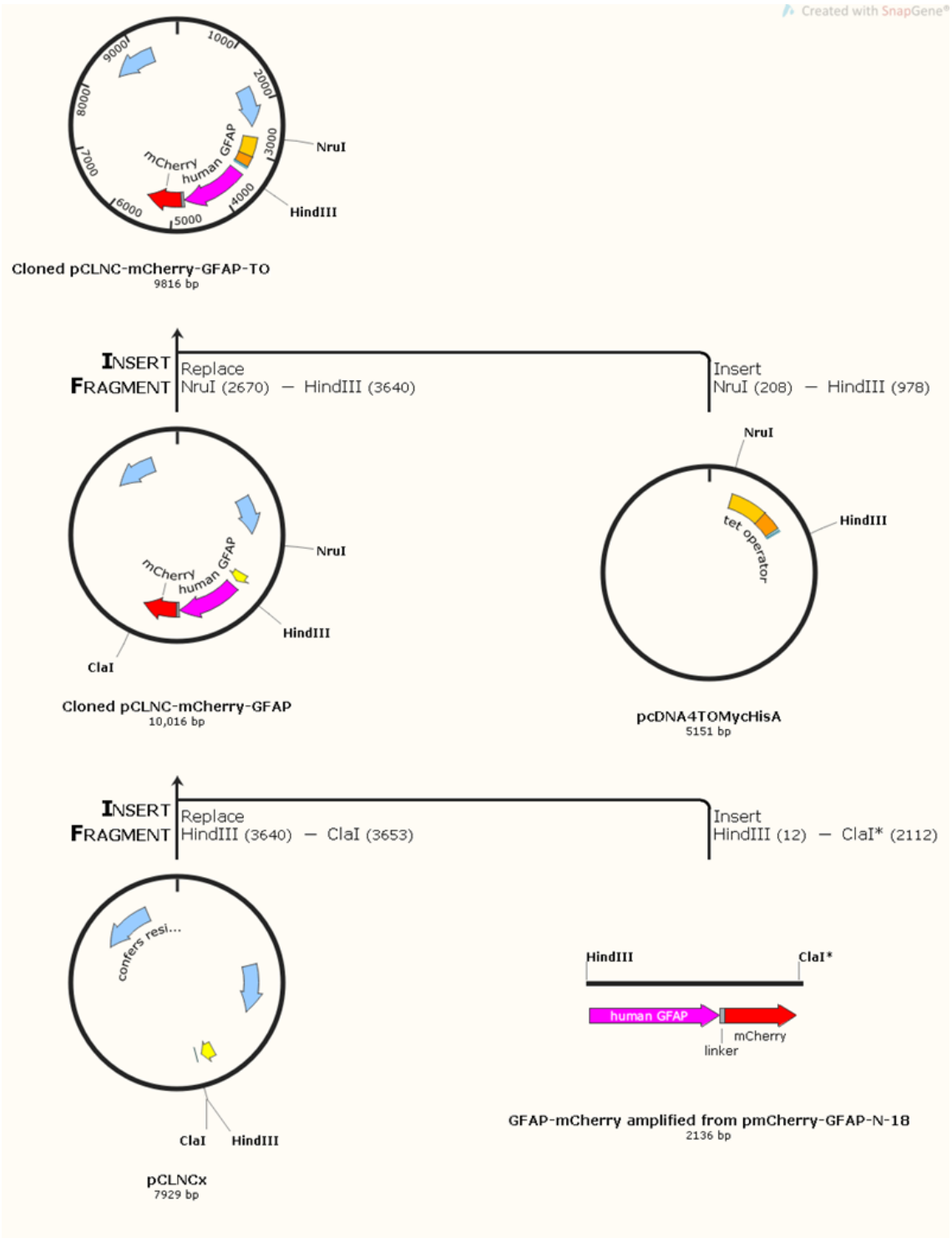

Figure 4-6: Diagram representing cloning history for creating pCLNC-mCherry-GFAP-TO. The initial pCLNC-mCherry-GFAP vector was created from cloning the amplified mCherry tagged GFAP sequence from the mCherry-GFAP-N-18 plasmid into the pCLNCx retroviral vector. This new pCLNC-mCherry-GFAP vector then had the CMV promoter removed and the TetO2 promoter cloned in from the pcDNA4™/TO/*myc*-His vector.

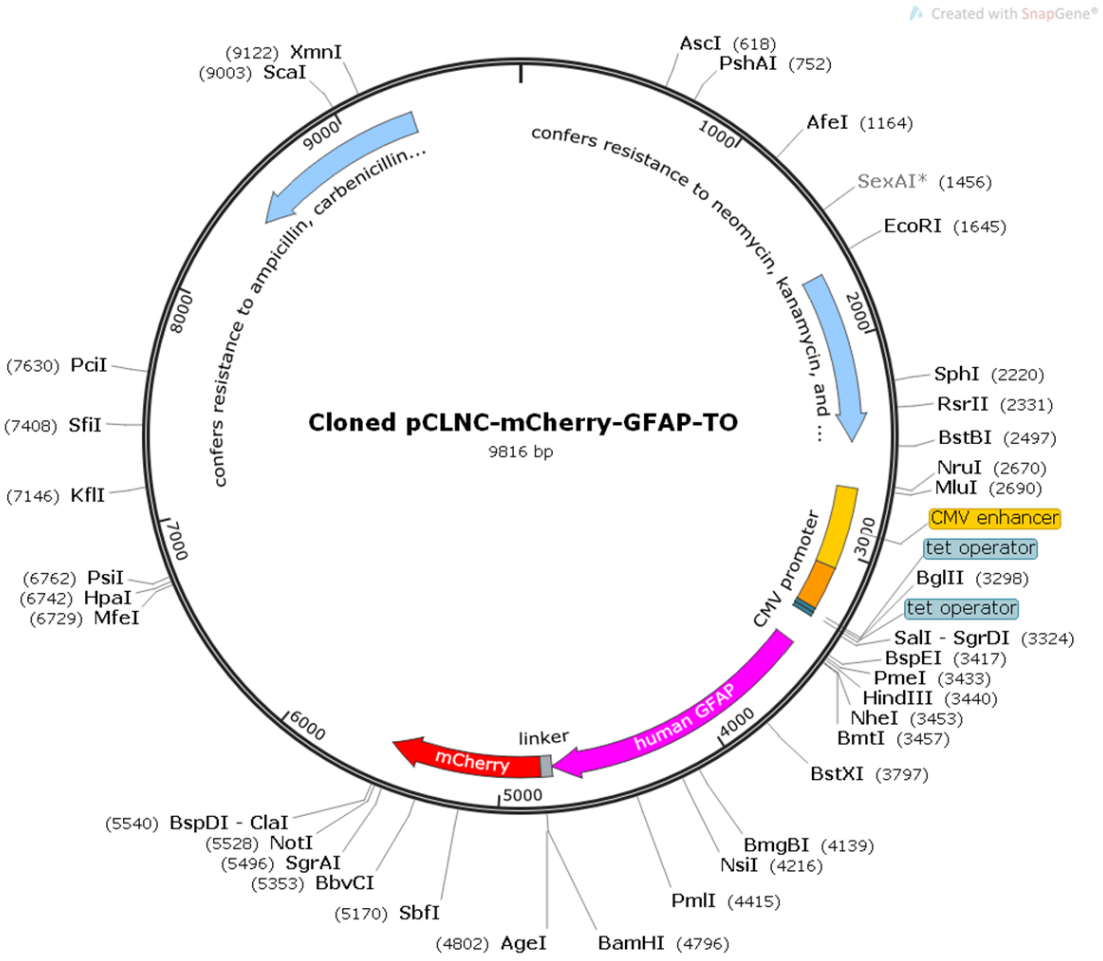

Figure 4-7: Map of cloned pCLNC-mCherry-GFAP-TO with relevant features and all restriction enzyme sites.
The original CMV promoter was replace by a TetO2 promoter between restriction enzyme sites NRuI and HindIII. The mCherry-GFAP sequence was inserted into the cloning sites between restriction enzyme sites HindIII and ClaI. The new cloned vector was 9816bp.

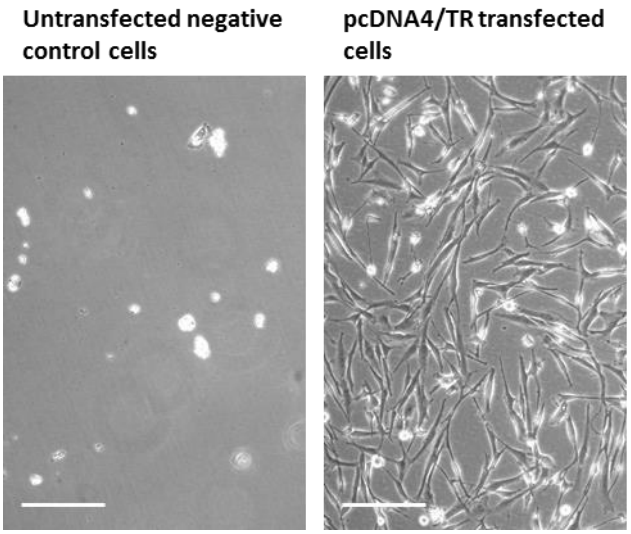

Figure 4-8: Phase microscope images of untransfected control MIO-M1 cells and cells transfected with pcDNA4/TR cultured with 1µg/ml blasticidin.
After two weeks of culturing cells with blasticidin, negative control untransfected cells died. However, transfected cells containing the blasticidin-resistance gene survived culture with this antibiotic and a stable line of MIO-M1 pcDNA4/TR cells was established. Scale bar represents 200µm.

4.3.2.1 MIO-M1 pcDNA4/TR cells transfected with the retroviral vector pCLNC-mCherry-GFAP-TO were not induced to express mCherry-GFAP by tetracycline

The newly created MIO-M1 pcDNA4/TR cell line was transfected with the retroviral vector pCLNC-mCherry-GFAP-TO or the control vector pCLNC-mCherry-TO. After transfection and selection with both blasticidin and G418 antibodies, these cells expressed a small amount of mCherry fluorescence even without tetracycline induction, when the promoter should be “turned off” (Figure 4-9). The control vector (Figure 4-9B) appeared to express more mCherry fluorescence than the vector containing GFAP (Figure 4-9A).

Transfected cells were exposed to tetracycline in order to derepress the TetO2 promoter to initiate expression of mCherry-GFAP or mCherry alone. To test the optimal TetO2 promoter induction, varying tetracycline concentrations (between 0.1 and 1µg/ml) and incubation times (8 to 24 hours) were tested. Cells were initially cultured in the absence or presence of 0.5 and 1µg/ml tetracycline for 8 and 18 hours (Figure 4-10). After 8 hours, cells transfected with the pCLNC-mCherry-GFAP-TO vector and treated with 0.5 and 1µg/ml tetracycline did not increase expression of mCherry fluorescence when compared to the cells cultured without tetracycline (Figure 4-10A). Further exposure for 18 hours, also did not induce the expression of mCherry fluorescence in the transfected cells at either of these tetracycline concentrations (Figure 4-10B). On this basis, it was decided to increase the concentration of tetracycline as well as the exposure time. Cells were cultured in the absence or presence of 5 and 10 µg/ml tetracycline for 24 hours. However, fluorescence microscopy images showed that neither 5 nor 10µg/ml of tetracycline induced an increase in mCherry fluorescence in MIO-M1 cells after 24 hours transfection with pCLNC-mCherry-GFAP-TO retroviral vector, compared to the same cells without tetracycline (Figure 4-11). The same lack of mCherry fluorescence was observed in cells transfected with the control vector pCLNC-mCherry-TO (not shown).

These observations indicated that tetracycline was not controlling the TetO2 promoter. Sequencing of the vectors revealed that both were correct and therefore the cells should be expressing the correct TetO2 promoter sequence. However, it might be possibly that there was not enough of the TetR regulatory

protein expression when compared to the TetO2 promoter. The retroviral vector pCLNCx may have been producing more mCherry-GFAP-TO compared to the pcDNA4/TR plasmid production of the TetR molecule in the MIO-M1 cell line. Therefore, to improve the control of the inducible promoter, copy numbers of the TetR were increased in further studies.

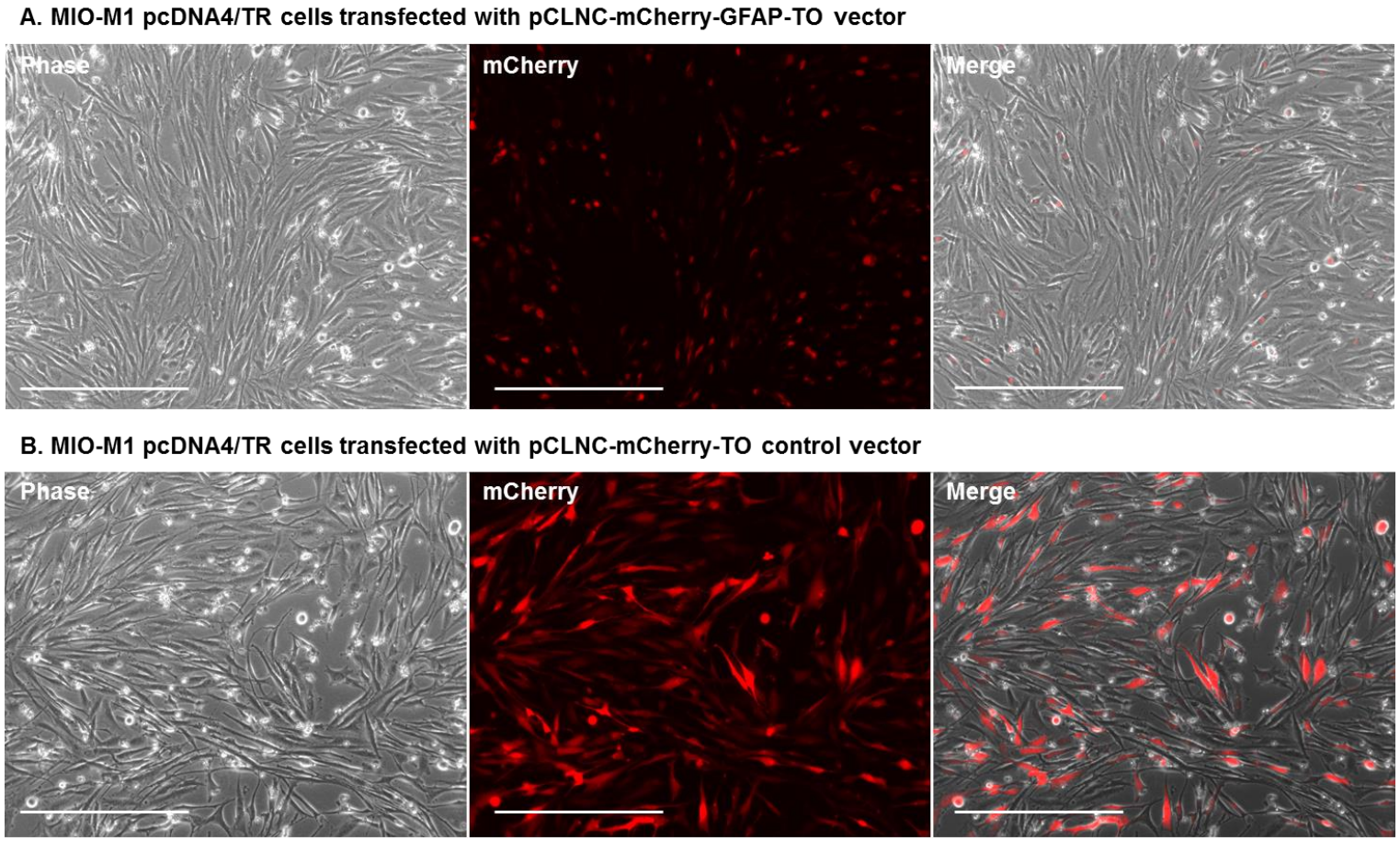

Figure 4-9: Representative phase and fluorescence microscope images of transfected MIO-M1 pcDNA4/TR cell line. Cells were transfected with **(A)** retroviral vector pCLNC-mCherry-GFAP-TO or **(B)** control vector pCLNC-mCherry-TO. Images show that even with the promoter "turned off" cells were expressing a small amount of mCherry fluorescence. Scale bar represents 400µm.

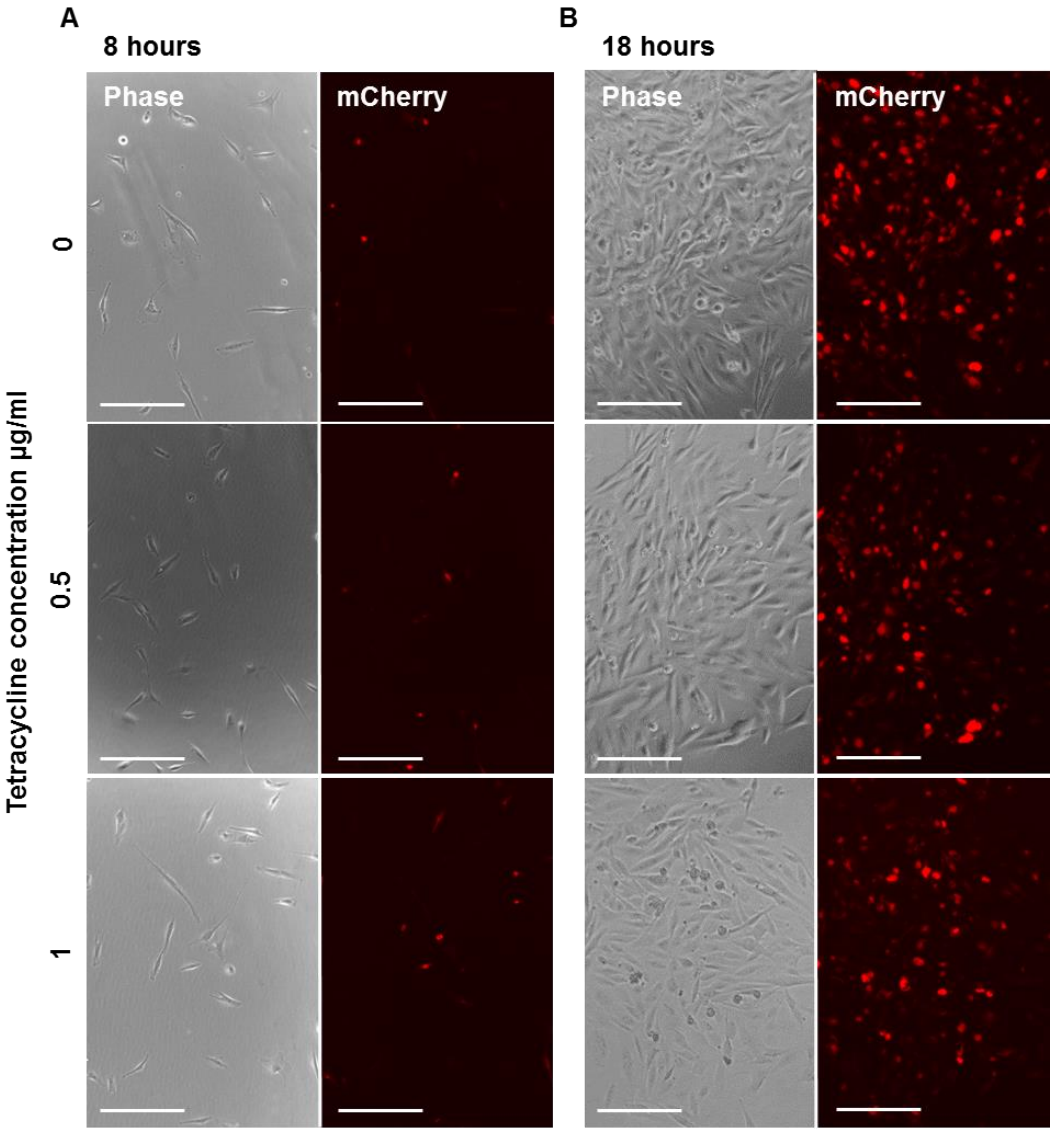

Figure 4-10: Representative phase and fluorescence microscope images of transfected MIO-M1 pcDNA4/TR cells cultured with increasing concentrations of tetracycline.
Cells transfected with retroviral vector pCLNC-mCherry-GFAP-TO were cultured with 0, 0.5 or 1µg/ml of tetracycline. **(A)** After 8 hours of culturing transfected cells with tetracycline, cells did not express more mCherry fluorescence when compared to cells cultured in the absence of tetracycline. **(B)** 18 hours of culture with increasing concentrations of tetracycline did not modify mCherry fluorescence expression by transfected MIO-M1 cells when compared to cells cultured in the absence of tetracycline. Scale bar represents 200µm.

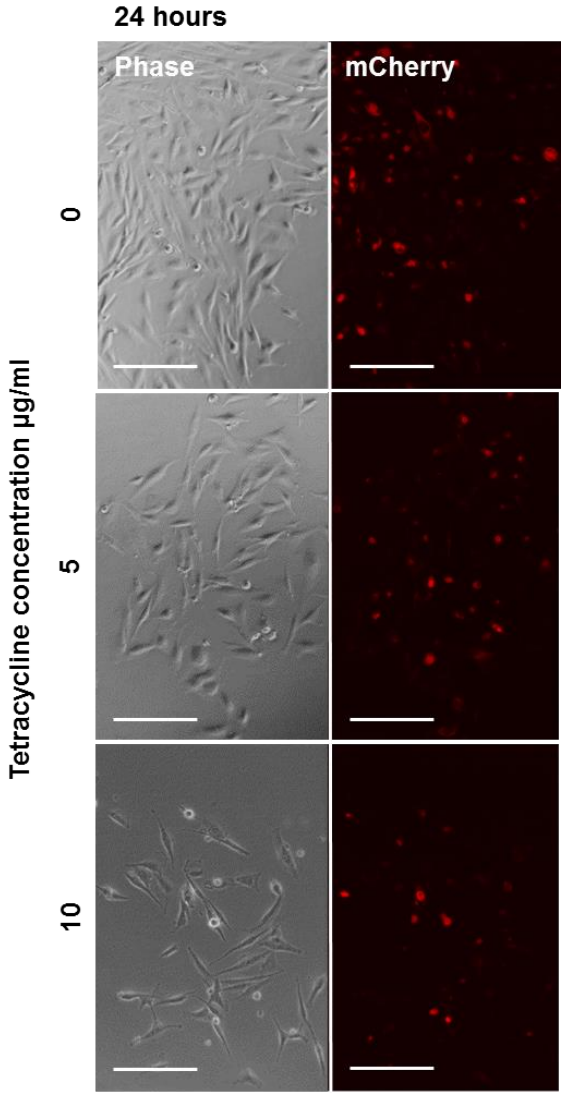

Figure 4-11: Representative phase and fluorescence microscope images of MIO-M1 pcDNA4/TR cells transfected with the retroviral vector pCLNC-mCherry-GFAP-TO and cultured with increasing concentrations of tetracycline.
Cells cultured for 24 hours with both 5 and 10µg/ml of tetracycline did not show increased expression of mCherry fluorescence when compared to cells cultured in the absence of tetracycline. Scale bar represents 200µm.

4.3.3 Co-transfection of MIO-M1 cells with the pCLNC-TetR vector and the pCLNC-mCherry-GFAP-TO vector or the control pCLNC-mCherry-TO vector

In order to increase copy numbers of the TetR gene, it was cloned into the retroviral vector pCLNCx. The restriction enzyme sites HindIII and ClaI in pCLNCx downstream of the CMV promoter were exploited to clone the TetR sequence from the pcDNA4/TR plasmid (Figure 4-12). The newly created retroviral vector was named pCLNC-TetR (Figure 4-13). MIO-M1 cells were co-transfected with viral medium containing the pCLNC-TetR vector and the pCLNC-mCherry-GFAP-TO vector or the pCLNC-TetR vector with the pCLNC-mCherry-TO control vector. Various ratios of TetR to TetO2 containing viral medium were used to increase copy numbers of the TetR gene relative to the TetO2 promoter. After co-transfection, cells were observed under a digital inverted microscope to check for lack of mCherry fluorescence. When the ratio of TetR viral medium increased during co-transfection, there were fewer observable mCherry positive cells (Figure 4-14).

Quantification of the proportion of mCherry fluorescence positive cells revealed that when MIO-M1 cells were co-transfected with retroviral vectors pCLNC-TetR and pCLNC-mCherry-GFAP-TO at increasing ratios of TetR to TetO2 inducible promoter, the percentage of cells expressing mCherry decreased (Figure 4-15). When the MIO-M1 cells containing the original pcDNA4/TR plasmid were transfected with pCLNC-mCherry-GFAP-TO vector, 27% of the cells were positive for mCherry fluorescence and this single transfection was used as a reference baseline. The percentage of mCherry positive cells increased to 43% in MIO-M1 cells that were co-transfected with viral medium containing the vectors pCLNC-TetR and pCLNC-mCherry-GFAP-TO at a ratio of 4:1. However, the percentage of mCherry positive cells then decreased as the ratio changed and increased amounts of pCLNC-TetR viral medium were used. At a ratio of 20:1 of pCLNC-TetR to pCLNC-mCherry-GFAP-TO, 18% of cells were positive for mCherry fluorescence and at a ratio of 50:1 this was reduced to 5% positive cells. Increasing the ratio further to 200:1 decreased the percentage of mCherry positive cells to 3% and at 500:1 this fell to 0% (Figure 4-15). This suggested that increasing the volume of viral medium containing the pCLNC-

TetR vector caused a corresponding TetR repression of the TetO2 promoter and subsequent reduction in mCherry-GFAP in transfected cells.

The trend of a decreasing proportion of mCherry positive cells was the same in MIO-M1 cells co-transfected with pCLNC-TetR and the control pCLNC-mCherry-TO vector at differing ratios. When the MIO-M1 pcDNA4/TR cell line was transfected with retroviral control vector pCLNC-mCherry-TO, 57% mCherry fluorescent positive cells was observed. However, after co-transfection with the vectors pCLNC-TetR and pCLNC-mCherry-TO at a ratio of 4:1 the percentage of mCherry positive cells decreased to 48%. Further decreases to 31%, 19%, 8% and 4% mCherry fluorescent cells were observed when the ratio of transfection was 20:1, 50:1, 200:1 and 500:1, respectively (Figure 4-15). This indicated that increasing the ratio of volume of viral medium containing the pCLNC-TetR vector to pCLNC-mCherry-TO vector caused sufficient increase in TetR to repress the expression of mCherry induced by the TetO2 promoter in transfected cells.

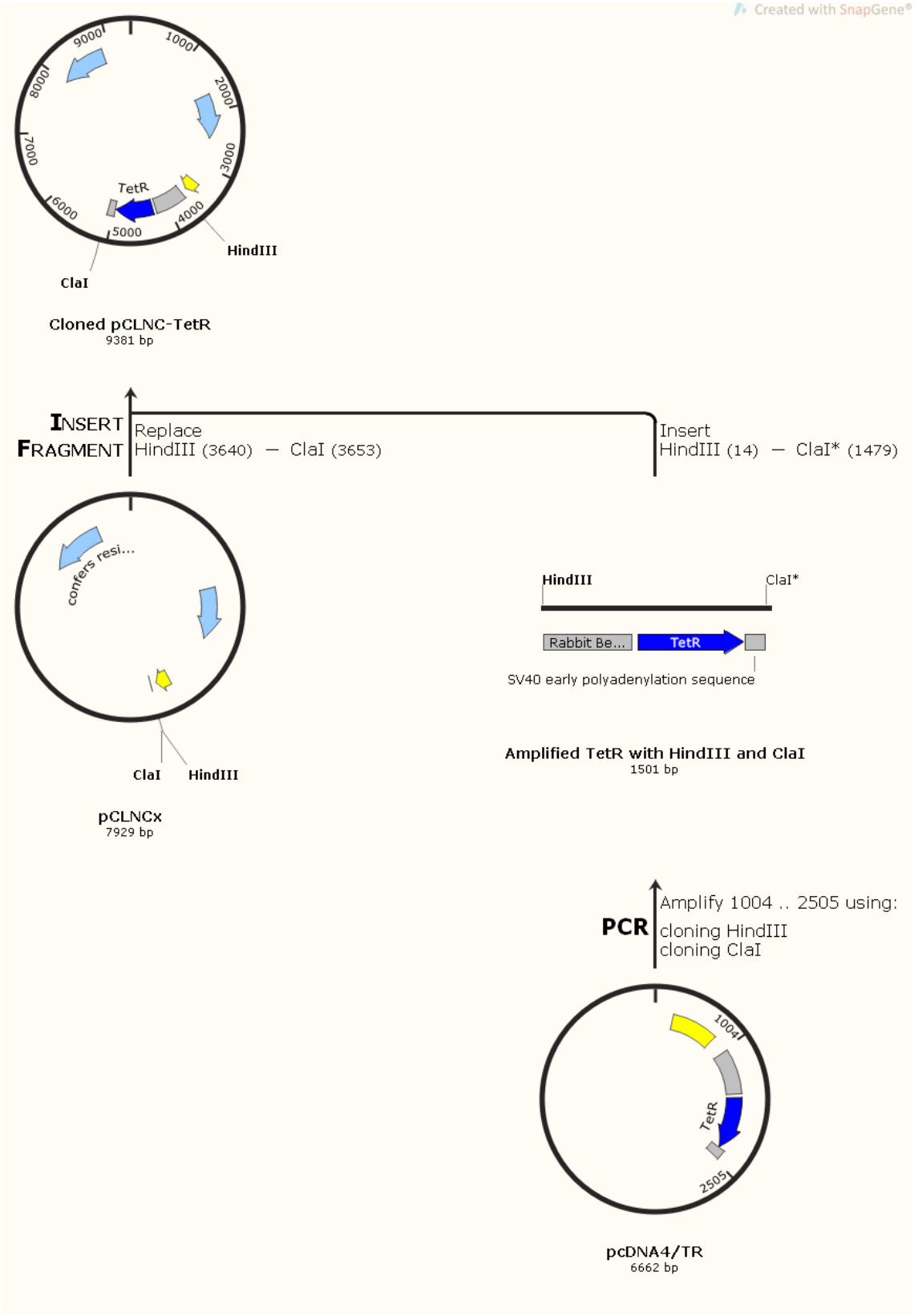

Figure 4-12: Diagram representing the cloning history of the pCLNC-TetR vector.
The TetR sequence from the pcDNA4/TR vector was amplified and cloned into the pCLNCx retroviral vector HindIII and ClaI cloning site.

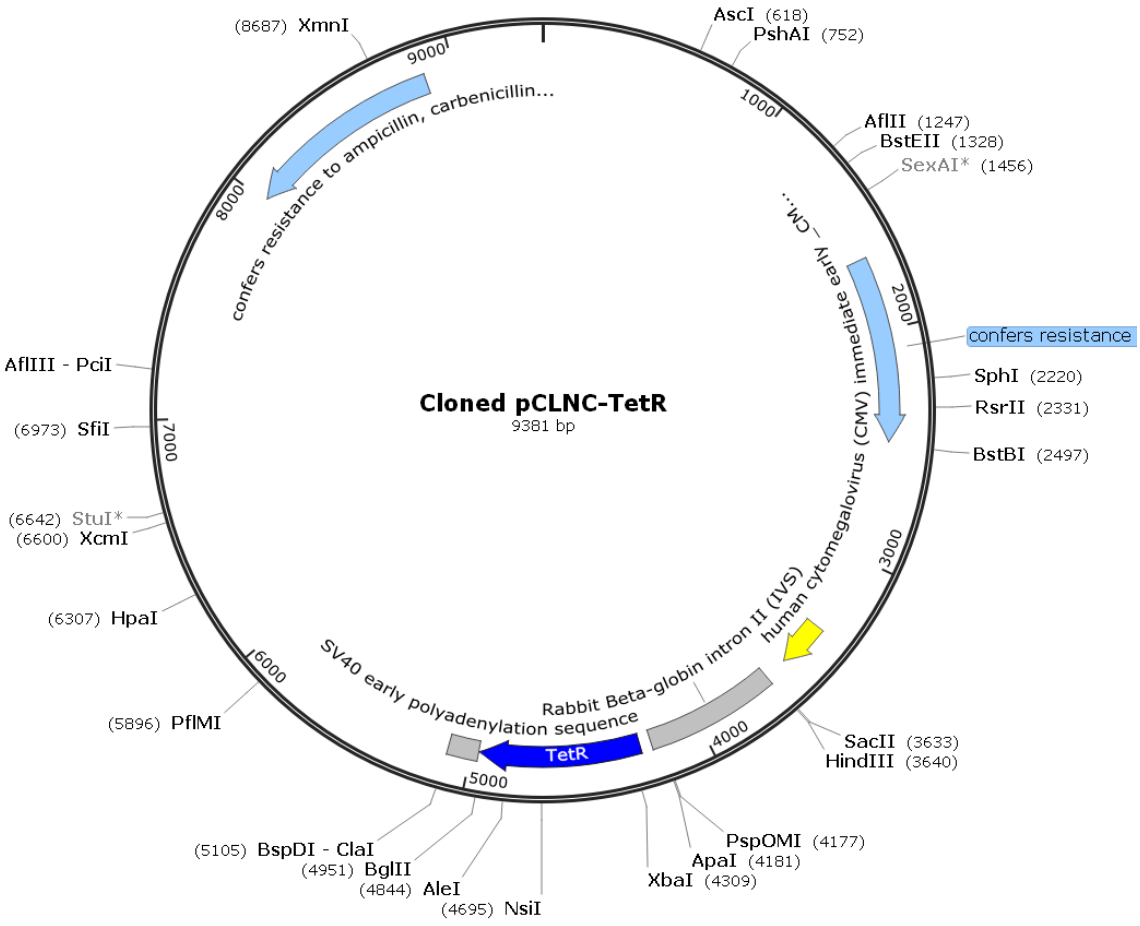

Figure 4-13: Map of the cloned pCLNC-TetR vector with relevant features and all restriction enzyme sites.
The TetR sequence was inserted into the cloning sites HindIII and ClaI of pCLNCx retroviral vector. The new cloned vector was 9381bp.

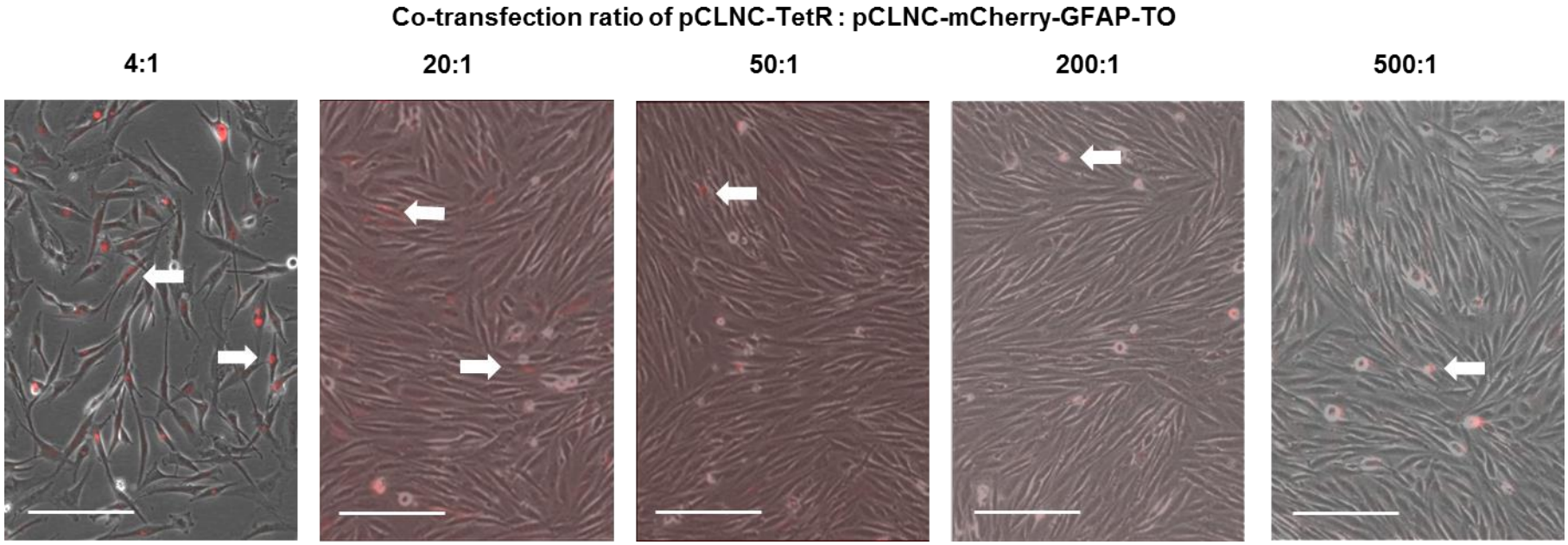

Figure 4-14: Representative merged phase and fluorescence microscope images of MIO-M1 cells co-transfected with retroviral vectors. Cells were co-transfected with pCLNC-TetR and pCLNC-mCherry-GFAP-TO retroviral vector medium applied at ratios ranging from 4:1 up to 1000:1. Images show representatives of ratios 4:1, 20:1, 50:1, 200:1 and 500:1. Increasing the volume of medium containing the pCLNC-TetR vector caused decrease in mCherry fluorescence. White arrows indicate mCherry positive cells.

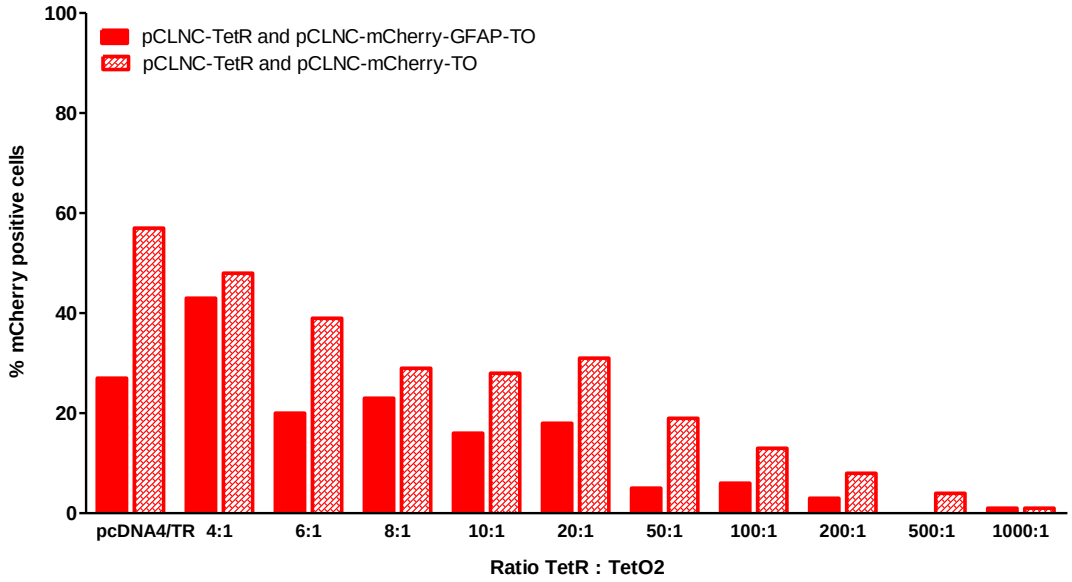

Figure 4-15: Percentage of mCherry fluorescence positive MIO-M1 cells after co-transfection with retroviral vectors at increasing ratios of TetR to TetO2 promoter. Solid red bar chart represents percentage of cells positive for mCherry after co-transfection with the pCLNC-TetR and pCLNC-mCherry-GFAP-TO vectors. Crosshatched red bar chart represents percentage of mCherry positive cells after co-transfection with the pCLNC-TetR vector and pCLNC-mCherry-TO control vector. As the proportion of pCLNC-TetR vector increased, the percentage of mCherry positive cells decreased. The bars represented by pcDNA4/TR are the percentage of mCherry positive cells within the MIO-M1 pcDNA4/TR cell line singularly transfected by either pCLNC-mCherry-GFAP-TO or pCLNC-mCherry-TO. These values were used as a “base-line” for expression of mCherry by cells co-transfected with various ratios of both vectors. N=1.

4.3.3.1 TetR gene expression was not increased as mCherry-GFAP or mCherry gene expression decreased in MIO-M1 cells that had been co-transfected

MIO-M1 cells were co-transfected with various ratios of viral medium containing the retroviral vectors pCLNC-TetR encoding for the TetR gene and pCLNC-mCherry-GFAP-TO encoding for the GFAP gene tagged to mCherry and under the transcriptional control of the TetO2 promoter. The relative expression of these genes was measured by qPCR in transfected cells, using the RNA from the MIO-M1 cells containing the pcDNA4/TR plasmid singularly transfected with the pCLNC-mCherry-GFAP-TO vector as a calibrator sample. Fold changes in gene expression were compared between cell groups (Figure 4-16). When the transfection ratio was 20:1 of pCLNC-TetR to pCLNC-mCherry-GFAP-TO, the relative expression of the TetR gene was significantly downregulated by 1.85-fold ($p<0.01$). The TetR gene expression was also significantly downregulated ($p<0.05$) when the ratio of transfection was 50:1 and 1000:1 and downregulated at 500:1, although not significantly, when compared to the calibrator sample. Relative expression of the TetR gene slightly increased to 1.106 and 1.064 when transfection ratio was 100:1 and 200:1, respectively, which corresponds to a non-significant 0.94 and 0.90-fold upregulation (Figure 4-16). On the other hand, the relative gene expression of mCherry-GFAP was significantly decreased in all samples when compared to the calibrator ($p<0.001$). When the co-transfection ratio was 20:1 or 1000:1 of pCLNC-TetR to pCLNC-mCherry-GFAP-TO vectors, the gene expression of mCherry-GFAP was significantly downregulated by 15-fold and 570-fold, respectively when compared to the calibrator ($p<0.001$). This correlated to the percentage of mCherry positive cells decreasing in these transfected cells.

MIO-M1 cells were also co-transfected with the retroviral vectors pCLNC-TetR and pCLNC-mCherry-TO encoding for the mCherry gene alone controlled by the TetO2 promoter. The relative expression of these genes was measured by qPCR in these cells and using the RNA from the MIO-M1 pcDNA4/TR cell line transfected with pCLNC-mCherry-TO as a calibrator sample, fold changes in gene expression were compared (Figure 4-17). In all co-transfection samples, relative expression of TetR gene was downregulated compared to the single transfection calibrator sample. When the ratio of co-transfection of pCLNC-TetR

to pCLNC-mCherry-TO was 20:1, 50:1, 200:1, 500:1 and 1000:1, TetR gene expression was significantly downregulated when compared to the calibrator sample ($p<0.05$). The largest fold change was at the ratio of 20:1 where the TetR gene was significantly downregulated by 4-fold ($p<0.01$). Even at the ratio of 100:1 there was a 1-fold downregulation although this was not significant (Figure 4-17). Gene expression of mCherry was significantly downregulated in MIO-M1 cells that were co-transfected with pCLNC-TetR and pCLNC-mCherry-TO at all ratios tested ($p<0.001$). At a transfection ratio of 20:1 of pCLNC-TetR to pCLNC-mCherry-TO vectors, the relative expression ratio of mCherry was 0.035 when compared to the calibrator sample, which was a significant downregulation of 29-fold ($p<0.001$). At a transfection ratio of 1000:1 the relative expression ratio of mCherry was further reduced to 0.002 compared to the calibrator, which was a 584-fold significant downregulation ($p<0.001$) (Figure 4-17).

The results show that transfecting MIO-M1 cells with pCLNC-TetR retroviral vector did not increase TetR gene expression when compared to TetR gene expression in cells transfected with the pcDNA4/TR plasmid. Although TetR gene expression in pCLNC-TetR transfected cells was reduced or the same as pcDNA4/TR transfected cells, increasing the ratio of viral pCLNC-TetR vector to pCLNC-mCherry-GFAP-TO vector, did significantly reduce the gene expression of mCherry-GFAP. This significant reduction in mCherry-GFAP with assumed corresponding reduction in TetO2 promoter expression allowed sufficient TetR mediated repression, as indicated by reduced mCherry fluorescence in these transfected cells.

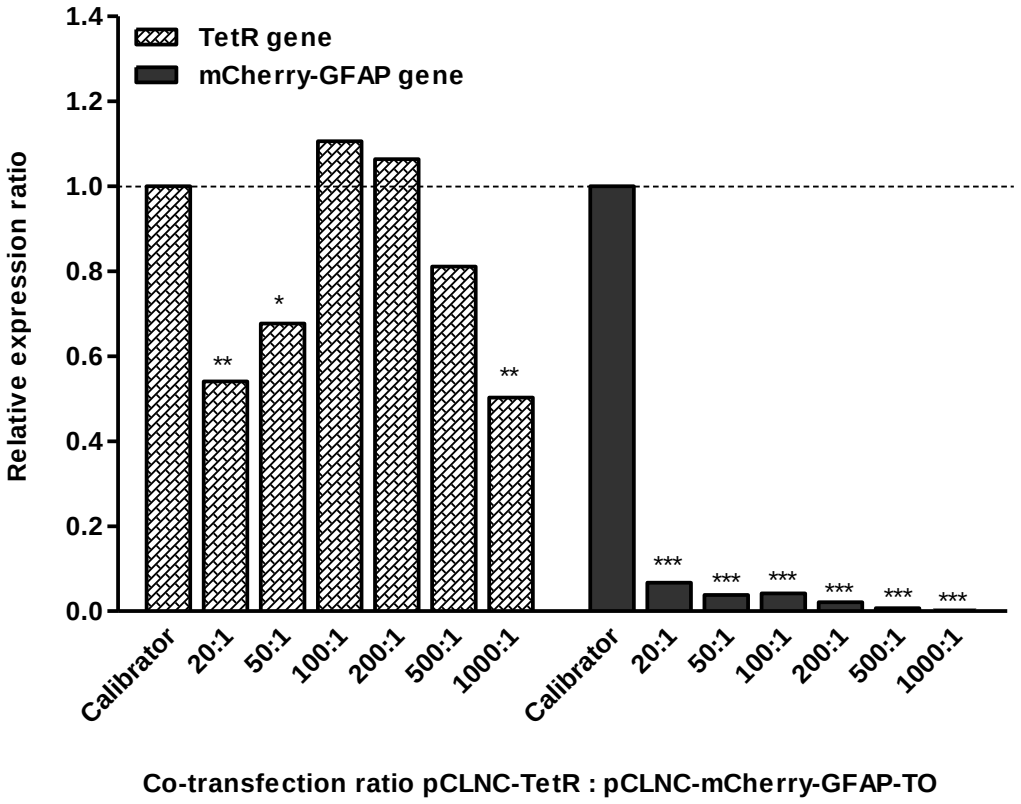

Figure 4-16: qPCR results showing relative expression of TetR and mCherry-GFAP genes in MIO-M1 cells transfected with varying ratios of pCLNC-TetR to pCLNC-mCherry-GFAP-TO retroviral vectors.
Bar charts represent relative expression ratios of TetR (crosshatched) and mCherry-GFAP (solid) genes calculated by ΔΔCt method. Relative expression of TetR significantly decreased or was unchanged by the different transfection ratios. Gene expression of mCherry-GFAP was significantly downregulated in all samples when compared to calibrator sample. Students T-test, $p<0.05$, N= 3 separate qPCR reactions

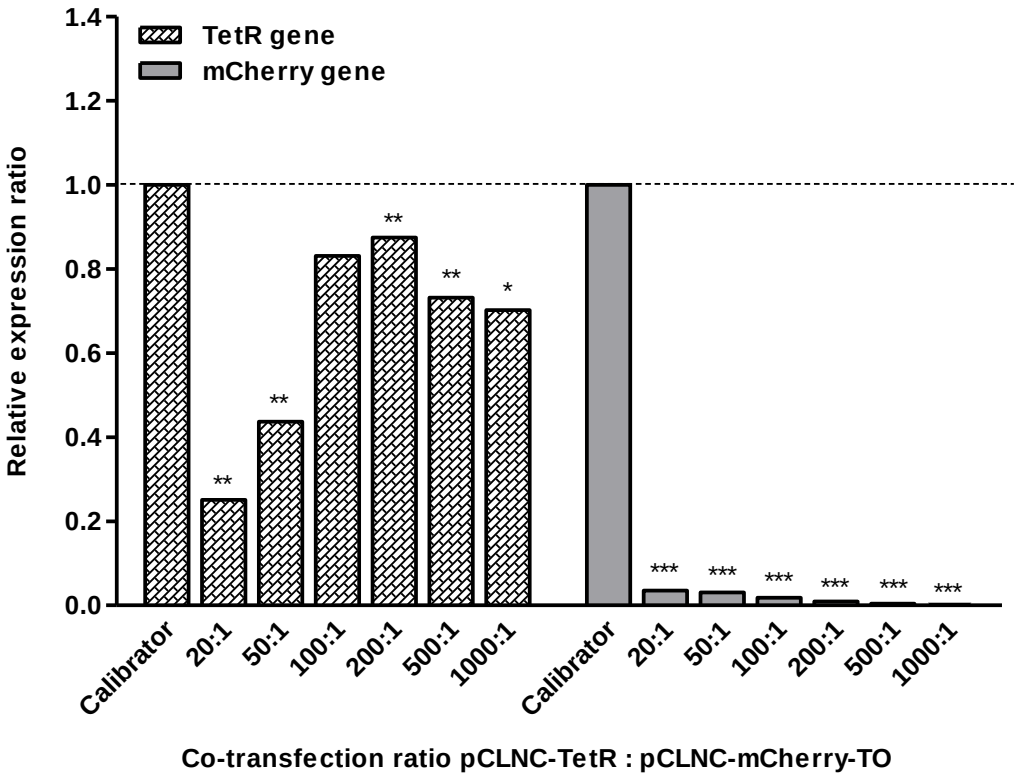

Figure 4-17: qPCR results showing relative expression of TetR and mCherry genes in MIO-M1 cells transfected with varying ratios of pCLNC-TetR to pCLNC-mCherry-TO retroviral vectors.
Bar charts represent relative expression ratios of TetR (crosshatched) and mCherry (solid) genes calculated by $\Delta\Delta$Ct method. Relative expression of TetR and mCherry genes were significantly decreased in all samples when compared to calibrator. Students T-test, $p<0.05$, N= 3 separate qPCR reactions

4.3.3.2 The ratio at which MIO-M1 cells are co-transfected with pCLNC-TetR and pCLNC-mCherry-GFAP-TO did not affect induction of the TetO2 promoter by tetracycline.

MIO-M1 cells were co-transfected with viral medium containing retroviral vectors pCLNC-TetR and pCLNC-mCherry-GFAP-TO at various ratios and then cultured with increasing concentrations of tetracycline in order to induce TetO2 promoter mediated activation of mCherry-GFAP transcription. When the co-transfection ratio was 20:1 of pCLNC-TetR to pCLNC-mCherry-GFAP-TO, these cells were on average 19% positive for mCherry fluorescence. After 8 hours culture of these cells with tetracycline at 0.5µg/ml there was a slight increase in the proportion of mCherry fluorescent cells to 21% but with higher concentrations of 1 and 5µg/ml tetracycline this decreased to 16% (Figure 4-18A). This change was not statistically significant when compared to cells cultured without tetracycline or when compared to individual concentrations of the antibiotic. Extending the culture of these cells with tetracycline to 24 hours did not significantly modify the percentage of mCherry positive cells either.

When the ratio of co-transfection was increased to 50:1 of the pCLNC-TetR to pCLNC-mCherry-GFAP-TO vectors and the cells were cultured with increasing concentrations of tetracycline for 8 and 24 hours there was no significant increase in the average percentage of mCherry positive cells when compared to cells not cultured with tetracycline (Figure 4-18B). MIO-M1 cells transfected at a ratio of 50:1 without tetracycline induction showed an average of 12% mCherry positive cells. Culturing these cells with the highest concentration of tetracycline used, at 5µg/ml, the average percentage of mCherry positive cells changed to 11% after 8 hours and 8% after 24 hours, which was not significant.

When the ratio of co-transfection was increased further to 200:1 and 500:1 pCLNC-TetR to pCLNC-mCherry-GFAP-TO vectors the average percentages of mCherry fluorescent cells without tetracycline induction were 5% and 2%, respectively (Figure 4-18C/D). When these cells were cultured with increasing concentrations of tetracycline for 8 or 24 hours there was no significant increase in the percentage of mCherry positive cells when compared to cells cultured without tetracycline. Neither the time of exposure nor the concentration of tetracycline affected the average percentage of mCherry fluorescent cells. For example, culturing 500:1 transfected cells with 0.5, 1 or 5µg/ml tetracycline for

24 hours did not change the percentage of mCherry positive cells when compared to cells cultured without tetracycline as this remained at 2% under all conditions (Figure 4-18D).

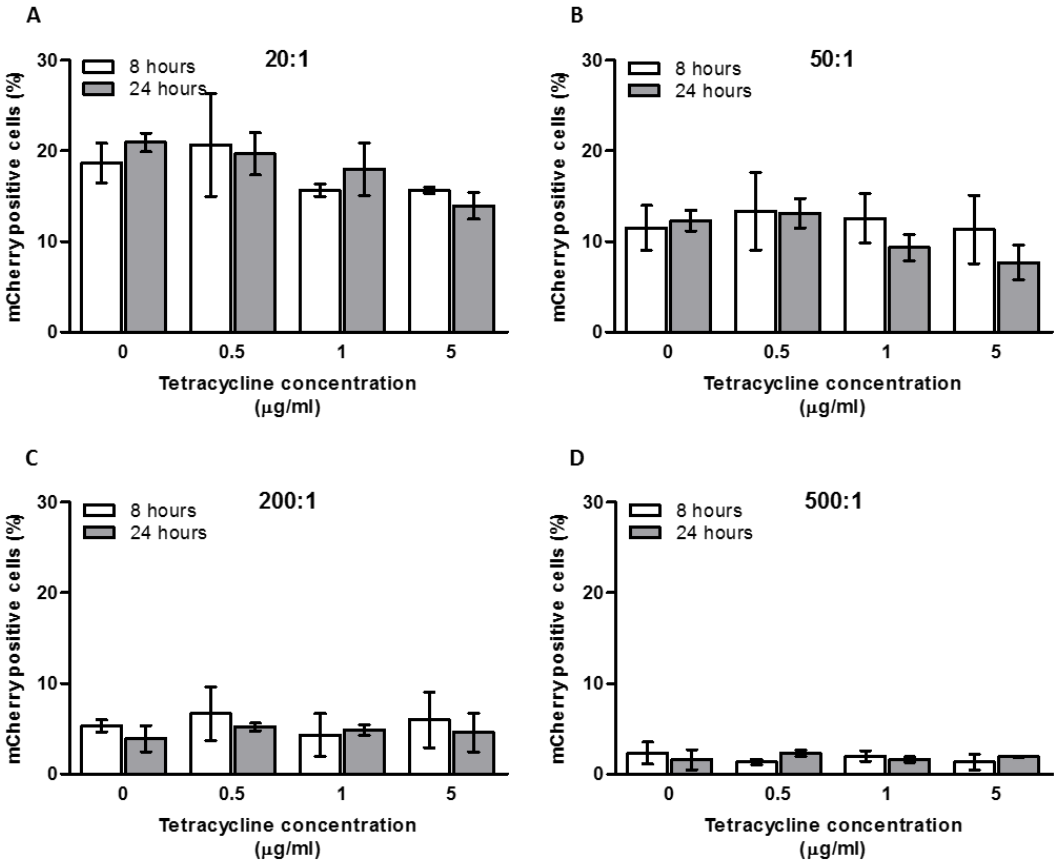

Figure 4-18: Percentage of mCherry positive cells within the population of co-transfected MIO-M1 cells after culture with increasing concentrations of tetracycline for 8 and 24 hours.

Bar charts represent proportion of mCherry fluorescence positive cells (mean +/- SEM). **(A)** MIO-M1 cells co-transfected with viral medium containing retroviral vector ratio of 20:1 of pCLNC-TetR: pCLNC-mCherry-GFAP-TO cultured with increasing concentrations of tetracycline for 8 or 24 hours, showed no significant increase in percentage of mCherry positive cells when compared to transfected cells cultured in the absence of tetracycline. **(B)** MIO-M1 cells transfected with retroviral vectors at a ratio of 50:1 were cultured with increasing concentrations of tetracycline. After 8 or 24 hours of tetracycline induction, cells did not increase expression of mCherry fluorescence when compared to cells cultured without tetracycline. **(C)** MIO-M1 cells were transfected with retroviral vectors at a ratio of 200:1 of pCLNC-TetR: pCLNC-mCherry-GFAP-TO. There was no increase in the percentage of mCherry fluorescence when cells were cultured in the presence of increasing concentrations of tetracycline for 8 or 24 hours when compared to cells cultured in the absence of tetracycline. **(D)** MIO-M1 cells were transfected at a ratio of 500:1 of the viral vectors pCLNC-TetR: pCLNC-mCherry-GFAP-TO. Culture of cells with increasing concentrations of tetracycline did not increase expression of mCherry fluorescence when compared to untreated control cells. Two-way ANOVA, $p>0.05$, N=3

4.3.4 Retroviral transfection of MIO-M1 cells with the pCLNC-mCherry-GFAP vector

As transfection of MIO-M1 cells with the tetracycline-inducible promoter was not successful, the original pCLNC-mCherry-GFAP vector with the CMV promoter was used for transfection (Figure 4-19). However, the ratio of virus particles to cell number was altered to attempt the insertion of varying amounts of vector into cells to cause gradient GFAP overexpression. After the gradient transfection, cells were sorted by FACS to obtain a pure population of transfected cells. FACS data analysis involved a step where a series of gates were defined to identify the population of interest. Cells were interrogated by their ability to uptake the live/dead fluorescent dye to gate out dead cells. Cells were then gated through the forward scatter (FSC), which relates to size, and the side scatter (SSC), which relates to morphology, to gate out cell aggregates. Live single cells were then selected for by their mCherry fluorescent protein (Figure 4-20). The transfection efficiency as well as the quantitation of mCherry fluorescence intensity could also be determined. The mCherry fluorescence intensity gave indication of the amount of vector transfected and thus the relative quantity of GFAP gene expression.

4.3.4.1 Increasing volume of viral medium containing pCLNC-mCherry-GFAP vector did not change transfection efficiency in MIO-M1 cells but increased mCherry fluorescence intensity

MIO-M1 cells that were transfected with increasing volumes of viral medium containing the retroviral vector pCLNC-mCherry-GFAP showed that an average transfection efficiency of 53% would be achieved (Figure 4-21). The lowest efficiency of 46% was found in cells transfected with 50% pCLNC-mCherry-GFAP viral medium and the highest efficiency was 61% in cells transfected with 100% viral medium. This transfection efficiency was much higher than that achieved using the EndoFectin Max reagent with the pmCherry-GFAP-N-18 plasmid. It also indicated that the transfection efficiency was not modified by the volume of viral medium used to transfect cells. As the volume of medium containing the vector used to transfect MIO-M1 cells increased, the median mCherry fluorescence intensity increased concurrently (Figure 4-21). Fluorescence intensity data was not available for cells transfected with 80% volume of pCLNC-mCherry-GFAP medium. When MIO-M1 cells were

transfected with a 5% volume of pCLNC-mCherry-GFAP medium containing the vector, the median mCherry fluorescence intensity was 1923, at 20% this was 2111, at 60% the fluorescence increased to 2500 and at 100% vector transfection the median fluorescence intensity was 3048 (Figure 4-21). This suggested that increasing vector quantity used in transfection increased mCherry fluorescence and therefore caused a corresponding increase in GFAP gene expression.

Since this preliminary data was consistent across the different volumes of viral medium used, it was decided to repeat the experiments with a further two passages of MIO-M1 cells, selecting 0%, 5%, 20%, 60% and 100% viral medium containing the pCLNC-mCherry-GFAP retroviral vector. A total of three passages were analysed through FACS for statistical analysis. Transfection efficiency in MIO-M1 cells transfected with 5% viral medium containing the pCLNC-mCherry-GFAP vector was 61%, which decreased slightly to 56% efficiency in cells transfected with 20% viral medium, 47% in cells with 60% viral transfection and 41% in cells with 100% transfection (Figure 4-22). When compared between volumes of medium used for transfection, this was not a significant change in transfection efficiency. Median mCherry fluorescence intensity in MIO-M1 cells transfected with pCLNC-mCherry-GFAP increased as volume of medium containing the retroviral vector increased (Figure 4-23). When the volume of medium used in transfection contained 5% pCLNC-mCherry-GFAP viral vector, the average median mCherry fluorescence intensity was 1483. As transfection medium volume increased to 20% viral vector, average median mCherry fluorescence intensity increased to 2841 in transfected cells. In cells transfected with 60% and 100% volume of medium containing pCLNC-mCherry-GFAP, fluorescence continued to increase to 3514 and 3596, respectively. There was a statistically significant increase of median fluorescence intensity in MIO-M1 cells transfected with 60% or 100% volume of medium containing viral vector pCLNC-mCherry-GFAP when compared to 5% transfection volume ($p<0.05$) (Figure 4-23). Therefore, further work was carried out using MIO-M1 cells transfected with 5% medium containing pCLNC-mCherry-GFAP as a “low” GFAP expressing cell line and the cells transfected with 100% volume of medium containing pCLNC-mCherry-GFAP as a “high” GFAP expressing cell line.

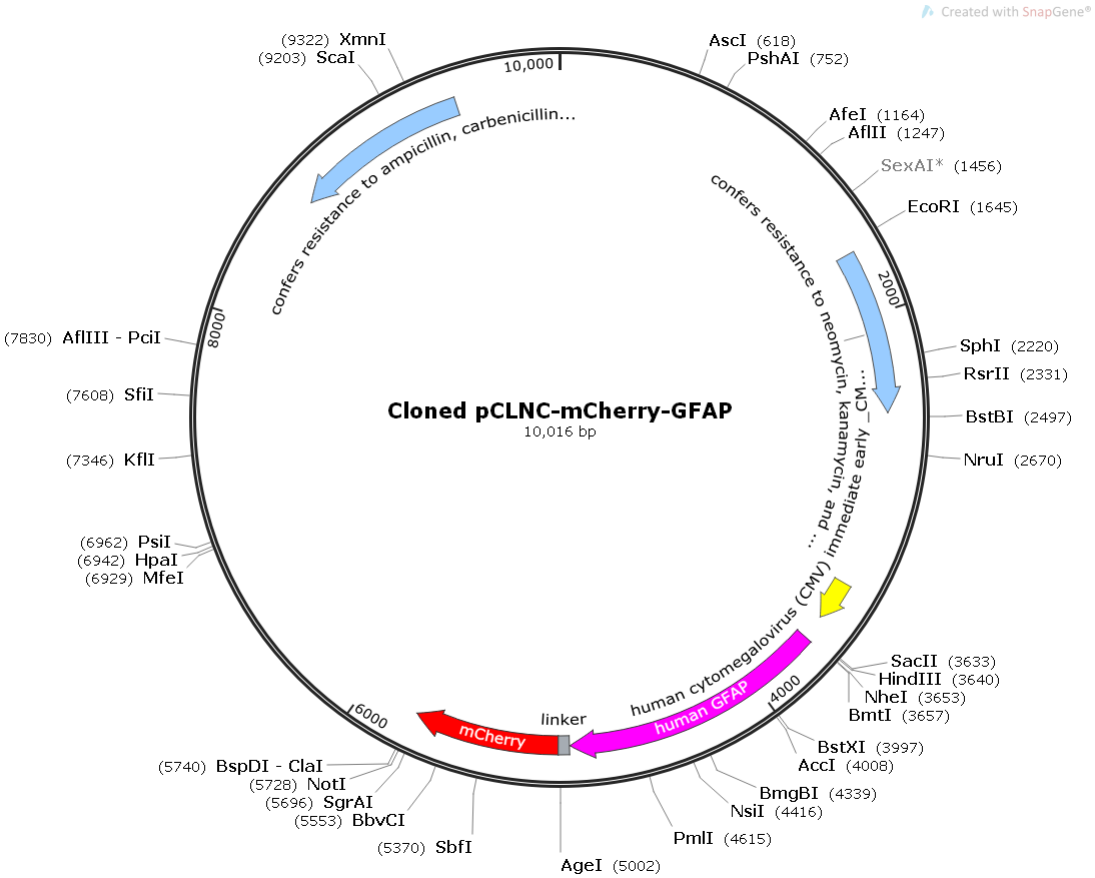

Figure 4-19: Map of the cloned pCLNC-mCherry-GFAP vector with relevant features and all restriction enzyme sites.
The mCherry-GFAP sequence extracted from the pmCherry-GFAP-N-18 was inserted into the cloning site between HindIII and ClaI in the pCLNCx vector. The new cloned vector was 10,016bp.

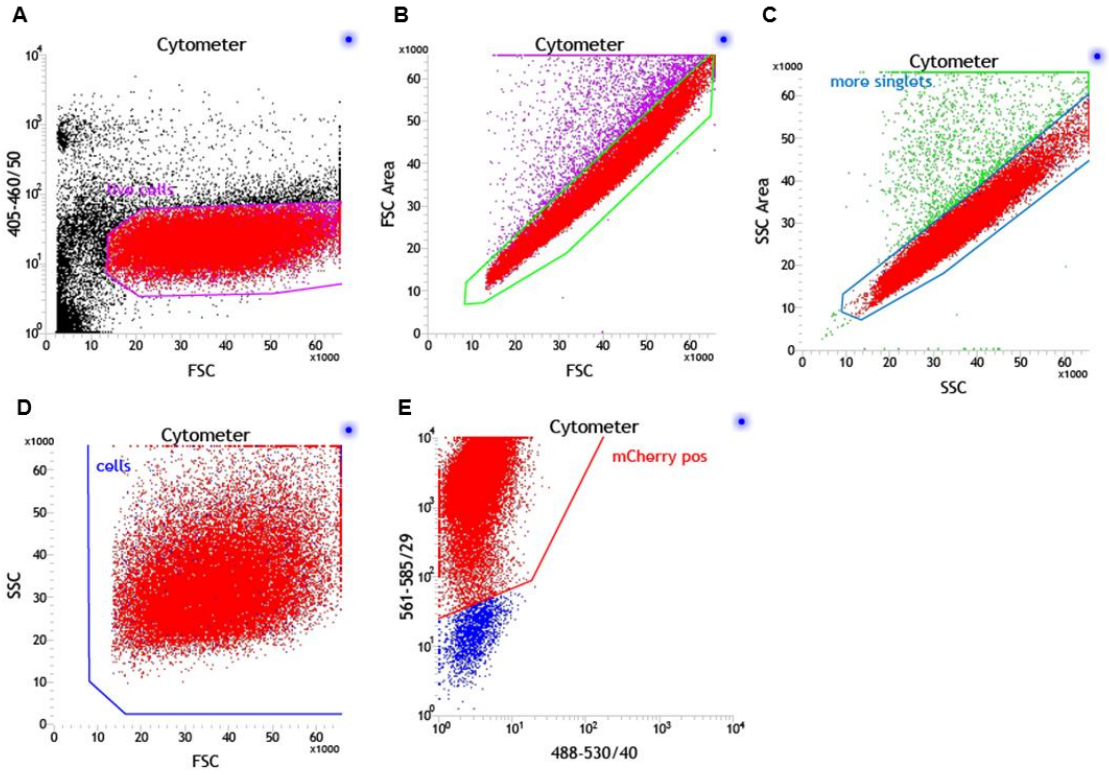

Figure 4-20: Gating parameters used in FACS sorting of MIO-M1 cells transfected with medium containing 100% retroviral vector pCLNC-mCherry-GFAP.
(A) Cells were firstly gated based on uptake of live/dead fluorescent dye to eliminate dead cells. **(B)** Cells were then gated based on forward scatter (FSC) to further separate live cells. **(C)** Live cells were gated through side scatter (SSC) to eliminate cell aggregates. **(D)** Live single cells were further gated. **(E)** Live single cells were then selected for by their mCherry fluorescent protein using a 561-585/29 bandpass filter to obtain a pure population.

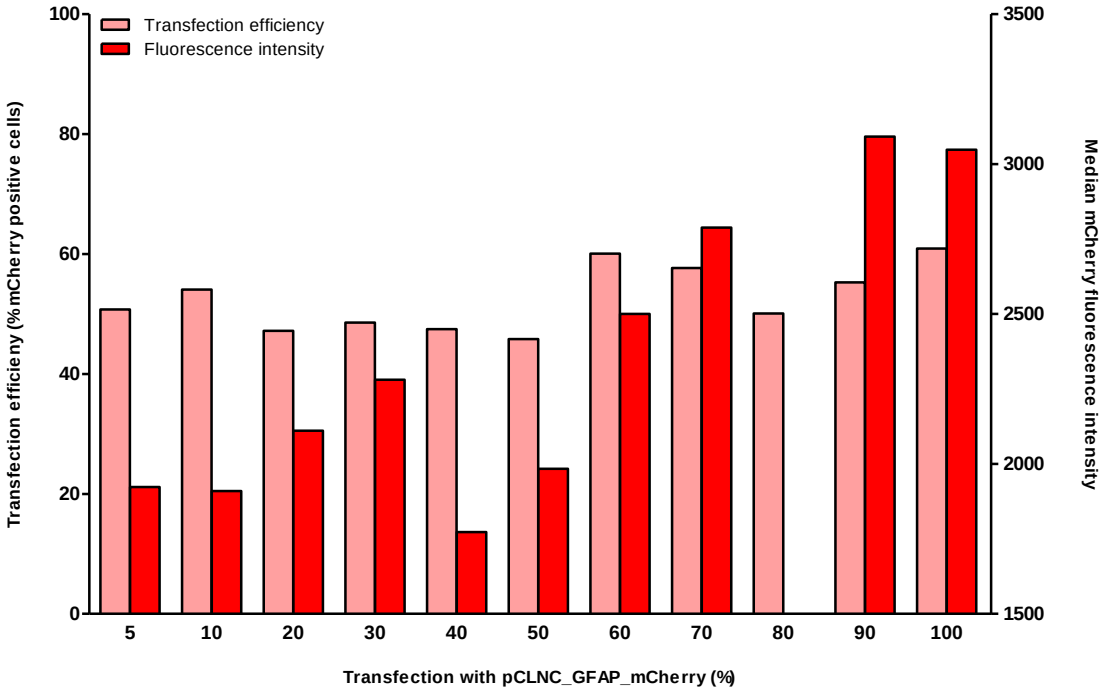

Figure 4-21: FACS analysis of MIO-M1 cells transfected with increasing volumes of viral medium containing pCLNC-mCherry-GFAP viral vector particles.
Bar charts represent transfection efficiency (pink bars) and median mCherry fluorescence intensity (red bar) of one passage of transfected MIO-M1 cells. Transfection efficiency remained stable but median fluorescence intensity increased as transfection percentage increased.

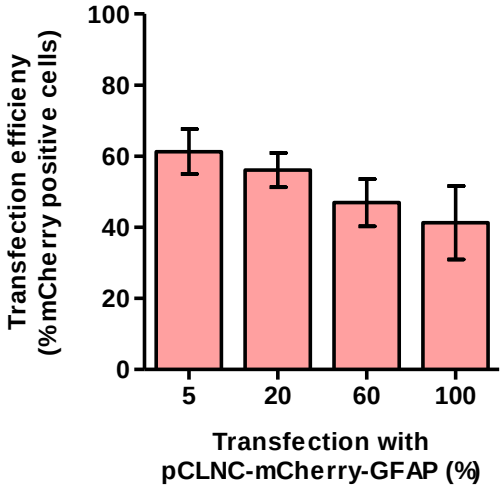

Figure 4-22: Transfection efficiency of MIO-M1 cells transfected with increasing volumes of medium containing pCLNC-mCherry-GFAP retroviral vector.
Bar chart represents average transfection efficiency of cells transfected with 5%, 20%, 60% or 100% medium containing pCLNC-mCherry-GFAP (mean +/- SEM). There was no significant difference in transfection efficiency between cells transfected with any volume of medium containing the pCLNC-mCherry-GFAP vector. One-way ANOVA and Tukey post-test, p>0.05, N=3.

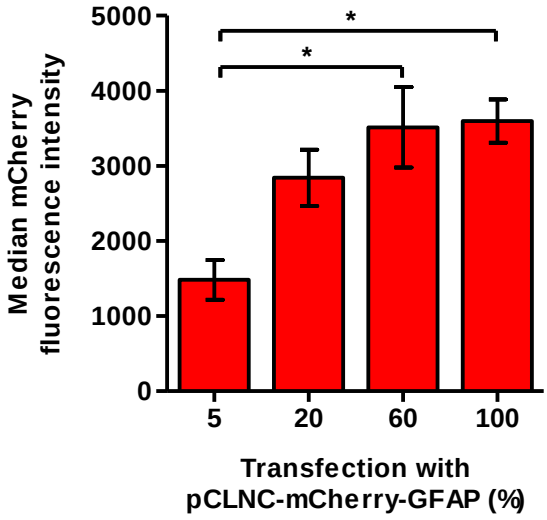

Figure 4-23: Median mCherry fluorescence intensity by MIO-M1 cells transfected with increasing volumes of pCLNC-mCherry-GFAP retroviral vector.
Bar chart represents average median mCherry fluorescence intensity by cells transfected with 5%, 20%, 60% or 100% medium containing pCLNC-mCherry-GFAP (mean +/- SEM). There was a significant increase in median fluorescence intensity in cells transfected with 60% or 100% retroviral vector medium when compared to 5% medium. One-way ANOVA and Tukey post-test, p<0.05, N=3.

4.4 Discussion

4.4.1 Resistance of MIO-M1 cells to transfection with an inducible promoter system

The method of retroviral transfection using TetR-expressing MIO-M1 cells with the pCLNC-mCherry-GFAP-TO vector provided stable expression of mCherry-GFAP when compared to the lipid-based transfection reagent EndoFectin Max, which only provided transient plasmid transfection. Upon culture and expansion of EndoFectin Max transfected cells they lacked mCherry fluorescence. The mCherry-GFAP-N-18 plasmid could have been released by the cells but also, after FACS sorting the cells were not maintained continuously in G418 selection antibiotic, which may have contributed to the loss of cells containing the plasmid. However, it is well known that gene transfer via non-viral vectors is inefficient and transient compared to viral vector transfer (Maier et al., 2010). Although transfection efficiency was similar, at around 30%, with either the EndoFectin Max reagent or the retroviral vector it was preferable to have a stable transfection in which cells could be passaged and progeny would express mCherry-GFAP so multiple long-term culture experiments could be performed. This was attempted using the T-REx™ tetracycline-induced system, which has two tetracycline operators (TetO2) inserted in the human CMV promoter controlling the mCherry-GFAP gene. The MIO-M1 cell line expressing TetR was transfected with the pCLNC-mCherry-GFAP-TO vector and addition of tetracycline to the cell culture medium should have increased expression of mCherry-GFAP, observed by increase in fluorescence. However, this effect was not seen in these transfected MIO-M1 cells and gene induction was not regulated by tetracycline, even up to a concentration of 10µg/ml for 24 hours. Surprisingly, without tetracycline in the culture medium the MIO-M1 cells were mCherry fluorescence positive, indicating that the initial repression by TetR had not worked. This contrasts with a previous report in HeLa cells co-transfected with a TetR-expressing plasmid and a plasmid containing the TetO2-CMV promoter fused to a reporter gene. In that study, there was a 100-fold repression after 24 hours, which was efficiently reversed by addition of 1µg/ml of tetracycline (Yao et al., 1998). However, the authors noted that efficacy of the tetracycline-mediated repression system was affected by cell type and the reporter gene used. In the present study, the method was attempted in MIO-M1

cells, so the data obtained strongly suggests that these cells are not susceptible to transfection using this system.

When the system was previously tested *in vitro* in primate cells the molar ratio of the two plasmids used in co-transfection had to be modified so that there was six times more TetR-expressing plasmid compared to the TetO2-CMV promoter plasmid (Yao et al., 1998). This indicated that repression of the transgene requires a high amount of the TetR molecule. This process was also explored in the present study with MIO-M1 cells, which were co-transfected with pCLNC-mCherry-GFAP-TO and the newly cloned pCLNC-TetR vector. When viral medium containing the pCLNC-TetR vector was increased in co-transfection the mCherry fluorescence decreased in Müller cells, suggesting that the mCherry-GFAP gene expression was repressed. Nevertheless, addition of tetracycline did not reverse this repression as mCherry fluorescence was not upregulated. Quantification by qPCR on the RNA from these co-transfected cells revealed that although the mCherry-GFAP gene was markedly downregulated, even up to 570-fold, the expression of the TetR gene was unchanged or even reduced when compared to the transfection in TetR-expressing MIO-M1 cell line. There was far less TetO2 promoter gene expression and sufficient TetR gene expression to produce repression of mCherry-GFAP as indicated by lack of mCherry fluorescence in transfected cells. However, because tetracycline did not increase mCherry fluorescence in these cells, it could be possible that the TetR protein could not be bound by tetracycline. Additionally, the co-transfection system was not tested in other cell types in this study and so perhaps the TetR gene sequence was missing an important regulatory element after cloning into pCLNCx, although this was not examined. Therefore, expressing both TetR and TetO2 promoter genes in pCLNCx retroviral vectors was not effective in ensuring the TetO2 promoter could be controlled by tetracycline in MIO-M1 cells.

4.4.2 Achieving effective and stable transfection of MIO-M1 cells with mCherry-GFAP

The viral load is a numerical expression of the quantity of virus in a given volume often measured as viral particles per ml. To increase the percentage of cells transfected a higher viral load is needed and it can be simply a matter of exposing the target cells to a larger volume of virus (Coffin et al., 1997).

Although viral load was not measured directly, MIO-M1 cells were transfected with increasing volumes of viral medium with the intention of introducing more retroviral pCLNC-mCherry-GFAP particles to the cells. The percentage of cells transfected was not modified in MIO-M1 cells transfected with increasing volumes of viral medium as transfection efficiency remained unchanged. However, efficiency was much higher than that achieved in cells transfected with the mCherry-GFAP-N-18 plasmid and in cell transfected with the pCLNC-mCherry-GFAP-TO inducible vector. More importantly though, the median mCherry fluorescence increased significantly in MIO-M1 cells transfected with the highest volume of viral medium compared to the lowest volume. This suggests that these MIO-M1 cells transfected with the highest volume of viral medium express more mCherry-GFAP when compared to the MIO-M1 cells transfected with the lowest viral load. Upon expansion in culture, these retrovirus transfected cells remained positive for mCherry and therefore stably transfected MIO-M1 cells were established, overexpressing the GFAP protein. These GFAP overexpressing MIO-M1 cells will be valuable in studying the effects of this intermediate filament protein *in vitro* as it is obvious that overexpression of this protein is detrimental in experimental models *in vivo*.

Chapter 5 Effects of GFAP overexpression in the MIO-M1 cell line

5.1 Introduction

5.1.1 Role of GFAP in gliosis

The response of Müller glial cells to inflammatory cytokines plays a major role in reactive gliosis in the human retina during disease. TNF-α is a major inflammatory cytokine associated with retinal degenerative diseases and an activator of Müller cell gliosis (Tezel et al., 2001, Fernandez-Bueno et al., 2013). Despite its pro-inflammatory role, in this study TNF-α was found to downregulate GFAP protein expression in MIO-M1 cells, resembling the anti-gliotic property of this cytokine in zebrafish retina (Nelson et al., 2013). In mammalian astrocytes, TNF-α reduces protein expression of GFAP *in vitro* and may not be responsible for reactive changes observed in astrocytes during neurodegenerative diseases (Edwards and Robinson, 2006).

The regulatory effect of TNF-α on Müller glial cells overexpressing GFAP has not yet been examined and there is little knowledge on the interaction of this molecule with other Müller cell proteins during gliosis. The MIO-M1 Müller glial cell line expresses other characteristic makers such as vimentin, CRALBP and glutamine synthetase (Limb et al., 2002) but the regulatory interaction between these proteins and GFAP has not been determined. Evidence has emerged that vimentin may be associated with GFAP regulation. As another type III IF protein found in glial cells, it is upregulated along with GFAP during Müller cell gliosis (Reichenbach and Bringmann, 2010). Astrocytes of GFAP deficient mice, do not completely lose vimentin protein expression and it has been suggested that because only subtle aberrations in these cells occur, vimentin may take over the functional role of GFAP (Messing and Brenner, 2003, Pekny et al., 1998). Transgenic mice overexpressing GFAP have shown co-localised GFAP and vimentin expression throughout the CNS *in vivo* and within the astrocyte cytoskeleton *in vitro* (Messing et al., 1998, Cho and Messing, 2009). Additionally, in p27 deficient mice overexpressing GFAP, Müller glial cells also show upregulated vimentin expression (Vázquez-Chona et al., 2011). Based on these studies it would be important to examine the expression of vimentin and other specific Müller glial cell markers in MIO-M1 cells overexpressing GFAP.

5.1.2 Role of GFAP in cell proliferation

Astrocyte cell growth is inhibited by GFAP overexpression, partly due to a decrease in their proliferation and partly due to increased cell death. This is demonstrated by observations that astrocytes overexpressing GFAP show increased apoptosis and reduced BrdU labelling *in vitro* (Cho and Messing, 2009). In rat astrocytoma C6 cells, overexpression of GFAP *in vitro* was shown to suppress cell proliferation (Toda et al., 1994). Furthermore, *in vivo* injection of GFAP overexpressing C6 cells into athymic mice significantly reduced glial tumour growth compared to mice injected with control C6 cells (Toda et al., 1999). Other studies demonstrated that the astrocytoma cell line U251 which overexpresses GFAP, following treatment with antisense complementary DNA, downregulate GFAP expression, enhance their proliferation and become more invasive (Rutka et al., 1994). However, the cause of this reduced cell proliferation in the CNS produced by GFAP overexpression is not known.

In the retina, chronic stimuli can cause non-proliferative reactive gliosis. *In vivo* chronic glaucoma models reveal increased GFAP protein expression by Müller glia. However, these cells do not incorporate BrdU and the total cell numbers are unchanged (Inman and Horner, 2007). This suggests that Müller glial cell proliferation is not modified by GFAP overexpression during glaucomatous changes in the retina. In contrast, *in vivo* acute damage to Müller glia causes upregulation of GFAP and increased Müller cell proliferation (Byrne et al., 2013). Therefore, the type of insult sustained by Müller glia may dictate the effect on their proliferation.

5.1.3 Role of GFAP in Müller glial stem cell state and neural differentiation

The MIO-M1 cells have stem cell properties as *in vitro* they express retinal stem cell markers Sox2, Sox9, Pax6 and Chx10 (Lawrence et al., 2007). In investigating potential mechanisms to promote endogenous regeneration by these cells it would be important to understand how gliotic modifications through GFAP overexpression could affect the progenicity of these cells. Inactivation of Pax6 in retinal progenitor cells narrows their multipotent state (Marquardt et al., 2001), whilst *in vivo* loss of Sox9 and *ex vivo* ablation of Sox2 in the retina show that both are essential for Müller glia survival and maintenance of progenicity (Surzenko et al., 2013, Poche et al., 2008). *In vitro* silencing of Sox2 in Müller

glial cells caused cells to become neuronal in morphology and to increase their expression of neuronal markers, whilst decreasing their expression of the glial marker vimentin (Bhatia et al., 2011).

With age, astrocytes increase expression of GFAP. When astrocytes from older animals were co-cultured with embryonic neurons, less neurite outgrowth was observed when compared to younger astrocytes expressing lower levels of GFAP (Rozovsky et al., 2005). When younger astrocytes were transfected with a GFAP-expressing plasmid, this overexpression also caused reduced neurite outgrowth, suggesting that GFAP is an independent factor in neurite outgrowth and could prevent neural differentiation. However, when the retinal explants from transgenic mice overexpressing GFAP were treated with growth permissive media there was greater neurite outgrowth when compared to explants of normal retina (Toops et al., 2012). In an induced glaucoma rat model, when activated Müller glial cells expressing GFAP were cultured *in vitro* with RGC, RGC grew longer neurites when in contact with GFAP positive glial cells (Lorber et al., 2012). This suggests that under the right conditions GFAP overexpression in activated Müller glia might not be detrimental but can be supportive to neurons and assist regeneration. It is therefore vital to understand the function of GFAP during *in vitro* MIO-M1 differentiation and its implications for potential promotion of *in vivo* regeneration.

5.2 Objectives

GFAP upregulation is intrinsically linked to retinal scarring, neural regeneration and is a characteristic feature of Müller cell gliosis (Sarthy, 2007). However, the role and regulation of GFAP has not been determined and mechanisms of GFAP overexpression are not fully understood. Because GFAP is a structural protein of Müller glia, by inducing overexpression in these cells we can examine the effects that this intermediate filament has on their functions and their stem cell characteristics. As TNF-α can downregulate GFAP expression in MIO-M1 cells, it would be beneficial to examine the effects of this inflammatory cytokine on cells overexpressing GFAP. Therapeutic approaches to regulate GFAP expression during disease or injury may need to be directed at controlling gliosis and scarring whilst also allowing for Müller glia proliferation and regeneration.

The objectives of this chapter were:

1. To investigate whether *in vitro* GFAP overexpression in MIO-M1 cells affects cell viability or proliferation.
2. To assess the regulation of induced overexpressed GFAP protein in MIO-M1 treated with the inflammatory cytokine TNF-α *in vitro*.
3. To examine whether *in vitro* induced rod photoreceptor precursor differentiation of MIO-M1 cells may be affected by overexpression of GFAP.
4. To determine whether induced overexpression of GFAP modulates expression of characteristic stem cell markers expressed by Müller glial cells.

Experimental design:

I. MIO-M1 cells transfected with the GFAP encoding gene tagged to a fluorescent mCherry protein and control untransfected cells were expanded in culture to undertake the above studies.

II. Extracted RNA and protein isolated from cell lysates were used to semi-quantify expression of GFAP by RT-PCR and western blot analysis.

III. To assess the viability and proliferation of MIO-M1 cells overexpressing GFAP, a hexosaminidase assay was performed together with immunocytochemistry staining of the proliferation marker Ki67. A colorimetric cell cytotoxicity assay measuring the release of LDH was also performed.

IV. Control and GFAP overexpressing cells were cultured with TNF-α for 6 days and protein isolated from these cells was used to measure expression of endogenous and exogenous GFAP using western blot analysis.

V. Control and GFAP overexpressing cells were cultured with FTRI (factors known to induce differentiation of these cells into rod photoreceptor precursors) and protein expression of NR2E3, a rod photoreceptor marker, was measured in cell lysates using western blot analysis.

VI. RNA was extracted from control and GFAP overexpressing cells and examined for mRNA expression of the Müller glial markers CRALBP,

glutamine synthetase and vimentin, as well as the retinal progenitor cell markers Pax6, Chx10, Sox9 and Sox2.

VII. Protein expression of vimentin was also semi-quantified using western blot analysis and immunocytochemistry.

5.3 Results

5.3.1 Expression of GFAP mRNA in MIO-M1 cells transfected with the retroviral vector pCLNC-mCherry-GFAP

MIO-M1 cells were previously transfected with viral medium containing 5% retroviral vector pCLNC-mCherry-GFAP, which was determined to be low GFAP overexpression when compared to cells transfected with viral medium containing 100% volume of the vector, which was established as high GFAP overexpression. These two MIO-M1 cell lines overexpressing GFAP are referred to as low and high transfection herein.

Two different primers were used in RT-PCR to quantify endogenous and total GFAP mRNA expression by the transfected cells. Total GFAP expression being the expression of endogenous GFAP plus the induced mCherry-GFAP. The mCherry-GFAP sequence does not include a non-coding region of exon 1 of the GFAP gene variant 1, which was exploited to create primers within this non-coding region to detect endogenous GFAP and primers outside this region to detect total GFAP. Endogenous GFAP mRNA expression was significantly downregulated in MIO-M1 cells transfected with low ($p<0.05$) and high ($p<0.01$) pCLNC-mCherry-GFAP vector when compared to untransfected control cells (Figure 5-1A). On the other hand, total GFAP mRNA expression was observed significantly upregulated in both low and high transfection cells when compared to untransfected control cells ($p<0.01$) (Figure 5-1B). Neither endogenous or total GFAP mRNA were modified between low and high transfected cells.

5.3.2 Expression of GFAP protein in MIO-M1 cells transfected with the retroviral vector pCLNC-mCherry-GFAP

GFAP protein was semi-quantitatively measured by western blot analysis probed with an anti-GFAP antibody. The antibody recognised endogenous GFAP, producing a band at 50kDa, the exogenous mCherry-GFAP, producing a band around 80kDa, and GFAP dimers, producing a band around 100kDa. To measure endogenous GFAP expression the optical density of the single band at 50kDa was analysed, whilst total protein expression was analysed by measuring the optical density of the entire column (Figure 5-2).

In low transfection MIO-M1 cells, endogenous GFAP protein was unchanged but total GFAP protein expression increased significantly compared to

untransfected control cells ($p<0.01$) (Figure 5-2). Total GFAP protein expression was also significantly increased in high transfection MIO-M1 cells when compared to control cells ($p<0.01$) (Figure 5-2B). Endogenous GFAP protein expression was not modified in highly transfected cells when compared to control untransfected cells (Figure 5-2A). There was no significant difference in total GFAP protein expression between low and high transfected cells.

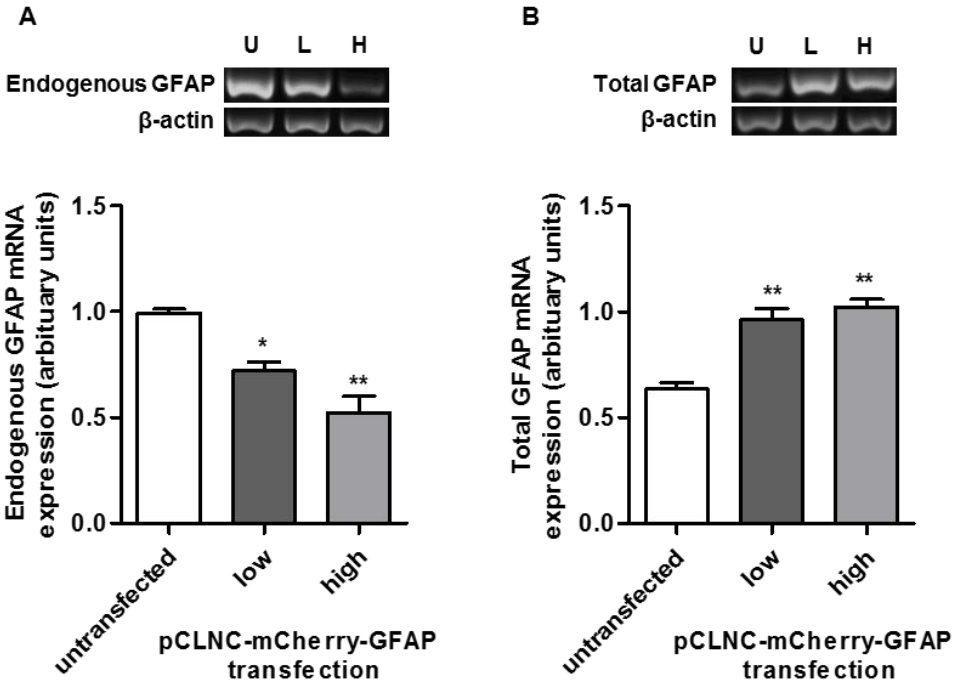

Figure 5-1: mRNA expression of GFAP by MIO-M1 cells transfected with low or high levels of pCLNC-mCherry-GFAP retroviral vector.
Representative images of PCR bands for β-actin, endogenous GFAP and total GFAP shown above bar charts. Bar charts represent relative expression of endogenous and total GFAP mRNA normalised to β-actin (mean +/- SEM). Two different primer pairs were used to distinguish between endogenous and total (endogenous plus mCherry-GFAP) expression. **(A)** There was a significant decrease in mRNA expression of endogenous GFAP in MIO-M1 cells transfected with low or high pCLNC-mCherry-GFAP when compared to untransfected controls. **(B)** There was a significant increase in total GFAP mRNA expression in MIO-M1 cells transfected with low or high pCLNC-mCherry-GFAP when compared to untransfected control cells. One-way ANOVA and Tukey's post-test, $p<0.05$, N=3. U: untransfected, L: low, H: high.

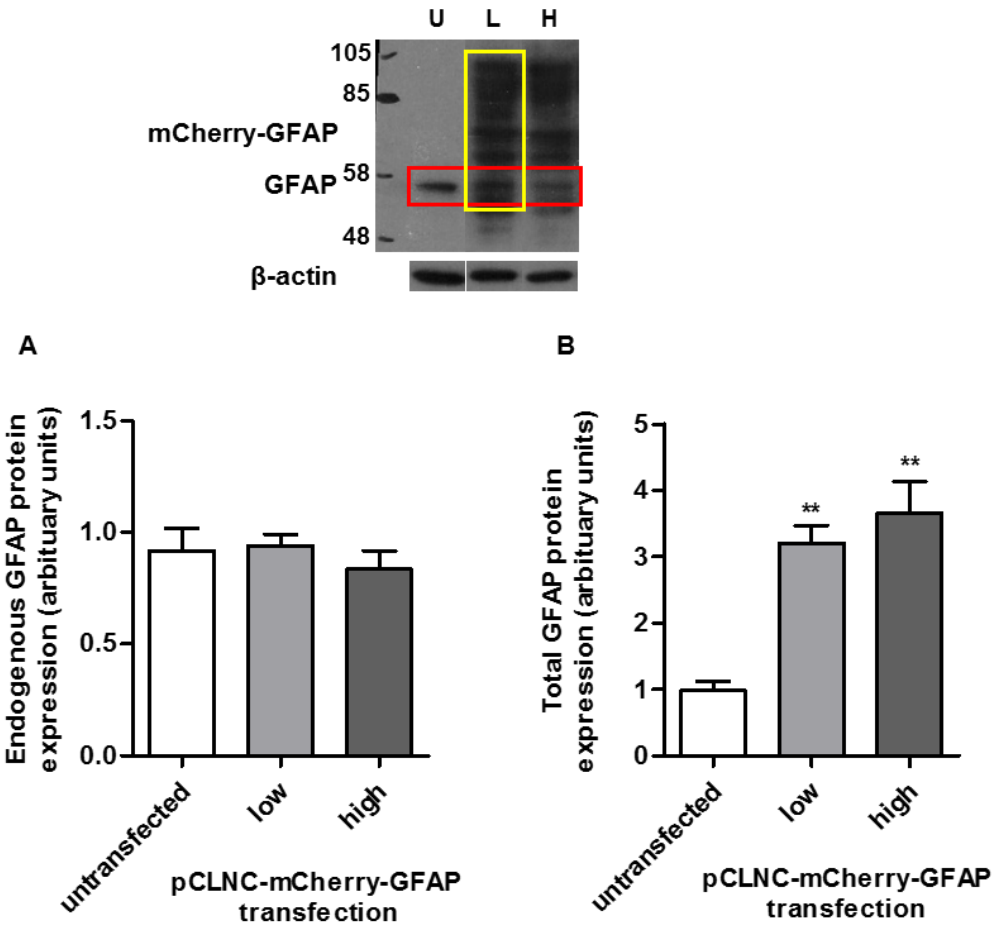

Figure 5-2: Protein expression of GFAP by MIO-M1 cells transfected with low or high levels of pCLNC-mCherry-GFAP retroviral vector.
Representative image of western blot probed with β-actin and anti-GFAP antibody shown above bar charts. Bands for endogenous GFAP at 50kDa, mCherry-GFAP at ~80kDa and GFAP dimers at ~100kD were seen. Bar charts represent relative expression of endogenous (red box) and total (yellow box) protein normalised to β-actin (mean +/- SEM). **(A)** There was no difference in protein expression of endogenous GFAP in pCLNC-mCherry-GFAP transfected cells when compared to untransfected control cells. **(B)** There was a significant increase in total GFAP protein expression in MIO-M1 cells transfected with low or high concentrations of pCLNC-mCherry-GFAP when compared to control cells. One-way ANOVA and Tukey's post-test, $p<0.05$, N=3. U: untransfected, L: low, H: high.

5.3.3 Overexpression of GFAP did not affect MIO-M1 cell proliferation

To investigate whether overexpression of GFAP modified cell proliferation when MIO-M1 cells were transfected with low or high concentrations of retroviral medium, two proliferation assays were performed. The human protein Ki67 is expressed in the cell nuclei specifically during active phases of the cell cycle and thus is an accurate cell proliferation marker. Immunocytochemistry performed using the anti-Ki67 antibody revealed that the proportion of growing, dividing cells was similar between untransfected and transfected cells (Figure 5-3). Cell counts of Ki67 positive cells within the GFAP transfected and untransfected cell populations indicated that proliferation was not modified. Within untransfected control MIO-M1 cells 25% of the cells were proliferating as determined by expression of Ki67 (Figure 5-4). When MIO-M1 cells were transfected with low concentration of pCLNC-mCherry-GFAP retroviral medium there was a slight but not significant decrease in proliferation as 18% of the cells stained for Ki67. Within the high transfection MIO-M1 cell population, proliferation was similar to control cells with 24% of cells staining for Ki67. Overall, there was no significant difference in the proportion of proliferating cells between cells transfected with low or high concentrations of pCLNC-mCherry-GFAP when compared to untransfected control cells (Figure 5-4).

Hexosaminidase is a lysosomal enzyme, the total activity of which is directly proportional to the number of living cells in a homogenous population because relative absorbance readings are directly proportional to cell numbers. This assay was used in this study to measure cell proliferation rate over time. Over 7 days, untransfected control MIO-M1 cells proliferated at the same rate as cells which had been transfected with either low or high concentrations of pCLNC-mCherry-GFAP retroviral medium (Figure 5-5). Further culture of these cells revealed that after 9 days the untransfected MIO-M1 cells continued to proliferate whereas the GFAP overexpressing cells reached a plateau in cell number. However, the relative absorbance reading of MIO-M1 cells transfected with either low or high pCLNC-mCherry-GFAP was not significantly different compared to control MIO-M1 cells at 2, 5, 7 and 9 days in culture (Figure 5-5). It was therefore concluded that overexpression of GFAP did not affect the proliferation rate of MIO-M1 cells.

5.3.4 Increasing GFAP overexpression did not modify MIO-M1 cell cytotoxicity

To determine whether GFAP overexpression was cytotoxic to MIO-M1 cells, transfected cells were cultured for 5 days in normal DMEM + 10% FCS medium, and a cytotoxicity assay kit was used. This colorimetric assay quantifies cell death based on measurement of LDH release into the cell culture supernatant. The pCLNC-mCherry-GFAP transfected cells were compared to untransfected control MIO-M1 cells to calculate the percentage of cytotoxicity (Figure 5-6). MIO-M1 cells transfected with low concentrations of pCLNC-mCherry-GFAP retroviral medium showed an average 13% cell death. Cells transfected with high level of retroviral medium showed an average cell death of 11%. There was no significant difference in cytotoxicity between low and high transfected MIO-M1 cells, indicating that different levels of GFAP overexpression did not modify cell viability (Figure 5-6).

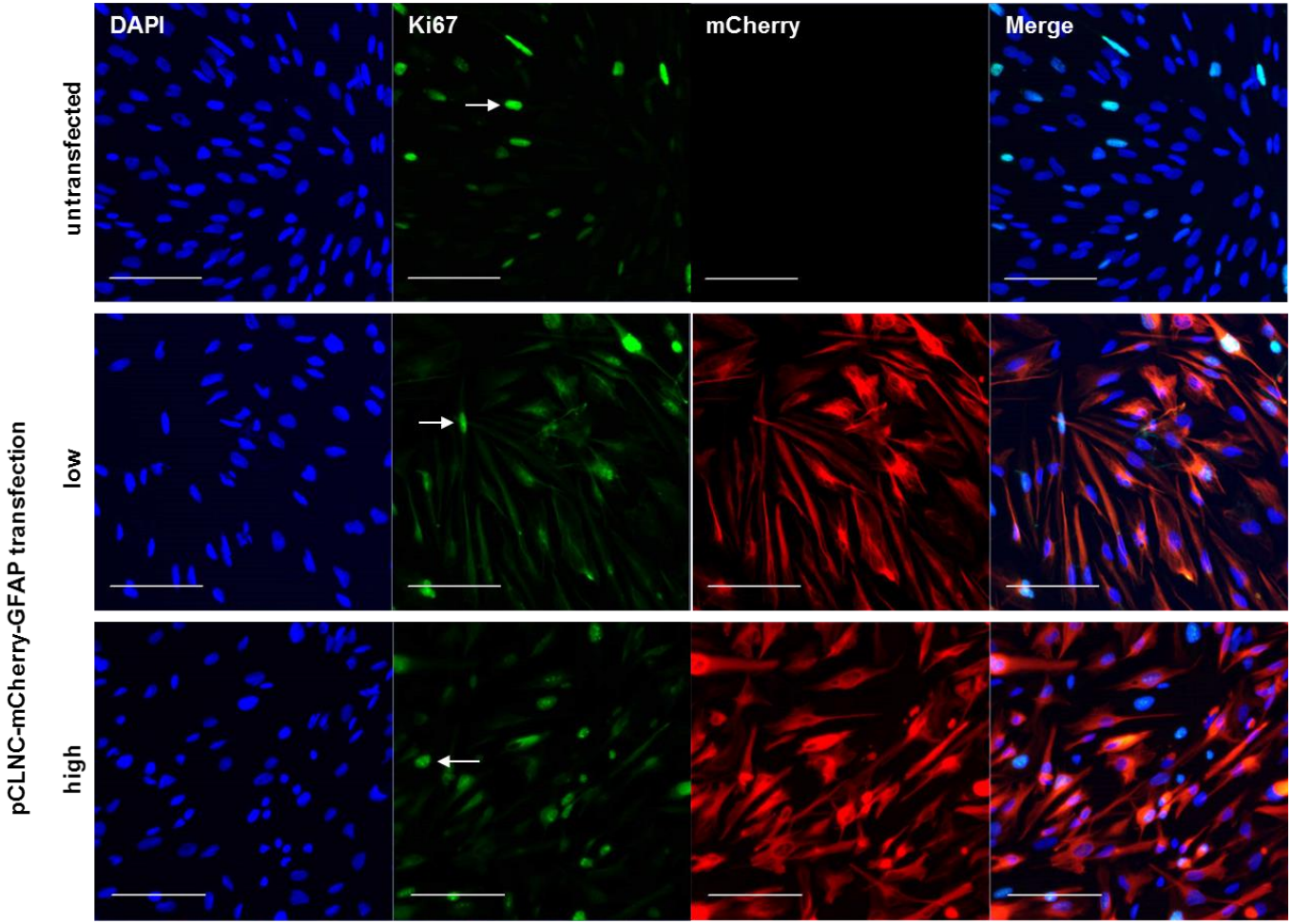

Figure 5-3: Immunofluorescence images of MIO-M1 cells transfected with low or high levels of pCLNC-mCherry-GFAP retroviral vector stained with anti-Ki67.

Representative immunocytochemistry images of untransfected and transfected Müller cells with low or high levels of pCLNC-mCherry-GFAP viral vector stained with anti-Ki67 (Alexa Flour 488, green) and fluorescent for mCherry (red). White arrows indicate Ki67 positive nuclei immunostaining. Scale bar represents 100um.

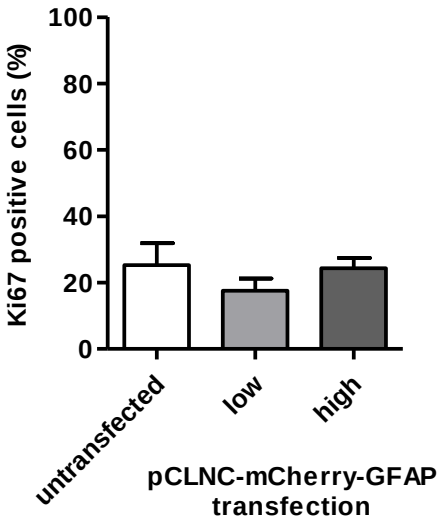

Figure 5-4: Quantification of the percentage of cell nuclei stained for Ki67 in MIO-M1 cells transfected with low or high levels of pCLNC-mCherry-GFAP retroviral vector.

Bar chart represents the percentage of immunostained cells (mean +/- SEM). There was no significant difference in Ki67 staining of transfected MIO-M1 cells compared to untransfected control cells or between cells transfected with low or high levels of retroviral vector. One-way ANOVA and Tukey's post-test $p>0.05$, N=3.

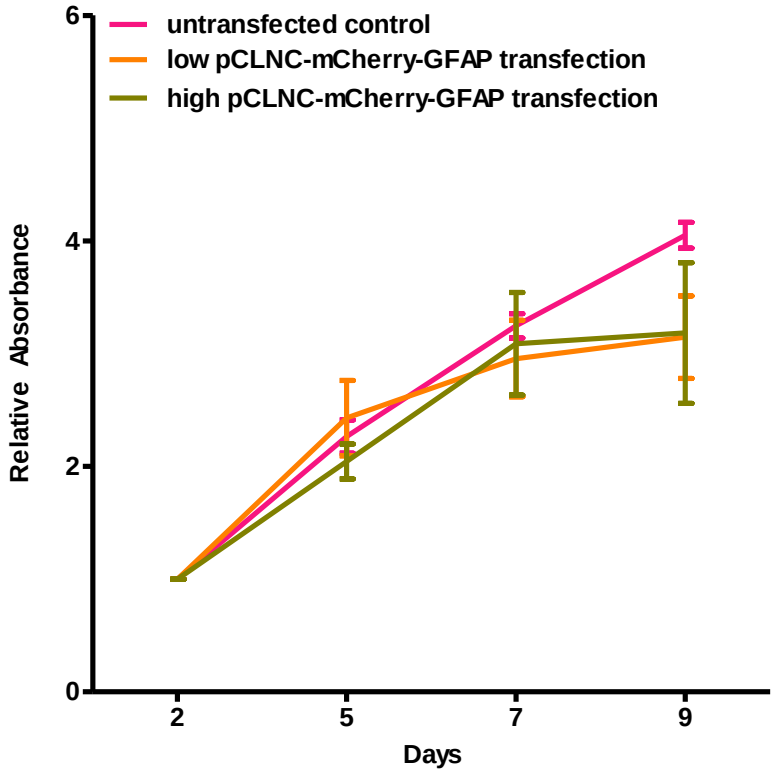

Figure 5-5: Proliferation rates of untransfected MIO-M1 cells and cells transfected with low or high levels of pCLNC-mCherry-GFAP retroviral vector as determined by hexosaminidase assay.
Pink coloured line represents untransfected control cells, orange line represents low transfection cells and green line represents high transfection cells (mean +/- SEM). Proliferation rate of untransfected MIO-M1 cells slightly increased after 9 days. However, there was no significant modification of cell proliferation in transfected cells at 2, 5, 7 or 9 days in culture when compared to untransfected control cells. Two-way ANOVA and Bonferroni post-test $p>0.05$, N=3.

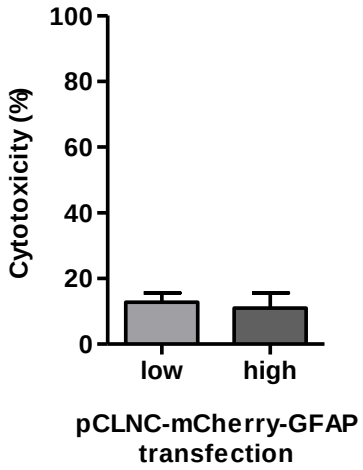

Figure 5-6: Percentage of cytotoxicity in MIO-M1 cells transfected with low or high levels of pCLNC-mCherry-GFAP retroviral vector.
Bar chart represents percentage of cytotoxicity (mean +/- SEM). As judged by proportion of dead cells there was no significant difference in cytotoxicity between MIO-M1 cells transfected with low or high levels of pCLNC-mCherry-GFAP when compared to each other. Students T-test $p>0.05$, N=3.

5.3.5 TNF-α downregulated endogenous but not total GFAP mRNA expression in MIO-M1 cells transfected with pCLNC-mCherry-GFAP

Because TNF-α was shown to downregulate GFAP mRNA and protein expression in MIO-M1 cells, it was examined whether this cytokine would regulate induced overexpression of GFAP in MIO-M1 cells. Total GFAP mRNA expression was measured by including both endogenous and vector induced expression. In untransfected cells, total expression was the same as endogenous expression. When untransfected MIO-M1 cells were cultured in the presence of 5ng/ml TNF-α, endogenous and total GFAP mRNA expression decreased significantly when compared to untreated control cells ($p<0.001$) (Figure 5-7). MIO-M1 cells transfected with both low or high concentrations of pCLNC-mCherry-GFAP retroviral medium cultured in the presence of TNF-α, also showed significant downregulation of endogenous GFAP mRNA expression when compared to transfected cells cultured in the absence of TNF-α ($p<0.01$) (Figure 5-7A). However, retroviral transfected MIO-M1 cells cultured in the presence of TNF-α did not show downregulation of total GFAP mRNA expression when compared to transfected cells cultured in the absence of TNF-α (Figure 5-7B).

5.3.6 TNF-α downregulated endogenous but not total GFAP protein expression in MIO-M1 cells transfected with pCLNC-mCherry-GFAP

MIO-M1 cells cultured with 5ng/ml TNF-α showed a significant downregulation of GFAP protein expression when compared to untreated control cells ($p<0.01$) (Figure 5-8A). When MIO-M1 cells were transfected with low level of pCLNC-mCherry-GFAP vector and were cultured with 5ng/ml TNF-α, there was a significant downregulation of endogenous GFAP protein expression ($p<0.01$) (Figure 5-8A). However, total GFAP protein expression, which includes endogenous and vector induced GFAP, was not modified by culturing low transfection cells with TNF-α when compared to transfected cells cultured in the absence of TNF-α (Figure 5-8B). When highly transfected MIO-M1 cells were cultured in the presence of TNF-α, the protein expression of endogenous GFAP was slightly decreased when compared to transfected cells cultured in the absence of TNF-α, although this was not statistically significant (Figure 5-8A). Additionally, total GFAP protein expression was unchanged when these highly

transfected cells were cultured with TNF-α compared to cells cultured without this cytokine (Figure 5-8B).

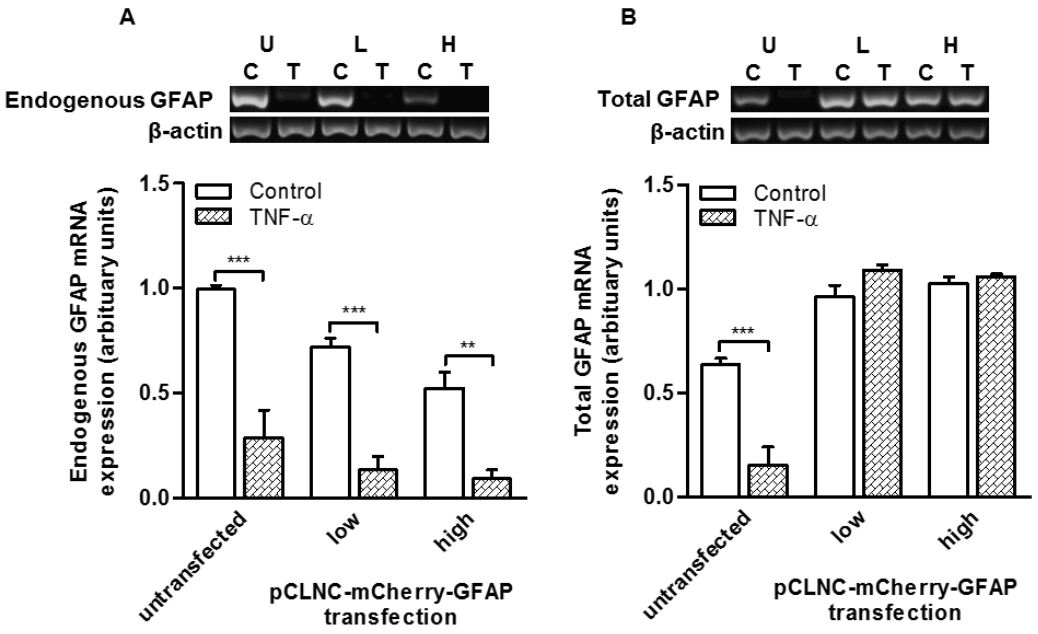

Figure 5-7: mRNA expression of GFAP by MIO-M1 cells transfected with low or high levels of pCLNC-mCherry-GFAP retroviral vector and cultured in the absence or presence of TNF-α.

Representative PCR bands of endogenous GFAP, total GFAP and β-actin are shown above bar charts. Bar charts represent GFAP mRNA expression normalised to β-actin (mean +/- SEM) in untransfected, low or high pCLNC-mCherry-GFAP transfected MIO-M1 cells. Empty white bars represent GFAP expression in cells cultured in the absence of TNF-α, whilst filled bars represent cells cultured in the presence of TNF-α. **(A)** Endogenous GFAP mRNA was significantly decreased in untransfected and transfected MIO-M1 cells in the presence of TNF-α when compared to cells cultured in the absence of this cytokine. **(B)** Total GFAP mRNA expression, including both endogenous and vector induced expression, was not modified in transfected MIO-M1 cells cultured with TNF-α when compared to transfected cells cultured without TNF-α. Two-way ANOVA and Bonferroni post-test $p<0.05$, N=3. C: control, T: TNF-α, U: untransfected, L: low, H: high.

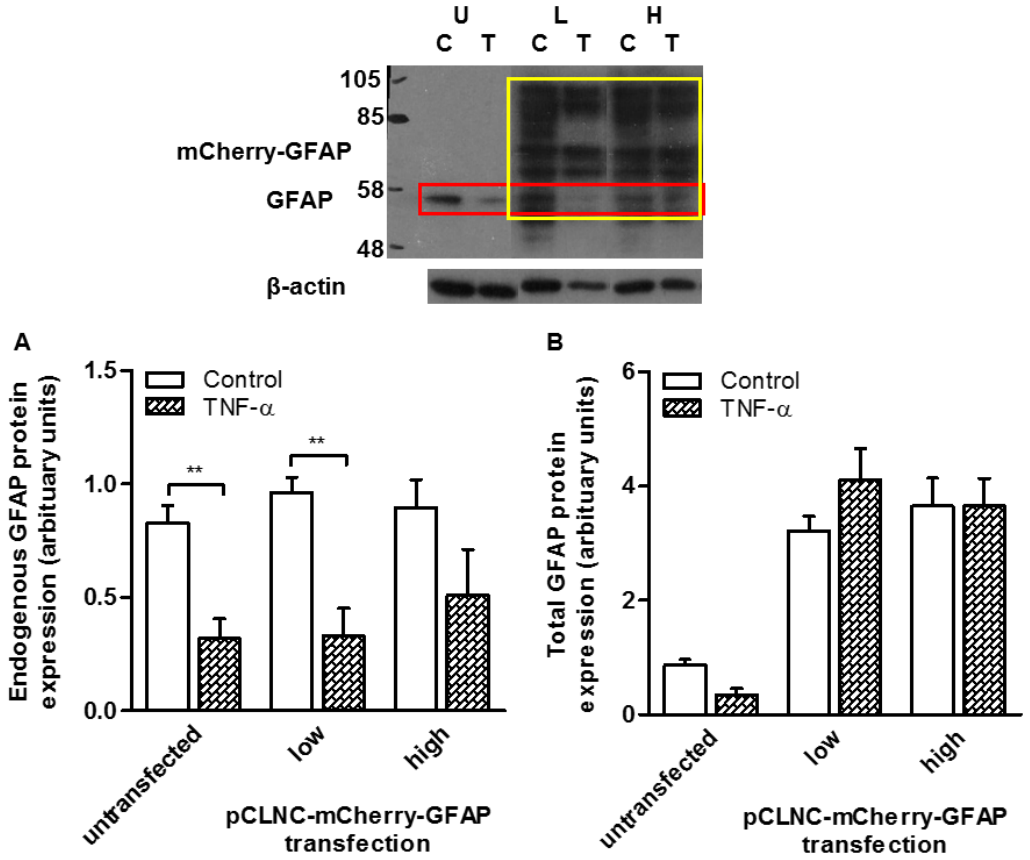

Figure 5-8: Protein expression of GFAP by MIO-M1 cells transfected with low or high levels of pCLNC-mCherry-GFAP retroviral vector and cultured in the absence or presence of TNF-α.
Representative image of western blot probed with β-actin and anti-GFAP antibody shown above bar charts. Bar charts represent GFAP protein expression normalised to β-actin (mean +/- SEM) in untransfected, low or high pCLNC-mCherry-GFAP transfected MIO-M1 cells. Empty white bars represent GFAP expression in cells cultured in the absence of TNF-α, whilst filled bars represent cells cultured in the presence of TNF-α. **(A)** Untransfected MIO-M1 cells and cells transfected with low level of retroviral vector when cultured in the presence of TNF-α, showed a significant decrease in endogenous GFAP protein expression when compared to cells cultured in the absence of TNF-α. Endogenous protein was measured by the band at 50kDa (red box). **(B)** When transfected MIO-M1 cells were cultured with TNF-α, total GFAP protein expression was not modified when compared to transfected cells cultured without TNF-α. Total GFAP protein was measured by the optical density of the entire column including all bands recognised by the anti-GFAP antibody (yellow box). Two-way ANOVA and Bonferroni post-test $p<0.05$, N=3. C: control, T: TNF-α, U: untransfected, L: low, H: high.

5.3.7 Culturing MIO-M1 cells transfected with pCLNC-mCherry-GFAP with FTRI

MIO-M1 cells were cultured with FTRI. Protein expression of NR2E3 was examined as a marker of rod photoreceptor precursor differentiation. As previously shown in this current study, MIO-M1 cells cultured with FTRI showed a significant increase in NR2E3 protein expression compared to untreated control cells ($p<0.05$) (Figure 5-9). When cells were cultured with FTRI in the presence of TNF-α, NR2E3 protein expression was significantly upregulated when compared to control cells ($p<0.01$) but did not differ from cells cultured with FTRI alone. This suggests that TNF-α does not modify the ability of MIO-M1 cells to express NR2E3 after culture with FTRI.

MIO-M1 cells transfected with low concentration of pCLNC-mCherry-GFAP retroviral medium and cultured in the presence of FTRI showed no increase in NR2E3 protein expression when compared to transfected untreated control cells (Figure 5-9). NR2E3 protein expression was not modified in low GFAP transfection cells cultured with TNF-α or with FTRI in the presence or absence of TNF-α when compared to transfected control cells. When MIO-M1 cells were transfected with high concentration of pCLNC-mCherry-GFAP retroviral medium and were cultured with FTRI there was also no significant increase in NR2E3 protein expression compared to transfected cells that were cultured in the absence of FTRI (Figure 5-9). NR2E3 protein expression was not modified in these high GFAP transfection cells by culture with FTRI in the presence of TNF-α or with TNF-α alone when compared to transfected untreated control cells. This suggests that GFAP overexpression may not allow for induced rod photoreception differentiation of MIO-M1 cells.

5.3.8 Expression of GFAP in transfected MIO-M1 cells cultured with FTRI

MIO-M1 cells cultured with FTRI in the absence or presence of TNF-α significantly downregulate their protein expression of GFAP when compared to control untreated cells ($p<0.05$) (Figure 5-10). When MIO-M1 cells were transfected with low level of pCLNC-mCherry-GFAP retroviral vector and cultured with FTRI in the absence or presence of TNF-α, protein expression of endogenous GFAP was not modified when compared to transfected control cells (Figure 5-10). In MIO-M1 cells transfected with high levels of pCLNC-mCherry-GFAP retroviral vector and cultured with FTRI in the absence or

presence of TNF-α, endogenous GFAP protein expression was also not modified when compared to transfected control (Figure 5-10). This indicates that FTRI does not downregulate GFAP expression in MIO-M1 cells overexpressing GFAP as observed in untransfected MIO-M1 cells.

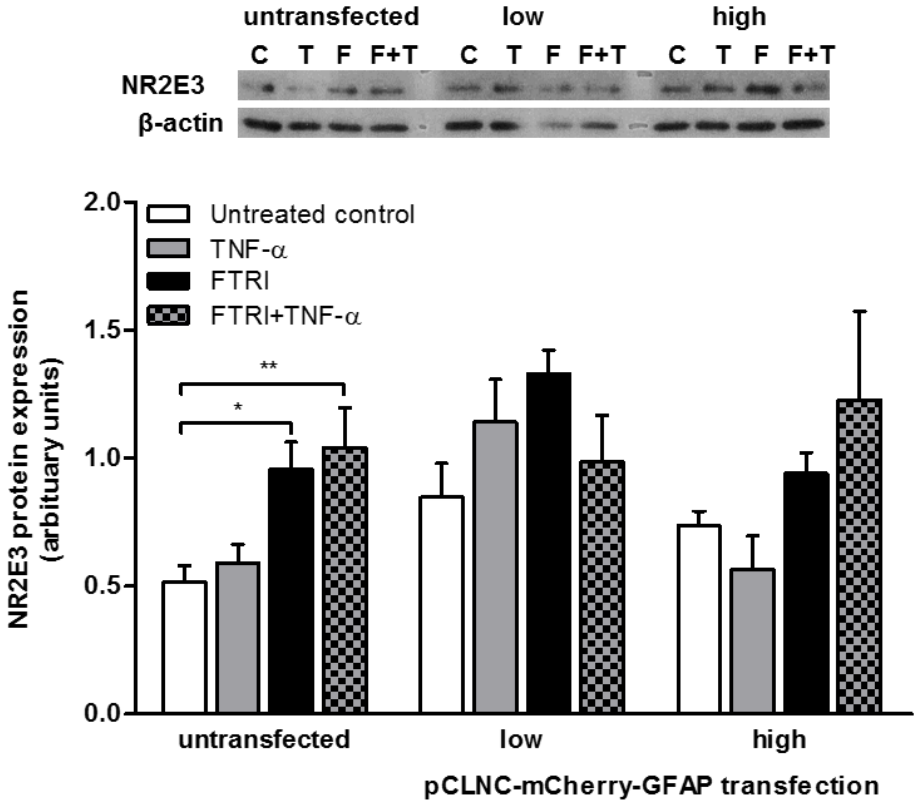

Figure 5-9: Protein expression of the rod photoreceptor marker NR2E3 by untransfected or pCLNC-mCherry-GFAP transfected MIO-M1 cells cultured with FTRI in the absence or presence of TNF-α.
Representative western blots bands of NR2E3 and β-actin shown above bar charts. Bar charts represent NR2E3 protein expression normalised to β-actin (mean +/- SEM). Protein expression of NR2E3 was significantly increased in untransfected MIO-M1 cells cultured with FTRI in the absence or presence of TNF-α when compared to untreated control cells. However, in MIO-M1 cells transfected with low or high levels of pCLNC-mCherry-GFAP vector and cultured with FTRI in the absence or presence of TNF-α, NR2E3 protein expression was not modified when compared to transfected untreated control cells. Two-way ANOVA and Bonferroni post-test $p<0.05$, N=3. C: control, T: TNF-α, F: FTRI, F+T: FTRI+TNF-α.

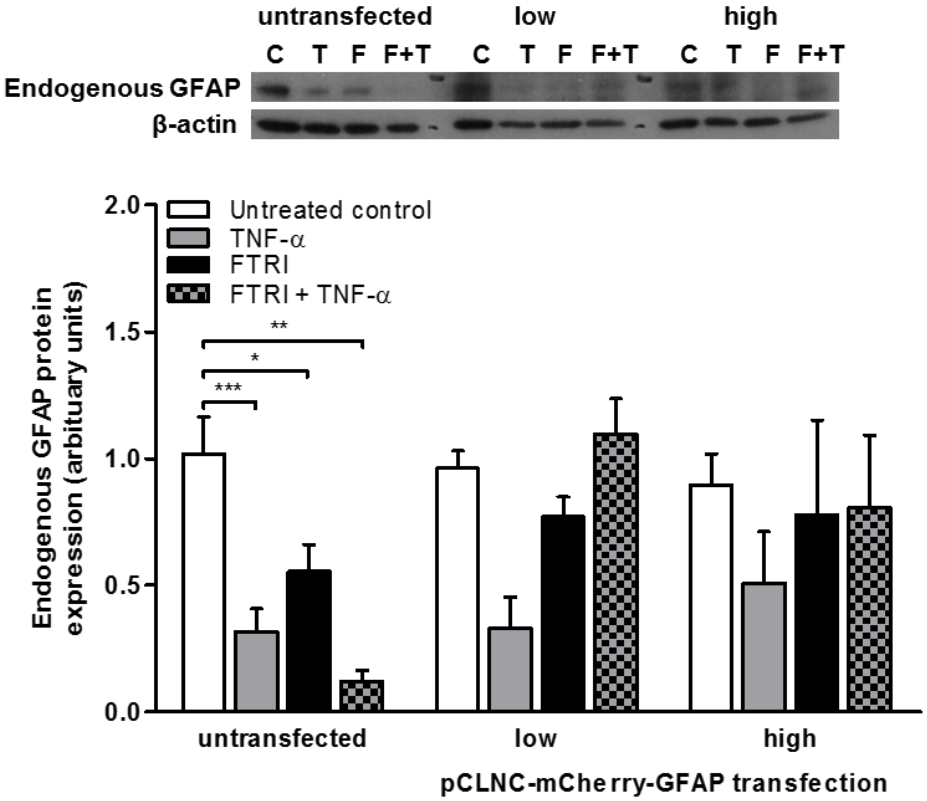

Figure 5-10: Protein expression of endogenous GFAP by untransfected or pCLNC-mCherry-GFAP transfected MIO-M1 cells cultured with FTRI in the absence or presence of TNF-α.
Representative western blots bands of endogenous GFAP and β-actin are shown above bar charts. Bar charts represent endogenous GFAP protein expression normalised to β-actin (mean +/- SEM). Protein expression of endogenous GFAP was downregulated in untransfected MIO-M1 cells cultured with FTRI in the absence or presence of TNF-α when compared to untreated control cells. In MIO-M1 cells transfected with low or high levels of pCLNC-mCherry-GFAP vector and cultured with FTRI in the absence or presence of TNF-α, endogenous GFAP protein expression was not modified when compared to transfected untreated control cells. Two-way ANOVA and Bonferroni post-test $p<0.05$, N=3. C: control, T: TNF-α, F: FTRI, F+T: FTRI+TNF-α.

5.3.9 GFAP overexpression did not modify mRNA expression of Müller glial and progenitor cell markers

RNA was extracted and cDNA obtained from MIO-M1 cells transfected with low or high concentrations of pCLNC-mCherry-GFAP retroviral medium and mRNA expression of Müller glia and progenitor cell markers were semi-quantitively measured. mRNA expression of the Müller glial cell markers CRALBP, glutamine synthetase and vimentin were not modified by low or high pCLNC-mCherry-GFAP transfection of MIO-M1 cells when compared to untransfected control cells (Figure 5-11A-C). mRNA expression by MIO-M1 cells of progenitor cell markers Pax6, Chx10, Sox9 and Sox2 were also not significantly modified in cells transfected with either low or high levels of pCLNC-mCherry-GFAP vector when compared to untransfected control cells (Figure 5-11D-G).

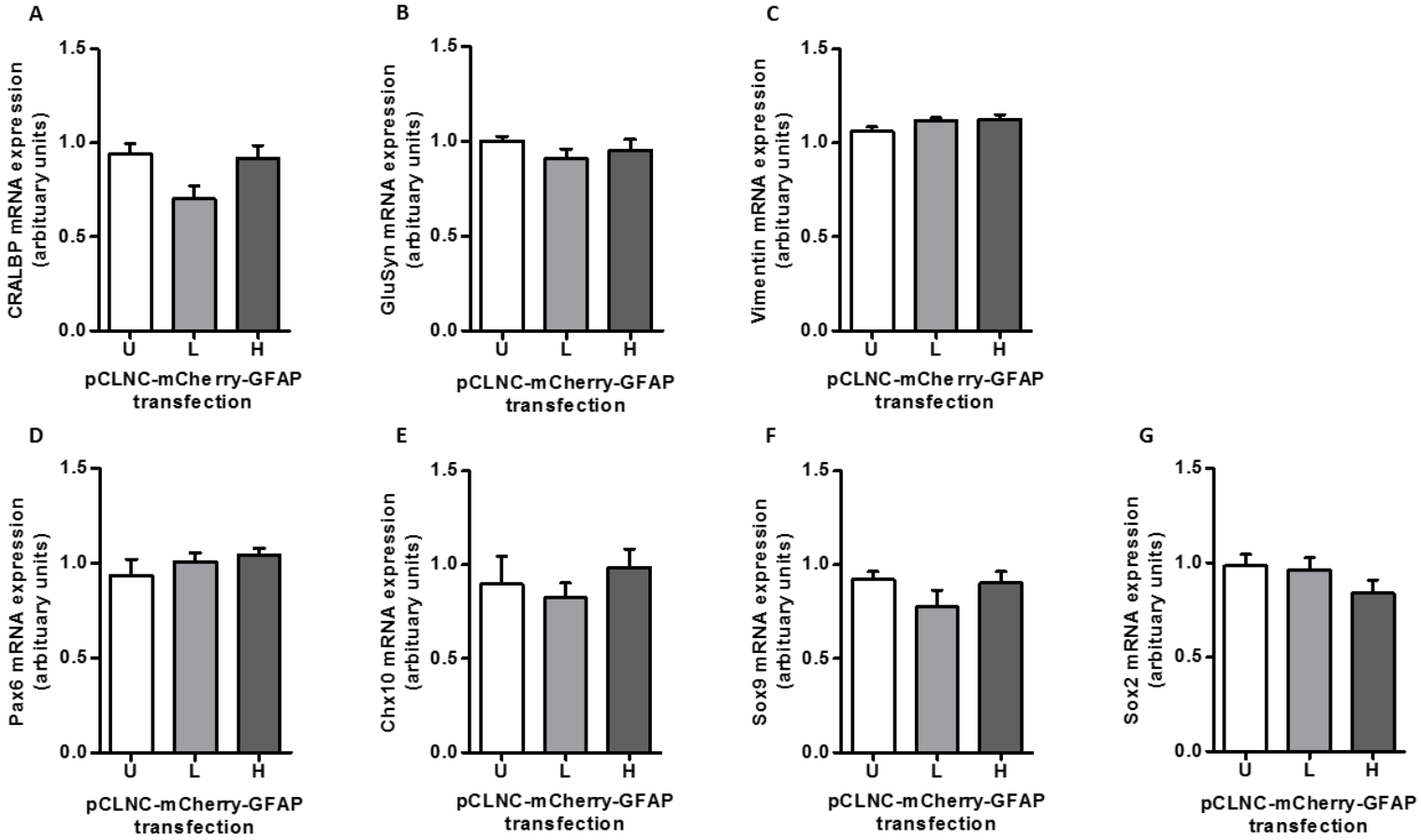

Figure 5-11: mRNA expression of Müller glial and progenitor cell markers by untransfected, low or high pCLNC-mCherry-GFAP transfected MIO-M1 cells.

Müller glial cell markers **(A)** CRALBP, **(B)** glutamine synthetase (GluSyn) and **(C)** vimentin mRNA expression was unchanged in MIO-M1 cells transfected with low or high levels of pCLNC-mCherry-GFAP when compared to untransfected cells. mRNA expression of progenitor cell markers **(D)** Pax6, **(E)** Chx10, **(F)** Sox9 and **(G)** Sox2 were not modified in low or high transfection MIO-M1 cells when compared to untransfected control cells. One-way ANOVA and Tukey post-test, $p>0.05$, N=3. U: untransfected, L: low, H: high.

5.3.10 GFAP overexpression caused downregulation of vimentin protein expression

The protein expression of vimentin was further investigated because GFAP and vimentin are closely associated within Müller glial cells. Untransfected and pCLNC-mCherry-GFAP transfected MIO-M1 cells were immunocytochemically stained with anti-vimentin antibody and imaged under a fluorescence microscope. Different populations were identified; cells expressing vimentin only, cells expressing mCherry only (and thus GFAP overexpression) and cells expressing vimentin plus mCherry. Within the GFAP overexpressing pCLNC-mCherry-GFAP transfected MIO-M1 cells, there was a subset of cells that expressed mCherry or vimentin but not both and another subset that expressed both (Figure 5-12). When MIO-M1 cells were transfected with either low or high concentrations of pCLNC-mCherry-GFAP retroviral medium and overexpressed exogenous mCherry-GFAP, there was a decrease in the percentage of cells expressing vimentin only (Figure 5-13). In untransfected MIO-M1 cells, 73% of cells expressed vimentin and this proportion decreased to 42% and 39% of cells in cells transfected with low or high levels of pCLNC-mCherry-GFAP vector, respectively. However, total vimentin expression, which includes both cells expressing vimentin only and cells expressing vimentin and mCherry, remained high at 70% and 75%, which is comparable to vimentin expression in untransfected control cells (Figure 5-13). This suggests that although similar proportions of vimentin positive cells were observed in untransfected and transfected cells, it could be that those transfected cells that lacked mCherry fluorescence were expressing lower levels of mCherry-GFAP that were not detectable by confocal microscopy.

Cell lysates from control untransfected and transfected GFAP overexpressing MIO-M1 cells were used to measure protein expression of vimentin using western blot analysis. Vimentin protein expression slightly decreased in MIO-M1 cells transfected with low or high levels of pCLNC-mCherry-GFAP vector but this was not statistically significant when compared to untransfected control cells (Figure 5-14). This suggests that GFAP overexpression may downregulate the protein expression of vimentin by MIO-M1 cells.

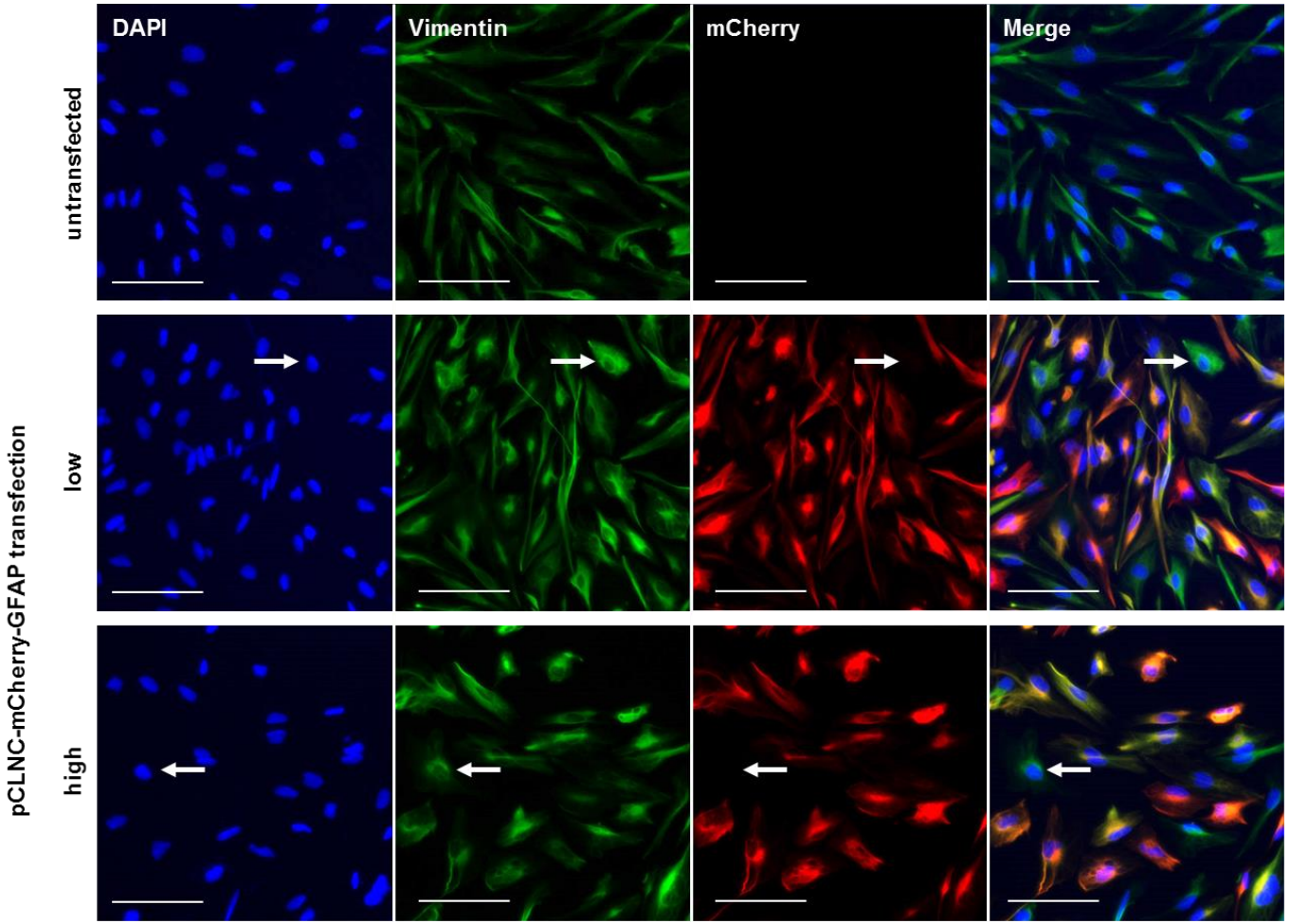

Figure 5-12: Immunofluorescence images of untransfected MIO-M1 cells and cells transfected with low or high levels of pCLNC-mCherry-GFAP retroviral vector stained with anti-vimentin antibody.
Representative immunocytochemistry images of untransfected and low or high transfection Müller cells (mCherry fluorescent, red) stained with anti-vimentin antibody (Alexa Flour 488, green). White arrows indicate vimentin positive immunostained but mCherry negative cells. Scale bar represents 100µm.

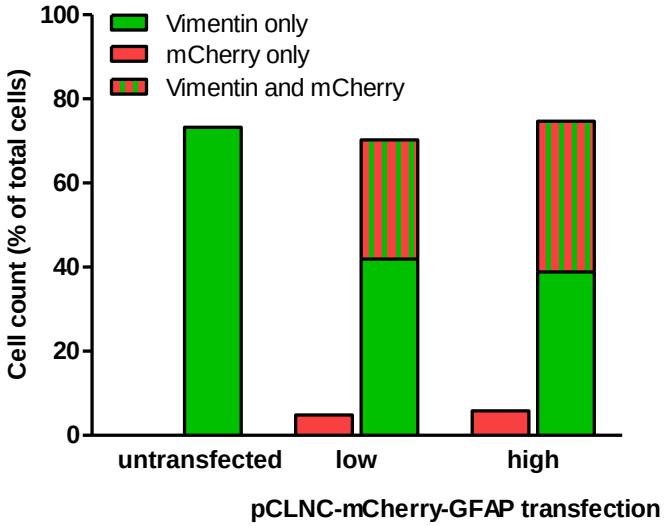

Figure 5-13: Quantification by immunocytochemistry of vimentin expression by MIO-M1 cells transfected with low or high levels of pCLNC-mCherry-GFAP retroviral vector.
Bar charts represent the percentage of cells immunostained for vimentin only (green), cells fluorescent for mCherry i.e. transfected cells (red), and cells positive for vimentin and mCherry combined (green and red striped). Percentage of cells expressing vimentin only decreased in MIO-M1 cells transfected with pCLNC-mCherry-GFAP.

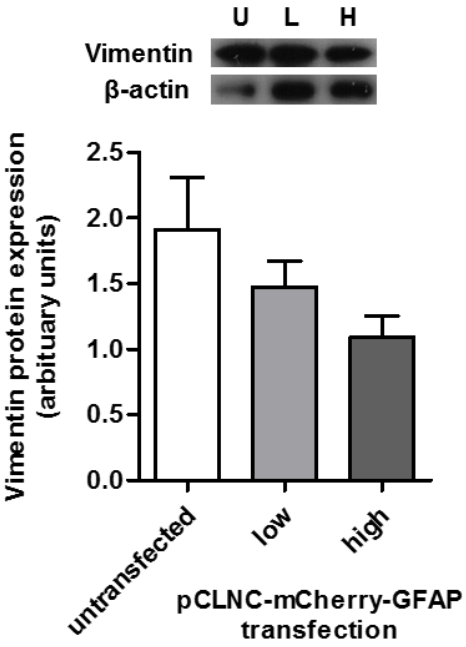

Figure 5-14: Protein expression of vimentin by untransfected and pCLNC-mCherry-GFAP transfected MIO-M1 cells.
Representative western blot bands of vimentin and β-actin shown above bar chart. Bar chart represents vimentin protein expression normalised to β-actin (mean +/- SEM). Protein expression of vimentin decreased in GFAP overexpressing MIO-M1 cells when compared to untransfected cells, although this difference was not statistically significant. One-way ANOVA, Tukey's post-test $p>0.05$, N=4. U: untransfected, L: low, H: high.

5.4 Discussion

5.4.1 Induced overexpression of GFAP does not modify Müller glial cell characteristics in MIO-M1 cells

The overexpression of GFAP is a hallmark for gliosis but it is not known if simply overexpressing GFAP causes other changes in Müller glia. MIO-M1 cells were transfected with low (5%) and high (100%) concentrations of pCLNC-mCherry-GFAP retroviral medium, which generated two cell lines with distinct mCherry fluorescence intensities. When cells were transfected with high level of retrovirus, their median fluorescence intensity was significantly increased compared to cells transfected with low level retrovirus. When protein isolated from cell lysates was analysed by western blotting and probed with anti-GFAP antibody there was an obvious protein accumulation with a large smear of bands detected, including bands for the endogenous GFAP, exogenous mCherry-GFAP and potential GFAP aggregates. This differential endogenous and induced protein has been previously reported in human astrocytes transfected with GFAP fused to a fluorescent protein (Tang et al., 2006). It was also observed that in induced GFAP overexpressing astrocytes the endogenous GFAP increased alongside the induced protein but this was not observed in Müller glial cells. In fact, the opposite was seen in MIO-M1 cells; endogenous GFAP mRNA expression significantly decreased in pCLNC-mCherry-GFAP transfected cells, which was accompanied by no changes in endogenous GFAP protein expression. Measuring the total GFAP mRNA and protein expression, by including endogenous as well as induced expression, revealed significant increases in both MIO-M1 cells transfected with low or high concentrations of pCLNC-mCherry-GFAP retroviral medium when compared to untransfected control cells. However, there was not a significant difference in total GFAP mRNA and protein expression between the low and high transfection cells. The flow cytometry analysis, in which the low and high transfections produced increasing fluorescence intensities in MIO-M1 cells, did not relate to the values observed by western blot analysis. This brings into question whether the two transfected cell lines are truly different from each other. The flow analysis was never repeated with the transfected MIO-M1 cells after passaging, so it is difficult to determine whether the mCherry fluorescence remained significantly higher in the highly transfected cells compared to the cells transfected with low concentration of retroviral medium.

The state and rate of proliferation of MIO-M1 cells was not affected by GFAP overexpression with either low or high levels of the pCLNC-mCherry-GFAP vector. This mimics that seen in Müller glial cells in an *in vivo* chronic glaucoma model where proliferation was unaffected by continuous GFAP upregulation over time (Inman and Horner, 2007). Although GFAP overexpression caused cytotoxicity in MIO-M1 cells when compared to untransfected cells, there was no difference in cytotoxicity between cells transfected with low or high levels of mCherry-GFAP. This could suggest that because there was not significant increase in total GFAP protein expression in high pCLNC-mCherry-GFAP vector transfected MIO-M1 cells, there was no additional effect on cell viability. Alternatively, it may be possible that low pCLNC-mCherry-GFAP transfection and low GFAP overexpression already reaches a threshold for cytotoxicity and any additional GFAP protein does not augment cell death. Nonetheless, the two pCLNC-mCherry-GFAP transfected MIO-M1 cell lines were used to compare the effects of low and high GFAP overexpression in further experiments.

Analysis of mRNA expression revealed that overexpression of GFAP did not modify expression of other Müller glial cell markers, including markers of neural progenitors expressed by these cells. Thus, CRALBP, glutamine synthetase and vimentin mRNA expression were unchanged in MIO-M1 cells transfected with either low or high pCLNC-mCherry-GFAP vector levels when compared to untransfected control cells. This suggests that the cells maintained their glial cell characteristics when GFAP was overexpressed. It is also possible that the transcriptional regulation of CRALBP, glutamine synthetase and vimentin is not influenced by GFAP expression.

5.4.2 TNF-α does not regulate induced mCherry-GFAP expression

As previously shown, when MIO-M1 cells were cultured with TNF-α GFAP mRNA and protein expression was downregulated. However, in both low and high levels of pCLNC-mCherry-GFAP transfected MIO-M1 cells, endogenous GFAP mRNA expression was significantly downregulated by TNF-α, although total GFAP mRNA was not modified. Additionally, endogenous GFAP protein expression was significantly decreased in MIO-M1 cells transfected with low level of pCLNC-mCherry-GFAP vector and cultured with TNF-α when compared to transfected untreated cells. However, in these low and high transfection cells, total GFAP protein expression was not modified by TNF-α. This indicates that

TNF-α does not regulate the exogenously induced mCherry-GFAP expression. TNF-α is known to activate the transcription factor NFκB and there is a conserved NFκB binding site in the upstream promoter sequence of the human GFAP gene (Bae et al., 2006, Gomes et al., 1999). This NFκB response element can mediate opposite transcriptional regulation of GFAP to different inflammatory cytokines (Krohn et al., 1999). It is evident that in MIO-M1 cells TNF-α can activate NFκB and the endogenous GFAP gene is responsive to this transcription factor although the exogenous mCherry-GFAP vector was not responsive in this study. It might be that cloning the mCherry-GFAP sequence into the pCLNCx retroviral vector may have caused loss of the NFκB binding site which is responsible for the GFAP gene regulation by TNF-α. From the original Addgene sequence only 25bp upstream of the GFAP gene were cloned into the pCLNCx vector, losing the promoter region of the GFAP gene and replacing it with the CMV promoter.

Alternatively, it may be possible to suggest that in MIO-M1 cells overexpressing GFAP, TNF-α does not alter total GFAP protein expression due to slow degradation of the GFAP protein. This is because when there is more GFAP protein, it requires longer time to degrade. In astrocytes, TNF-α has been shown to decrease GFAP mRNA but not protein, or it decreases GFAP protein much less than mRNA (Oh et al., 1993, Selmaj et al., 1991). This could be due to the fact that GFAP protein half-life is 8 days in astrocytes *in vitro* and therefore protein downregulation requires longer than 8 days to become evident (Chiu and Goldman, 1984). The transfected MIO-M1 cells were cultured with TNF-α for 6 days, for which it is possible that the cells needed longer time in culture to observe total GFAP protein decrease. This merits further investigations.

5.4.3 Overexpression of GFAP does not modify Müller glial stem cell characteristics but is not permissive for rod photoreceptor precursor differentiation of MIO-M1 cells

Overexpression of GFAP did not modify mRNA expression of progenitor markers in MIO-M1 cells. This was shown by observations that in pCLNC-mCherry-GFAP retroviral transfected MIO-M1 cells, mRNA expression of Pax6, Chx10, Sox9 and Sox2 were unchanged when compared to control untransfected cells.

MIO-M1 cells transfected with low or high levels of pCLNC-mCherry-GFAP retroviral vector were induced to differentiate into rod photoreceptor precursors *in vitro* using the established FTRI method (Jayaram et al., 2014). As previously reported, when untransfected MIO-M1 cells were cultured with FTRI they increased protein expression of the rod photoreceptor marker NR2E3 whilst decreasing protein expression of GFAP. MIO-M1 cells transfected with low or high levels of pCLNC-mCherry-GFAP vector and cultured with FTRI, showed no changes in NR2E3 or GFAP protein expression, suggesting that GFAP overexpression in MIO-M1 cells may not be a permissive environment for rod photoreceptor precursor differentiation. It has been shown that in p27 deficient mice with transiently upregulated GFAP expression in Müller glial cells, the homeostatic support functions of Müller glia were not altered, indicating that Müller cell gliosis can be accommodating of normal retinal function in distinct circumstances (Vázquez-Chona et al., 2011). However, this was not evident in the current study as observed by lack of rod photoreceptor precursor differentiation, which could indicate species differences in the Müller glia reaction to upregulated GFAP.

5.4.4 Overexpression of GFAP in MIO-M1 cells modifies expression of vimentin protein

MIO-M1 cells transfected with low level pCLNC-mCherry-GFAP vector showed reduced but not significant vimentin protein expression when compared to untransfected control cells. Vimentin protein expression decreased further but again not significantly, in MIO-M1 cells transfected with high level pCLNC-mCherry-GFAP vector when compared to low transfection. These observations may indicate that GFAP regulates vimentin expression in MIO-M1 cells but this needs further clarification. There was a small number of experiments undertaken to measure vimentin protein expression which could decrease the significance of the statistical analysis. Alternatively, the high variability observed with western blot analysis indicates the possibility of experimental error. Immunocytochemical analysis of transfected cells revealed a subset of cells with low undetectable mCherry fluorescence but high vimentin expression, suggesting that when GFAP expression was reduced, vimentin levels were potentially increased to compensate. This however, needs more studies.

Although *in vitro* mouse Müller glial cells induced to overexpress endogenous GFAP also upregulate vimentin, *in vivo* GFAP multicopy mutation causes astrocytes to form GFAP aggregates without vimentin expression (Tanaka et al., 2007, Vázquez-Chona et al., 2011). Rat C6 glioma cells transfected with eGFP-GFAP have lower levels of vimentin but Toda et al found vimentin levels unchanged in C6 cells transfected with murine GFAP cDNA (Toda et al., 1994, Tseng et al., 2006). Current literature on vimentin protein regulation is limited but suggests that the methods used to study this expression may need refinement. In addition, modification of vimentin expression may be variable between different cell populations and this may reflect the changes observed in MIO-M1 cells. In fish brain-derived glial cultures labelled for GFAP and vimentin, there was a population of cells negative for vimentin but positive for GFAP, and another population of cells positive for vimentin but negative for GFAP (Cohen et al., 1994). It may be possible that there exist subpopulations of glial cells that express either vimentin or GFAP only, as observed in MIO-M1 cells transfected with pCLNC-mCherry-GFAP. This merits further investigation, potentially by flow cytometry analysis of vimentin and GFAP expression in these cells because immuncytochemistry can be subjective and low expression can be misinterpreted.

Chapter 6 General discussion

6.1 Effects of inflammatory cytokines on the expression of gliosis-associated proteins in MIO-M1 cells

Reactive Müller cell gliosis initiates an inflammatory response within the retina, whilst causing destructive tissue alterations and scar formation, leading to retinal degeneration (Lewis and Fisher, 2003, Xue et al., 2011). Vimentin is one of the proteins associated with gliosis because it is increased in Müller glial cells during retinal disease and in experimental models of retinal inflammation (Hoerster et al., 2014, Lahmar et al., 2014). However, in this study, vimentin mRNA expression was unchanged when MIO-M1 cells were cultured with the inflammatory cytokines TNF-α, IL-6, CNTF or TGF-β1 *in vitro*. The inflammatory cytokine TGF-β1 is known to induce vimentin gene and protein expression *in vitro* when used at lower concentrations than those used in this study. At higher concentrations, it has also been shown to have an inhibitory effect on vimentin gene expression (Wu et al., 2007, Carey and Zehner, 1995). It was therefore surprising that TGF-β1 had no effect on vimentin gene expression in MIO-M1 cells *in vitro*. The human vimentin promoter can be upregulated by active β-catenin, which is the downstream component of the canonical Wnt signalling pathway (Gilles et al., 2003). However, previous work has demonstrated that TGF-β1 downregulates the canonical Wnt signalling pathway in MIO-M1 cells (Angbohang et al., 2015), so potentially this could have resulted in lack of vimentin regulation. This signalling pathway however, was not explored in this study and should be considered for future investigations.

Galectin-1 is another Müller cell gliosis-associated protein examined in this study. Its expression was not affected by culturing MIO-M1 cells with any of the inflammatory cytokines, even though it is known to be involved in the inflammatory response (Kim et al., 2012, Camby et al., 2006). In the CNS, galectin-1 promotes adult neural progenitor cell proliferation and in the zebrafish, galectin is involved in Müller cell mediated regeneration of rod photoreceptors (Craig et al., 2010, Sakaguchi et al., 2006). Upregulation of galectin in zebrafish retina precedes regeneration, suggesting an important role for galectin in directing progenitor cell differentiation (Eastlake et al., 2017). Unfortunately, the expression of galectin was not examined in MIO-M1 cells

induced to differentiate into rod photoreceptor precursors and this should be a subject of further studies. Also, as galectin-1 is a secreted protein, it would have been of interest to investigate the secretion of this protein by MIO-M1 cells cultured with the inflammatory cytokines examined, as well as the effect of exogenous galectin-1 on MIO-M1 cells induced to differentiate into neuronal precursors *in vitro*.

Of the proteins investigated, tenascin was the only protein that was shown to be modulated by the inflammatory cytokine TGF-β1. Upregulation of tenascin is associated with many retinal diseases including glaucoma, AMD and diabetic retinopathy, suggesting the inflammatory response may regulate tenascin (Reinhard et al., 2017). Surprisingly, MIO-M1 cells downregulated their tenascin mRNA expression when cultured with TGF-β1, unlike that previously reported in astrocytes (Smith and Hale, 1997), suggesting that the TGF-β1 signalling pathway may regulate tenascin in different glial cell types. The expression of tenascin was not examined in MIO-M1 cells cultured with factors known to induce differentiation of these cells into photoreceptor precursors (Jayaram et al., 2014). After spinal cord injury in tenascin deficient mice, there is reduced locomotor recovery and axonal regrowth, indicating the importance of tenascin in regeneration (Chen et al., 2010). Furthermore, when human astrocytes are grown *in vitro* in the presence of exogenous tenascin they adopt a quiescent phenotype, suggesting that tenascin could inhibit astrocyte scar formation (Holley et al., 2005). However, culturing of MIO-M1cells with exogenous tenascin was not performed in this study, for which it would be interesting to examine the role of this protein in MIO-M1 cell proliferation and induced rod photoreceptor precursor differentiation.

6.2 TNF-α signalling potentially regulates GFAP expression in MIO-M1 cells

Culturing MIO-M1 cells with TNF-α caused downregulation of GFAP expression through activation of NFκB signalling (summarised in Figure 6-1). In mice, intraocular injection of exogenous TNF-α rapidly activates NFκB in Müller glial cells but this is not seen in all cells suggesting that not all Müller glia respond equally (Mac Nair et al., 2014). Studies using an *in vivo* optic nerve crush model was shown to increase TNF-α expression in the retina in the absence of NFκB activation in these animals. It is possible that levels of endogenous TNF-α are

reduced as a result of crush injury when compared to intraocular injection of TNF-α, which is also more localised and independent of the retina levels of TNF-α produced *in vivo*. This suggests that MIO-M1 cells cultured *in vitro* with exogenous TNF-α may not respond in the same way as cells *in vivo*. This could explain why TNF-α is associated with retinal degenerative diseases as it is possible that the majority of cells become reactive.

In this study, it was also observed that MIO-M1 cells modulate the expression of TNFR2 in response to exogenous TNF-α. Activation of this receptor is known to initiate a neuroprotective signalling as opposed to signalling through TNFR1 which is known to initiate apoptosis (Sedger and McDermott, 2014). During cell culture, interactions between different Müller glial cell populations are also likely to occur. Although transmembrane TNF-α was not examined in this study, it is possible that MIO-M1 cells may express transmembrane TNF-α which can interact with TNFR2 present on neighbouring cells. There is also the possibility that soluble TNFR2 is stabilising the exogenous TNF-α in culture and slowly releasing TNF-α, as suggested by long term studies in leukocytes (Aderka et al., 1992). In the present study, MIO-M1 cells expressed activated NFκB protein for up to 6 days *in vitro,* suggesting a prolonged activation possibly by sTNFR2. Further investigations are therefore needed to determine what factors render MIO-M1 cells receptive to TNF-α in this way. A logical next step would be to study the effect of exogenous TNF-α in an organotypic retinal explant tissue culture system, which mimics *in vivo* glial reactivity (Johnson and Martin, 2008) and examine the expression of NFκB signalling molecules.

Although *in vitro* culture of MIO-M1 cells with TNF-α caused a dose-response downregulation in the expression of mRNA and protein coding for GFAP, untreated control MIO-M1 cells already expressed basal levels of GFAP. This was expected because GFAP is normally present at low levels in Müller glial cells *in vivo*. Originally when the MIO-M1 cell line was first established, GFAP was not detected in cell lysates by western blot analysis, similar to what was observed in other cultured mammalian Müller glial cells (Limb et al., 2002, McGillem et al., 1998). Potentially, the MIO-M1 cells may have increased their expression of GFAP over time. It has been proposed that *in vitro* culturing of primary human Müller glia on plastic tissue culture plates is a stressful environment as cells robustly express GFAP (Lupien et al., 2004). Hauck et al

found the proteomic profile of 2 week old cultured primary porcine Müller glial cells to be profoundly different to freshly isolated cells (Hauck et al., 2003). However, the MIO-M1 cell line is not a primary cell line as they became spontaneously immortalised. Furthermore, the MIO-M1 cell line is well characterised and stably retains Müller glia markers such as CRALBP and glutamine synthetase (Limb et al., 2002), although changes in these proteins were not analysed in this study. *In vitro* cells do naturally respond to changes in culture medium, serum factors and gas concentrations so it is worth considering these factors as they can unintentionally change cell phenotype over time e.g. with changing batches of reagents or suppliers. It should also be considered that these cells are not receiving natural stimuli from the retinal environment and this may account for the increase in GFAP protein observed after long term culture of these cells.

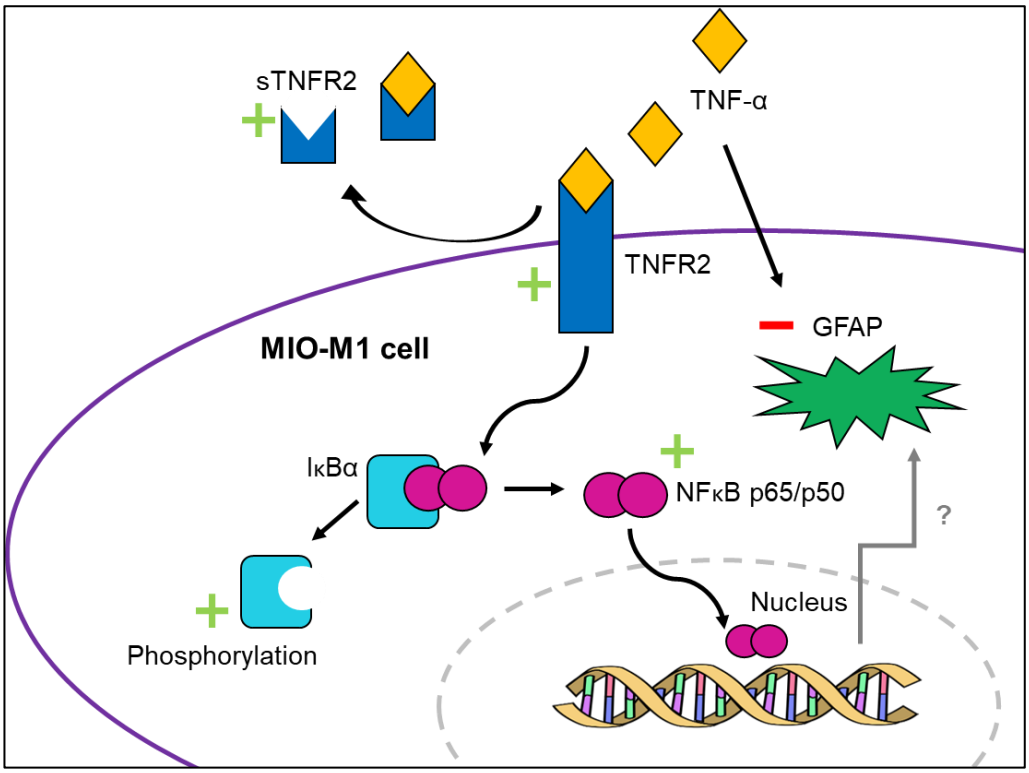

Figure 6-1: Possible mechanism regulating GFAP expression in MIO-M1 cells by TNF-α.

Culturing MIO-M1 cells with TNF-α caused robust downregulation of GFAP. There was also upregulation of TNFR2 and the soluble TNFR2 (sTNFR2) in MIO-M1 cells cultured with TNF-α. sTNFR2 can bind TNF-α and prolong the affects seen through TNFR2 signalling. Downstream of TNFR2, there was upregulation of phosphorylated IκBα, suggesting that this protein was degraded and allowed NFκB to translocate to the nucleus for gene transcription. Supporting this, NFκB p65 phosphorylation and NFκB p50 protein expression were increased significantly in MIO-M1 cells cultured with TNF-α, suggesting that the NFκB signalling pathway was activated. NFκB translocates to the nucleus as a transcription factor, which in MIO-M1 cells may potentially regulate gene transcription of GFAP. Further work is needed to confirm this. Green + signs indicates upregulation, red – sign indicates downregulation, grey ? indicates possible unconfirmed mechanism.

6.3 Culture of MIO-M1 cells with FGF, taurine, retinoic acid and IGF-1

When MIO-M1 cells were cultured with FGF, taurine, retinoic acid and IGF-1 (FTRI) (Jayaram et al., 2014), increase in mRNA expression of NR2E3 proved difficult to measure. Since increase in mRNA coding for this photoreceptor protein was previously reported as being significantly upregulated, new specific primers were designed and rigorously tested to optimise the PCR method. However, inconsistencies in detecting upregulation of this gene was observed in the present study. When qPCR was performed it did not show a significant upregulation as NR2E3 expression only increased 1.09-fold. Previous work in the lab had found a significant increase in NR2E3 expression, which account for a 1.3-fold change (unpublished). Six separate experiments were performed using qPCR in the previous study, whereas this study included only three replicates. It is conceivable that by increasing the sample number it might be possible to achieve statistical significance but it might make the results biologically irrelevant. Nonetheless, protein expression of NR2E3 was observed to be significantly increased in MIO-M1 cells induced to differentiate into photoreceptor precursors in this study. It might be that mRNA expression of NR2E3 is constitutively stable, which may have made it difficult to assess small differences in mRNA levels, whereas de novo NR2E3 protein synthesis may have facilitated the observation of increased protein expression. Additionally, it was observed that GFAP mRNA and protein expression significantly decreased in MIO-M1 cells cultured with FTRI. As GFAP is not expressed in photoreceptor precursor cells this indicates that these cells were downregulating their glial markers and may be re-entering the cell cycle as that seen in Müller glia in the chick retina (Fischer and Reh, 2003). Alternatively, it may be that these differentiation factors independently cause the downregulation of GFAP expression. It would be interesting to examine the effects of the factors separately on GFAP expression, which merits further studies.

MIO-M1 cells were also cultured with FTRI in the presence of TNF-α. The results showed that decreased protein expression of GFAP was accompanied by increase of NR2E3 protein expression in these cells, suggesting that TNF-α does not inhibit the neural differentiation potential of MIO-M1 cells. In the regenerating zebrafish retina, TNF-α released from dying neurons has been

suggested to be necessary for induction of Müller glia proliferation. In damaged chick retinae, TNF-α is associated with Müller glial cell progenitor formation (Fischer et al., 2014, Nelson et al., 2013). Additionally, present observations show that TNFR2 and activated NFκB protein expression is increased in MIO-M1 cells cultured with FTRI in the presence of TNF-α. This suggests that this signalling pathway may facilitate MIO-M1 cell differentiation into rod photoreceptor precursors. This concept is supported by studies in the mouse CNS, where TNFR2 signalling promotes progenitor cell proliferation (Arnett et al., 2001).

6.4 Development of methods to induce GFAP overexpression in MIO-M1 cells

Transgenic mice overexpressing GFAP have been developed as *in vivo* models for studying CNS abnormalities associated with Alexandre disease and astrocytes from these animals have been examined *in vitro* to study GFAP protein accumulation (Hagemann et al., 2006). However, there are limited studies on the effects of GFAP overexpression in the retina or Müller glial cells. The present study explored various methods to investigate whether regulation of GFAP expression could be achieved in MIO-M1 cells. Tetracycline inducible GFAP expression was not possible in MIO-M1 cells, despite attempts to adjust and refine the retroviral transfection method. It is recommended that the host cell is cotransfected with a ratio of at least 6:1 tetracycline repressor TetR to the tetracycline operator TetO2 in order to repress transcription of the gene of interest. Even with low TetO2 expression compared to TetR expression, mCherry-GFAP repression was not reversed by the presence of tetracycline. Potentially the MIO-M1 cell line is not compatible with this system or it is possible that that the cloning method altered the TetR molecule rendering it unable to bind the TetO2 site or tetracycline. It may also be possible that the tetracycline antibiotic was not effective but other antibiotic derivatives were not tested in this study. However, retroviral transfection of MIO-M1 cells with pCLNC-mCherry-GFAP proved to be efficient in inducing overexpression of GFAP, although expression of the vector could not be regulated *in vitro*. Nevertheless, the method facilitated studies on the overexpression of GFAP in MIO-M1 cells.

6.5 Effect of GFAP overexpression in MIO-M1 cells

Transfecting MIO-M1 cells with increasing volumes of retroviral medium containing the pCLNC-mCherry-GFAP vector created two cell lines stably expressing mCherry-GFAP at low and high levels as measured by mCherry fluorescence intensity. Through mRNA and protein expression analysis it was evident that the transfected MIO-M1 cells were expressing exogenous GFAP fused to mCherry and GFAP aggregates, as well as endogenous GFAP. Although the phenotypic Müller glia characteristics were not modified by overexpressing GFAP, exogenous mCherry-GFAP was not regulated by TNF-α in the same manner as that seen with endogenous GFAP. Retroviral transfected MIO-M1 cells cultured with TNF-α did not show downregulation of the induced GFAP mRNA or protein expression, unlike endogenous GFAP which was significantly decreased in the presence of TNF-α. The pCLNC-mCherry-GFAP inserted sequence produces the correct GFAP protein but it does not contain the GFAP gene promoter sequence. However, the results obtained with this vector provide further evidence that TNF-α is regulating GFAP at the transcriptional level, possibly via NFκB activation acting at the κB binding site upstream of the GFAP promoter.

GFAP overexpression in MIO-M1 cells inhibited induced rod photoreceptor precursor differentiation by FTRI, suggesting that overexpression of GFAP may hinder MIO-M1 cell's stem cell characteristics. In the zebrafish, which can regenerate the retina after injury, Müller cell gliosis occurs before and during cell cycle re-entry (Thomas et al., 2016), suggesting that controlling reactive gliosis may be important for inducing regeneration in the mammalian eye.

6.6 Conclusions

This work has demonstrated that the inflammatory cytokine TNF-α can downregulate expression of GFAP in MIO-M1 cell line *in vitro* through downstream signalling via TNFR2 and NFκB activation. This mechanism needs to be validated within the retina using *ex vivo* or *in vivo* models. Further research is also necessary to investigate the genetic targets of NFκB producing this effect because this would identify potential genes that could be involved in preventing retinal scarring. Additionally, this study demonstrated that TNF-α does not inhibit rod photoreceptor precursor differentiation of MIO-M1 cells, indicating that TNF-α may not hinder regeneration in these cells *in vitro*. As

TNF-α does not act alone within the retina environment, further work is needed to identify other factors that may promote neural differentiation of Müller glia with stem cell features.

This study has also shown that it is possible to induce overexpression of GFAP MIO-M1 cells *in vitro* using an optimised retroviral transfection method. Cell proliferation, viability and stem cell characteristics were not altered by GFAP overexpression, whilst the potential to differentiate into rod photoreceptor precursors was inhibited. Although the exact role of GFAP in degeneration is unknown, this study has revealed that perhaps within MIO-M1 cells it may not be disadvantageous or harmful but controlling its expression may be very important for regeneration. However, further work with this established GFAP-overexpressing cell line is needed to confirm these observations. It would also be of interest to examine the production of gliosis-associated factors in these cells, for example expression of inflammatory cytokines or extracellular matrix proteins.

In conclusion, reactive gliosis characterised by GFAP overexpression in MIO-M1cells, may be controlled by TNF-α *in vitro* which has the potential to encourage endogenous regeneration. Further studies are needed to develop therapeutic treatments for retinal degenerative diseases.

Chapter 7 Materials and Methods

7.1 MIO-M1 cell culture

The established Müller glial stem cell line MIO-M1 (Moorfields Institute of Ophthalmology-Müller1) (Lawrence et al., 2007) was maintained in Dulbecco's Modified Eagle Media (DMEM, high glucose, GlutaMAX™, pyruvate; Cat no. 31966-047; Gibco, Life Technologies; Carlsbad, CA, USA) with 10% Fetal Calf Serum (FCS; Biosera; Boussens, France) supplemented with penicillin and streptomycin (Cat no 15070-063; Gibco, Life Technologies) at final concentrations of 20 U/ml and 20µg/ml, respectively. Cells were incubated in a 37°C incubator with 5% CO_2. When a confluent monolayer was reached cells were passaged by removing media and detaching the cells from the flasks using 2ml of TrypLE™ Express Enzyme (1X, Cato no. 12604; Gibco, Life Technologies) by incubation at 37°C for 3 minutes. Approximately 3ml of media containing 10% FCS was added to deactivate the trypsin and the suspended cell solution transferred to a 15ml falcon tube and centrifuged at 1500RPM for 5 minutes to obtain a cell pellet. The supernatant was removed and the cell pellet re-suspended in fresh media and subcultured at an approximate dilution of 1 in 5 of the original cell density. Cells were passaged in this way in T75 flasks once a week. Cell passages from p5 to p35 were used in this study and each cell passage constituted an "N" number as a biological repeat.

7.1.1 Cryopreservation

Cryopreservation for storage was carried out by re-suspending the cell pellet from a T75 flask in 1ml of freezing media consisting of 50% DMEM containing penicillin and streptomycin, 40% FCS and 10% Dimethyl Sulfoxide (DMSO; Cat no. D4540; Sigma-Aldrich, Dorset, UK). The suspension was transferred to a cryovial and placed in an isopropanol freezing container at -80°C for 24 hours to allow controlled slow freezing, optimal for cell preservation. After 24 hours cryovials were transferred to liquid nitrogen at -150°C for long term storage.

7.1.2 Cell counting

After detaching cells from a flask and obtaining a cell pellet, cells were re-suspended in fresh media and diluted 1 in 4 in Trypan Blue solution (Cat no T8154; Sigma Aldrich). Live cells could be counted on a haemocytometer under a microscope. Cells were counted so they could be plated correctly; 200,000

cells/ml were used in a T25; 75,000 cells/ml used in each well in a six well plate and 8,000 cells/ml in each well in a 24 well plate.

7.1.3 Phase contrast microscopy

Cells were examined under an inverted phase contrast microscope (Leica DC IL) and images acquired using the Leica DC200 camera with a 10X objective unless otherwise stated.

7.2 Cytokine treatment of MIO-M1 cells

MIO-M1 cells were cultured with the following cytokines: human recombinant Tumour Necrosis Factor-α (TNF-α; Cat no 300-01A, Peprotech; UK), human recombinant Interleukin-6 (IL-6; Cat no AF-200-06 Peprotech), human recombinant Transforming Growth Factor-β1 (TGF-β1; Cat no 100-21, Peprotech) and human recombinant Ciliary Neurotrophic Factor (CNTF; Cat no 450-13, Peprotech). Lyophilised cytokines were reconstituted in sterile 0.1% Bovine Serum Albumin (BSA; Acros Organics, Thermo Fisher Scientific; Pittsburgh, PA, USA) in phosphate buffered saline (PBS) as per the manufacturer's instructions and stored as working aliquots at -20°C. For dose-response experiments final concentrations of IL-6, CNTF and TGF-β1 were 0.1ng/ml, 1ng/ml, 10ng/ml and 100ng/ml, whilst concentrations of TNF-α were 0.5ng/ml, 5ng/ml, 50ng/ml and 500ng/ml. For all other experiments final concentrations were used at doses previously established in the laboratory as follows: 10ng/ml for IL-6, 10ng/ml for CNTF, 5ng/ml for TNF-α and 50ng/ml for TGF-β1. Cytokines were added at time of plating and replenished on day 3 of a 6 day experiment.

7.2.1 Time-lapse TNF-α treatment of MIO-M1 cells

For ELISA experiments (as described below) MIO-M1 cells were cultured with 5ng/ml TNF-α and cell lysates collected at various time points. Cells were cultured for 15 minutes, 30 minutes, 3 hours, 6 hours and 24 hours in the absence or presence of TNF-α. In these instances, cell lysates were extracted using the protein extraction buffer provided in the ELISA kit.

7.3 Inhibition of NFκB in MIO-M1 cells

NFκB activation was inhibited in MIO-M1 cells using two different chemical compounds. Caffeic acid phenethyl ester (CAPE; Cat no. 2734; Bio-Techne Ltd.;UK) and RO1069920 (Cat no. 1778; Bio-Techne Ltd.) were reconstituted in

DMSO as per the manufacturer's instructions and stored as working aliquots at -20°C. Initial experiments to test the effect of the inhibitors on cell survival used concentrations of CAPE at 5, 10, 20, 30, 40 and 50 µg/ml, whilst concentrations of RO1069920 were 0.1, 1, 3, 10, 30 µM. 4000 cells were seeded onto 48 well plates and inhibitors were added at time of plating in DMEM supplemented with 2% FCS and penicillin and streptomycin incubated at 37°C for 24 hours. After 24 hours, media was removed and wells covered in Trypan Blue solution mixed 1:1 with PBS so dead blue cells could be counted. The concentrations of inhibitor in which cell death was over 15% were not used. Following experiments used final concentrations of CAPE at 5 and 10 µg/ml, whilst RO1069920 was used at concentrations of 0.1, 1 and 3 µM.

Further experiments tested if addition of TNF-α after or during inhibition of NFκB activation could regulate GFAP expression. This was to determine if the TNF-α downregulation of GFAP was achieved through NFκB signalling. Cells were seeded at 2.5 x 10^5 in T25 flasks using DMEM supplemented with 2% FCS and penicillin and streptomycin. When using CAPE, all conditions were cultured for 24 hours with the inhibitor and the following day media was replenished. The control conditions had media only and treatment conditions had media supplemented with 5ng/ml TNF-α and cells were incubated for further 5 days. When using RO1069920, at time of plating the cells media was either supplemented with inhibitor alone or with the inhibitor in the presence of 5ng/ml TNF-α and incubated for 6 days.

7.4 Rod photoreceptor precursor differentiation of MIO-M1 cells

To induce differentiation of MIO-M1 cells, cells were cultured with growth factors in tissue culture flasks coated with basement membrane proteins. ECM gel (ECM Gel from Engelbreth-Holm-Swarm murine sarcoma; Cat no E1270; Sigma-Aldrich) was reconstituted as per the manufacturer's instruction and stock concentrations stored at -20°C. To achieve a working solution with final concentration of 50µg/ml the stock was diluted in a buffer solution of 15mM Na_2CO_3 and 35mM $NaHCO_3$ at pH 9.6. Working solution was kept at 4°C. Enough working solution was used to cover the entire surface of the flask or plate (1ml for a T25 flask) and incubated at 37°C for a minimum of 2 hours prior

to use. After incubation the solution was completely removed by aspiration and the cells cultured on this coated surface.

The growth factors used for rod photoreceptor precursor differentiation were as previously described by the group (Jayaram et al., 2014) and constituted a mixture of human Fibroblast Growth Factor- 2 (FGF-2; Cat no F0291; Sigma-Aldrich), taurine (Cat no T8691; Sigma-Aldrich), retinoic acid (Cat no R2625; Sigma-Aldrich) and recombinant human Insulin-like Growth Factor-1 (IGF-1; Cat no 291-G1-200; R&D Systems, Inc.; MN, USA). All growth factors were reconstituted as per manufacturer's instructions and stored as aliquots of stock solutions at -20°C. These were used at final concentrations of FGF-2 at 20ng/ml, taurine at 20µM, retinoic acid at 5µM and IGF-1 at 100ng/ml. The differentiation protocol used DMEM supplemented with 2% FCS and penicillin and streptomycin. Growth factors were added at the time of plating and replenished on day 3 of a 6 day experiment.

7.5 Cell viability LIVE/DEAD assay

To test cytokine's cytotoxicity on MIO-M1 cells, a LIVE/DEAD® Viability/ Cytotoxicity Assay Kit (For mammalian cells; Cat no L-3224; Life Technology) was used. The kit allows for simultaneous determination of live and dead cells based on two colour fluorescence; live cells will fluoresce green as calcein dye is retained within live cells and dead cells will fluoresce red as ethidium homodimer-1 (EthD-1) enters damaged cell membranes.

For the assay cells were grown on glass coverslips coated with ECM gel as described above and cytokines were added to the media at the concentrations indicated above. Kit reagents were stored at -20°C until cells were ready and the working solution was used fresh at the time of use and was prepared in sterile DPBS at a concentration of 1µM calcein and 0.1µM EthD-1 as per manufacturer's instructions. Cells were incubated with this solution for 30 minutes at room temperature and immediately mounted onto a microscope slide, sealed with nail varnish and imaged under a fluorescence microscope. At least three representative images for each condition were acquired and red fluorescent cells (dead cells) were counted manually. Cell death was calculated as the percentage of red EthD-1 stained cells compared to total number of cells.

7.6 Cell proliferation as determined by hexosaminidase assay

Hexosaminidase is a lysosomal enzyme, the total activity of which is directly proportional to the number of living cells in a homogenous population. The assay is a colorimetric determination of hexosaminidase level and absorbance values obtained are directly proportional to both the number of cells and the length of incubation with substrate (Landegren, 1984). The substrate 4-nitrophenyl-N-acetyl-ß-D glucosaminide (Cat No. N9376; Sigma Aldrich) was used for the hexosaminidase assay. This was dissolved in sodium citrate solution (pH 5.0) at a concentration of 0.25%, and then added to 0.5% Triton X-100 solution (Cat No. X100; Sigma Aldrich).

4000 cells were seeded per well in a 96 well plate and cultured between 2 and 9 days. To assess quantity of living cells at a given time point, media was aspirated from the plates, wells rinsed twice with PBS and 60µl of substrate solution was added. The plates were then incubated for 2 hours at 37°C, after which the reaction was blocked by adding 90µl of 0.1M glycine-NaOH buffer solution (pH 10.4). The final absorbance was measured using a Safire UV-VIS spectrophotometer (Tecan, Mannedorf, Switzerland) at 405nm wavelength with a refence of 620nm. Values obtained were averaged as each condition was performed in triplicate and repeated over three cell passages.

7.7 Cell cytotoxicity assay

A Cytotoxicity Detection Kit^{PLUS} (LDH) (Cat no. 04744926001, Roche) was used to measure cytotoxicity and cell death of MIO-M1 cells overexpressing GFAP. It is a colorimetric assay based on the measurement of lactate dehydrogenase (LDH) activity released from the cytosol of damaged cells into the supernatant.

Working solutions were prepared immediately before use as per manufacturer's instructions and three controls were included in each experiment. The controls being a background control of DMEM only, a low control of MIO-M1 untreated normal cells, and a high control of normal MIO-M1 to which lysis reagent was added to estimate maximum releasable LDH. Every condition was done in triplicate and repeated over 3 passages.

4000 cells were seeded per well in a 96 well plate and cultured for 6 days at 37°C. To each well that contained a high control, 5µl of lysis reagent was added and the plate incubated for further 15 minutes. To determine LDH activity, 100µl

of the reaction mixture was added to each well and the plate incubated for 30 minutes, after which 50µl of a stop solution was added and the plate shaken for 10 seconds. The final absorbance was measured using a Safire UV-VIS spectrophotometer (Tecan, Mannedorf, Switzerland) at 490nm wavelength with a refence of 620nm.

To determine the percentage cytotoxicity the average absorbance of the triplicate samples and controls were calculated, and then for each value the background control was subtracted. The resulting experimental values were substituted in the following equation:

$$Cytotoxicity\ (\%) = \frac{experimental\ value - low\ control}{high\ control - low\ control} \times 100$$

7.8 Reverse Transcription (RT)-PCR

7.8.1 RNA extraction

To isolate RNA, an RNeasy Plus Mini Kit (Cat no 74134; Qiagen; Hilden, Germany) was used. After cells were grown to a confluent monolayer, media was removed, cells were detached using a cell scraper and collected in a falcon tube using sterile PBS. The cell suspension was centrifuged and the cell pellet was re-suspended in Buffer RLT Plus (from the kit) plus β-mercaptoenthanol at a dilution of 1 in 100. The suspension was either frozen at -80°C for future use or homogenised immediately using a needle to ensure cell lysis. RNA extraction was performed as per manufacturer's instructions, which included the use of a gDNA Eliminator spin column to remove any genomic DNA contamination. RNA was eluted using 30µl of RNase-free water and its concentration measured using a spectrophotometer (Nanodrop-1000, Thermo Scientific). Samples were stored at -80°C and thawed on ice prior to use.

7.8.2 Reverse transcription

The amount of RNA yield from the extraction varied between 500ng and 1µg of RNA for the RT reaction to generate cDNA. Volumes of RNA used in the RT reactions were calculated according to the concentration obtained in each reaction. In all cases, samples within the same experiment had the same amount of RNA reverse transcribed as to make the samples comparable. There were two methods used to perform RT:

1) A Tetro cDNA Synthesis Kit (Cat no BIO-65043; Bioline; London, UK) was first used. A single reaction mixture was made up consisting of 1µl Oligo $d(T)_{18}$, 1µl 10mM dNTP mix, 4µl 5X RT buffer, 1µl RiboSafe RNase Inhibitor, 1µl Tetro Reverse Transcriptase, *n*µl RNA for the required concentration and DEPC-treated water up to 20µl total volume. Samples were mixed gently, briefly centrifuged and transferred to a thermal cycler (Mastercycler® Gradient; Eppendorf, UK or Mastercycler® Pro: vapo protect; Eppendorf, UK) for incubation at 45°C for 30 minutes followed by 85°C for 5 minutes.

2) A first-strand cDNA synthesis kit (Cat no 18090010; SuperScript® IV First-Strand Synthesis System; Life Technologies) was also used. An initial mixture was prepared consisting of 1µl Oligo $d(T)_{12-18}$ primer (Cat no 18418-012; Life Technologies), 1µl dNTP mix (Cat no U151A; Promega; Madison, WI, USA), template RNA and DNase free water up to 13.5µl. The mix was gently vortexed and briefly centrifuged before being transferred to a thermocycler (Eppendorf, UK). The mix was heated to 65°C for 5 minutes and then placed on ice for at least 1 minute. Whilst the initial mixture was incubating another mixture was made up of 4µl 5X RT buffer, 1µl 100mM DTT, 0.5µl RNasin® Plus RNase inhibitor (Cat no N2611; Promega) and 1µl SuperScript® IV reverse transcriptase. This was vortexed and centrifuged and then added to the initial reaction mixture. The combined reaction mixture was incubated at 55°C for 10 minutes and then 80°C for 10 minutes as per the manufacturer's instruction. The cDNA produced was then either used immediately in a PCR reaction or stored at -20°C for future use.

7.8.3 Polymerase chain reaction (PCR)

PCR of cDNA products was performed using GoTaq® Green Master Mix (Cat no M712; Promega) which is a premixed solution containing *Taq* DNA polymerase enzyme, dNTPs, $MgCl_2$ and reaction buffer. A reaction mix was made up consisting of 10µl GoTaq, 1µl of forward and 1µl of reverse primers, 1µg of sample cDNA which was either 1µl or 2µl (depending on amount which was reversed transcribed) and enough RNase free water to total a 20µl reaction. Primers were obtained from Sigma or Invitrogen and reconstituted as per manufacturer's instructions to 100µM concentration in RNase free water and further diluted 1 in 100 to a working concentration stock of 10µM. See appendix 1 for list of primers used. The mix was vortexed, centrifuged and

transferred to a thermal cycler. Samples were incubated at 95°C for 5 minutes as an initial denaturation step, followed by 95°C for 1 minute, then the optimised annealing temperature for 1 minute and an extension step of 72°C for 1 minute. This was repeated an appropriate number of cycles before a final extension at 72°C for 5 minutes and refrigeration at 4°C.

7.8.4 Gel electrophoresis

Gel electrophoresis was used to run 10µl of the PCR product at 100V for 60 minutes. The gel consisted of 2% agarose with 1 in 15,000 GelRed™ nucleic acid gel stain (10,000X in water; Cat no 41003; Biotium Inc., Hayward, CA, USA). The GoTaq master mix contains loading dye that allows monitoring of progress and a 100bp DNA ladder (Cat no G210; Promega) was also run alongside the samples. Gels were examined under UV light and images taken using Genesnap Image Acquisition Software (www.syngene.com) under consistent exposure.

7.8.5 Image and statistical analysis

Images were analysed by densitometry of bands using ImageJ (Java, USA) software and results exported to Microsoft Excel and GraphPad Prism 5 (GraphPad Software Inc.; La Jolla, CA, USA) which were used for semi quantitative analysis. Genes of interest were normalised to β-actin used as a housekeeping gene. The same experiment was repeated at least three times to ensure reproducibility and increase reliability. Results were expressed as means +/- standard error of the mean (SEM) at 95% confidence intervals. For experiments comparing two different conditions a paired student's T test was used and experiments comparing variations of the same condition (dose-response experiments) a one-way-repeated-measures-ANOVA was used. A P value of <0.05 was considered statistically significant.

7.9 Real Time Quantitative PCR (qPCR)

The two-step quantitative reverse transcription PCR method was used. RNA extraction and reverse transcription using the first-strand cDNA synthesis kit was performed as described above to obtain 1µg of cDNA. This was further diluted with water to 250ng of cDNA for use.

7.9.1 Primer optimisation

Before running formal qPCR reactions, primers for each gene of interest were optimised. Custom primers were designed with Invitrogen OligoPerfect™ Designer to be 20 nucleotides long and the amplicon length around 100 base pairs (see appendix 2). Primer concentrations were used at 10μM. When performing qPCR with SYBR Green dye, a total volume of 25μl was used in each reaction and primers accounting for no more than 4μl. Various ratios of forward to reverse primer were tested in μl – 1:3, 2:2, 3:1, 1:1. Three repeats of each combination was performed. When performing qPCR with Luna master mix, a total volume of 20μl was used in each reaction with primers making up 1μl; 0.5μl forward and 0.5μl reverse primer were used. Primers were tested by post-amplification melting-curve analysis to check for primer-dimer artefacts and to ensure reaction specificity.

7.9.2 Reaction preparation

A SYBR® Green JumpStart™ Taq ReadyMix™ (Cat no. S4438, Sigma-Aldrich, UK) was used to prepare the qPCR reaction mix. In this procedure, nucleotides are tagged to SYBR Green I dye which is a fluorescent DNA-binding dye that binds to the minor groove of any dsDNA. Each reaction consisted of 12.5μl of the master mix, 0.25μl of the indicator dye (provided with the master mix), 4μl of the primers and water to make up the remaining volume to 20μl. Three repeats of each condition were prepared as one master mix to minimise pipetting errors. The repeats were loaded into MicroAmp® Optical 96-Well Reaction Plates (Cat no. N8010560, Thermo Fisher) and 5μl of the diluted cDNA added to each well for a total of 25μl.

A second master mix, Luna® Universal qPCR Master Mix (Cat no. M3003L, New England Biolabs® Inc), was used which is based on the same principle as the SYBR Green I dye. The reaction was prepared consisting of 10μl of the master mix, 0.5μl of each primer and water to make up the remaining volume to 15μl. Master mixes for each condition were made and aliquoted into 96-well plates and 5μl of cDNA was added at the end for a total of 20μl.

Each run also contained reactions for housekeeping gene β-actin used for normalisation. All reactions were prepared on ice and plates sealed with an adhesive film to avoid evaporation.

7.9.3 qPCR run

Two different machines were used, 7900HT Fast Real-Time PCR System and QuantStudio™ 6 Flex Real-Time PCR System, both from Applied Biosystems™. For both machines, plates were centrifuged briefly to bring all reagents to the bottom of the well and then transferred to the machine. For the 7900HT machine the plates were covered with a heat mat before being placed in the machine. Using the software on the PC attached to the machines, the thermal cyclers were set up as follows: an initial hold step at 50°C for 2 minutes and then 95°C for 10 minutes, followed by the PCR step for 40 cycles of 95°C for 15 seconds and 60°C for 1 minute, finally a melt curve step of 95°C for 15 seconds, 60°C for 1 minute and a dissociation stage of 95°C for 15 seconds. Data was collected between the 60°C and 72°C stage of each cycle as well as during dissociation. Ramp rates were set to 100% for all the stages except for the last step of dissociation which was at 2%.

7.9.4 Analysis

After completion of the run, the threshold cycle (Ct) data was exported from the software for analysis. The software allowed amplification plots and dissociation curves to be viewed and could be exported as images. The Ct is the cycle number at which the fluorescent signal (from the SYBR Green I dye) of the reaction crosses the threshold level, which is a statistically significant increase in signal compared to the baseline signal level calculated during the initial cycles of PCR when there is little change in fluorescent signal.

The raw data was imported into an Excel spreadsheet for relative quantification. Relative quantification allows gene expression levels to be calculated as an up- or down-regulation in a calibrator (untreated control) sample and an experimental sample, focusing on a fold change in the gene of interest in the experiment compared to calibrator. The ΔΔCt method used compares Ct values from the experimental sample with both the calibrator sample and housekeeping gene; the Ct value of the gene of interest in the experiment and calibrator is adjusted to the normalising housekeeping gene. The ΔΔCt values obtained represent a fold difference in expression. Relative quantification followed the steps below:

Normalise samples and calibrator to housekeeping gene:

$$Ct_{gene\ of\ interest} - Ct_{housekeeing\ gene} = \Delta Ct$$

Normalise experimental sample to calibrator:

$$\Delta Ct_{sample} - \Delta Ct_{calibrator} = \Delta\Delta Ct$$

Substitute into the equation:

$$2^{-\Delta\Delta Ct} = fold\ change$$

7.10 Western blotting

7.10.1 Protein isolation

Whole cell lysates were isolated for analysis of protein expression. After cells were grown under various experimental conditions, media was aspirated, cells were washed briefly with PBS to remove any residual media and cells were then detached using a cell scraper. Cells were suspended in PBS and transferred to a Falcon tube to obtain a cell pellet by centrifugation. After removing the PBS, cell pellets were either stored at -20°C for future use or used immediately for protein isolation. 1ml of Radio Immunoprecipitation Assay (RIPA) lysis buffer (Cat no R0278; Sigma-Aldrich) containing 10µl of protease inhibitor cocktail (P8340, Sigma-Aldrich, UK), 0.5mM Dithiothreitol (DTT), 1mM Phenyl Methyl Sulphonyl Fluoride (PMSF) and 3mM Sodium Orthovanadate (Na_3VO_4) was freshly prepared. For this purpose, cell pellets were re-suspended in 100µl of ice cold RIPA buffer, pipetted thoroughly and vortexed to reach a homogenous suspension. The suspension was then placed on ice for 5 minutes to allow cells to swell and lyse and then centrifuged for 5 minutes at 10,000 rpm to pellet any cellular debris. The supernatant containing the proteins was collected and stored at -20°C.

Relative protein concentrations were calculated using the Thermo Scientific Pierce™ BCA (Bicinchoninic Acid) Protein Assay Kit (Cat no 23225; Life Technologies), which is a colorimetric assay based on a reaction between the protein in the sample and the detection reagent. When Cu^{2+} ions are reduced by protein to Cu^{1+}, bicinchoninic acid forms a coloured product which is measured by spectrophotometry. The product has a strong linear absorbance at 562nm with increasing protein concentration. Assays were performed in 96-well plates in which samples (water plus protein), blank (water), zero (water plus lysis buffer) and standards (standard plus lysis buffer), which were made up as

per the manufacturer's instructions and had known increasing concentrations, were loaded in duplicate. The BCA reagent was made up according to the manufacturer's instructions and added to each well. Plates were incubated for 30 minutes at 37°C. Plates were then measured immediately at 562nm in a Safire plate reader (Tecan; Mannedorf, Switerzland). A standard curve was prepared based on the known concentrations of the standard solutions and using the linear equation generated, values obtained by the unknown samples were extrapolated to the standard curve to asses protein concentrations. Additionally, standards and samples were normalised to the zero and blank, respectively.

7.10.2 Protein gel electrophoresis

NuPAGE® (Life Technologies) electrophoresis and buffer systems were used for protein gel electrophoresis. Pre-cast Novex® 4-12% Bis-Tris polyacrylamide gels (Cat no NP0336BOX; Life Technologies) were used along with 800ml of 1X MOPS (3-(N-morpholino) propane sulfonic acid) SDS (sodium dodecyl sulfate) Running Buffer (20X; Cat no NP0001; Life Technologies) to separate proteins within the range of 15kDa to 260kDa. Alternatively, Novex™ 7% Tris-Acetate gels (Cat no EA03555BOX; Life Technologies) were used with Tris-Acetate SDS Running Buffer (20X; Cat no LA0041; Life Technologies) to sperate larger molecular weight proteins within the range of 30kDa to 500kDa. Gels were 1.5mm thick and had 15 wells which could carry up to 25µl of protein load. Loading samples (15µl each) were prepared with 3.75µl of loading buffer (LDS 4X; Cat no NP0007; Life Technologies), 1.5µl of reducing agent (10X; Cat no NP0009; Life Technologies) and a maximum of 9.75µl of protein. To load equal amounts of protein, the volume of protein lysate was calculated from the concentration readings to give either 2µg or 5µg of protein, with the remaining volume made up with water. Loading samples were briefly vortexed, centrifuged and boiled at 80°C for 10 minutes to denature the proteins.

Meanwhile, gels were removed from their packaging and rinsed in distilled water. Combs from the wells were gently removed and the white tape seal removed to allow contact of the gel with buffer during electrophoresis. Gels were placed in XCell SureLock™ Mini-Cell Electrophoresis System (Life Technologies) tanks and secured in place to form a water-tight compartment. This inner compartment was filled with 200ml of MOPS or Tris-Acetate buffer

supplemented with 500µl of antioxidant (Cat no NP0005; Life Technologies). The other 600ml of the buffer filled the outer compartment of the tank. Samples (15µl each) were then loaded into the wells in parallel with 5µl of pre-stained protein standard ladder (Broad Range 11-190kDa; Cat no P7706; New England Biolabs; Ipswich, MA, USA). The gel was run at 180V for 60 minutes.

7.10.3 Gel transfer

A semi-dry transfer method was used in this study. Poly VinyliDene Fluoride (PVDF) membranes (Immobilon-FL PVDF, 0.45 µm; Cat no IPFL00010; Merck Millipore; Darmstadt, Germany) were cut to the appropriate size of the gels and soaked in methanol for 2 minutes, then rinsed in distilled water and soaked in transfer buffer. A 1X transfer buffer (20X; Cat no NP0006; Life Technologies) was made up with 15% methanol in 100ml of distilled water which was used to soak the PVDF membrane and extra thick filter paper (Cat no 1703968; Bio-Rad Laboratories; West Berkley, CA, USA). Once the gel had run, the case was removed and the gel rinsed with transfer buffer. The pre-wet filter paper was placed on the bottom platinum anode of the Trans-Blot® SD Semi-Dry Transfer Cell (Bio-Rad Laboratories), the pre-wet membrane on top of the filter paper and the gel placed faced-down on top of the membrane followed by another pre-wet filter paper. The top cathode was secured in place and the transfer was carried out at 10V for 30 minutes for one gel or 25V for 30 minutes for two gels.

7.10.4 Immunoblotting

Following protein transfer to the PVDF membranes, these were blocked in Tris-buffered saline (TBS) with 0.1% Tween-20, 5% milk and 5% FCS for 2 hours at 37°C. The primary antibody (see appendix 3) was diluted appropriately in the blocking reagent and membranes were incubated with the antibody overnight at 4°C on a shaker. The next day membranes were washed 3 times for 30 minutes with TBS with 0.1% Tween-20 at room temperature on a shaker. Membranes were then incubated for 1 hour at room temperature with secondary antibody (Jackson ImmunoResearch Laboratories Inc.; PA, USA), which was a species specific HRP conjugated IgG, diluted at 1 in 5000 with blocking reagent. Three washes were then repeated as before. The bound secondary antibody reacted with Luminata Western HRP Substrate (Classico cat no WBLUC0500 or Crescendo cat no WBLUR0500; Millipore Corporation; Billerica, MA, USA) which was applied to the membrane for 2 minutes. Excess solution was

removed and the membrane placed in a cassette and the protein was visualised using Fuji X-ray film (Cat no AUT-300-040D; Thermo Fisher Scientific) developed in a dark room.

7.10.5 Stripping membranes of antibodies for re-probing

Following visualisation membranes could be stripped of antibodies by briefly washing with TBS and incubating in stripping buffer consisting of 200mM glycine and 5mM NaCl at pH2.5 for 30 minutes at room temperature. Membranes were then washed 3 times for 5 minutes in TBS at room temperature before re-probing with primary antibody, or were stored at 4°C in TBS for up to two weeks for future use.

7.10.6 Image analysis

After X-ray films were scanned into a computer, optical density of bands was quantified using ImageJ and results were exported to Excel. Statistical analysis was performed in GraphPad Prism as described previously.

7.11 Immunocytochemistry and immunohistochemistry

7.11.1 Fixation and sectioning of tissue

Tissue samples were placed in 4% paraformaldehyde (PFA) for 24 hours at 4°C and then cryoprotected in 30% sucrose for 24 hours. Tissue samples were then embedded by placing in OCT (optimum cutting temperature) embedding matrix (Cat no KMA-0100-00A; CellPath; Newton, UK) and snap frozen on dry ice. Once embedded, samples were stored at -20°C. Tissues were sectioned at 10µm thickness on a cryostat (Leica CM1850).

7.11.2 Fixation of cells

Cells were grown in 24 well plates on sterile circular glass cover slips, which had been coated with ECM gel prior to use, as described above. Following cell culture, media was removed from the wells and cells were fixed with 4% PFA for 5 minutes. PFA was removed and disposed of in a fume hood and 30% sucrose was then added to the wells for 15 minutes for cryopreservation. Once sucrose was removed and glass slides dried the plate was either used for immunostaining immediately or stored at -20°C for later use.

7.11.3 Staining

If frozen, microcoverslips were allowed to defrost at room temperature for at least 30 minutes prior to staining. Cells were washed 3 times for 5 minutes in

TBS before being blocked for 1 hour at room temperature. Blocking reagent was made up of TBS with 0.3% Triton (X100; Cat no 9002-93-1; Sigma Aldrich) and 5% normal donkey serum (Cat no 017-000-121; Jackson ImmunoResearch Laboratories Inc.). The primary antibody (listed in appendix 3) was diluted as required in the blocking reagent and added to the cells for overnight incubation at 4°C on a shaker. Parallel to this, a control experiment in which no primary antibody was used, was run to exclude for any background or non-specific staining of the secondary antibody. The following day the cells were washed 3 times for 5 minutes in TBS before the secondary antibody was applied. The secondary antibody (donkey anti species from primary antibody), labelled with Alexa-Fluor fluorochromes (Jackson ImmunoResearch Laboratories Inc.), was diluted in TBS with 0.3% Triton at a 1 in 500 dilution and cells were incubated with this for 3 hours at room temperature. Cells were then washed 3 times in TBS as above. Cell nuclei were counter stained with DAPI (4', 6-diamidino-2-phenylindole; Cat no D9542; Sigma Aldrich) diluted at 1 in 5000 with TBS for 2 minutes before a final rinse with distilled water. Microscope slides were prepared with Vectashield mounting medium (Vector Laboratories; Burlingame, CA, USA) and glass cover slips removed from wells and placed cell side down on the slides. Cover slips were sealed with nail varnish.

Immunhistochemistry was performed using the same protocol except washes were 10 minutes.

7.11.4 Fluorescence microscopy and image analysis

Fluorescence images were acquired either on an epifluorescence microscope (Leica DMRB) or a confocal microscope (ZEISS Confocal Laser Scanning Microscope LSM 700 or 710; Carl Zeiss AG; Oberkochen, Germany). For epifluorescence either 10X or 20X objectives were used and images taken on a ProgRes® microscope camera (Jenoptik; Jena, Germany). For confocal microscopy 10X, 20X or 40X objectives were used. The Zeiss LSM 700 40X objective was for oil immersion, whilst the Zeiss LSM 710 40X objective was for water immersion. Exposure times for each fluorescence filter and microscope settings were adjusted appropriately and kept constant within experiments. At least three representative images of each experimental condition were acquired using the ZEN Imaging Software (ZEISS). Cell counting of positively stained

cells in these images was done manually and results were analysed on Excel and statistical analysis performed on GraphPad prism.

7.12 Enzyme-Linked Immunosorbent Assay (ELISA)

An enzyme-linked immunosorbent assay (ELISA) is a quantitative technique to detect the presence of antigens that are recognized by an antibody, which is coupled to an easily-assayed enzyme. For this assay, 96 well microplates are pre-coated with a specific antibody (to detect the protein of interest) and standards and samples are subsequently applied to the plate. Any antigen present is bound to the plate via the immobilised antibody. After incubation, the wells are washed to remove any unbound substance and an enzyme-linked antibody specific for the antigen is added and the plate incubated again. An additional wash removes any unbound antibody-enzyme reagent and a substrate solution is then added to the wells. After further incubation a colour develops in proportion to the amount of antigen bound in the initial step. A stop solution is added at a defined endpoint and intensity of the colour is measured. The absorbance value is proportional to the quantity of protein of interest. Standards and samples are duplicated and an average absorbance is calculated and the zero control (diluent of the standards alone) is subtracted. A standard curve is created using the known standard concentrations and absorbance values. Concentrations of the samples are calculated by extrapolation to the standard curve.

Three different quantitative sandwich enzyme immunoassay kits were used in this study. The Quantikine® ELISA human TNF-RII/TNFRSF1B kit (Cat no. DRT200; R&D Systems Inc.; MN, USA) measured human soluble TNF-Receptor II concentration in cell culture supernatants and was performed as per manufacturer's instructions. The NFκB p65 (pS536) SimpleStep ELISA™ kit (Cat no. ab176647; Abcam; Cambridge, UK) measured phosphorylated NFκB p65 in human cell lysates and was performed following manufacturer's instructions. The IκBα (pS32/36) SimpleStep ELISA™ kit (Cat no. ab176643; Abcam) was used to measure phosphorylated IκBα in human cell lysates following manufacturer's instructions.

7.13 Methods to induce GFAP overexpression in MIO-M1 cell line

7.13.1 Transfection of MIO-M1 cells with plasmid mCherry-GFAP-N-18

The mCherry-GFAP-N-18 plasmid was a gift from Michael Davidson (Addgene plasmid # 55051). mCherry is a mutant fluorescent protein which has excitation and emission maxima at 587nm and 610nm, respectively, allowing for detection of the protein. The plasmid sequence is shown in appendix 4.

7.13.1.1 Isolation of plasmid DNA from bacteria

Bacterial cells containing the mCherry-GFAP-N-18 plasmid were cultured overnight at 37°C on LB agar plate containing kanamycin at final concentration of 50µg/ml (Cat no 60615; Sigma-Aldrich) for selection of single colonies containing the plasmid, which contained kanamycin resistance. Six single colonies were picked with a pipette and used to inoculate 6ml of LB broth plus kanamycin. The bacterial culture was incubated at 37°C on a shaker for 12-16 hours. Following incubation, 500µl of the broth containing the bacteria was removed and stored at 4°C for future use. Additionally, 500µl was mixed with 500µl of 50% glycerol in a cryovial for long term storage at -80C. The remaining bacterial culture was used to isolate plasmid DNA using a Qiagen Plasmid Mini Kit (Cat no 12123; Qiagen) according to the manufacturer's instruction. Plasmid DNA was stored at -20°C.

7.13.1.2 Diagnostic restriction enzyme digest

To verify that the plasmid contained the correct GFAP gene sequence, isolated plasmid DNA was digested with the restriction enzymes PstI, AflII and KpnI. A 10µl reaction containing 3µl of DNA, 0.2µl of each enzyme, 1µl of the appropriate buffer and 3µl 30X BSA was completed with distilled water. The reaction mix was incubated at 37°C for 1 hour. Products, as well as uncut plasmid, were run on a 1% agarose gel at 200V for 30 minutes with a 1kb ladder which had added buffer to achieve similar salt concentrations as the reaction mix. Gel products were checked for correct sized bands.

7.13.1.3 Sequencing

To ensure the GFAP insert was correct, isolated plasmid DNA was sequenced using the Sanger sequencing method. The DNA was prepared for sequencing in two separate 20µl reactions comprising of 0.5µl BigDye® Terminator ready

reaction mix (Applied Biosystems), 3.75µl BigDye Sequencing Buffer (Applied Biosystems), 1µl of forward or reverse sequencing primer (see appendix 5), 1µl DNA and distilled water up to 20µl. The two mixtures were transferred to a thermo cycler and the reaction denatured at 96°C for 1 minute, the sequencing reaction proceeded for 30 cycles of 96°C for 30 seconds, 55°C for 30 seconds and 60°C for 4 minutes. The sequencing reaction was precipitated to remove unincorporated fluorescent nucleotides by incubation with 3M NaOAc (2µl), 0.5M EDTA (0.59µl) and 95% Ethanol (50µl) at room temperature in the dark for 15 minutes. The mixtures were centrifuged at 13000 RPM for 30 minutes and the supernatants discarded. 70µl of 70% Ethanol was then added to each preparation and centrifuged again at 13000 RPM for 15 minutes to obtain pellets. Each pellet was then left to dry at room temperature for 15 minutes in the dark. The dried pellet was then re-suspended in 15µl of Hi-Di™ Formamide (Life Technologies) and denatured at 96°C for 5 minutes and 4°C for 5 minutes. The DNA was then loaded in an Applied Biosystems 3730 DNA analyser for sequencing.

7.13.1.4 Expanding plasmid DNA

The original bacteria aliquot, which was stored at 4°C, was used to inoculate 250µl into 125ml of LB broth containing kanamycin in a conical flask. Flasks were covered with aluminium foil and incubated at 37°C overnight, shaking at 200-230 rpm. The bacterial broth was then centrifuged to obtain a bacterial pellet and a Qiagen Plasmid Maxi Kit (Cat no 12162; Qiagen) was used to isolate the plasmid DNA as per manufacturer's instructions. DNA concentrations were measured using a spectrophotometer and stored at -20°C.

7.13.1.5 EndoFectin Max transfection

Müller glial cells were transfected with the plasmid DNA using the EndoFectin Max transfection reagent (Cat no EFM1004; tebu-bio, France). Cells were seeded in a 24 well plate to ensure that 80% confluence was reached overnight. The 24-well plate contained glass coverslips coated in ECM so the cells could be viewed under a fluorescence microscope. Various combinations of plasmid DNA and EndoFectin Max reagent volumes were used to assess the optimal conditions for transfection. For this purpose in Eppendorf tubes, 0.5µg or 1µg of the plasmid DNA was diluted in 50µl of DMEM media and separately 0.5µl, 1µl, 2µl, 3µl or 4µl of EndoFectin Max reagent was diluted with 50µl of DMEM. The

diluted EndoFectin Max reagent was added to the diluted DNA solution and the combined solution gently mixed. The mixture was incubated at room temperature for 25 minutes before being added directly to each well containing the cells in 0.5ml of DMEM + 10% FCS. Cells were incubated with EndoFectin Max at 37°C for 48 hours at which point glass coverslips were removed from the wells, placed cell side down on the microscope slides covered with Vectashield and sealed with nail varnish. Microscope slides were then viewed under a LSM 700 confocal microscope to determine the proportion of cells that had been transfected. Those cells which had been transfected with the mCherry-GFAP plasmid were detected by their fluorescence.

In order to transfect a larger number of cells, T25 flasks were used and the optimised protocol was modified. There was 1µg of plasmid DNA diluted in 250µl of DMEM and 2µl of EndoFectin Max reagent diluted in 250µl of DMEM. Diluted solutions were combined and incubated for 25 minutes at room temperature and added to the flask with 5ml of DMEM + 10% FCS and incubated at 37°C for 48 hours. Flasks of cells could be viewed under a fluorescent digital inverted microscope (The EVOS® FL Imaging System).

7.13.1.6 Selection of transfected cells

After transfection the media was removed from the remaining wells and the T25 flask and replaced with fresh DMEM media with 10% FCS containing G418 antibiotic (G418 Sulfate, Geneticin® Selective Antibiotic Powder; Cat no 11811-023; Life Technologies) at a final concentration of 400µg/ml. The plasmid contained the Neomycin resistant gene and thus transfected cells would show resistance to G418, which allowed for their positive selection. After 48 hours incubation with G418 at 37°C, the cells attached to coverslips were checked again for fluorescence as described above. The cells in the T25 flask that had survived had the media replaced with fresh DMEM media with 10% FCS and penicillin/ streptomycin and were allowed to grow to confluence.

7.13.1.7 Fluorescence-activated cell sorting

In order to ensure a pure population of transfected cells, fluorescence- activated cell sorting (FACS) was used. This method allows enrichment of cell populations on the basis of their fluorescent characteristics. Once cells had grown to confluence in a T25 flask, they were detached from the flask using

TrypLE™ and centrifuged to obtain a cell pellet. The pellet was resuspended in 400µl DMEM + 2% FCS supplemented with 1% penicillin and streptomycin. The suspension was filtered to remove any cellular debris or clumped cells and a single cell suspension was obtained. A DRAQ7™ live/dead discriminator (Cat no DR71000; BioStatus; UK) was added to this single cell suspension, which was applied through a 100µm nozzle at 30psi along with a sheath fluid (Cat no. 342003; BD FACSFlow™; BD Biosciences; USA) in a custom made BD Influx flow cytometer (BD Biosciences; USA). Dead cells could be eliminated and cells expressing mCherry were detected by fluorescent lasers at 587nm. mCherry positive cells become electrically charged and as they passed through an electrostatic deflection system they are directed into a separate container. The container used for collection was a 15ml falcon tube with DMEM + 10% FCS with 1% pen/strep. The selected cells were then transferred into a 24-well plate with DMEM + 10% FCS and 1% pen/strep and were allowed to grow to confluence.

7.13.2 Transfection of MIO-M1 cells with the retroviral pCLNCx vector under the control of an inducible promoter

7.13.2.1 Subcloning mCherry-GFAP into pCLNCx

7.13.2.1.1 PCR amplification

In order to subclone mCherry-GFAP into a retroviral vector the mCherry-GFAP sequence had to be amplified from the original mCherry-GFAP-N-18 plasmid. Cloning primers upstream and downstream from the desired sequence were created containing HindIII and ClaI restriction sites which could be used for cloning into matching sites in retroviral vector pCLNCx, a gift from Dr. Amanda Carr. The forward primer created a HindIII site on amplification and the reverse primer created a ClaI site on amplification (see appendix 6). A reaction mix was made up consisting of 10µl GoTaq, 1µl of forward and 1µl of reverse primers, 1µl pmCherry-GFAP-N-18 DNA and RNase free water up to a total of 20µl reaction. The mix was vortexed, centrifuged and transferred to a thermal cycler. Samples were incubated at 95°C for 5 minutes as an initial denaturation step, followed by 36 cycles of 95°C for 1 minute, 58°C for 2.5 minutes and an extension step of 72°C for 1 minute, and a final extension at 72°C for 5 minutes. PCR products were separated on a 1% agarose gel at 200V for 30 minutes

alongside a 1kb ladder as a reference. The amplicon at the correct size for the mCherry-GFAP construct was excised from the gel using a UV light box and purified using a Qiagen QIAquick Gel Extraction Kit (Cat no 28704; Qiagen) as per manufacturer's instructions. DNA concentrations were measured using a spectrophotometer and stored at -20°C.

7.13.2.1.2 Restriction enzyme digest

Isolated mCherry-GFAP DNA obtained from the PCR amplification and the retroviral vector pCLNCx were digested with the restriction enzymes HindIII and ClaI to create complementary sticky ends. The 50µl reactions containing 2µg of DNA, 5µl of the appropriate buffer, 3µl of each enzyme, and made up with distilled water were incubated at 37°C for 2 hours. Products were separated on a 1% agarose gel at 200V for 30 minutes and the restriction digest amplicon for mCherry-GFAP and pCLNCx were excised from the gel as described above. DNA concentrations were measured using a spectrophotometer and stored at -20°C.

7.13.2.1.3 DNA Ligation

The restriction digested mCherry-GFAP DNA was ligated into the pCLNCx vector to create a new vector pCLNC-mCherry-GFAP. T4 DNA ligase (Cat no M180A; Promega) was used to generate a 10µl ligation reaction mix consisting of 1µl vector pCLNCx DNA, 1µl ligase, 1µl 10X buffer, 1-7µl insert mCherry-GFAP DNA and made up with nuclease-free water. Seven separate reactions were made, which were incubated at 4°C overnight.

7.13.2.1.4 Transformation

The following day the new ligated vector pCLNC-mCherry-GFAP preparation was transformed into TOP10 Chemically Competent *E. coli* cells (One Shot®; Cat no C4040-10; Invitrogen) for plasmid propagation as per manufacturer's instructions. Briefly, the *E. coli* cells were thawed on ice and 25µl was added to each ligation reaction and the mix was incubated on ice for 30 minutes. The cells were then heat shocked in a pre-warmed water bath at 42°C for 30 seconds and then placed back on ice, 200µl of room temperature S.O.C. medium was added and cells incubated at 37°C for 1 hour shaking at 225rpm. Each reaction mixture was then spread on a LB + ampicillin agar plate pre-warmed to 37°C, left to dry and then inverted and incubated at 37°C overnight.

The pCLNCx backbone vector contained ampicillin resistance which allowed for selection of bacterial cells containing the plasmid.

7.13.2.1.5 Verification of transformation and plasmid expansion

Plates were transferred to 4°C and single bacterial colonies were used to inoculate individual tubes containing 6ml of LB media plus ampicillin. The bacterial culture was incubated at 37°C on a shaker for 12-16 hours. Following incubation and bacterial growth, 500µl was removed and stored at 4°C for future use and 500µl was added to 500µl of 50% glycerol in a cryovial for long term storage at -80C. The other 5ml was used to isolate plasmid DNA using a Qiagen Plasmid Mini Kit (Cat no 12123; Qiagen) as per manufacturer's instructions. A diagnostic restriction enzyme digest was performed on the isolated DNA digested with HindIII and ClaI enzymes to verify that transformation had worked correctly and the plasmids produced contained the mCherry-GFAP insert. The original bacteria aliquot was then expanded by inoculating 125ml of LB broth plus ampicillin in a conical flask with 250µl plasmid-containing bacteria. The flask was incubated at 37°C overnight in a shaking incubator. Plasmid DNA was finally isolated using a Qiagen Plasmid Maxi Kit (Cat no 12162; Qiagen) and DNA concentration was measured using a spectrophotometer and stored at -20°C.

7.13.2.2 Subcloning the tetracycline operator 2 (TetO2) inducible promoter into the pCLNC-mCherry-GFAP vector

Both the pCLNC-mCherry-GFAP and pcDNA4™/TO/*myc*-HisB (Cat no V103020, Invitrogen) (a gift from Prof. Karl Matter) vectors had restriction enzyme sites for NruI and HindIII either side of the promoters which could be exploited for cloning. The CMV promoter in the pCLNCx backbone vector could be removed using NruI and HindIII as well as the TetO2 promoter from the pcDNA4™/TO/*myc*-HisB. A restriction enzyme digest was performed as described above using 2µg of plasmid DNA cut with NruI and HindIII enzymes. Digested products were separated on a 1% gel at 200V for 30 minutes and bands of the correct size for the TetO2 promoter and the pCLNC-mCherry-GFAP were isolated and extracted from the gel as previously described. A ligation reaction of pCLNC-mCherry-GFAP and the TetO2 promoter was set up overnight and subsequently transformed into competent E coli as described above. The E coli strain used was methyltransferase deficient *dam-/dcm-*

Competent E. coli (Cat. no. C29251; NEB, UK) in order to ensure restriction enzyme sites were not altered. Transformation of these cells was performed as per manufacturer's instructions. The *E. coli* cells were thawed on ice and 50µl added to each 5µl ligation reaction and the mix was incubated on ice for 30 minutes. The cells were then heat shocked in a water bath at 42°C for 30 seconds and then placed back on ice for 5 minutes. Each reaction was mixed with 950µl of room temperature S.O.C. medium and incubated at 37°C for 1 hour shaking at 250rpm. After incubation, a 10-fold dilution was performed using S.O.C. medium and 100µl of each transformation reaction was spread onto an LB + ampicillin agar plate pre-warmed at 37°C, left to dry and then inverted and incubated at 37°C overnight. Verification and plasmid expansion were performed as described above using the restriction enzymes HindIII and NruI. The newly created plasmid pCLNC-mCherry-GFAP-TO DNA was stored at -20°C.

7.13.2.2.1 Creating a control plasmid containing mCherry only

In order to create an mCherry only control plasmid, the retroviral vector pCLNC-mCherry-GFAP-TO plasmid was restriction digested to remove the mCherry-GFAP sequence and replaced with mCherry only. The mCherry sequence was PCR amplified from the original mCherry-GFAP-N-18 plasmid. Cloning primers (see appendix 6) flanking the mCherry sequence were created containing HindIII and ClaI restriction sites that could be used for cloning into matching sites in pCLNC-mCherry-GFAP-TO after the mCherry-GFAP had been removed. Amplification PCR was performed as described above and the mCherry PCR product along with pCLNC-mCherry-GFAP-TO vector were digested with the restriction enzymes HindIII and ClaI. This process removed the mCherry-GFAP sequence from the retroviral vector and exposed HindIII and ClaI sites matching those of the amplified mCherry sequence. The DNA ligation of the mCherry into the pCLNCx-TO vector, transformation into *dam-/dcm-* Competent E. coli, plasmid verification, expansion and isolation were all performed as described above. Control plasmid pCLNC-mCherry-TO DNA was stored at -20°C.

7.13.2.2.2 Sequencing new pCLNC-mCherry-GFAP-TO vector and control vector pCLNC-mCherry-TO

Both plasmids were sequenced using the Sanger Sequencing Service provided by Source BioScience (Nottingham, UK). Specially designed primers (see appendix 5) were used to generate readings of the plasmids from the NeoR site in the pCLNCx backbone through the TetO2 promoter and mCherry with or without GFAP until the SV40 backbone region. Sequencing readings were compared to vector maps using Serial Cloner 2.6.1 molecular biology software. The results confirmed that both plasmid were correct.

7.13.2.3 Development of a stable MIO-M1 cell line expressing the pcDNA4/TR regulatory plasmid

Before the retroviral transfection of the tetracycline-inducible promoter into cells, a stable MIO-M1 cell line expressing the regulatory vector, pcDNA4/TR (Cat no V102520, Invitrogen) a gift from Prof. Karl Matter, containing the TetR gene and expressing high levels of TetR molecule, was established for use as hosts for inducible promoter-based constructs. Plasmid DNA was expanded and isolated as described above.

7.13.2.3.1 Determining antibiotic sensitivity

The regulatory plasmid pcDNA4/TR contains the blasticidin resistance gene allowing for selection of the plasmid using blasticidin antibiotic (Cat. No. R21001, Invitrogen). Therefore it was necessary to produce a kill curve, to determine the appropriate blasticidin concentration which would kill the untransfected MIO-M1 cells. Cells were seeded at 25% confluence on 6 well plates the day before treatment to ensure cells were actively dividing. A dose response curve experiment using 0, 0.5, 1, 1.5, 2, 4, 6, 8 and 10µg/ml blasticidin was created. The selection media was replenished every 3-4 days and the percentage of surviving cells was observed after two weeks under a phase microscope. The concentration of blasticidin determined as being appropriate for selection was 1µg/ml.

7.13.2.3.2 Transfection and selection of MIO-M1 cells expressing the regulatory plasmid

MIO-M1 cells at passage 20 or under were seeded onto 6 well plates to reach 80% confluence the next day. The cells were transfected with pcDNA4/TR using

the EndoFectin Max reagent as described above. Briefly, 2µg of plasmid DNA was diluted with 200µl DMEM alone whilst 4µl of EndoFectin was also diluted with DMEM. Both were mixed together and incubated at room temperature for 25 minutes. The mixture was then added to the cells along with 2.5ml of DMEM plus 10% FCS and incubated at 37°C for 24 hours. An untransfected negative control was also prepared, which was incubated with EndoFectin only without the plasmid DNA. After 24 hours cells were washed and fresh medium was added. 48 hours after transfection the cells were split into fresh medium containing 1µg/ml blasticidin. Cells were kept at low density such that they were no more than 25% confluent for the antibiotic treatment. Selective medium was replaced every 3-4 days until the cells reached confluence and were split again and a stable cell line was established after 2 weeks. Negative control cells were killed by the antibiotic after the 2 week period.

7.13.2.4 Retroviral transfection of MIO-M1 cells

In order to create retrovirus, the pCLNC-mCherry-GFAP-TO vector was transfected into GP2-293 packaging cells with the envelope plasmid pMD.G and a carrier plasmid pBSK (a gift from Dr. Amanda Carr). GP2-293 cells were cultured on 0.1% gelatin-coated 10cm^2 dishes. To coat the dishes, 5ml of 0.1% gelatin was used to cover the entire surface of the dish and incubated at 37°C for a minimum of 30 minutes prior to use. After incubation the solution was completely removed by aspiration and the cells cultured on this coated surface. The day before transfection the GP2-293 cells were split 1:5 onto the plates in 8ml DMEM supplemented with 10% FCS and 1% pen/strep.

The following day the GP2-293 packaging cells were transfected with the plasmids using the calcium phosphate precipitation method as follows. Solution A was prepared containing 375µl of 2X HEPES-buffered saline solutions (HBS) at pH7.1 and 7.5µl of 100X PO_4, whilst solution B was prepared containing 15µg of pCLNC-mCherry-GFAP-TO, 5µg of pMD.G and 10µg pBSK, 45µl of 2M $CaCl_2$ in a total volume of 372.5µl made up with water. The two solutions were combined by adding solution B dropwise using a Pasteur pipette to solution A whilst bubbling air through solution A using a 2ml stripette. A calcium phosphate DNA co-precipitate is formed, the calcium phosphate helps the DNA bind to the surface of cells, where it is then taken in by endocytosis. The calcium-phosphate/DNA precipitate solution was then added to the GP2-293 cells,

mixed gently and the cells incubated at 37°C for 6 hours. After the 6 hours the medium was removed and replaced with 10ml of fresh pre-warmed DMEM with 10% FCS and pen/strep. The cells were incubated overnight at 37°C and the next day the medium was replaced and the cells incubated at 37°C for 48 hours. During this incubation the GP2-293 cells were producing the retrovirus containing the pCLNC-mCherry-GFAP-TO sequence as confirmed by the presence of mCherry positive GP2-293 cells under a fluorescent digital inverted microscope (The EVOS® FL Imaging System).

The medium, containing the retrovirus, was removed following the 48 hours incubation and 1ml FCS supplemented with 1µl of polybrene (40mg/ml stock; Hexadimethrine bromide, Cat. No. H9268, Sigma) was added to it. This mixture was then filtered through a 0.45µm filter to remove any packaging cells and added to 10ml of DMEM containing 10% FCS and pen/strep. This mixture of approximately 20ml was split into 5ml aliquots which were stored at 4°C. One aliquot was used immediately; 5ml of the viral medium was added to a T25 culture flask which had been seeded with $3.5x10^5$ MIO-M1 cells the previous day. The MIO-M1 cells were incubated with the viral medium for 6 hours at 37°C at which point the medium was replaced with another pre-warmed aliquot of fresh viral medium which had been stored at 4°C. The MIO-M1 cells were incubated with the viral medium overnight at 37°C and the process was repeated twice the following day in the morning and evening.

After two days incubation of the MIO-M1 cells with viral medium this was removed and replaced with DMEM containing 10% FCS and 1% pen/strep and cells were cultured until they reached confluence. Cells were then split to 25% confluence and G418 and blasticidin were added to the media for selection of the transfected cells. The blasticidin allows selection of the MIO-M1 cells containing regulatory plasmid pcDNA4/TR and G418 selects for cells with plasmid pCLNCx backbone. At this stage cells were checked for lack of mCherry fluorescence under a digital inverted microscope, as the inducible promoter is “switched off” until tetracycline is added. Once a pure population of transfected cells was obtained some cells were frozen down for long term storage and the remaining cells were allowed to expand in culture.

7.13.2.5 Tetracycline induction of MIO-M1 cells containing pcDNA4/TR regulatory plasmid transfected with pCLNC-mCherry-GFAP-TO or control pCLNC-mCherry-TO vectors

Transfected cells were seeded onto 48 well-plates at 25% confluence and allowed to settle overnight in DMEM media. The next day the selection antibiotics blasticidin and G418 were added along with various concentrations of tetracycline. Final concentrations of tetracycline used were 0, 0.1, 0.5, 1, 2, 3, 4, 5, 6, 7, 8, 9 and 10µg/ml and cells were cultured for 8, 16, 24 and 76 hours. At each time point images were captured under a fluorescence digital inverted microscope to observe the mCherry fluorescence as the inducible promoter was “switched on” by tetracycline.

7.13.3 Co-transfection of MIO-M1 cells with the retroviral vectors pCLNC-TetR and pCLNC-mCherry-GFAP-TO or control vector pCLNC-mCherry-TO

7.13.3.1 Subcloning the tetracycline repressor (TetR) into pCLNCx

The TetR gene was cloned into the retroviral vector pCLNCx. Sequences either side of the TetR gene were also cloned to include the β-globin intron, the T7 promoter upstream and the SV40 poly(A) signal downstream. The restriction enzyme sites HindIII and ClaI in pCLNCx downstream of the CMV promoter were used to expose the cloning site. Cloning primers flanking the desired sequence in pcDNA4/TR were created containing 5'-HindIII and 3'-ClaI restriction sites. The forward primer created a HindIII site on amplification and the reverse primer created a ClaI site on amplification (see appendix 6). The pcDNA4/TR plasmid was used as a template to amplify the TetR gene sequence. Gel electrophoresis and gel extraction were performed as described above. Restriction enzyme digests of 2µg of amplified DNA and pCLNCx using HindIII and ClaI enzymes were obtained and the digested products separated on a 1% gel at 200V for 30 minutes. Bands of the correct size for the amplified TetR product and the digested pCLNCx were isolated and extracted from the gel as previously described. A ligation reaction of pCLNCx and the TetR product was set up overnight and subsequently transformed into deficient *dam-/dcm-* Competent E. coli. Verification and plasmid expansion were performed as described before using the restriction enzymes HindIII and ClaI. The newly created plasmid pCLNC-TetR DNA was stored at -20°C and glycerol stocks of bacterial cultures were stored at -80°C.

7.13.3.2 Retroviral co-transfection of MIO-M1 cells

The retroviral transfection protocol was performed identically as described above but GP2-293 packaging cells were separately transfected with pCLNC-mCherry-GFAP-TO, pCLNC-mCherry-TO or pCLNC-TetR. MIO-M1 cells at passage lower than p20 were seeded into 12-well plates at a concentration of $1X10^5$ per well. Cells were co-transfected with viral medium containing the pCLNC-TetR vector and pCLNC-mCherry-GFAP-TO vector or pCLNC-mCherry-TO control vector at various ratios (Table 6-1). After transfection cells were selected by using G418 and checked for mCherry fluorescence under a digital inverted microscope.

Ratio	pCLNC-TetR µl viral medium	pCLNC-mCherry-GFAP-TO **or** pCLNC-mCherry-TO µl viral medium
4:1	1000	250
6:1	1000	166.67
8:1	1000	125
10:1	1000	100
20:1	1000	50
50:1	1000	20
100:1	1000	10
200:1	1000	5
500:1	1000	2
1000:1	1000	1
Control	1000	0
Control	0	1000

Table 7-1: Volume (µl) of viral medium applied to MIO-M1 cells during co-transfection to achieve various ratios between constructed vectors.
Decreasing volumes of viral medium containing vector pCLNC-mCherry-GFAP-TO or pCLNC-mCherry-TO were applied to cells along with 1000µl of viral medium containing the pCLNC-TetR vector

.

7.13.3.3 Quantification of TetR gene expression compared to mCherry-GFAP and mCherry alone using qPCR

To quantify gene expression of the tetracycline regulator in comparison to mCherry-GFAP or mCherry gene under the TetO2 promoter, a two-step quantitative reverse transcription PCR was performed. RNA was isolated from transfected cells, reverse transcribed and subjected to qPCR as previously described. Primers for each gene were optimised prior to running the qPCR reactions (see appendix 2). RNA extracted from a canine kidney cell line stably transfected with pcDNA4/TR, a gift from Prof. Karl Matter, was used as a positive control to optimise the primers for the TetR gene. The calibrator sample was the RNA from MIO-M1 cells containing the pcDNA4/TR regulatory plasmid transfected with the pCLNC-mCherry-GFAP-TO vector or the control pCLNC-mCherry-TO vector. Ct values were analysed using the $\Delta\Delta$Ct method and

expression level of each gene compared to calibrator was calculated for each sample (different ratios of transfection).

7.13.3.4 Tetracycline induction of GFAP in MIO-M1 cells co-transfected with the pCLNC-TetR and pCLNC-mCherry-GFAP-TO or control pCLNC-mCherry-TO

The transfected cells were seeded onto 48 well-plates at 25% confluence and allowed to settle overnight in DMEM media supplemented with 10% FCS and G418. After 24 hours, various concentrations of tetracycline were added. Final concentrations of tetracycline used were 0, 0.5, 1 and 5µg/ml and cells were incubated for 8 and 24 hours. At each time point images were taken under a fluorescence digital inverted microscope to capture mCherry fluorescence. This was repeated three times for quantification; from each image, at least 100 cells were analysed and the number of mCherry positive cells within that representative sample were calculated.

7.13.4 Retroviral transfection of MIO-M1 cells with pCLNC-mCherry-GFAP

As the tetracycline-inducible promoter was not successfully working in the MIO-M1 cell line, the original pCLNC-mCherry-GFAP vector was used for transfection. However, the ratio of virus particles to cell number was altered to attempt the insertion of varying amounts of vector into cells to cause gradient GFAP overexpression. Retroviral transfection was performed as previously described above. The protocol was only altered in regards to the amount of viral medium, and therefore number of virus particles, that was applied to the MIO-M1 cells. For example, 100% transfection was achieved by addition of 5ml of viral medium to the T25 culture flask of confluent MIO-M1 cells, and 50% transfection was achieved by addition of 2.5ml of viral medium mixed with 2.5ml DMEM to the same size flask of MIO-M1 cells (Table 6-2).

After an initial gradient transfection, cells were grown to confluence and then sorted by FACS to obtain a pure population of transfected cells. FACS also allowed determination of the transfection efficiency by counting the mCherry positive cell numbers as well as the quantitation of mCherry fluorescence intensity of transfected cells. The mCherry fluorescence intensity gave indication of the amount of vector transfected and thus the relative quantity of GFAP gene expression. Cells selected by FACS were then grown to confluence

and expanded in G418 selection antibiotic to maintain a pure population. Transfection was repeated with a further two passages of MIO-M1 cells using 0%, 5%, 20%, 60% and 100% viral medium containing the pCLNC-mCherry-GFAP retroviral vector. A total of three passages were analysed through FACS for statistical analysis. Following expansion some cells were stored in freezing medium at -80°C and some were used for further experimental work. RNA and protein lysates were collected from transfected and untransfected control cells and RT-PCR and western blot were performed to measure mRNA and protein expression of GFAP in these cells.

Transfection with pCLNC-mCherry-GFAP (%)	ml of viral medium	ml of DMEM
100	5	0
90	4.5	0.5
80	4	1
70	3.5	1.5
60	3	2
50	2.5	2.5
40	2	3
30	1.5	3.5
20	1	4
10	0.5	4.5
5	0.25	4.75
0	0	5

Table 7-2: Volume (ml) of viral medium containing the pCLNC-mCherry-GFAP vector applied to MIO-M1 cells for transfection.
Decreasing volumes of viral medium were applied to cells to reduce the number of virus particles and reduce the amount of GFAP overexpression

Chapter 8 Bibliography

ADERKA, D., ENGELMANN, H., MAOR, Y., BRAKEBUSCH, C. & WALLACH, D. 1992. Stabilization of the bioactivity of tumor necrosis factor by its soluble receptors. *J Exp Med,* 175**,** 323-9.

AGARWAL, R. & AGARWAL, P. 2012. Glaucomatous neurodegeneration: An eye on tumor necrosis factor-alpha. *Indian Journal of Ophthalmology,* 60**,** 255-261.

AL-LAMKI, R. S., LU, W., WANG, J., YANG, J., SARGEANT, T. J., WELLS, R., SUO, C., WRIGHT, P., GODDARD, M., HUANG, Q., LEBASTCHI, A. H., TELLIDES, G., HUANG, Y., MIN, W., POBER, J. S. & BRADLEY, J. R. 2013. TNF, acting through inducibly expressed TNFR2, drives activation and cell cycle entry of c-Kit+ cardiac stem cells in ischemic heart disease. *STEM CELLS,* 31**,** 1881-1892.

ALBERT S. BALDWIN, J. 1996. THE NF-κB AND IκB PROTEINS: New Discoveries and Insights. *Annual Review of Immunology,* 14**,** 649-681.

ALEXOPOULOU, L., KRANIDIOTI, K., XANTHOULEA, S., DENIS, M., KOTANIDOU, A., DOUNI, E., BLACKSHEAR, P. J., KONTOYIANNIS, D. L. & KOLLIAS, G. 2006. Transmembrane TNF protects mutant mice against intracellular bacterial infections, chronic inflammation and autoimmunity. *European Journal of Immunology,* 36**,** 2768-2780.

ALGE, C. S., PRIGLINGER, S. G., KOOK, D., SCHMID, H., HARITOGLOU, C., WELGE-LUSSEN, U. & KAMPIK, A. 2006. Galectin-1 Influences Migration of Retinal Pigment Epithelial Cells. *Investigative Ophthalmology & Visual Science,* 47**,** 415-426.

ANDERSON, D. H., GUÉRIN, C. J., ERICKSON, P. A., STERN, W. H. & FISHER, S. K. 1986. Morphological recovery in the reattached retina. *Investigative Ophthalmology & Visual Science,* 27**,** 168-83.

ANGBOHANG, A., WU, N., CHARALAMBOUS, T., EASTLAKE, K., LEI, Y., KIM, Y. S., SUN, X. H. & LIMB, G. A. 2015. Downregulation of the Canonical WNT Signaling Pathway by TGFbeta1 Inhibits Photoreceptor Differentiation of Adult Human Muller Glia with Stem Cell Characteristics. *Stem Cells Dev*.

ARNETT, H. A., MASON, J., MARINO, M., SUZUKI, K., MATSUSHIMA, G. K. & TING, J. P. Y. 2001. TNFα promotes proliferation of oligodendrocyte progenitors and remyelination. *Nature Neuroscience,* 4**,** 1116.

BACIGALUPO, M. L., MANZI, M., RABINOVICH, G. A. & TRONCOSO, M. F. 2013. Hierarchical and selective roles of galectins in hepatocarcinogenesis, liver fibrosis and inflammation of hepatocellular carcinoma. *World J Gastroenterol,* 19**,** 8831-49.

BAE, M.-K., KIM, S.-R., LEE, H.-J., WEE, H.-J., YOO, M.-A., OCK OH, S., BAEK, S.-Y., KIM, B.-S., KIM, J.-B., SIK, Y. & BAE, S.-K. 2006. Aspirin-induced blockade of NF-κB activity restrains up-regulation of glial fibrillary acidic protein in human astroglial cells. *Biochimica et Biophysica Acta (BBA) - Molecular Cell Research,* 1763**,** 282-289.

BAILEY, T. J., FOSSUM, S. L., FIMBEL, S. M., MONTGOMERY, J. E. & HYDE, D. R. 2010. The inhibitor of phagocytosis, O-phospho-L-serine, suppresses Müller glia proliferation and cone cell regeneration in the light-damaged zebrafish retina. *Experimental eye research,* 91**,** 601-612.

BALLIOS, B. G., CLARKE, L., COLES, B. L. K., SHOICHET, M. S. & VAN DER KOOY, D. 2012. The adult retinal stem cell is a rare cell in the ciliary epithelium whose progeny can differentiate into photoreceptors. *Biology Open*.

BARKER, R. A. B., STEPHEN; NEAL, MICHAEL J. 1999. *Neuroscience at a Glance*, BLACKWELL SCIENCE LTD.

BEG, A. A. & BALTIMORE, D. 1996. An essential role for NF-kappaB in preventing TNF-alpha-induced cell death. *Science,* 274**,** 782-4.

BEG, A. A., SHA, W. C., BRONSON, R. T., GHOSH, S. & BALTIMORE, D. 1995. EMBRYONIC LETHALITY AND LIVER DEGENERATION IN MICE LACKING THE RELA COMPONENT OF NF-KAPPA-B. *Nature,* 376**,** 167-170.

BELECKY-ADAMS, T. L., CHERNOFF, E. C., WILSON, J. M. & DHARMARAJAN, S. 2013. Reactive Muller Glia as Potential Retinal Progenitors. *In:* BONFANTI, L. (ed.) *Neural Stem Cells - New Perspectives.* Rijeka: InTech.

BERNARDOS, R. L., BARTHEL, L. K., MEYERS, J. R. & RAYMOND, P. A. 2007. Late-Stage Neuronal Progenitors in the Retina Are Radial Müller Glia That Function as Retinal Stem Cells. *The Journal of Neuroscience,* 27**,** 7028-7040.

BESSA, T. F., CORDEIRO, C. A., GONÇALVES, R. M., YOUNG, L. H., CAMPOS, W. R., ORÉFICE, F. & TEIXEIRA, A. L. 2012. Increased serum levels of soluble tumor necrosis factor receptor-2 (sTNFR2) in patients with active toxoplasmic retinochoroiditis. *The Brazilian Journal of Infectious Diseases,* 16**,** 540-544.

BESSER, M., JAGATHEASWARAN, M., REINHARD, J., SCHAFFELKE, P. & FAISSNER, A. 2012. Tenascin C regulates proliferation and differentiation processes during embryonic retinogenesis and modulates the de-differentiation capacity of Müller glia by influencing growth factor responsiveness and the extracellular matrix compartment. *Developmental Biology,* 369**,** 163-176.

BHATIA, B., SINGHAL, S., LAWRENCE, J. M., KHAW, P. T. & LIMB, G. A. 2009. Distribution of Müller stem cells within the neural retina: Evidence for the existence of a ciliary margin-like zone in the adult human eye. *Experimental Eye Research,* 89**,** 373-382.

BHATIA, B., SINGHAL, S., TADMAN, D. N., KHAW, P. T. & LIMB, G. A. 2011. SOX2 Is Required for Adult Human Müller Stem Cell Survival and Maintenance of Progenicity In Vitro. *Investigative Ophthalmology & Visual Science,* 52**,** 136-145.

BHATTACHARYA, S., DAS, A. V., MALLYA, K. B. & AHMAD, I. 2008. Ciliary neurotrophic factor-mediated signaling regulates neuronal versus glial differentiation of retinal stem cells/progenitors by concentration-dependent recruitment of mitogen-activated protein kinase and Janus kinase-signal transducer and activator of transcription pathways in conjunction with Notch signaling. *STEM CELLS,* 26**,** 2611-24.

BRENNER, M., JOHNSON, A. B., BOESPFLUG-TANGUY, O., RODRIGUEZ, D., GOLDMAN, J. E. & MESSING, A. 2001. Mutations in GFAP, encoding glial fibrillary acidic protein, are associated with Alexander disease. *Nat Genet,* 27**,** 117-20.

BRINGMANN, A., IANDIEV, I., PANNICKE, T., WURM, A., HOLLBORN, M., WIEDEMANN, P., OSBORNE, N. N. & REICHENBACH, A. 2009. Cellular signaling and factors involved in Muller cell gliosis: neuroprotective and detrimental effects. *Prog Retin Eye Res,* 28**,** 423-51.

BRINGMANN, A., PANNICKE, T., GROSCHE, J., FRANCKE, M., WIEDEMANN, P., SKATCHKOV, S. N., OSBORNE, N. N. & REICHENBACH, A. 2006. Müller cells in the healthy and diseased retina. *Progress in Retinal and Eye Research,* 25**,** 397-424.

BRINGMANN, A. & REICHENBACH, A. 2001. Role of Muller cells in retinal degenerations. *Front Biosci,* 6**,** E72-92.

BROWN, D. M. & REGILLO, C. D. 2007. Anti-VEGF Agents in the Treatment of Neovascular Age-related Macular Degeneration: Applying Clinical Trial Results to the Treatment of Everyday Patients. *American Journal of Ophthalmology,* 144**,** 627-637.e2.

BROWN, K., GERSTBERGER, S., CARLSON, L., FRANZOSO, G. & SIEBENLIST, U. 1995. Control of I kappa B-alpha proteolysis by site-specific, signal-induced phosphorylation. *Science,* 267**,** 1485-1488.

BROWN, K., PARK, S., KANNO, T., FRANZOSO, G. & SIEBENLIST, U. 1993. Mutual regulation of the transcriptional activator NF-kappa B and its inhibitor, I kappa B-alpha. *Proceedings of the National Academy of Sciences,* 90**,** 2532-2536.

BURKE, J. M. & SMITH, J. M. 1981. Retinal proliferation in response to vitreous hemoglobin or iron. *Investigative Ophthalmology and Visual Science,* 20**,** 582-592.

BURMEISTER, M., NOVAK, J., LIANG, M.-Y., BASU, S., PLODER, L., HAWES, N. L., VIDGEN, D., HOOVER, F., GOLDMAN, D., KALNINS, V. I., RODERICK, T. H., TAYLOR, B. A., HANKIN, M. H. & MCLNNES, R. R. 1996. Ocular retardation mouse caused by Chx10 homeobox null allele: impaired retinal progenitor proliferation and bipolar cell differentiation. *Nat Genet,* 12**,** 376-384.

BUSH, T. G., PUVANACHANDRA, N., HORNER, C. H., POLITO, A., OSTENFELD, T., SVENDSEN, C. N., MUCKE, L., JOHNSON, M. H. & SOFRONIEW, M. V. 1999. Leukocyte Infiltration, Neuronal Degeneration, and Neurite Outgrowth after Ablation of Scar-Forming, Reactive Astrocytes in Adult Transgenic Mice. *Neuron,* 23**,** 297-308.

BYRNE, L. C., KHALID, F., LEE, T., ZIN, E. A., GREENBERG, K. P., VISEL, M., SCHAFFER, D. V. & FLANNERY, J. G. 2013. AAV-Mediated, Optogenetic Ablation of Müller Glia Leads to Structural and Functional Changes in the Mouse Retina. *PLoS ONE,* 8**,** e76075.

CAMBY, I., LE MERCIER, M., LEFRANC, F. & KISS, R. 2006. Galectin-1: a small protein with major functions. *Glycobiology,* 16**,** 137R-157R.

CAREY, I. & ZEHNER, Z. 1995. *Regulation of chicken vimentin gene expression by serum, phorbol ester, and growth factors: Identification of a novel fibroblast growth factor- inducible element*.

CASACCIA-BONNEFIL, P., GU, C. & CHAO, M. V. 1999. Neurotrophins in cell survival/death decisions. *Adv Exp Med Biol,* 468**,** 275-82.

CEPKO, C. L., AUSTIN, C. P., YANG, X., ALEXIADES, M. & EZZEDDINE, D. 1996. Cell fate determination in the vertebrate retina. *Proceedings of the National Academy of Sciences,* 93**,** 589-595.

CHANG, M.-L., WU, C.-H., JIANG-SHIEH, Y.-F., SHIEH, J.-Y. & WEN, C.-Y. 2007. Reactive changes of retinal astrocytes and Müller glial cells in kainate-induced neuroexcitotoxicity. *Journal of Anatomy,* 210**,** 54-65.

CHEN, J., JOON LEE, H., JAKOVCEVSKI, I., SHAH, R., BHAGAT, N., LOERS, G., LIU, H.-Y., MEINERS, S., TASCHENBERGER, G., KÜGLER, S., IRINTCHEV, A. & SCHACHNER, M. 2010. The Extracellular Matrix Glycoprotein Tenascin-C Is Beneficial for Spinal Cord Regeneration. *Molecular Therapy,* 18**,** 1769-1777.

CHEN, J., RATTNER, A. & NATHANS, J. 2005. The rod photoreceptor-specific nuclear receptor Nr2e3 represses transcription of multiple cone-specific genes. *J Neurosci,* 25**,** 118-29.

CHEN, K.-H., WU, C.-C., ROY, S., LEE, S.-M. & LIU, J.-H. 1999. Increased Interleukin-6 in Aqueous Humor of Neovascular Glaucoma. *Investigative Ophthalmology & Visual Science,* 40**,** 2627-2632.

CHEN, Z., HAGLER, J., PALOMBELLA, V. J., MELANDRI, F., SCHERER, D., BALLARD, D. & MANIATIS, T. 1995. Signal-induced site-specific phosphorylation targets I kappa B alpha to the ubiquitin-proteasome pathway. *Genes Dev,* 9**,** 1586-97.

CHERNOIVANENKO, I. S., MININ, A. A. & MININ, A. A. 2013. Role of vimentin in cell migration. *Russian Journal of Developmental Biology,* 44**,** 144-157.

CHIAO, P. J., MIYAMOTO, S. & VERMA, I. M. 1994. Autoregulation of I kappa B alpha activity. *Proceedings of the National Academy of Sciences,* 91**,** 28-32.

CHIU, F.-C. & GOLDMAN, J. E. 1984. Synthesis and Turnover of Cytoskeletal Proteins in Cultured Astrocytes. *Journal of Neurochemistry,* 42**,** 166-174.

CHO, W. & MESSING, A. 2009. Properties of astrocytes cultured from GFAP over-expressing and GFAP mutant mice. *Experimental Cell Research,* 315**,** 1260-1272.

COFFIN, J. M., HUGHES, S. H. & VARMOS, H. E. 1997. *Retroviruses,* Cold Spring Harbor (NY), Cold Spring Harbor Laboratory Press.

COHEN, I., SIVRON, T., LAVIE, V., BLAUGRUND, E. & SCHWARTZ, M. 1994. Vimentin immunoreactive glial cells in the fish optic nerve: implications for regeneration. *Glia,* 10**,** 16-29.

CONNER, C., ACKERMAN, K. M., LAHNE, M., HOBGOOD, J. S. & HYDE, D. R. 2014. Repressing Notch Signaling and Expressing TNFα Are Sufficient to Mimic Retinal Regeneration by Inducing Müller Glial Proliferation to Generate Committed Progenitor Cells. *The Journal of Neuroscience,* 34**,** 14403-14419.

COOREY, N. J., SHEN, W., CHUNG, S. H., ZHU, L. & GILLIES, M. C. 2012. The role of glia in retinal vascular disease. *Clinical and Experimental Optometry,* 95**,** 266-281.

CRAIG, S. E. L., THUMMEL, R., AHMED, H., VASTA, G. R., HYDE, D. R. & HITCHCOCK, P. F. 2010. The Zebrafish Galectin Drgal1-L2 Is Expressed by Proliferating Müller Glia and Photoreceptor Progenitors and Regulates the Regeneration of Rod Photoreceptors. *Investigative Ophthalmology & Visual Science,* 51**,** 3244-3252.

CUEVA VARGAS, J. L., OSSWALD, I. K., UNSAIN, N., AUROUSSEAU, M. R., BARKER, P. A., BOWIE, D. & DI POLO, A. 2015. Soluble Tumor Necrosis Factor Alpha Promotes Retinal Ganglion Cell Death in Glaucoma via Calcium-Permeable AMPA Receptor Activation. *The Journal of Neuroscience,* 35**,** 12088-12102.

DAHL, D. 1979. The radial glia of Müller in the rat retina and their response to injury. An immunofluorescence study with antibodies to the glial fibrillary acidic (GFA) protein. *Experimental Eye Research,* 28**,** 63-69.

DAS, A. V., MALLYA, K. B., ZHAO, X., AHMAD, F., BHATTACHARYA, S., THORESON, W. B., HEGDE, G. V. & AHMAD, I. 2006. Neural stem cell properties of Müller glia in the mammalian retina: Regulation by Notch and Wnt signaling. *Developmental Biology,* 299**,** 283-302.

DEL DEBBIO, C. B., BALASUBRAMANIAN, S., PARAMESWARAN, S., CHAUDHURI, A., QIU, F. & AHMAD, I. 2010. Notch and Wnt Signaling Mediated Rod Photoreceptor Regeneration by Müller Cells in Adult Mammalian Retina. *PLoS ONE,* 5**,** e12425.

DEMIRCAN, N., SAFRAN, B. G., SOYLU, M., OZCAN, A. A. & SIZMAZ, S. 2006. Determination of vitreous interleukin-1 (IL-1) and tumour necrosis factor (TNF) levels in proliferative diabetic retinopathy. *Eye (Lond),* 20**,** 1366-9.

DINARELLO, C. A. 2000. Proinflammatory Cytokines. *Chest,* 118**,** 503-508.

DUBOIS-DAUPHIN, M., POITRY-YAMATE, C., DE BILBAO, F., JULLIARD, A. K., JOURDAN, F. & DONATI, G. 1999. Early postnatal Müller cell death leads to retinal but not

optic nerve degeneration in NSE-Hu-Bcl-2 transgenic mice. *Neuroscience,* 95**,** 9-21.

DVORIANTCHIKOVA, G. & IVANOV, D. 2014. Tumor necrosis factor-alpha mediates activation of NF-κB and JNK signaling cascades in retinal ganglion cells and astrocytes in opposite ways. *European Journal of Neuroscience,* 40**,** 3171-3178.

DYER, M. A. 2003. Regulation of proliferation, cell fate specification and differentiation by the homeodomain proteins Prox1, Six3, and Chx10 in the developing retina. *Cell Cycle,* 2**,** 350-7.

DYER, M. A. & CEPKO, C. L. 2001. Regulating proliferation during retinal development. *Nat Rev Neurosci,* 2**,** 333-342.

EASTLAKE, K., BANERJEE, P. J., ANGBOHANG, A., CHARTERIS, D. G., KHAW, P. T. & LIMB, G. A. 2016. Muller glia as an important source of cytokines and inflammatory factors present in the gliotic retina during proliferative vitreoretinopathy. *Glia,* 64**,** 495-506.

EASTLAKE, K., HEYWOOD, W. E., TRACEY-WHITE, D., AQUINO, E., BLISS, E., VASTA, G. R., MILLS, K., KHAW, P. T., MOOSAJEE, M. & LIMB, G. A. 2017. Comparison of proteomic profiles in the zebrafish retina during experimental degeneration and regeneration. *Sci Rep,* 7**,** 44601.

ECKES, B., COLUCCI-GUYON, E., SMOLA, H., NODDER, S., BABINET, C., KRIEG, T. & MARTIN, P. 2000. Impaired wound healing in embryonic and adult mice lacking vimentin. *J Cell Sci,* 113 (Pt 13)**,** 2455-62.

ECKES, B., DOGIC, D., COLUCCI-GUYON, E., WANG, N., MANIOTIS, A., INGBER, D., MERCKLING, A., LANGA, F., AUMAILLEY, M., DELOUVEE, A., KOTELIANSKY, V., BABINET, C. & KRIEG, T. 1998. Impaired mechanical stability, migration and contractile capacity in vimentin-deficient fibroblasts. *J Cell Sci,* 111 (Pt 13)**,** 1897-907.

EDWARDS, M. M. & ROBINSON, S. R. 2006. TNF alpha affects the expression of GFAP and S100B: implications for Alzheimer's disease. *J Neural Transm,* 113**,** 1709-15.

EISENFELD, A. J., BUNT-MILAM, A. H. & SARTHY, P. V. 1984. Müller cell expression of glial fibrillary acidic protein after genetic and experimental photoreceptor degeneration in the rat retina. *Investigative Ophthalmology & Visual Science,* 25**,** 1321-8.

ENG, L. F., LEE, Y. L., KWAN, H., BRENNER, M. & MESSING, A. 1998. Astrocytes cultured from transgenic mice carrying the added human glial fibrillary acidic protein gene contain Rosenthal fibers. *J Neurosci Res,* 53**,** 353-60.

ERICKSON, P. A., FISHER, S. K., ANDERSON, D. H., STERN, W. H. & BORGULA, G. A. 1983. Retinal detachment in the cat: the outer nuclear and outer plexiform layers. *Investigative Ophthalmology & Visual Science,* 24**,** 927-42.

ERICKSON, P. A., FISHER, S. K., GUÉRIN, C. J., ANDERSON, D. H. & KASKA, D. D. 1987. Glial fibrillary acidic protein increases in Müller cells after retinal detachment. *Experimental Eye Research,* 44**,** 37-48.

FAISSNER, A., ROLL, L. & THEOCHARIDIS, U. 2017. Tenascin-C in the matrisome of neural stem and progenitor cells. *Molecular and Cellular Neuroscience,* 81**,** 22-31.

FAN, W., LIN, N., SHEEDLO, H. J. & TURNER, J. E. 1996. Muller and RPE cell response to photoreceptor cell degeneration in aging Fischer rats. *Exp Eye Res,* 63**,** 9-18.

FAULKNER, J. R., HERRMANN, J. E., WOO, M. J., TANSEY, K. E., DOAN, N. B. & SOFRONIEW, M. V. 2004. Reactive astrocytes protect tissue and preserve function after spinal cord injury. *J Neurosci,* 24**,** 2143-55.

FAUSETT, B. & GOLDMAN, D. 2006. A role for alpha1 tubulin-expressing Muller glia in regeneration of the injured zebrafish retina. *J Neurosci,* 26**,** 6303 - 6313.

FAUSETT, B. V., GUMERSON, J. D. & GOLDMAN, D. 2008. The Proneural Basic Helix-Loop-Helix Gene Ascl1a Is Required for Retina Regeneration. *The Journal of Neuroscience,* 28**,** 1109-1117.

FAUTSCH, M. P., SILVA, A. O. & JOHNSON, D. H. 2003. Carbohydrate binding proteins galectin-1 and galectin-3 in human trabecular meshwork. *Experimental Eye Research,* 77**,** 11-16.

FERNANDEZ-BUENO, I., GARCIA-GUTIERREZ, M. T., SRIVASTAVA, G. K., GAYOSO, M. J., GONZALO-ORDEN, J. M. & PASTOR, J. C. 2013. Adalimumab (tumor necrosis factor-blocker) reduces the expression of glial fibrillary acidic protein immunoreactivity increased by exogenous tumor necrosis factor alpha in an organotypic culture of porcine neuroretina. *Mol Vis,* 19**,** 894-903.

FIMBEL, S. M., MONTGOMERY, J. E., BURKET, C. T. & HYDE, D. R. 2007. Regeneration of Inner Retinal Neurons after Intravitreal Injection of Ouabain in Zebrafish. *The Journal of Neuroscience,* 27**,** 1712-1724.

FINCO, T. S. & BALDWIN, A. S. 1995. Mechanistic aspects of NF-κB regulation: The emerging role of phosphorylation and proteolysis. *Immunity,* 3**,** 263-272.

FISCHER, A. J. 2005. Neural regeneration in the chick retina. *Progress in Retinal and Eye Research,* 24**,** 161-182.

FISCHER, A. J. & BONGINI, R. 2010. Turning Müller Glia into Neural Progenitors in the Retina. *Molecular Neurobiology,* 42**,** 199-209.

FISCHER, A. J., MCGUIRE, C. R., DIERKS, B. D. & REH, T. A. 2002. Insulin and Fibroblast Growth Factor 2 Activate a Neurogenic Program in Müller Glia of the Chicken Retina. *The Journal of Neuroscience,* 22**,** 9387-9398.

FISCHER, A. J. & REH, T. A. 2001. Muller glia are a potential source of neural regeneration in the postnatal chicken retina. *Nat Neurosci,* 4**,** 247-252.

FISCHER, A. J. & REH, T. A. 2002. Exogenous growth factors stimulate the regeneration of ganglion cells in the chicken retina. *Dev Biol,* 251**,** 367-79.

FISCHER, A. J. & REH, T. A. 2003. Potential of Müller glia to become neurogenic retinal progenitor cells. *Glia,* 43**,** 70-76.

FISCHER, A. J., SCOTT, M. A. & TUTEN, W. 2009. Mitogen-activated protein kinase-signaling stimulates Müller glia to proliferate in acutely damaged chicken retina. *Glia,* 57**,** 166-181.

FISCHER, A. J., ZELINKA, C., GALLINA, D., SCOTT, M. A. & TODD, L. 2014. Reactive microglia and macrophage facilitate the formation of Muller glia-derived retinal progenitors. *Glia,* 62**,** 1608-28.

FISHER, S. K., ERICKSON, P. A., LEWIS, G. P. & ANDERSON, D. H. 1991. Intraretinal proliferation induced by retinal detachment. *Investigative Ophthalmology & Visual Science,* 32**,** 1739-48.

FISHER, S. K. & LEWIS, G. P. 2003. Müller cell and neuronal remodeling in retinal detachment and reattachment and their potential consequences for visual recovery: a review and reconsideration of recent data. *Vision research,* 43**,** 887-897.

FLANAGAN, L. A., JU, Y.-E., MARG, B., OSTERFIELD, M. & JANMEY, P. A. 2002. Neurite branching on deformable substrates. *Neuroreport,* 13**,** 2411-2415.

FONTAINE, V., KINKL, N., SAHEL, J., DREYFUS, H. & HICKS, D. 1998. Survival of purified rat photoreceptors in vitro is stimulated directly by fibroblast growth factor-2. *J Neurosci,* 18**,** 9662-72.

FONTAINE, V., MOHAND-SAID, S., HANOTEAU, N., FUCHS, C., PFIZENMAIER, K. & EISEL, U. 2002. Neurodegenerative and neuroprotective effects of tumor Necrosis factor (TNF) in retinal ischemia: opposite roles of TNF receptor 1 and TNF receptor 2. *J Neurosci,* 22**,** Rc216.

FRANCKE, M., FAUDE, F., PANNICKE, T., UCKERMANN, O., WEICK, M., WOLBURG, H., WIEDEMANN, P., REICHENBACH, A., UHLMANN, S. & BRINGMANN, A. 2005. Glial cell-mediated spread of retinal degeneration during detachment: a hypothesis based upon studies in rabbits. *Vision Res,* 45**,** 2256-67.

FRANKS, W. A., LIMB, G. A., STANFORD, M. R., OGILVIE, J., WOLSTENCROFT, R. A., CHIGNELL, A. H. & DUMONDE, D. C. 1992. Cytokines in human intraocular inflammation. *Current Eye Research,* 11**,** 187-191.

FRANTZ, C., STEWART, K. M. & WEAVER, V. M. 2010. The extracellular matrix at a glance. *Journal of Cell Science,* 123**,** 4195-4200.

FRANZE, K., GROSCHE, J., SKATCHKOV, S. N., SCHINKINGER, S., FOJA, C., SCHILD, D., UCKERMANN, O., TRAVIS, K., REICHENBACH, A. & GUCK, J. 2007. Müller cells are living optical fibers in the vertebrate retina. *Proceedings of the National Academy of Sciences,* 104**,** 8287-8292.

FRASSON, M., PICAUD, S., LEVEILLARD, T., SIMONUTTI, M., MOHAND-SAID, S., DREYFUS, H., HICKS, D. & SABEL, J. 1999. Glial cell line-derived neurotrophic factor induces histologic and functional protection of rod photoreceptors in the rd/rd mouse. *Invest Ophthalmol Vis Sci,* 40**,** 2724-34.

FURUKAWA, T., MORROW, E. M., LI, T., DAVIS, F. C. & CEPKO, C. L. 1999. Retinopathy and attenuated circadian entrainment in Crx-deficient mice. *Nat Genet,* 23**,** 466-470.

FURUKAWA, T., MUKHERJEE, S., BAO, Z. Z., MORROW, E. M. & CEPKO, C. L. 2000. rax, Hes1, and notch1 promote the formation of Muller glia by postnatal retinal progenitor cells. *Neuron,* 26**,** 383-94.

GALLINA, D., TODD, L. & FISCHER, A. J. 2014. A comparative analysis of Müller glia-mediated regeneration in the vertebrate retina. *Experimental Eye Research,* 123**,** 121-130.

GHANEM AA, A. L., ELEWA AM 2010. Tumor Necrosis Factor-α and Interleukin-6 Levels in Patients with Primary Open-Angle Glaucoma. *J Clinic Experiment Ophthalmol*.

GILLES, C., POLETTE, M., MESTDAGT, M., NAWROCKI-RABY, B., RUGGERI, P., BIREMBAUT, P. & FOIDART, J. M. 2003. Transactivation of vimentin by beta-catenin in human breast cancer cells. *Cancer Res,* 63**,** 2658-64.

GOLDMAN, D. 2014. Muller glial cell reprogramming and retina regeneration. *Nat Rev Neurosci,* 15**,** 431-442.

GOMES, F. C., PAULIN, D. & MOURA NETO, V. 1999. Glial fibrillary acidic protein (GFAP): modulation by growth factors and its implication in astrocyte differentiation. *Braz J Med Biol Res,* 32**,** 619-31.

GOSSEN, M. & BUJARD, H. 1992. Tight control of gene expression in mammalian cells by tetracycline-responsive promoters. *Proceedings of the National Academy of Sciences of the United States of America,* 89**,** 5547-5551.

GOUREAU, O., AMIOT, F., DAUTRY, F. & COURTOIS, Y. 1997. Control of Nitric Oxide Production by Endogenous TNF-α in Mouse Retinal Pigmented Epithelial and Muller Glial Cells. *Biochemical and Biophysical Research Communications,* 240**,** 132-135.

GOUREAU, O., RHEE, K. D. & YANG, X. J. 2004. Ciliary neurotrophic factor promotes muller glia differentiation from the postnatal retinal progenitor pool. *Dev Neurosci,* 26**,** 359-70.

GRAF, T., FLAMMER, J., PRUNTE, C. & HENDRICKSON, P. 1993. Gliosis-like retinal alterations in glaucoma patients. *J Glaucoma,* 2**,** 257-9.

GRELL, M., DOUNI, E., WAJANT, H., LOHDEN, M., CLAUSS, M., MAXEINER, B., GEORGOPOULOS, S., LESSLAUER, W., KOLLIAS, G., PFIZENMAIER, K. & SCHEURICH, P. 1995. The transmembrane form of tumor necrosis factor is the prime activating ligand of the 80 kDa tumor necrosis factor receptor. *Cell,* 83**,** 793-802.

GRELL, M., WAJANT, H., ZIMMERMANN, G. & SCHEURICH, P. 1998. The type 1 receptor (CD120a) is the high-affinity receptor for soluble tumor necrosis factor. *Proc Natl Acad Sci U S A,* 95**,** 570-5.

HAGEMANN, T. L., CONNOR, J. X. & MESSING, A. 2006. Alexander Disease-Associated Glial Fibrillary Acidic Protein Mutations in Mice Induce Rosenthal Fiber Formation and a White Matter Stress Response. *The Journal of Neuroscience,* 26**,** 11162-11173.

HARADA, T., HARADA, C., NAKAYAMA, N., OKUYAMA, S., YOSHIDA, K., KOHSAKA, S., MATSUDA, H. & WADA, K. 2000. Modification of glial-neuronal cell interactions prevents photoreceptor apoptosis during light-induced retinal degeneration. *Neuron,* 26**,** 533-41.

HATAKEYAMA, J. & KAGEYAMA, R. 2004. Retinal cell fate determination and bHLH factors. *Semin Cell Dev Biol,* 15**,** 83-9.

HATAKEYAMA, J., TOMITA, K., INOUE, T. & KAGEYAMA, R. 2001. Roles of homeobox and bHLH genes in specification of a retinal cell type. *Development,* 128**,** 1313-1322.

HAUCK, S. M., SUPPMANN, S. & UEFFING, M. 2003. Proteomic profiling of primary retinal Müller glia cells reveals a shift in expression patterns upon adaptation to in vitro conditions. *Glia,* 44**,** 251-263.

HAYES, S., NELSON, B. R., BUCKINGHAM, B. & REH, T. A. 2007. Notch signaling regulates regeneration in the avian retina. *Developmental Biology,* 312**,** 300-311.

HENDRICKSON, A., BUMSTED-O'BRIEN, K., NATOLI, R., RAMAMURTHY, V., POSSIN, D. & PROVIS, J. 2008. Rod photoreceptor differentiation in fetal and infant human retina. *Experimental Eye Research,* 87**,** 415-426.

HISATOMI, T., SAKAMOTO, T., YAMANAKA, I., SASSA, Y., KUBOTA, T., UENO, H., OHNISHI, Y. & ISHIBASHI, T. 2002. Photocoagulation-Induced Retinal Gliosis Is Inhibited by Systemically Expressed Soluble TGF-[bgr] Receptor Type II via Adenovirus Mediated Gene Transfer. *Lab Invest,* 82**,** 863-870.

HOERSTER, R., MUETHER, P. S., VIERKOTTEN, S., HERMANN, M. M., KIRCHHOF, B. & FAUSER, S. 2014. Upregulation of TGF-ss1 in experimental proliferative vitreoretinopathy is accompanied by epithelial to mesenchymal transition. *Graefes Arch Clin Exp Ophthalmol,* 252**,** 11-6.

HOLLBORN, M., FRANCKE, M., IANDIEV, I., BÜHNER, E., FOJA, C., KOHEN, L., REICHENBACH, A., WIEDEMANN, P., BRINGMANN, A. & UHLMANN, S. 2008. Early Activation of Inflammation- and Immune Response-Related Genes after Experimental Detachment of the Porcine Retina. *Investigative Ophthalmology & Visual Science,* 49**,** 1262-1273.

HOLLEY, J. E., GVERIC, D., WHATMORE, J. L. & GUTOWSKI, N. J. 2005. Tenascin C induces a quiescent phenotype in cultured adult human astrocytes. *Glia,* 52**,** 53-58.

HOLTKAMP, G. M., KIJLSTRA, A., PEEK, R. & DE VOS, A. F. 2001. Retinal Pigment Epithelium-immune System Interactions: Cytokine Production and Cytokine-induced Changes. *Progress in Retinal and Eye Research,* 20**,** 29-48.

HORIUCHI, T., MITOMA, H., HARASHIMA, S.-I., TSUKAMOTO, H. & SHIMODA, T. 2010. Transmembrane TNF-α: structure, function and interaction with anti-TNF agents. *Rheumatology (Oxford, England),* 49**,** 1215-1228.

IGARASHI, Y., CHIBA, H., UTSUMI, H., MIYAJIMA, H., ISHIZAKI, T., GOTOH, T., KUWAHARA, K., TOBIOKA, H., SATOH, M., MORI, M. & SAWADA, N. 2000. Expression of receptors for glial cell line-derived neurotrophic factor (GDNF) and neurturin in the inner blood-retinal barrier of rats. *Cell Struct Funct,* 25**,** 237-41.

IKESHIMA-KATAOKA, H., SHEN, J. S., ETO, Y., SAITO, S. & YUASA, S. 2008. Alteration of inflammatory cytokine production in the injured central nervous system of tenascin-deficient mice. *In Vivo,* 22**,** 409-13.

INMAN, D. M. & HORNER, P. J. 2007. Reactive nonproliferative gliosis predominates in a chronic mouse model of glaucoma. *Glia,* 55**,** 942-953.

IOACHIM, E., STEFANIOTOU, M., GOREZIS, S., TSANOU, E., PSILAS, K. & AGNANTIS, N. J. 2005. Immunohistochemical study of extracellular matrix components in epiretinal membranes of vitreoproliferative retinopathy and proliferative diabetic retinopathy. *Eur J Ophthalmol,* 15**,** 384-91.

ITO, K., STANNARD, K., GABUTERO, E., CLARK, A., NEO, S.-Y., ONTURK, S., BLANCHARD, H. & RALPH, S. 2012. Galectin-1 as a potent target for cancer therapy: role in the tumor microenvironment. *Cancer and Metastasis Reviews,* 31**,** 763-778.

IZUMI, Y., SHIMAMOTO, K., BENZ, A. M., HAMMERMAN, S. B., OLNEY, J. W. & ZORUMSKI, C. F. 2002. Glutamate transporters and retinal excitotoxicity. *Glia,* 39**,** 58-68.

JADHAV, A. P., MASON, H. A. & CEPKO, C. L. 2006. Notch 1 inhibits photoreceptor production in the developing mammalian retina. *Development,* 133**,** 913-23.

JADHAV, A. P., ROESCH, K. & CEPKO, C. L. 2009. Development and neurogenic potential of Muller glial cells in the vertebrate retina. *Prog Retin Eye Res,* 28**,** 249-62.

JAKOVCEVSKI, I., MILJKOVIC, D., SCHACHNER, M. & ANDJUS, P. R. 2013. Tenascins and inflammation in disorders of the nervous system. *Amino Acids,* 44**,** 1115-1127.

JANY, P. L., HAGEMANN, T. L. & MESSING, A. 2013. GFAP Expression as an Indicator of Disease Severity in Mouse Models of Alexander Disease. *ASN Neuro,* 5.

JAYARAM, H., BECKER, S. & LIMB, G. A. 2011. *Stem Cell Based Therapies for Glaucoma*.

JAYARAM, H., JONES, M. F., EASTLAKE, K., COTTRILL, P. B., BECKER, S., WISEMAN, J., KHAW, P. T. & LIMB, G. A. 2014. Transplantation of Photoreceptors Derived From Human Müller Glia Restore Rod Function in the P23H Rat. *Stem Cells Translational Medicine,* 3**,** 323-333.

JIN LIM, M., AHN, J., YOUN YI, J., KIM, M.-H., SON, A. R., LEE, S.-L.-O., LIM, D.-S., SOO KIM, S., AE KANG, M., HAN, Y. & SONG, J.-Y. 2014. Induction of galectin-1 by TGF-β1 accelerates fibrosis through enhancing nuclear retention of Smad2. *Experimental Cell Research,* 326**,** 125-135.

JOHNSON, E. C., JIA, L., CEPURNA, W. O., DOSER, T. A. & MORRISON, J. C. 2007. Global Changes in Optic Nerve Head Gene Expression after Exposure to Elevated

Intraocular Pressure in a Rat Glaucoma Model. *Investigative ophthalmology & visual science,* 48**,** 3161-3177.

JOHNSON, T. V. & MARTIN, K. R. 2008. Development and Characterization of an Adult Retinal Explant Organotypic Tissue Culture System as an In Vitro Intraocular Stem Cell Transplantation Model. *Investigative Ophthalmology & Visual Science,* 49**,** 3503-3512.

JONES, B. W., WATT, C. B., FREDERICK, J. M., BAEHR, W., CHEN, C.-K., LEVINE, E. M., MILAM, A. H., LAVAIL, M. M. & MARC, R. E. 2003. Retinal remodeling triggered by photoreceptor degenerations. *The Journal of Comparative Neurology,* 464**,** 1-16.

KANG, S. M., TRAN, A. C., GRILLI, M. & LENARDO, M. J. 1992. NF-kappa B subunit regulation in nontransformed CD4+ T lymphocytes. *Science,* 256**,** 1452-6.

KARL, M. O., HAYES, S., NELSON, B. R., TAN, K., BUCKINGHAM, B. & REH, T. A. 2008. Stimulation of neural regeneration in the mouse retina. *Proceedings of the National Academy of Sciences,* 105**,** 19508-19513.

KASSEN, S. C., RAMANAN, V., MONTGOMERY, J. E., T. BURKET, C., LIU, C.-G., VIHTELIC, T. S. & HYDE, D. R. 2007. Time course analysis of gene expression during light-induced photoreceptor cell death and regeneration in albino zebrafish. *Developmental Neurobiology,* 67**,** 1009-1031.

KASSEN, S. C., THUMMEL, R., CAMPOCHIARO, L. A., HARDING, M. J., BENNETT, N. A. & HYDE, D. R. 2009. CNTF induces photoreceptor neuroprotection and Müller glial cell proliferation through two different signaling pathways in the adult zebrafish retina. *Experimental Eye Research,* 88**,** 1051-1064.

KIM, S. J., JIN, J., KIM, Y. J., KIM, Y. & YU, H. G. 2012. Retinal Proteome Analysis in a Mouse Model of Oxygen-Induced Retinopathy. *Journal of Proteome Research,* 11**,** 5186-5203.

KINOUCHI, R., TAKEDA, M., YANG, L., WILHELMSSON, U., LUNDKVIST, A., PEKNY, M. & CHEN, D. F. 2003. Robust neural integration from retinal transplants in mice deficient in GFAP and vimentin. *Nature Neuroscience,* 6**,** 863.

KIRSCH, M., LEE, M.-Y., MEYER, V., WIESE, A. & HOFMANN, H.-D. 1997. Evidence for Multiple, Local Functions of Ciliary Neurotrophic Factor (CNTF) in Retinal Development: Expression of CNTF and Its Receptor and In Vitro Effects on Target Cells. *Journal of Neurochemistry,* 68**,** 979-990.

KLAUSMEYER, A., GARWOOD, J. & FAISSNER, A. 2007. Differential expression of phosphacan/RPTPβ isoforms in the developing mouse visual system. *The Journal of Comparative Neurology,* 504**,** 659-679.

KOHNO, K., HAMANAKA, R., ABE, T., NOMURA, Y., MORIMOTO, A., IZUMI, H., SHIMIZU, K., ONO, M. & KUWANO, M. 1993. Morphological change and destabilization of beta-actin mRNA by tumor necrosis factor in human microvascular endothelial cells. *Exp Cell Res,* 208**,** 498-503.

KOIKE, C., NISHIDA, A., UENO, S., SAITO, H., SANUKI, R., SATO, S., FURUKAWA, A., AIZAWA, S., MATSUO, I., SUZUKI, N., KONDO, M. & FURUKAWA, T. 2007. Functional Roles of Otx2 Transcription Factor in Postnatal Mouse Retinal Development. *Molecular and Cellular Biology,* 27**,** 8318-8329.

KOLB, H., NELSON, R., AHNELT, P. & CUENCA, N. 2001. Chapter 1 Cellular organization of the vertebrate retina. *In:* HELGA KOLB, H. R. S. W. H. K. S. M.-S. W. J. E. D. (ed.) *Progress in Brain Research.* Elsevier.

KROHN, K., ROZOVSKY, I., WALS, P., TETER, B., ANDERSON, C. P. & FINCH, C. E. 1999. Glial Fibrillary Acidic Protein Transcription Responses to Transforming Growth

Factor-β1 and Interleukin-1β Are Mediated by a Nuclear Factor-1-Like Site in the Near-Upstream Promoter. *Journal of Neurochemistry,* 72**,** 1353-1361.
KUMAR, A., PANDEY, R. K., MILLER, L. J., SINGH, P. K. & KANWAR, M. 2013. Müller Glia in Retinal Innate Immunity: A perspective on their roles in endophthalmitis. *Critical reviews in immunology,* 33**,** 119-135.
KUMAR, A. & SHAMSUDDIN, N. 2012. Retinal Muller Glia Initiate Innate Response to Infectious Stimuli via Toll-Like Receptor Signaling. *PLoS ONE,* 7**,** e29830.
KUO, H.-K., CHEN, Y.-H., WU, P.-C., WU, Y.-C., HUANG, F., KUO, C.-W., LO, L.-H. & SHIEA, J. 2012. Attenuated Glial Reaction in Experimental Proliferative Vitreoretinopathy Treated with Liposomal Doxorubicin. *Investigative Ophthalmology & Visual Science,* 53**,** 3167-3174.
KUZMANOVIC, M., DUDLEY, V. J. & SARTHY, V. P. 2003. GFAP Promoter Drives Müller Cell–Specific Expression in Transgenic Mice. *Investigative Ophthalmology & Visual Science,* 44**,** 3606-3613.
LAHMAR, I., PFAFF, A. W., MARCELLIN, L., SAUER, A., MOUSSA, A., BABBA, H. & CANDOLFI, E. 2014. Müller cell activation and photoreceptor depletion in a mice model of congenital ocular toxoplasmosis. *Experimental Parasitology,* 144**,** 22-26.
LANDEGREN, U. 1984. Measurement of cell numbers by means of the endogenous enzyme hexosaminidase. Applications to detection of lymphokines and cell surface antigens. *J Immunol Methods,* 67**,** 379-88.
LANGMANN, T. 2007. Microglia activation in retinal degeneration. *J Leukoc Biol,* 81**,** 1345-51.
LAPING, N. J., MORGAN, T. E., NICHOLS, N. R., ROZOVSKY, I., YOUNG-CHAN, C. S., ZAROW, C. & FINCH, C. E. 1994. Transforming growth factor-β1 induces neuronal and astrocyte genes: Tubulin α1, glial fibrillary acidic protein and clusterin. *Neuroscience,* 58**,** 563-572.
LAVAIL, M. M., UNOKI, K., YASUMURA, D., MATTHES, M. T., YANCOPOULOS, G. D. & STEINBERG, R. H. 1992. Multiple growth factors, cytokines, and neurotrophins rescue photoreceptors from the damaging effects of constant light. *Proceedings of the National Academy of Sciences of the United States of America,* 89**,** 11249-11253.
LAWRENCE, J. M., SINGHAL, S., BHATIA, B., KEEGAN, D. J., REH, T. A., LUTHERT, P. J., KHAW, P. T. & LIMB, G. A. 2007. MIO-M1 Cells and Similar Müller Glial Cell Lines Derived from Adult Human Retina Exhibit Neural Stem Cell Characteristics. *STEM CELLS,* 25**,** 2033-2043.
LEBRUN-JULIEN, F., DUPLAN, L., PERNET, V., OSSWALD, I., SAPIEHA, P., BOURGEOIS, P., DICKSON, K., BOWIE, D., BARKER, P. A. & DI POLO, A. 2009. Excitotoxic Death of Retinal Neurons In Vivo Occurs via a Non-Cell-Autonomous Mechanism. *The Journal of Neuroscience,* 29**,** 5536-5545.
LEE, Y., MESSING, A., SU, M. & BRENNER, M. 2008. GFAP promoter elements required for region-specific and astrocyte-specific expression. *Glia,* 56**,** 481-493.
LENDAHL, U., ZIMMERMAN, L. B. & MCKAY, R. D. 1990. CNS stem cells express a new class of intermediate filament protein. *Cell,* 60**,** 585-95.
LENKOWSKI, J. R., QIN, Z., SIFUENTES, C. J., THUMMEL, R., SOTO, C. M., MOENS, C. B. & RAYMOND, P. A. 2013. Retinal regeneration in adult zebrafish requires regulation of TGFβ signaling. *Glia,* 61**,** 1687-1697.
LENKOWSKI, J. R. & RAYMOND, P. A. 2014. Muller glia: Stem cells for generation and regeneration of retinal neurons in teleost fish. *Prog Retin Eye Res,* 40**,** 94-123.

LEVINE, E. M., ROELINK, H., TURNER, J. & REH, T. A. 1997. Sonic Hedgehog Promotes Rod Photoreceptor Differentiation in Mammalian Retinal Cells In Vitro. *The Journal of Neuroscience,* 17**,** 6277-6288.

LEWIS, G. & FISHER, S. 2003. Up-regulation of glial fibrillary acidic protein in response to retinal injury: its potential role in glial remodeling and a comparison to vimentin expression. *Int Rev Cytol,* 230**,** 263 - 290.

LEWIS, G. P. & FISHER, S. K. 2000. Müller Cell Outgrowth after Retinal Detachment: Association with Cone Photoreceptors. *Investigative Ophthalmology & Visual Science,* 41**,** 1542-1545.

LEWIS, G. P., MATSUMOTO, B. & FISHER, S. K. 1995. Changes in the organization and expression of cytoskeletal proteins during retinal degeneration induced by retinal detachment. *Investigative Ophthalmology & Visual Science,* 36**,** 2404-16.

LIETH, E., BARBER, A. J., XU, B., DICE, C., RATZ, M. J., TANASE, D. & STROTHER, J. M. 1998. Glial reactivity and impaired glutamate metabolism in short-term experimental diabetic retinopathy. Penn State Retina Research Group. *Diabetes,* 47**,** 815-820.

LILLIEN, L. 1995. Changes in retinal cell fate induced by overexpression of EGF receptor. *Nature,* 377**,** 158-62.

LIMB, G. A., ALAM, A., EARLEY, O., GREEN, W., CHIGNELL, A. H. & DUMONDE, D. C. 1994a. Distribution of cytokine proteins within epiretinal membranes in proliferative vitreoretinopathy. *Curr Eye Res,* 13**,** 791-8.

LIMB, G. A., CHIGNELL, A. H., GREEN, W., LEROY, F. & DUMONDE, D. C. 1996. Distribution of TNF alpha and its reactive vascular adhesion molecules in fibrovascular membranes of proliferative diabetic retinopathy. *Br J Ophthalmol,* 80**,** 168-73.

LIMB, G. A., EARLEY, O., JONES, S. E., LEROY, F., CHIGNELL, A. H. & DUMONDE, D. C. 1994b. Expression of mRNA coding for TNF alpha, IL-1 beta and IL-6 by cells infiltrating retinal membranes. *Graefes Arch Clin Exp Ophthalmol,* 232**,** 646-51.

LIMB, G. A., SALT, T. E., MUNRO, P. M., MOSS, S. E. & KHAW, P. T. 2002. In vitro characterization of a spontaneously immortalized human Muller cell line (MIO-M1). *Invest Ophthalmol Vis Sci,* 43**,** 864-9.

LIMB, G. A., SOOMRO, H., JANIKOUN, S., HOLLIFIELD, R. D. & SHILLING, J. 1999. Evidence for control of tumour necrosis factor-alpha (TNF-alpha) activity by TNF receptors in patients with proliferative diabetic retinopathy. *Clin Exp Immunol,* 115**,** 409-14.

LIN, Y.-P., OUCHI, Y., SATOH, S. & WATANABE, S. 2009. Sox2 Plays a Role in the Induction of Amacrine and Müller Glial Cells in Mouse Retinal Progenitor Cells. *Investigative Ophthalmology & Visual Science,* 50**,** 68-74.

LITTLE, A. R., BENKOVIC, S. A., MILLER, D. B. & O'CALLAGHAN, J. P. 2002. Chemically induced neuronal damage and gliosis: enhanced expression of the proinflammatory chemokine, monocyte chemoattractant protein (MCP)-1, without a corresponding increase in proinflammatory cytokines1. *Neuroscience,* 115**,** 307-320.

LIU, F.-T., PATTERSON, R. J. & WANG, J. L. 2002. Intracellular functions of galectins. *Biochimica et Biophysica Acta (BBA) - General Subjects,* 1572**,** 263-273.

LÖFFLER, K., SCHÄFER, P., VÖLKNER, M., HOLDT, T. & KARL, M. O. 2015. Age-dependent Müller glia neurogenic competence in the mouse retina. *Glia,* 63**,** 1809-1824.

LORBER, B., GUIDI, A., FAWCETT, J. W. & MARTIN, K. R. 2012. Activated retinal glia mediated axon regeneration in experimental glaucoma. *Neurobiol Dis,* 45**,** 243-52.

LU, Y.-B., FRANZE, K., SEIFERT, G., STEINHÄUSER, C., KIRCHHOFF, F., WOLBURG, H., GUCK, J., JANMEY, P., WEI, E.-Q., KÄS, J. & REICHENBACH, A. 2006. Viscoelastic properties of individual glial cells and neurons in the CNS. *Proceedings of the National Academy of Sciences of the United States of America,* 103**,** 17759-17764.

LU, Y.-B., IANDIEV, I., HOLLBORN, M., KÖRBER, N., ULBRICHT, E., HIRRLINGER, P. G., PANNICKE, T., WEI, E.-Q., BRINGMANN, A., WOLBURG, H., WILHELMSSON, U., PEKNY, M., WIEDEMANN, P., REICHENBACH, A. & KÄS, J. A. 2011. Reactive glial cells: increased stiffness correlates with increased intermediate filament expression. *The FASEB Journal,* 25**,** 624-631.

LUO, C., YANG, X., KAIN, A. D., POWELL, D. W., KUEHN, M. H. & TEZEL, G. 2010. Glaucomatous Tissue Stress and the Regulation of Immune Response through Glial Toll-like Receptor Signaling. *Investigative Ophthalmology & Visual Science,* 51**,** 5697-5707.

LUPIEN, C., BRENNER, M., GUÉRIN, S. L. & SALESSE, C. 2004. Expression of glial fibrillary acidic protein in primary cultures of human Müller cells. *Experimental Eye Research,* 79**,** 423-429.

MAC NAIR, C. E., FERNANDES, K. A., SCHLAMP, C. L., LIBBY, R. T. & NICKELLS, R. W. 2014. Tumor necrosis factor alpha has an early protective effect on retinal ganglion cells after optic nerve crush. *Journal of Neuroinflammation,* 11**,** 194.

MACHOLD, R., HAYASHI, S., RUTLIN, M., MUZUMDAR, M. D., NERY, S., CORBIN, J. G., GRITLI-LINDE, A., DELLOVADE, T., PORTER, J. A., RUBIN, L. L., DUDEK, H., MCMAHON, A. P. & FISHELL, G. 2003. Sonic Hedgehog Is Required for Progenitor Cell Maintenance in Telencephalic Stem Cell Niches. *Neuron,* 39**,** 937-950.

MACLAREN, R. E., PEARSON, R. A., MACNEIL, A., DOUGLAS, R. H., SALT, T. E., AKIMOTO, M., SWAROOP, A., SOWDEN, J. C. & ALI, R. R. 2006. Retinal repair by transplantation of photoreceptor precursors. *Nature,* 444**,** 203-207.

MAIER, P., VON KALLE, C. & LAUFS, S. 2010. Retroviral vectors for gene therapy. *Future Microbiol,* 5**,** 1507-23.

MAKRIDES, S. C. 2003. *Gene Transfer and Expression in Mammalian Cells*.

MARQUARDT, T., ASHERY-PADAN, R., ANDREJEWSKI, N., SCARDIGLI, R., GUILLEMOT, F. & GRUSS, P. 2001. Pax6 is required for the multipotent state of retinal progenitor cells. *Cell,* 105**,** 43 - 55.

MARTÍNEZ-FERNÁNDEZ DE LA CÁMARA, C., OLIVARES-GONZÁLEZ, L., HERVÁS, D., SALOM, D., MILLÁN, J. M. & RODRIGO, R. 2014. Infliximab reduces Zaprinast-induced retinal degeneration in cultures of porcine retina. *Journal of Neuroinflammation,* 11**,** 172.

MCCOY, M. K. & TANSEY, M. G. 2008. TNF signaling inhibition in the CNS: implications for normal brain function and neurodegenerative disease. *Journal of Neuroinflammation,* 5**,** 45.

MCGILLEM, G. S., GUIDRY, C. & DACHEUX, R. F. 1998. Antigenic changes of rabbit retinal Müller cells in culture. *Investigative Ophthalmology & Visual Science,* 39**,** 1453-1461.

MCKEON, R., SCHREIBER, R., RUDGE, J. & SILVER, J. 1991. Reduction of neurite outgrowth in a model of glial scarring following CNS injury is correlated with

the expression of inhibitory molecules on reactive astrocytes. *The Journal of Neuroscience,* 11**,** 3398-3411.

MCMAHON, P. J., PANCZYKOWSKI, D. M., YUE, J. K., PUCCIO, A. M., INOUE, T., SORANI, M. D., LINGSMA, H. F., MAAS, A. I. R., VALADKA, A. B., YUH, E. L., MUKHERJEE, P., MANLEY, G. T., OKONKWO, D. O., CASEY, S. S., CHEONG, M., COOPER, S. R., DAMS-O'CONNOR, K., GORDON, W. A., HRICIK, A. J., LAWLESS, K., MENON, D., SCHNYER, D. M. & VASSAR, M. J. 2014. Measurement of the Glial Fibrillary Acidic Protein and Its Breakdown Products GFAP-BDP Biomarker for the Detection of Traumatic Brain Injury Compared to Computed Tomography and Magnetic Resonance Imaging. *Journal of Neurotrauma,* 32**,** 527-533.

MEARS, A. J., KONDO, M., SWAIN, P. K., TAKADA, Y., BUSH, R. A., SAUNDERS, T. L., SIEVING, P. A. & SWAROOP, A. 2001. Nrl is required for rod photoreceptor development. *Nat Genet,* 29**,** 447-452.

MENET, V., GIMENEZ Y RIBOTTA, M., CHAUVET, N., DRIAN, M. J., LANNOY, J., COLUCCI-GUYON, E. & PRIVAT, A. 2001. Inactivation of the glial fibrillary acidic protein gene, but not that of vimentin, improves neuronal survival and neurite growth by modifying adhesion molecule expression. *J Neurosci,* 21**,** 6147-58.

MESSING, A. & BRENNER, M. 2003. GFAP: Functional implications gleaned from studies of genetically engineered mice. *Glia,* 43**,** 87-90.

MESSING, A., HEAD, M. W., GALLES, K., GALBREATH, E. J., GOLDMAN, J. E. & BRENNER, M. 1998. Fatal encephalopathy with astrocyte inclusions in GFAP transgenic mice. *Am J Pathol,* 152**,** 391-8.

MEYERS, J. R., HU, L., MOSES, A., KABOLI, K., PAPANDREA, A. & RAYMOND, P. A. 2012. beta-catenin/Wnt signaling controls progenitor fate in the developing and regenerating zebrafish retina. *Neural Dev,* 7**,** 30.

MIDDELDORP, J. & HOL, E. M. 2011. GFAP in health and disease. *Progress in Neurobiology,* 93**,** 421-443.

MUETHER, P. S., NEUHANN, I., BUHL, C., HERMANN, M. M., KIRCHHOF, B. & FAUSER, S. 2013. Intraocular growth factors and cytokines in patients with dry and neovascular age-related macular degeneration. *Retina,* 33**,** 1809-14.

MUTO, A., IIDA, A., SATOH, S. & WATANABE, S. 2009. The group E Sox genes Sox8 and Sox9 are regulated by Notch signaling and are required for Müller glial cell development in mouse retina. *Experimental Eye Research,* 89**,** 549-558.

NAKAYAMA, K., ISHIDA, N., SHIRANE, M., INOMATA, A., INOUE, T., SHISHIDO, N., HORII, I. & LOH, D. Y. 1996. Mice lacking p27(Kip1) display increased body size, multiple organ hyperplasia, retinal dysplasia, and pituitary tumors. *Cell,* 85**,** 707-20.

NAKAZAWA, T., HISATOMI, T., NAKAZAWA, C., NODA, K., MARUYAMA, K., SHE, H., MATSUBARA, A., MIYAHARA, S., NAKAO, S., YIN, Y., BENOWITZ, L., HAFEZI-MOGHADAM, A. & MILLER, J. W. 2007a. Monocyte chemoattractant protein 1 mediates retinal detachment-induced photoreceptor apoptosis. *Proceedings of the National Academy of Sciences,* 104**,** 2425-2430.

NAKAZAWA, T., MATSUBARA, A., NODA, K., HISATOMI, T., SHE, H., SKONDRA, D., MIYAHARA, S., SOBRIN, L., THOMAS, K. L., CHEN, D. F., GROSSKREUTZ, C. L., HAFEZI-MOGHADAM, A. & MILLER, J. W. 2006a. Characterization of cytokine responses to retinal detachment in rats. *Mol Vis,* 12**,** 867-878.

NAKAZAWA, T., NAKAZAWA, C., MATSUBARA, A., NODA, K., HISATOMI, T., SHE, H., MICHAUD, N., HAFEZI-MOGHADAM, A., MILLER, J. W. & BENOWITZ, L. I. 2006b. Tumor Necrosis Factor-α Mediates Oligodendrocyte Death and Delayed Retinal

Ganglion Cell Loss in a Mouse Model of Glaucoma. *The Journal of Neuroscience,* 26**,** 12633-12641.

NAKAZAWA, T., TAKEDA, M., LEWIS, G. P., CHO, K.-S., JIAO, J., WILHELMSSON, U., FISHER, S. K., PEKNY, M., CHEN, D. F. & MILLER, J. W. 2007b. Attenuated Glial Reactions and Photoreceptor Degeneration after Retinal Detachment in Mice Deficient in Glial Fibrillary Acidic Protein and Vimentin. *Investigative Ophthalmology & Visual Science,* 48**,** 2760-2768.

NASSAR, K., GRISANTI, S., TURA, A., LÜKE, J., LÜKE, M., SOLIMAN, M. & GRISANTI, S. 2014. A TGF-β receptor 1 inhibitor for prevention of proliferative vitreoretinopathy. *Experimental Eye Research,* 123**,** 72-86.

NATARAJAN, K., SINGH, S., BURKE, T. R., JR., GRUNBERGER, D. & AGGARWAL, B. B. 1996. Caffeic acid phenethyl ester is a potent and specific inhibitor of activation of nuclear transcription factor NF-kappa B. *Proc Natl Acad Sci U S A,* 93**,** 9090-5.

NELSON, C. M., ACKERMAN, K. M., O'HAYER, P., BAILEY, T. J., GORSUCH, R. A. & HYDE, D. R. 2013. Tumor necrosis factor-alpha is produced by dying retinal neurons and is required for Muller glia proliferation during zebrafish retinal regeneration. *J Neurosci,* 33**,** 6524-39.

NELSON, C. M., GORSUCH, R. A., BAILEY, T. J., ACKERMAN, K. M., KASSEN, S. C. & HYDE, D. R. 2012. Stat3 defines three populations of müller glia and is required for initiating maximal müller glia proliferation in the regenerating zebrafish retina. *The Journal of Comparative Neurology,* 520**,** 4294-4311.

NG, L., HURLEY, J. B., DIERKS, B., SRINIVAS, M., SALTO, C., VENNSTROM, B., REH, T. A. & FORREST, D. 2001. A thyroid hormone receptor that is required for the development of green cone photoreceptors. *Nat Genet,* 27**,** 94-98.

NG, L., MA, M., CURRAN, T. & FORREST, D. 2009. Developmental expression of thyroid hormone receptor β2 protein in cone photoreceptors in the mouse. *Neuroreport,* 20**,** 627-631.

NISHI, Y., SANO, H., KAWASHIMA, T., OKADA, T., KURODA, T., KIKKAWA, K., KAWASHIMA, S., TANABE, M., GOTO, T., MATSUZAWA, Y., MATSUMURA, R., TOMIOKA, H., LIU, F. T. & SHIRAI, K. 2007. Role of galectin-3 in human pulmonary fibrosis. *Allergol Int,* 56**,** 57-65.

NISHIDA, A., FURUKAWA, A., KOIKE, C., TANO, Y., AIZAWA, S., MATSUO, I. & FURUKAWA, T. 2003. Otx2 homeobox gene controls retinal photoreceptor cell fate and pineal gland development. *Nat Neurosci,* 6**,** 1255-1263.

O'BRIEN, K. M. B., CHENG, H., JIANG, Y., SCHULTE, D., SWAROOP, A. & HENDRICKSON, A. E. 2004. Expression of Photoreceptor-Specific Nuclear Receptor NR2E3 in Rod Photoreceptors of Fetal Human Retina. *Investigative Ophthalmology & Visual Science,* 45**,** 2807-2812.

OH, E. C. T., CHENG, H., HAO, H., JIA, L., KHAN, N. W. & SWAROOP, A. 2008. Rod differentiation factor NRL activates the expression of nuclear receptor NR2E3 to suppress the development of cone photoreceptors. *Brain Research,* 1236**,** 16-29.

OH, E. C. T., KHAN, N., NOVELLI, E., KHANNA, H., STRETTOI, E. & SWAROOP, A. 2007. Transformation of cone precursors to functional rod photoreceptors by bZIP transcription factor NRL. *Proceedings of the National Academy of Sciences,* 104**,** 1679-1684.

OH, Y. J., MARKELONIS, G. J. & OH, T. H. 1993. Effects of interleukin-1β and tumor necrosis factor-α on the expression of glial fibrillary acidic protein and transferrin in cultured astrocytes. *Glia,* 8**,** 77-86.

OHNUMA, S., PHILPOTT, A., WANG, K., HOLT, C. E. & HARRIS, W. A. 1999. p27Xic1, a Cdk inhibitor, promotes the determination of glial cells in Xenopus retina. *Cell,* 99**,** 499-510.

OKADA, M., MATSUMURA, M., OGINO, N. & HONDA, Y. 1990. Müller cells in detached human retina express glial fibrillary acidic protein and vimentin. *Graefe's Archive for Clinical and Experimental Ophthalmology,* 228**,** 467-474.

OKANO, K., TSURUTA, Y., YAMASHITA, T., TAKANO, M., ECHIDA, Y. & NITTA, K. 2010. Suppression of renal fibrosis by galectin-1 in high glucose-treated renal epithelial cells. *Exp Cell Res,* 316**,** 3282-91.

OOTO, S., AKAGI, T., KAGEYAMA, R., AKITA, J., MANDAI, M., HONDA, Y. & TAKAHASHI, M. 2004. Potential for neural regeneration after neurotoxic injury in the adult mammalian retina. *Proc Natl Acad Sci USA,* 101**,** 13654 - 13659.

OSAKADA, F., OOTO, S., AKAGI, T., MANDAI, M., AKAIKE, A. & TAKAHASHI, M. 2007. Wnt signaling promotes regeneration in the retina of adult mammals. *J Neurosci,* 27**,** 4210 - 4219.

PATEL, J. R., WILLIAMS, J. L., MUCCIGROSSO, M. M., LIU, L., SUN, T., RUBIN, J. B. & KLEIN, R. S. 2012. Astrocyte TNFR2 is required for CXCL12-mediated regulation of oligodendrocyte progenitor proliferation and differentiation within the adult CNS. *Acta Neuropathologica,* 124**,** 847-860.

PEKNY, M. 2001. Astrocytic intermediate filaments: lessons from GFAP and vimentin knock-out mice. *Progress in Brain Research.* Elsevier.

PEKNY, M., ELIASSON, C., CHIEN, C. L., KINDBLOM, L. G., LIEM, R., HAMBERGER, A. & BETSHOLTZ, C. 1998. GFAP-deficient astrocytes are capable of stellation in vitro when cocultured with neurons and exhibit a reduced amount of intermediate filaments and an increased cell saturation density. *Exp Cell Res,* 239**,** 332-43.

PEKNY, M., JOHANSSON, C. B., ELIASSON, C., STAKEBERG, J., WALLÉN, Å., PERLMANN, T., LENDAHL, U., BETSHOLTZ, C., BERTHOLD, C.-H. & FRISÉN, J. 1999. Abnormal Reaction to Central Nervous System Injury in Mice Lacking Glial Fibrillary Acidic Protein and Vimentin. *The Journal of Cell Biology,* 145**,** 503-514.

PENA, J. D., VARELA, H. J., RICARD, C. S. & HERNANDEZ, M. R. 1999a. Enhanced tenascin expression associated with reactive astrocytes in human optic nerve heads with primary open angle glaucoma. *Exp Eye Res,* 68**,** 29-40.

PENA, J. D. O., TAYLOR, A. W., RICARD, C. S., VIDAL, I. & HERNANDEZ, M. R. 1999b. Transforming growth factor β isoforms in human optic nerve heads. *British Journal of Ophthalmology,* 83**,** 209-218.

PITTLER, S. J., ZHANG, Y., CHEN, S., MEARS, A. J., ZACK, D. J., REN, Z., SWAIN, P. K., YAO, S., SWAROOP, A. & WHITE, J. B. 2004. Functional Analysis of the Rod Photoreceptor cGMP Phosphodiesterase α-Subunit Gene Promoter: Nrl AND Crx ARE REQUIRED FOR FULL TRANSCRIPTIONAL ACTIVITY. *Journal of Biological Chemistry,* 279**,** 19800-19807.

POCHE, R. A., FURUTA, Y., CHABOISSIER, M. C., SCHEDL, A. & BEHRINGER, R. R. 2008. Sox9 is expressed in mouse multipotent retinal progenitor cells and functions in Muller glial cell development. *J Comp Neurol,* 510**,** 237-50.

POGUE, A. I., CUI, J. G., LI, Y. Y., ZHAO, Y., CULICCHIA, F. & LUKIW, W. J. 2010. Micro RNA-125b (miRNA-125b) function in astrogliosis and glial cell proliferation. *Neuroscience Letters,* 476**,** 18-22.

POW, D. V. & CROOK, D. K. 1996. Direct immunocytochemical evidence for the transfer of glutamine from glial cells to neurons: Use of specific antibodies directed

against thed-stereoisomers of glutamate and glutamine. *Neuroscience,* 70**,** 295-302.
PRELICH, G. 2012. Gene Overexpression: Uses, Mechanisms, and Interpretation. *Genetics,* 190**,** 841-854.
PRENDES, M. A., HARRIS, A., WIROSTKO, B. M., GERBER, A. L. & SIESKY, B. 2013. The role of transforming growth factor β in glaucoma and the therapeutic implications. *British Journal of Ophthalmology,* 97**,** 680-686.
QU, Y., ZHAO, G. & LI, H. 2017. Forward and Reverse Signaling Mediated by Transmembrane Tumor Necrosis Factor-Alpha and TNF Receptor 2: Potential Roles in an Immunosuppressive Tumor Microenvironment. *Frontiers in Immunology,* 8**,** 1675.
RAMACHANDRAN, R., ZHAO, X. F. & GOLDMAN, D. 2011. Ascl1a/Dkk/beta-catenin signaling pathway is necessary and glycogen synthase kinase-3beta inhibition is sufficient for zebrafish retina regeneration. *Proc Natl Acad Sci U S A,* 108**,** 15858-63.
RAPAPORT, D. H., WONG, L. L., WOOD, E. D., YASUMURA, D. & LAVAIL, M. M. 2004. Timing and topography of cell genesis in the rat retina. *The Journal of Comparative Neurology,* 474**,** 304-324.
RAYMOND, P., BARTHEL, L., BERNARDOS, R. & PERKOWSKI, J. 2006. Molecular characterization of retinal stem cells and their niches in adult zebrafish. *BMC Developmental Biology,* 6**,** 36.
REESE, B. E. 2011. Development of the Retina and Optic Pathway. *Vision research,* 51**,** 613-632.
REICHENBACH, A. & BRINGMANN, A. 2010. *Müller Cells in the Healthy and Diseased Retina,* New York, Dordrecht, Heidelberg, London, Springer.
REICHENBACH, A. & BRINGMANN, A. 2013. New functions of Muller cells. *Glia,* 61**,** 651-78.
REINEHR, S., REINHARD, J., WIEMANN, S., STUTE, G., KUEHN, S., WOESTMANN, J., DICK, H. B., FAISSNER, A. & JOACHIM, S. C. 2016. Early remodelling of the extracellular matrix proteins tenascin-C and phosphacan in retina and optic nerve of an experimental autoimmune glaucoma model. *Journal of Cellular and Molecular Medicine,* 20**,** 2122-2137.
REINHARD, J., JOACHIM, S. C. & FAISSNER, A. 2015. Extracellular matrix remodeling during retinal development. *Exp Eye Res,* 133**,** 132-40.
REINHARD, J., ROLL, L. & FAISSNER, A. 2017. Tenascins in Retinal and Optic Nerve Neurodegeneration. *Frontiers in Integrative Neuroscience,* 11**,** 30.
RHEE, K. D., GOUREAU, O., CHEN, S. & YANG, X. J. 2004. Cytokine-induced activation of signal transducer and activator of transcription in photoreceptor precursors regulates rod differentiation in the developing mouse retina. *J Neurosci,* 24**,** 9779-88.
RHEE, K. D., NUSINOWITZ, S., CHAO, K., YU, F., BOK, D. & YANG, X.-J. 2013. CNTF-mediated protection of photoreceptors requires initial activation of the cytokine receptor gp130 in Müller glial cells. *Proceedings of the National Academy of Sciences of the United States of America,* 110**,** E4520-E4529.
RHEE, K. D. & YANG, X.-J. 2010. Function and Mechanism of CNTF/LIF Signaling in Retinogenesis. *Advances in experimental medicine and biology,* 664**,** 647-654.
ROBERTSON, J. V., GOLESIC, E., GAULDIE, J. & WEST-MAYS, J. A. 2010. Ocular Gene Transfer of Active TGF-β Induces Changes in Anterior Segment Morphology and

Elevated IOP in Rats. *Investigative Ophthalmology & Visual Science,* 51**,** 308-318.

ROBITAILLE, J., MACDONALD, M. L. E., KAYKAS, A., SHELDAHL, L. C., ZEISLER, J., DUBE, M.-P., ZHANG, L.-H., SINGARAJA, R. R., GUERNSEY, D. L., ZHENG, B., SIEBERT, L. F., HOSKIN-MOTT, A., TRESE, M. T., PIMSTONE, S. N., SHASTRY, B. S., MOON, R. T., HAYDEN, M. R., GOLDBERG, Y. P. & SAMUELS, M. E. 2002. Mutant frizzled-4 disrupts retinal angiogenesis in familial exudative vitreoretinopathy. *Nat Genet,* 32**,** 326-330.

ROMO, P., MADIGAN, M. C., PROVIS, J. M. & CULLEN, K. M. 2011. Differential effects of TGF-beta and FGF-2 on in vitro proliferation and migration of primate retinal endothelial and Muller cells. *Acta Ophthalmol,* 89**,** e263-8.

ROZOVSKY, I., WEI, M., MORGAN, T. E. & FINCH, C. E. 2005. Reversible age impairments in neurite outgrowth by manipulations of astrocytic GFAP. *Neurobiology of Aging,* 26**,** 705-715.

RUNGGER-BRANDLE, E., DOSSO, A. A. & LEUENBERGER, P. M. 2000. Glial reactivity, an early feature of diabetic retinopathy. *Invest Ophthalmol Vis Sci,* 41**,** 1971-80.

RUTKA, J. T., HUBBARD, S. L., FUKUYAMA, K., MATSUZAWA, K., DIRKS, P. B. & BECKER, L. E. 1994. Effects of antisense glial fibrillary acidic protein complementary DNA on the growth, invasion, and adhesion of human astrocytoma cells. *Cancer Res,* 54**,** 3267-72.

SAKAGUCHI, M., SHINGO, T., SHIMAZAKI, T., OKANO, H. J., SHIWA, M., ISHIBASHI, S., OGURO, H., NINOMIYA, M., KADOYA, T., HORIE, H., SHIBUYA, A., MIZUSAWA, H., POIRIER, F., NAKAUCHI, H., SAWAMOTO, K. & OKANO, H. 2006. A carbohydrate-binding protein, Galectin-1, promotes proliferation of adult neural stem cells. *Proceedings of the National Academy of Sciences,* 103**,** 7112-7117.

SANKAR GHOSH, MICHAEL J. MAY, A. & KOPP, E. B. 1998. NF-κB AND REL PROTEINS: Evolutionarily Conserved Mediators of Immune Responses. *Annual Review of Immunology,* 16**,** 225-260.

SARTHY, P. V. & FU, M. 1989. Transcriptional Activation of an Intermediate Filament Protein Gene in Mice with Retinal Dystrophy. *DNA,* 8**,** 437-446.

SARTHY, V. 2007. Focus on Molecules: Glial fibrillary acidic protein (GFAP). *Experimental Eye Research,* 84**,** 381-382.

SARTHY, V. & EGAL, H. 1995. Transient induction of the glial intermediate filament protein gene in Muller cells in the mouse retina. *DNA Cell Biol,* 14**,** 313-20.

SARTHY, V. P., PIGNATARO, L., PANNICKE, T., WEICK, M., REICHENBACH, A., HARADA, T., TANAKA, K. & MARC, R. 2005. Glutamate transport by retinal Müller cells in glutamate/aspartate transporter-knockout mice. *Glia,* 49**,** 184-196.

SASAKI, T., HIRABAYASHI, J., MANYA, H., KASAI, K.-I. & ENDO, T. 2004. Galectin-1 induces astrocyte differentiation, which leads to production of brain-derived neurotrophic factor. *Glycobiology,* 14**,** 357-363.

SCHELLER, J., CHALARIS, A., SCHMIDT-ARRAS, D. & ROSE-JOHN, S. 2011. The pro- and anti-inflammatory properties of the cytokine interleukin-6. *Biochimica et Biophysica Acta (BBA) - Molecular Cell Research,* 1813**,** 878-888.

SCHÜTTE, M. & WERNER, P. 1998. Redistribution of glutathione in the ischemic rat retina. *Neuroscience Letters,* 246**,** 53-56.

SEDGER, L. M. & MCDERMOTT, M. F. 2014. TNF and TNF-receptors: From mediators of cell death and inflammation to therapeutic giants – past, present and future. *Cytokine & Growth Factor Reviews,* 25**,** 453-472.

SELMAJ, K., SHAFIT-ZAGARDO, B., AQUINO, D. A., FAROOQ, M., RAINE, C. S., NORTON, W. T. & BROSNAN, C. F. 1991. Tumor necrosis factor-induced proliferation of astrocytes from mature brain is associated with down-regulation of glial fibrillary acidic protein mRNA. *J Neurochem,* 57**,** 823-30.

SETHI, C. S., LEWIS, G. P., FISHER, S. K., LEITNER, W. P., MANN, D. L., LUTHERT, P. J. & CHARTERIS, D. G. 2005. Glial Remodeling and Neural Plasticity in Human Retinal Detachment with Proliferative Vitreoretinopathy. *Investigative Ophthalmology & Visual Science,* 46**,** 329-342.

SHASTRY, B. S. 1995. Overexpression of genes in health and sickness. A bird's eye view. *Comparative Biochemistry and Physiology Part B: Biochemistry and Molecular Biology,* 112**,** 1-13.

SHEN, W., FRUTTIGER, M., ZHU, L., CHUNG, S. H., BARNETT, N. L., KIRK, J. K., LEE, S., COOREY, N. J., KILLINGSWORTH, M., SHERMAN, L. S. & GILLIES, M. C. 2012. Conditional Mullercell ablation causes independent neuronal and vascular pathologies in a novel transgenic model. *J Neurosci,* 32**,** 15715-27.

SHEN, W., LI, S., CHUNG, S. H. & GILLIES, M. C. 2010. Retinal vascular changes after glial disruption in rats. *J Neurosci Res,* 88**,** 1485-99.

SHOHAMI, E., GINIS, I. & HALLENBECK, J. M. 1999. Dual role of tumor necrosis factor alpha in brain injury. *Cytokine & Growth Factor Reviews,* 10**,** 119-130.

SIDDIQUI, S., HORVAT-BROECKER, A. & FAISSNER, A. 2009. Comparative screening of glial cell types reveals extracellular matrix that inhibits retinal axon growth in a chondroitinase ABC-resistant fashion. *Glia,* 57**,** 1420-1438.

SIMS, S. M., HOLMGREN, L., CATHCART, H. M. & SAPPINGTON, R. M. 2012. Spatial regulation of interleukin-6 signaling in response to neurodegenerative stressors in the retina. *American Journal of Neurodegenerative Disease,* 1**,** 168-179.

SINGHAL, S., BHATIA, B., JAYARAM, H., BECKER, S., JONES, M. F., COTTRILL, P. B., KHAW, P. T., SALT, T. E. & LIMB, G. A. 2012. Human Müller Glia with Stem Cell Characteristics Differentiate into Retinal Ganglion Cell (RGC) Precursors In Vitro and Partially Restore RGC Function In Vivo Following Transplantation. *Stem Cells Translational Medicine,* 1**,** 188-199.

SINGHAL, S., LAWRENCE, J. M., BHATIA, B., ELLIS, J. S., KWAN, A. S., MACNEIL, A., LUTHERT, P. J., FAWCETT, J. W., PEREZ, M.-T., KHAW, P. T. & LIMB, G. A. 2008. Chondroitin Sulfate Proteoglycans and Microglia Prevent Migration and Integration of Grafted Müller Stem Cells into Degenerating Retina. *STEM CELLS,* 26**,** 1074-1082.

SMETANA, K., JR., SZABO, P., GAL, P., ANDRE, S., GABIUS, H. J., KODET, O. & DVORANKOVA, B. 2015. *Emerging role of tissue lectins as microenvironmental effectors in tumors and wounds*, Histol Histopathol. 2014 Oct 13.

SMITH, G. M. & HALE, J. H. 1997. Macrophage/Microglia regulation of astrocytic tenascin: synergistic action of transforming growth factor-beta and basic fibroblast growth factor. *J Neurosci,* 17**,** 9624-33.

SMITH, S. B., BRODJIAN, S., DESAI, S. & SARTHY, V. 1997. *Glial fibrillary acidic protein (GFAP) is synthesized in the early stages of the photoreceptor cell degeneration of the mivit/mivit (vitiligo) mouse*, Exp Eye Res. 1997 Apr;64(4):645-50.

SOFRONIEW, M. V. 2015a. Astrocyte barriers to neurotoxic inflammation. *Nat Rev Neurosci,* 16**,** 249-263.

SOFRONIEW, M. V. 2015b. Astrogliosis. *Cold Spring Harbor Perspectives in Biology,* 7.

SPIRA, A. W. & HOLLENBERG, M. J. 1973. Human retinal development: Ultrastructure of the inner retinal layers. *Developmental Biology,* 31**,** 1-21.

SRINIVAS, M., NG, L., LIU, H., JIA, L. & FORREST, D. 2006. Activation of the blue opsin gene in cone photoreceptor development by retinoid-related orphan receptor beta. *Mol Endocrinol,* 20**,** 1728-41.

SURZENKO, N., CROWL, T., BACHLEDA, A., LANGER, L. & PEVNY, L. 2013. SOX2 maintains the quiescent progenitor cell state of postnatal retinal Muller glia. *Development,* 140**,** 1445-56.

SWAROOP, A., KIM, D. & FORREST, D. 2010. Transcriptional regulation of photoreceptor development and homeostasis in the mammalian retina. *Nat Rev Neurosci,* 11**,** 563-576.

SWINNEY, D. C., XU, Y. Z., SCARAFIA, L. E., LEE, I., MAK, A. Y., GAN, Q. F., RAMESHA, C. S., MULKINS, M. A., DUNN, J., SO, O. Y., BIEGEL, T., DINH, M., VOLKEL, P., BARNETT, J., DALRYMPLE, S. A., LEE, S. & HUBER, M. 2002. A small molecule ubiquitination inhibitor blocks NF-kappa B-dependent cytokine expression in cells and rats. *J Biol Chem,* 277**,** 23573-81.

TANAKA, K. F., TAKEBAYASHI, H., YAMAZAKI, Y., ONO, K., NARUSE, M., IWASATO, T., ITOHARA, S., KATO, H. & IKENAKA, K. 2007. Murine model of Alexander disease: Analysis of GFAP aggregate formation and its pathological significance. *Glia,* 55**,** 617-631.

TANG, G., XU, Z. & GOLDMAN, J. E. 2006. Synergistic Effects of the SAPK/JNK and the Proteasome Pathway on Glial Fibrillary Acidic Protein (GFAP) Accumulation in Alexander Disease. *Journal of Biological Chemistry,* 281**,** 38634-38643.

TANG, G., YUE, Z., TALLOCZY, Z., HAGEMANN, T., CHO, W., MESSING, A., SULZER, D. L. & GOLDMAN, J. E. 2008. Autophagy induced by Alexander disease-mutant GFAP accumulation is regulated by p38/MAPK and mTOR signaling pathways. *Human Molecular Genetics,* 17**,** 1540-1555.

TEZEL, G. 2008. TNF-alpha signaling in glaucomatous neurodegeneration. *Prog Brain Res,* 173**,** 409-21.

TEZEL, G., LI, L. Y., PATIL, R. V. & WAX, M. B. 2001. TNF-α and TNF-α Receptor-1 in the Retina of Normal and Glaucomatous Eyes. *Investigative Ophthalmology & Visual Science,* 42**,** 1787-1794.

TEZEL, G. & WAX, M. B. 2000. Increased production of tumor necrosis factor-alpha by glial cells exposed to simulated ischemia or elevated hydrostatic pressure induces apoptosis in cocultured retinal ganglion cells. *J Neurosci,* 20**,** 8693-700.

TEZEL, G., YANG, X., YANG, J. & WAX, M. B. 2004. Role of tumor necrosis factor receptor-1 in the death of retinal ganglion cells following optic nerve crush injury in mice. *Brain Research,* 996**,** 202-212.

THOMAS, J. L., RANSKI, A. H., MORGAN, G. W. & THUMMEL, R. 2016. Reactive gliosis in the adult zebrafish retina. *Experimental Eye Research,* 143**,** 98-109.

THOMPSON, J. E., PHILLIPS, R. J., ERDJUMENT-BROMAGE, H., TEMPST, P. & GHOSH, S. 1995. IκB-β regulates the persistent response in a biphasic activation of NF-κB. *Cell,* 80**,** 573-582.

TO, M., GOZ, A., CAMENZIND, L., OERTLE, P., CANDIELLO, J., SULLIVAN, M., HENRICH, P. B., LOPARIC, M., SAFI, F., ELLER, A. & HALFTER, W. 2013. Diabetes-induced morphological, biomechanical, and compositional changes in ocular basement membranes. *Exp Eye Res,* 116**,** 298-307.

TODA, M., MIURA, M., ASOU, H., SUGIYAMA, I., KAWASE, T. & UYEMURA, K. 1999. Suppression of Glial Tumor Growth by Expression of Glial Fibrillary Acidic Protein. *Neurochemical Research,* 24**,** 339-343.

TODA, M., MIURA, M., ASOU, H., TOYA, S. & UYEMURA, K. 1994. Cell Growth Suppression of Astrocytoma C6 Cells by Glial Fibrillary Acidic Protein cDNA Transfection. *Journal of Neurochemistry,* 63**,** 1975-1978.

TOOPS, K. A., HAGEMANN, T. L., MESSING, A. & NICKELLS, R. W. 2012. The effect of glial fibrillary acidic protein expression on neurite outgrowth from retinal explants in a permissive environment. *BMC Research Notes,* 5**,** 693-693.

TOUT, S., CHAN-LING, T., HOLLANDER, H. & STONE, J. 1993. The role of Muller cells in the formation of the blood-retinal barrier. *Neuroscience,* 55**,** 291-301.

TROPEPE, V., COLES, B. L. K., CHIASSON, B. J., HORSFORD, D. J., ELIA, A. J., MCINNES, R. R. & VAN DER KOOY, D. 2000. Retinal Stem Cells in the Adult Mammalian Eye. *Science,* 287**,** 2032-2036.

TSENG, W.-C., LU, K.-S., LEE, W.-C. & CHIEN, C.-L. 2006. Redistribution of GFAP and αB-crystallin after thermal stress in C6 glioma cell line. *Journal of Biomedical Science,* 13**,** 681-694.

TURNER, D. L. & CEPKO, C. L. 1987. A common progenitor for neurons and glia persists in rat retina late in development. *Nature,* 328**,** 131-136.

TURNER, D. L., SNYDER, E. Y. & CEPKO, C. L. 1990. Lineage-independent determination of cell type in the embryonic mouse retina. *Neuron,* 4**,** 833-845.

UEHARA, F., OHBA, N. & OZAWA, M. 2001. Isolation and Characterization of Galectins in the Mammalian Retina. *Investigative Ophthalmology & Visual Science,* 42**,** 2164-2172.

URSCHEL, K. & CICHA, I. 2015. TNF-α in the cardiovascular system: from physiology to therapy. *International Journal of Interferon, Cytokine and Mediator Research,* 7.

VAN RAAY, T. J. & VETTER, M. L. 2004. Wnt/Frizzled Signaling during Vertebrate Retinal Development. *Developmental Neuroscience,* 26**,** 352-358.

VANDER, A. J., SHERMAN, J. H. & LUCIANO, D. S. 2003. *Human Physiology: The Mechanism of Body Function*, The McGraw-Hill Companies.

VÁZQUEZ-CHONA, F., SONG, B. K. & GEISERT, E. E. 2004. Temporal Changes in Gene Expression after Injury in the Rat Retina. *Investigative ophthalmology & visual science,* 45**,** 2737.

VÁZQUEZ-CHONA, F. R., SWAN, A., FERRELL, W. D., JIANG, L., BAEHR, W., CHIEN, W.-M., FERO, M., MARC, R. E. & LEVINE, E. M. 2011. Proliferative reactive gliosis is compatible with glial metabolic support and neuronal function. *BMC Neuroscience,* 12**,** 98-98.

VECINO, E., RODRIGUEZ, F. D., RUZAFA, N., PEREIRO, X. & SHARMA, S. C. 2016. Glia–neuron interactions in the mammalian retina. *Progress in Retinal and Eye Research,* 51**,** 1-40.

VERARDO, M. R., LEWIS, G. P., TAKEDA, M., LINBERG, K. A., BYUN, J., LUNA, G., WILHELMSSON, U., PEKNY, M., CHEN, D.-F. & FISHER, S. K. 2008. Abnormal Reactivity of Müller Cells after Retinal Detachment in Mice Deficient in GFAP and Vimentin. *Investigative Ophthalmology & Visual Science,* 49**,** 3659-3665.

WAHLIN, K. J., CAMPOCHIARO, P. A., ZACK, D. J. & ADLER, R. 2000. Neurotrophic factors cause activation of intracellular signaling pathways in Muller cells and other cells of the inner retina, but not photoreceptors. *Invest Ophthalmol Vis Sci,* 41**,** 927-36.

WALCOTT, J. C. & PROVIS, J. M. 2003. Müller cells express the neuronal progenitor cell marker nestin in both differentiated and undifferentiated human foetal retina. *Clinical & Experimental Ophthalmology,* 31**,** 246-249.

WALSH, N., VALTER, K. & STONE, J. 2001. Cellular and subcellular patterns of expression of bFGF and CNTF in the normal and light stressed adult rat retina. *Exp Eye Res,* 72**,** 495-501.

WAN, J., RAMACHANDRAN, R. & GOLDMAN, D. 2012. HB-EGF Is Necessary and Sufficient for Müller Glia Dedifferentiation and Retina Regeneration. *Developmental Cell,* 22**,** 334-347.

WAN, J., ZHENG, H., XIAO, H.-L., SHE, Z.-J. & ZHOU, G.-M. 2007. Sonic hedgehog promotes stem-cell potential of Müller glia in the mammalian retina. *Biochemical and Biophysical Research Communications,* 363**,** 347-354.

WANG, J.-S. & KEFALOV, V. J. 2011. The Cone-specific visual cycle. *Progress in Retinal and Eye Research,* 30**,** 115-128.

WANG, M., MA, W., ZHAO, L., FARISS, R. N. & WONG, W. T. 2011. Adaptive Müller cell responses to microglial activation mediate neuroprotection and coordinate inflammation in the retina. *Journal of Neuroinflammation,* 8**,** 173-173.

WANG, Y., SMITH, S. B., OGILVIE, J. M., MCCOOL, D. J. & SARTHY, V. 2002. Ciliary neurotrophic factor induces glial fibrillary acidic protein in retinal Muller cells through the JAK/STAT signal transduction pathway. *Curr Eye Res,* 24**,** 305-12.

WARE, C. F., CROWE, P. D., VANARSDALE, T. L., ANDREWS, J. L., GRAYSON, M. H., JERZY, R., SMITH, C. A. & GOODWIN, R. G. 1991. Tumor necrosis factor (TNF) receptor expression in T lymphocytes. Differential regulation of the type I TNF receptor during activation of resting and effector T cells. *The Journal of Immunology,* 147**,** 4229-4238.

WASSLE, H. 2004. Parallel processing in the mammalian retina. *Nat Rev Neurosci,* 5**,** 747-757.

WATANABE, T. & RAFF, M. C. 1988. Retinal astrocytes are immigrants from the optic nerve. *Nature,* 332**,** 834-837.

WEN, R., SONG, Y., CHENG, T., MATTHES, M. T., YASUMURA, D., LAVAIL, M. M. & STEINBERG, R. H. 1995. Injury-induced upregulation of bFGF and CNTF mRNAS in the rat retina. *J Neurosci,* 15**,** 7377-85.

WEN, R., TAO, W., LI, Y. & SIEVING, P. A. 2012. CNTF AND RETINA. *Progress in Retinal and Eye Research,* 31**,** 136-151.

WILHELMSSON, U., LI, L., PEKNA, M., BERTHOLD, C.-H., BLOM, S., ELIASSON, C., RENNER, O., BUSHONG, E., ELLISMAN, M., MORGAN, T. E. & PEKNY, M. 2004. Absence of Glial Fibrillary Acidic Protein and Vimentin Prevents Hypertrophy of Astrocytic Processes and Improves Post-Traumatic Regeneration. *The Journal of Neuroscience,* 24**,** 5016-5021.

WU, K. H. C., MADIGAN, M. C., BILLSON, F. A. & PENFOLD, P. L. 2003. Differential expression of GFAP in early v late AMD: a quantitative analysis. *British Journal of Ophthalmology,* 87**,** 1159-1166.

WU, Y., ZHANG, X., SALMON, M., LIN, X. & ZEHNER, Z. E. 2007. TGFbeta1 regulation of vimentin gene expression during differentiation of the C2C12 skeletal myogenic cell line requires Smads, AP-1 and Sp1 family members. *Biochim Biophys Acta,* 3**,** 427-39.

WUNDERLICH, K. A., TANIMOTO, N., GROSCHE, A., ZRENNER, E., PEKNY, M., REICHENBACH, A., SEELIGER, M. W., PANNICKE, T. & PEREZ, M.-T. 2015. Retinal functional alterations in mice lacking intermediate filament proteins glial fibrillary acidic protein and vimentin. *The FASEB Journal,* 29**,** 4815-4828.

XIAO, M. & HENDRICKSON, A. 2000. Spatial and temporal expression of short, long/medium, or both opsins in human fetal cones. *The Journal of Comparative Neurology,* 425**,** 545-559.

XU, H., CHEN, M. & FORRESTER, J. V. 2009. Para-inflammation in the aging retina. *Prog Retin Eye Res,* 28**,** 348-68.

XUE, L. P., LU, J., CAO, Q., HU, S., DING, P. & LING, E. A. 2006. Müller glial cells express nestin coupled with glial fibrillary acidic protein in experimentally induced glaucoma in the rat retina. *Neuroscience,* 139**,** 723-732.

XUE, W., COJOCARU, R. I., DUDLEY, V. J., BROOKS, M., SWAROOP, A. & SARTHY, V. P. 2011. Ciliary Neurotrophic Factor Induces Genes Associated with Inflammation and Gliosis in the Retina: A Gene Profiling Study of Flow-Sorted, Müller Cells. *PLOS ONE,* 6**,** e20326.

YANG, X., LUO, C., CAI, J., POWELL, D. W., YU, D., KUEHN, M. H. & TEZEL, G. 2011. Neurodegenerative and Inflammatory Pathway Components Linked to TNF-α/TNFR1 Signaling in the Glaucomatous Human Retina. *Investigative Ophthalmology & Visual Science,* 52**,** 8442-8454.

YAO, F., SVENSJO, T., WINKLER, T., LU, M., ERIKSSON, C. & ERIKSSON, E. 1998. Tetracycline repressor, tetR, rather than the tetR-mammalian cell transcription factor fusion derivatives, regulates inducible gene expression in mammalian cells. *Hum Gene Ther,* 9**,** 1939-50.

YARON, O., FARHY, C., MARQUARDT, T., APPLEBURY, M. & ASHERY-PADAN, R. 2006. Notch1 functions to suppress cone-photoreceptor fate specification in the developing mouse retina. *Development,* 133**,** 1367-1378.

YOSHIDA, S., SOTOZONO, C., IKEDA, T. & KINOSHITA, S. 2001. Interleukin-6 (IL-6) production by cytokine-stimulated human Müller cells. *Current Eye Research,* 22**,** 341-347.

ZHANG, H., YAN, D., SHI, X., LIANG, H., PANG, Y., QIN, N., CHEN, H., WANG, J., YIN, B., JIANG, X., FENG, W., ZHANG, W., ZHOU, M. & LI, Z. 2008. Transmembrane TNF-α mediates “forward” and “reverse” signaling, inducing cell death or survival via the NF-κB pathway in Raji Burkitt lymphoma cells. *Journal of Leukocyte Biology,* 84**,** 789-797.

ZHANG, L., ZHAO, W., LI, B., ALKON, D. L., BARKER, J. L., CHANG, Y. H., WU, M. & RUBINOW, D. R. 2000. TNF-alpha induced over-expression of GFAP is associated with MAPKs. *Neuroreport,* 11**,** 409-12.

ZHANG, W., POTROVITA, I., TARABIN, V., HERRMANN, O., BEER, V., WEIH, F., SCHNEIDER, A. & SCHWANINGER, M. 2005. Neuronal Activation of NF-κB Contributes to Cell Death in Cerebral Ischemia. *Journal of Cerebral Blood Flow & Metabolism,* 25**,** 30-40.

ZHAO, X.-F., WAN, J., POWELL, C., RAMACHANDRAN, R., MYERS, M. G. & GOLDMAN, D. 2014. Leptin and IL-6 Family Cytokines Synergize to Stimulate Müller Glia Reprogramming and Retina Regeneration. *Cell reports,* 9**,** 272-284.

Chapter 9 Appendices

Appendix 1: RT-PCR Primers

Gene of interest	Sequence	Source
β-actin	Forward: CATGTACGTTGCTATCCAGGC Reverse: CTCCTTAATGTCACGCACGAT	Sigma Aldrich
Glial fibrillary acidic protein (GFAP)	Forward: CTGGGCTCAAGCAGTCTACC Reverse: GAGTCATCGCTCAGGAGGTC	Sigma Aldrich
Tenascin (TNC)	Forward: TCAAGGCTGCTACGCCTTAT Reverse: TTCTGGGCTGCCTCTACTGT	Sigma Aldrich
Galectin-1 (LGALS1)	Forward: CTCTCGGGTGGAGTCTTCTG Reverse: ACGAAGCTCTTAGCGTCAGG	Sigma Aldrich
Vimentin (VIM)	Forward: GAGAACTTTGCCGTTGAAGC Reverse: TCCAGCAGCTTCCTGTAGGT	Sigma Aldrich
Procollagen Galactosyltransferase (GLT25D1)	Forward: ACAGACTCCCAGTTGGGTTG Reverse: GCAAGGAGGTAAAGCACAGG	Sigma Aldrich
Nuclear Receptor Subfamily 2, Group E, Member 3 (NR2E3)	Forward: GGCGTGGAGTGAACTCTTTC Reverse: CTGGCTTGAAGAGGACCAAG	Invitrogen
Recoverin (RCVRN)	Forward: AGCTCCTTCCAGACGATGAA Reverse: CAAACTGGATCAGTCGCAGA	Sigma Aldrich
NR2E3 Hari	Forward: AGCATGGAGTCCAACACTGAG Reverse: GGTCATTGCTGGTGACATCAA	Sigma Aldrich
Recoverin Hari	Forward: CTCCTTCCAGACGATGAAAACA Reverse: GCCAGTGTCCCCTCAATGAA	Sigma Aldrich
NFκB1	Forward: GAAGCACGAATGACAGAGGC Reverse: GCTTGGCGGATTAGCTCTTTT	Sigma Aldrich
NFκB2	Forward: ATGGAGAGTTGCTACAACCCA Reverse: CTGTTCCACGATCACCAGGTA	Sigma Aldrich
TNF-R1	Forward: TCACCGCTTCAGAAAACCACC Reverse: GGTCCAGTGTGCAAGAAGAGA	Sigma Aldrich
TNF-R2	Forward: CGGGCCAACATGCAAAAGTC Reverse: CAGATGCGGTTCTGTTCCC	Sigma Aldrich

Appendix 2: qPCR Primers

Gene of interest	Sequence	Source
β-actin	Forward: CCAACCGCGAGAAGATGA Reverse: CCAGAGGCGTACAGGGATAG	Sigma Aldrich
NR2E3	Forward: AGCATGGAGTCCAACACTG Reverse: GGTCATTGCTGGTGACATC	Sigma Aldrich
TetR	Forward: AAAAATAAGCGGGCTTTGCT Reverse: CCCCTTCTAAAGGGCAAAAG	Sigma Aldrich
GFAP	Forward: ATCCACGCTGTTTTGACCTC Reverse: GTGATGCGTCCTCTCCAT	Sigma Aldrich
mCherry	Forward: ATCCACGCTGTTTTGACCTC Reverse: ACCTTGAAGCGCATGAACTC	Sigma Aldrich

Appendix 3: Primary Antibodies

Primary Antibody	Source	Host	Use	Dilution used
Monoclonal Anti-β-actin	Sigma Aldrich (Cat no. A2228)	Mouse	Western blot	1:5000
Polyclonal Anti-Glial fibrillary acidic protein (GFAP)	DAKO (Cat no. Z033401-2)	Rabbit	Western blot Immunocytochemistry	1:1000
Polyclonal Anti-NR2E3 (B-4)	Santa Cruz Biotechnology (Cat no. sc-374513)	Mouse	Western blot	1:100
Polyclonal Anti-NR2E3	Merck Millipore (Cat no. AB2299)	Rabbit	Immunocytochemistry	1:100
Polyclonal Anti-Vimentin	Santa Cruz Biotechnology (Cat no. sc-5565)	Rabbit	Immunocytochemistry Western blot	1:100 1:500
Monoclonal Anti-Nestin	Merck Millipore (Cat no. MAB5326)	Mouse	Immunocytochemistry	1:100
Monoclonal Anti-TNF RI/TNFRSF1A (16805)	Novus Biological (Cat. No MAB625-SP)	Mouse	Western blot	2µg/ml
Polyclonal Anti-TNF Receptor II	Abcam (Cat. No ab15563)	Rabbit	Western blot	1:5000
Monoclonal Anti-NFkB p105/50 (5D10D11)	Novus Biological (Cat. No NBP2-22178)	Mouse	Immunocytochemistry Western blot	1:200 1:1000
Polyclonal Anti-NFkB p100/52	Novus Biological (Cat. No NB100-82063)	Rabbit	Immunocytochemistry Western blot	1:100 1:500
Monoclonal IkB-alpha Antibody (6A920)	Novus Biological (Cat. No NB100-56507SS)	Mouse	Western blot	2µg/ml

Appendix 4: Addgene plasmid information

pmCherry-GFAP-N-18 **Sequence Number: GFAP-10x**

GCCACGATG - mCherry Sequence (708 Nucleotides - 236 Amino Acids AY678264)
ATGTACGGC - mCherry Chromophore (MYG)
ATGGTGGGT - Human GFAP Sequence (1296 Nucleotides - 432 Amino Acids)

LINKER - 18 Amino Acids (54 Nucleotides) between mCherry and GFAP

ATG - Methionine Start Codon

TAG TAA TGA - Stop Codons **Antibiotic = Kan/Neo**

GFAP is Human glial fibrillary acidic protein (NM_002055.2)

GTCAGATCCGCTAGCGCCACCATGGAGAGGAGACGCATCACCTCCGCTGCTCGCCGCTCCTACGT
CTCCTCAGGGGAGATGATGGTGGGGGGCCTGGCTCCTGGCCGCCGTCTGGGTCCTGGCACCCGCC
TCTCCCTGGCTCGAATGCCCCCTCCACTCCCAACCCGGGTGGATTTCTCCCTGGCTGGGGCACTCA
ATGCTGGCTTCAAGGAGACCCGGGCCAGTGAGCGGGCAGAGATGATGGAGCTCAATGACCGCTTT
GCCAGCTACATCGAGAAGGTTCGCTTCCTGGAACAGCAAAACAAGGCGCTGGCTGCTGAGCTGAA
CCAGCTGCGGGCCAAGGAGCCCACCAAGCTGGCAGACGTCTACCAGGCTGAGCTGCGAGAGCTG
CGGCTGCGGCTCGATCAACTCACCGCCAACAGCGCCCGGCTGGAGGTTGAGAGGGACAATCTGGC
ACAGGACCTGGCCACTGTGAGGCAGAAGCTCCAGGATGAAACCAACCTGAGGCTGGAAGCCGAG
AACAACCTGGCTGCCTATAGACAGGAAGCAGATGAAGCCACCCTGGCCCGTCTGGATCTGGAGAG
GAAGATTGAGTCGCTGGAGGAGGAGATCCGGTTCTTGAGGAAGATCCACGAGGAGGAGGTTCGGG
AACTCCAGGAGCAGCTGGCCCGACAGCAGGTCCATGTGGAGCTTGACGTGGCCAAGCCAGACCTC
ACCGCAGCCCTGAAAGAGATCCGCACGCAGTATGAGGCAATGGCGTCCAGCAACATGCATGAAGC
CGAAGAGTGGTACCGCTCCAAGTTTGCAGACCTGACAGACGCTGCTGCCCGCAACGCGGAGCTGC
TCCGCCAGGCCAAGCACGAAGCCAACGACTACCGGCGCCAGTTGCAGTCCTTGACCTGCGACCTG
GAGTCTCTGCGCGGCACGAACGAGTCCCTGGAGAGGCAGATGCGCGAGCAGGAGGAGCGGCACG
TGCGGGAGGCGGCCAGTTATCAGGAGGCGCTGGCGCGGCTGGAGGAAGAGGGGCAGAGCCTCAA
GGACGAGATGGCCCGCCACTTGCAGGAGTACCAGGACCTGCTCAATGTCAAGCTGGCCCTGGACA
TCGAGATCGCCACCTACAGGAAGCTGCTAGAGGGCGAGGAGAACCGGATCACCATTCCCGTGCAG
ACCTTCTCCAACCTGCAGATTCGAGAAACCAGCCTGGACACCAAGTCTGTGTCAGAAGGCCACCTC
AAGAGGAACATCGTGGTGAAGACCGTGGAGATGCGGGATGGAGAGGTCATTAAGGAGTCCAAGCA
GGAGCACAAGGATGTGATGAGCAGCGGTGGAGCAAGCGCAGCCAGTGGTAGCGCGGATCCACCG
GTCGCCACCATGGTGAGCAAGGGCGAGGAGGATAACATGGCCATCATCAAGGAGTTCATGCGCTT
CAAGGTGCACATGGAGGGCTCCGTGAACGGCCACGAGTTCGAGATCGAGGGCGAGGGCGAGGGC
CGCCCCTACGAGGGCACCCAGACCGCCAAGCTGAAGGTGACCAAGGGTGGCCCCCTGCCCTTCGC
CTGGGACATCCTGTCCCCTCAGTTCATGTACGGCTCCAAGGCCTACGTGAAGCACCCCGCCGACAT
CCCCGACTACTTGAAGCTGTCCTTCCCCGAGGGCTTCAAGTGGGAGCGCGTGATGAACTTCGAGGA
CGGCGGCGTGGTGACCGTGACCCAGGACTCCTCCCTGCAGGACGGCGAGTTCATCTACAAGGTGA
AGCTGCGCGGCACCAACTTCCCCTCCGACGGCCCCGTAATGCAGAAGAAGACCATGGGCTGGGAG
GCCTCCTCCGAGCGGATGTACCCCGAGGACGGCGCCCTGAAGGGCGAGATCAAGCAGAGGCTGA
AGCTGAAGGACGGCGGCCACTACGACGCTGAGGTCAAGACCACCTACAAGGCCAAGAAGCCCGT
GCAGCTGCCCGGCGCCTACAACGTCAACATCAAGTTGGACATCACCTCCCACAACGAGGACTACA
CCATCGTGGAACAGTACGAACGCGCCGAGGGCCGCCACTCCACCGGCGGCATGGACGAGCTGTA
CAAGTAAAGCGGCCGCGACTCTAGATCATAATCAGCCATACCACAT

mCherry-GFAP-N-18 in HeLa Cells

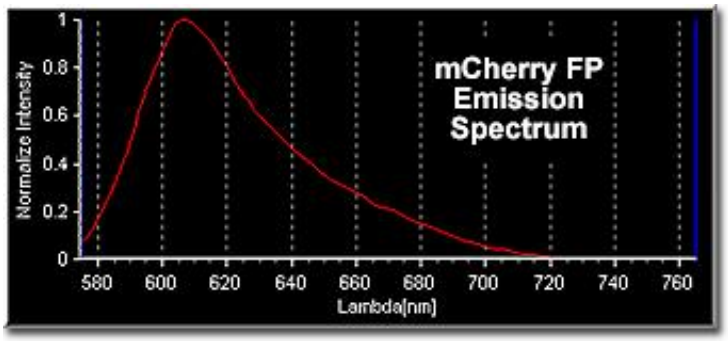

Appendix 5: Sequencing primers for constructed vectors

5.1 Source BioScience sequencing

Name of plasmid	Name/ Sequence of primers	Source
pCLNC_mCherry_GFAP_TO	NeoR_Forward: CGACCAAGCGAAACATC TO_seq_Forward: GCTGCTTCGCGATGTACG PCLNCx_seq_Reverse: CTTTTATTGAGCTCGGGGAG GFAP_mCherry_Forward1: TCCGCTAGCGCCACCATG GFAP_mCherry_Forward2: GAGATCCGGTTCTTGAGGAA GFAP_mCherry_Forward3: ACCAAGTCTGTGTCAGAAGGC	Sigma Aldrich
pCLNC_mCherry_TO	NeoR_Forward: CGACCAAGCGAAACATC TO_seq_Forward: GCTGCTTCGCGATGTACG PCLNCx_seq_Reverse: CTTTTATTGAGCTCGGGGAG	Sigma Aldrich
pcDNA4/TR	CMV_seq_Forward: TCACTTTTTTTTCAAGGCAATCA SV40_seq_Reverse: CCAGACATGATAAGATACATTGA	Sigma Aldrich

5.2 Sanger sequencing

Name of plasmid	Sequence of primers	Source
mCherry-GFAP-N-18	Forward: GCTGGTTTAGTGAACCGTCAGA Reverse: ATGTTGACGTTGTAGGCGCCGG	Sigma Aldrich

Appendix 6: Cloning primers

Sequence to be amplified	Sequence of primers	Source
mCherry-GFAP	Forward: CCGCGACTATCGATCATAATCAGCC Reverse: GGCTGATTATGATCGATAGTCGCGG	Sigma Aldrich
mCherry	Forward: GCGGTGGAGCAAGCTTAGCCAGTGG Reverse: ATGGCTGATATCGATCTAGAGTCGC	Sigma Aldrich
TetR	Forward: CGGATCGATCCTGAAGCTTCAGGGTGAG Reverse: CGAGCGGCCGCCAGTGTGATCGATTCGAC	Sigma Aldrich

Appendix 7: pCLNCX retrovirus expression vector

IMGENEX

11175 Flintkote Ave., Suite E, San Diego, CA 92121
www.imgenex.com. Biomol GmbH: www.biomol.de info@biomol.de
T: 0800-2466651/+49-8532600, F: Tel.: 0800-2466652/+49-85326022

pCLNCX Retrovirus Expression Vector

Catalog No.: 10042P

Contents: 10 µg in 20 µl 1x TE (10 mM Tris, pH 7.5, 1 mM EDTA)

BACKGROUND:

The pCLNCX expression vector is a part of the RetroMax expression system (Cat#10040K and 10041K) and has been designed to maximize recombinant–retrovirus titers in a simple, efficient, and flexible experimental system. All members of the RetroMax expression vector family (pCLXSN, pCLNCX, pCLNRX, and pCLNDX) have an extended packaging signal (ψ+) and are derived from safety-modified retrovirus vectors in which the *gag* open reading frame has been stopped by a point mutation (1), thereby minimizing the opportunity for replication competent retrovirus production by recombination with packaging genome.

The RetroMax system is designed for maximal virus titer in 293 cells. It takes advantages of two properties of 293 cells, i) high level of transfectibility, ii) strong E1A-mediated stimulation of CMV promoter controlled transcription. 293 cells are of nonmurine origin, hence the problem of **selective packaging and transfer of VL30 genomes (present in all murine packaging cells) are avoided.** Vector supernatants are free of helper virus and are of sufficiently high titer within 2 days of transient transfection in 293 cells to permit infection of more than 50% of dividing target cells in culture.

STORAGE:

For long-term storage, store at –20°C. For amplification, transform DH-5a or similar bacteria and plate on LB plates containing 50 mg/ml ampicillin.

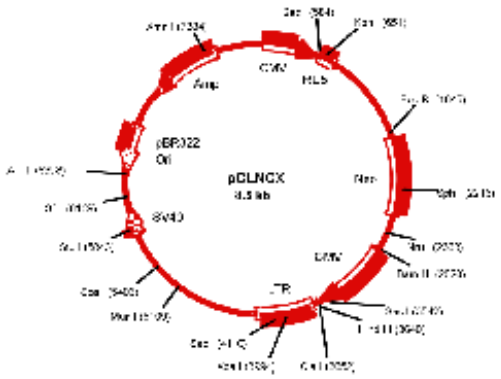

Schematic presentation of pCLNCX vector: CMV immediate early promoter/enhancer allows high-efficiency transcription in 293 cells. However, this is lost during viral replication. Hence, the gene of interest cloned into ***Eco RI*** cloning site is driven by Moloney MLV and murine sarcoma virus LTR (RU5). For expression under the control of CMV early promoter/enhancer, the gene of interest should be cloned into ***Hind III*** or ***Cla I*** site.

REFERENCES:

1. Naviaux, RK, Costanzi, E, Haas, M and Verma, I. The pCL vector system: Rapid production of helper-free, high titer, recombinant retroviruses. *J. Virol* 70: 5701-5705 (1996).